Extraction of canola proteins and assessment of their applications: cruciferin for encapsulation of bioactives and napin as a chaperone-like molecule

by

Ali Akbari

A thesis submitted in partial fulfillment of the requirements for the degree of

Doctor of Philosophy

in

Food Science and Technology

Department of Agricultural, Food and Nutritional Science
University of Alberta

Abstract

Canola is a farm-gate crop in Canada. Canola meal after oil extraction is used mostly as animal feed with limited value-added applications. Canola proteins are known to have great potential for use in food and non-food applications due to their nutritional, biological and functional properties. Canola contains two major proteins: cruciferin and napin, but with distinct properties. Cruciferin is resistant to gastric digestion and has excellent functional properties; it was hypothesized that it might be an appropriate material for encapsulation of bioactive compounds. Napin, a small molecule that is extremely thermal resistant, may represent chaperon-like activity. Therefore, the overall objectives of the thesis are 1) to develop an integrated method of extraction for these two main canola proteins, 2) to explore the potential application of cruciferin for encapsulation of bioactive compounds, 3) to study *in vitro* cellular uptake and trans-cellular transport of cruciferin-based particles, 4) to evaluate the potential chaperone-like activity of napin.

An integrated, simple and scalable method, including acidic washing (pH 4), alkaline extraction (pH 12.5), isoelectric precipitation (pH 4), and ultrafiltration, was developed to isolate two main canola proteins: cruciferin and napin. Negatively-charged Cruciferin/calcium (Cru/Ca) nanoparticles were prepared using a cold gelation method. To study the potential application of cruciferin to coat and protect chitosan particles at stomach low pH, positively-charged spherical cruciferin/chitosan (Cru/Cs) nanoparticles were also prepared. Cru/Ca particles were resistant in simulated gastric fluid, but released 70-90% of encapsulated compounds in simulated intestinal fluids while Cru/Cs particles were resistant in both simulated gastric and intestinal fluids and released less than 20% of the compounds. Although the surface of both particles was composed

of gastric-resistant cruciferin which was degraded in simulated intestinal fluid, the particles showed different release behavior in simulated intestinal fluid which reveals that the particle cores controlled the release rate of encapsulated compounds.

The cellular uptake and trans-cellular transport of Cru/Ca and Cru/Cs particles were also investigated using Caco-2 and Caco-2/HT29 co-culture systems. Our results showed that the presence of mucus secreted by HT29 cells, co-cultured with Caco-2, had negligible influence on the uptake and transport of both particles. The uptake of negatively-charged Cru/Ca particles was ~3 times higher than positively-charged Cru/Cs. Whereas digestion in simulated intestinal conditions led to dissociation of Cru/Ca particles, only cruciferin coating was digested from Cru/Cs particle surface; and as a result, the cellular uptake and transport of digested Cru/Cs particles were higher than the undigested form. The presence of mucus in Caco-2/HT29 co-culture decreased the cellular uptake and transport of digested Cru/Cs particles compared to the undigested particles which might be due to the mucoadhesive property of exposed chitosan-based particle core. Energy-dependent mechanisms were dominated for uptake of the undigested and digested particles.

In the last part of the thesis, the potential chaperone-like activity of napin was evaluated. The results showed that napin had a chaperone-like activity against thermal aggregation of ovotransferrin (OT) in a heat treatment. The chaperone-like activity of napin might be due to formation hydrophobic interactions between napin and OT fibril cores. The interactions decreased β-sheet and random coil structures in the fibril cores while increased α-helix.

The results of this thesis supported the potential application of cruciferin for encapsulation of bioactive compounds, and also show a chaperone-like activity for napin. The difference in the

application of the proteins was due to their distinct properties; while cruciferin formed particles through aggregation, napin has potential to suppress aggregation of other proteins.

PREFACE

This thesis is an original work done by Ali Akbari. The thesis is consisted of eight chapters: Chapter 1 provides a general introduction and the objectives of the thesis. Chapter 2 is literature review on canola proteins, encapsulation and delivery of bioactive compounds, and chaperone-like activity of proteins (A modified version of the chaperone part of this chapter is ready for submission); A version of chapter 3 has been published as "An integrated method of isolating napin and cruciferin from defatted canola meal" in *LWT - Food Science and Technology*; A version of chapter 4 has been published as "Cruciferin nanoparticles: Preparation, characterization and their potential application in delivery of bioactive compounds" in *Food Hydrocolloids*; A version of chapter 5 entitled as "Cruciferin coating improves the stability of chitosan nanoparticles at low pHs " has been accepted for publication in *Journal of Materials Chemistry B*; Chapter 6 entitled as "Cellular uptake and trans-cellular transport of cruciferin-based nanoparticles in Caco-2 and its co-culture with /HT29-MTX cells" and chapter 7 entitled as "Napin shows a chaperone-like activity through limiting fibril formation" are ready for submission; Chapter 8 provides some concluding remarks and future research directions. I was responsible for literature reviews required for the study, experimental designs, performing experiments, data collection and analysis, and writing the manuscripts. My supervisor, Dr. Jianping Wu, contributed to the experimental designs, data interpretations, manuscripts preparations and edit.

DEDICATION

To my parents who taught me to love learning,

to Fatemeh, my wife, who always supports me

and

to Arman, my son, who gives me hope and passion.

ACKNOWLEDGEMENTS

I want to take this opportunity to thank all the great people who helped me and participated in this work and made it possible. First and foremost, I want to thank my supervisor, Dr. Jianping Wu, for giving me the opportunity to work in his research laboratory. His support, encouragement and guidance were invaluable and will not be forgotten. I would like to thank my supervisory committee members, Dr. Afsaneh Lavasanifar and Dr. Lingyun Chen, for their guidance, constructive comments and suggestions that were infinitely important to complete my thesis. I would also like to express my sincere thanks to Dr. Larry D. Unsworth and Dr. Loong-Tak Lim for accepting the invitation to serve as internal and external examiners and devoted their time to read and evaluate this thesis.

I am deeply grateful for all the support given by the Graduate Program Administrators and lab managers of the Department of Agricultural Food and Nutritional Sciences (AFNS), Mrs. Jody Forslund, Ms. Krasna Kos, Dr. Lynn Elmes, Dr. Urmila Basu, Mrs. Nancy Turchinsky and Mrs. Heather Vandertol-Vanier. I would like to express my thanks to my fellow graduate students, both past and present, from Dr. Wu's and Dr. Lavasanifar's laboratories: Dr. Shengwen Shen, Dr. Jiapei Wang, Dr. Aman Ullah, Dr. Mohammad Reza Vakili, Dr. Nazila Safaei Nikouei, April Milne, Maria Offengenden, Alexandra Acero, Kaustav Majumder, Li Sen, Chamila Nimalaratne, Mejo Remanan, Wenlin Yu, Yuchen Gu, Yussef Esparza, Xiahong Sun, Sareh Panahi, Forough Jahandideh, Nan Shang, Wang Liao, Selene Gonzalez Toledo, Dr. Chalamaiah Meram, Liang Chen, Hongbing Fan, Shreyak Chaplot, Dr. Qingbiao Xu, Dr. Hui Hong, Dr. Myoungjin Son, Dr. Subhadeep Chakrabarti and Dr. Ping Liu.

The financial supports received as research grants or scholarship/fellowship from Natural Sciences and Engineering Research Council of Canada (NSERC), Alberta Livestock and Meat Agency Ltd. (ALMA), Alberta Innovates Bio Solutions (AI Bio), the Department of AFNS, the Faculty of Graduate Studies and Research, and Graduate Students' Association of University of Alberta, and Institute of Food Technologists (IFT) are highly appreciated.

Table of Contents

CHAPTER 4. Cruciferin nanoparticles: preparation, characterization and their potential application in delivery of bioactive compounds

List of Tables

List of Figures

Abbreviations:

Cru/Ca: Cruciferin/calcium

Cru/Cs: Cruciferin/chitosan

OT: Ovotransferrin

GRAS: Generally recognized as safe

USDA: United States Department of Agriculture

pI: Isoelectric point

GI: Gastrointestinal

HT29: HT29-MTX cell

Gly: Glycine

Gln: Glutamine

Tyr: Tyrosine

Pro: Proline

SDS: Sodium dodecyl sulfate

PVP: Polyvinylpolypyrrolidone

EDTA: Ethylenediaminetetraacetic acid

PMM: Protein micellar mass

SLN: Solid lipid nanoparticles

LML: Luminal mucus layer

AML: Adherent mucus layer

LDL: Low density lipoprotein

Hsps: Heat-shock proteins

HMC: High-molecular weight chitosan

LMC: Low- molecular weight chitosan

DV: Diavolume

CF: Concentration factors

NDF: Non-digestible fiber

TCA: Trichloroacetic acid

EAI: Emulsifying activity index

ME: Mercaptoethanol

DMEM: Dulbecco's modified eagle medium

HEPES: 4-(2-hydroxyethyl)-1-piperazineethanesulfonic acid

HBSS: Hanks' balanced salt solution

FBS: Fetal bovine serum

MTT: 3-(4,5-dimethylthiazol-2-yl)-2,5-diphenyltetrazolium bromide

DMSO: Dimethyl sulfoxide

ANS: 1-anilinonaphthalene-8-sulfonic acid

DTT: Dithiothreitol

DAPI: 4',6-diamidino-2-phenylindole

TEM: Transmission electron microscopy

CD: Circular Dichroism

FTIR: Fourier transform infrared

PBS: Phosphate-buffered saline

CLMS: Confocal laser scanning microscope

BB: Brilliant blue

EE: Encapsulation efficiency

LC: Loading capacity

PPY: Particle preparation yield

SGF: Simulated gastric fluid

SIF: Simulated intestinal fluid

PDI: Polydispersity index

DLS: Dynamic light scattering

DSC: Differential scanning calorimeter

C6: Coumarin-6

S_0: Surface hydrophobicity

FCS: Flow cytometry standard

MFI: Mean fluorescence intensity

TEER: Trans-epithelial electrical resistance

P_{app}: Apparent permeability coefficient

D_{eff}: Effective diffusion coefficient

Th T: Thioflavin T

ATR-FTIR: Attenuated total reflectance Fourier-transform infrared

CHAPER 1- General introduction and thesis objectives

Food proteins, a diverse group of biopolymers, have excellent functional properties along with high nutritional value (Wan et al., 2015). Generally food proteins are GRAS (Generally recognized as safe), biodegradable and biocompatible which are important for food applications (Elzoghby et al., 2012). The abundance and variety of protein sources are also other encouraging factors for their use in different purposes. Canola/rapeseed meal, a by-product of oil extraction, with global production of 38 million metric tons (USDA, 2013) and 35-40% protein (Wu, et al., 2008a), is an abundant and inexpensive protein source.

Encapsulation of bioactive compounds has recently attracted increasing attention in the development of new nutraceutical and pharmaceutical products. Bioactive compounds including vitamins, phytosterols, polyphenols, minerals, bioactive peptides and probiotics play vital roles in human metabolism making them essential for health. Enrichment of different food products by incorporation of the bioactive compounds improves public health (Wan et al., 2015). However, many of these compounds are sensitive to harsh conditions in food processing, storage and human digestive system. Poor solubility, unpleasant off-flavor, appearance and mouthfeel of bioactive compounds, and their undesirable interactions with other food component might also limit their incorporation in food products. Encapsulation is an appropriate method to overcome these limitations and improve the bioavailability of the compounds (McClements, 2015).

The delivery systems might be uptaken by intestinal epithelial cells and/or release the encapsulated bioactive compounds. The composition and physicochemical properties such as size, shape and charge of the systems are the main factors which influence the uptake and/or release efficiency of the compounds (Martins et al., 2015). Mucoadhesive particles are able to adhere to mucus layers, semipermeable barriers covering epithelial cells, and prolong residence time of the particles and as a result, sustainably release the bioactive compounds (Smart, 2005). However, mucus-penetrating particles can traverse across the mucus layers to the epithelial cells to be uptaken and/or release the compound close to the cells (Lai et al., 2009).

Most of food proteins form heat-set hydrogels and based on the gel structure, different compounds can be encapsulated and slowly be released. However, heat-set gels are not suitable for encapsulation of heat-sensitive compounds. An alternative method is cold gelation which needs a preheating step and adding multivalent ions to make a network with soluble protein aggregates.

The bioactive compounds are added before forming the network. This method was previously applied in encapsulation matrices of whey protein (Barbut and Foegeding, 1993; Marangoni et al., 2000; Cavallieri and Da Cunha, 2008), β-lactoglobulin (Remondetto and Subirade, 2003), soy protein (Maltais et al., 2005), and bovine serum albumin (Kundu et al., 2013).

Cruciferin, a major canola protein (60-65% of total protein) with isoelectric point (pI) of ~ 7.2, is composed of six subunits, each subunit contains one acidic 30 kDa α-chain and one basic 20 kDa β-chain (Wanasundara, 2011). It was hypothesized that cruciferin, a resistant protein to gastric digestion (Bos et al., 2007) with a high denaturation temperature of 91 °C and good gelling and emulsifying properties (Schwenke et al., 1998; Wu and Muir, 2008b), might be an appropriate wall material for encapsulation.

Functional, nutritional and bioactive characteristics of proteins in food matrices are closely associated with their structure. Food processing such as heating and high pressure treatment generally alter the techno- and bio-functionality of proteins through changing their structures and/or exposure of interactive residues (hydrophobic patches and sulfhydryl groups) (Visschers and de Jongh, 2005). These changes might facilitate the intermolecular cross-links leading to less solubility and aggregation. At least two distinct competitive pathways have been proposed for protein aggregation: one is reversible non-nucleation growth in which oligomers and worm-like (semi-flexible) fibrils are rapidly assembled, while the 2nd one is nucleation-dependent, where rigid long-straight fibrils (amyloids) are formed through lag-phased nucleation and growth (Miti et al., 2015; Gosal et al., 2005). Although protein aggregation is required for some functional properties such as gelling and thickening, it may result in undesirable appearance and flow behaviour in high protein beverage products (Nicolai and Durand, 2013). Ingested pre-formed aggregates might also act as fibrillization seeds to trigger extensive aggregation in the body (Chiti and Dobson, 2006). The ordered-structure amyloid fibrils are also recognized as a major contributing factor in amyloid-related diseases such as Alzheimer's and Huntington's (Hartl et al., 2011).

Chaperones are a large group of proteins which prevent aggregation and fibrillation of intrinsically disordered or partially unfolded proteins (Ellis, 2006; Liberek et al., 2008). In addition to cellular heat-shock proteins, chaperone-like activity was reported for casein (Librizzi et al., 2014), polyphenols (Hudson et al., 2009; Singh et al., 2013; Wang et al., 2008), cyclodextrin (Machida et al., 2000), heme-containing proteins (Khodarahmi et al., 2009). Amphiphilicity and flexibility are two important properties for a protein with chaperone activity (Koudelka et al., 2009).

Napin is the second major canola protein accounting for 20-25% of total canola protein. Napin with pI 10.7 and molecular weight of ~14.5 kDa, is composed of 4.5 kDa (40 amino acids) and 9.5 kDa (90 amino acids) chains. Napin, with high denaturation point of 110 °C is resistant to heat aggregation (Wu and Muir, 2008b). Napin, also contains 6.4% proline (Aider and Barbana, 2011), a hydrophobic residue, which provides more flexibility to protein structures (Yong and Forgeding, 2010). Therefore, it was hypothesized that the loosely folded and relatively flexible structure of napin, along with highly positive charge and presence of surface hydrophobic groups can facilitate its interaction with other proteins, and due to the high thermal stability, napin has ability to increase the heat resistance of the complex.

Therefore, two hypotheses were proposed in this thesis research: 1) Cruciferin, a resistant protein to gastric digestion, would be an appropriate material for encapsulation, protection and delivery of bioactive compounds. 2) Napin, a small molecule with high thermal resistant, can show chaperone-like activity.

The objectives of the research were:

1. To develop an integrated method of isolation of two main canola proteins, cruciferin and napin, from defatted canola meal.
2. To prepare cruciferin/calcium particles, evaluate their potential for encapsulation of bioactive compounds, and study the release of the compounds in simulated gastrointestinal (GI) tract.
3. To study the potential of cruciferin to coat chitosan particles, evaluate cruciferin/chitosan particles for encapsulation of bioactive compounds, and study the release of the compounds in simulated GI tract.
4. To study the *in vitro* cellular uptake and trans-cellular transport of cruciferin/calcium and cruciferin/chitosan particles in Caco-2 and its co-culture with /HT29-MTX cells.
5. To evaluate the potential chaperone-like activity of napin.

1.1. References

Aider, M. & Barbana, C. (2011). Canola proteins: Composition, extraction, functional properties, bioactivity, applications as a food ingredient and allergenicity - A practical and critical review. *Trends in Food Science & Technology,* 22(1), 21-39.

Barbut, S. & Foegeding, E. A. (1993). Ca^{2+}-Induced gelation of pre-heated whey-protein isolate. *Journal of Food Science*, 58(4), 867-871.

Bos, C., Airinei, G., Mariotti, F., Benamouzig, R., Berot, S., Evrard, J., Fenart, E., Tome, D., & Gaudichon, C. (2007). The poor digestibility of rapeseed protein is balanced by its very high metabolic utilization in humans. *Journal of Nutrition,* 137(3), 594-600.

Cavallieri, A. L. F. & Da Cunha, R. L. (2008). The effects of acidification rate, pH and ageing time on the acidic cold set gelation of whey proteins. *Food Hydrocolloids,* 22(3), 439-448.

Chiti, F. & Dobson, C. M. (2006). Protein misfolding, functional amyloid, and human disease. *Annual Review of Biochemistry,* 75, 333-366.

Ellis, R. J. (2006). Molecular chaperones: Assisting assembly in addition to folding. *Trends in Biochemical Sciences,* 31(7), 395-401.

Elzoghby, A. O., Samy, W. M., & Elgindy, N. A. (2012). Protein-based nanocarriers as promising drug and gene delivery systems. *Journal of Controlled Release,* 161(1), 38-49.

Gosal, W. S., Morten, I. J., Hewitt, E. W., Smith, D. A., Thomson, N. H., & Radford, S. E. (2005). Competing pathways determine fibril morphology in the self-assembly of beta(2)-microglobulin into amyloid. *Journal of Molecular Biology,* 351(4), 850-864.

Hartl, F. U., Bracher, A., & Hayer-Hartl, M. (2011). Molecular chaperones in protein folding and proteostasis. *Nature,* 475(7356), 324-332.

Hudson, S. A., Ecroyd, H., Dehle, F. C., Musgrave, I. F., & Carver, J. A. (2009). (-)-Epigallocatechin-3-gallate (EGCG) maintains kappa-casein in its pre-fibrillar state without redirecting its aggregation pathway. *Journal of Molecular Biology,* 392(3), 689-700.

Khodarahmi, R., Soori, H., & Karimi, S. A. (2009). Chaperone-like activity of heme group against amyloid-like fibril formation by hen egg ovalbumin: Possible mechanism of action. *International Journal of Biological Macromolecules,* 44(1), 98-106.

Koudelka, T., Hoffmann, P., & Carver, J. A. (2009). Dephosphorylation of alpha(s)- and beta-caseins and its effect on chaperone activity: A structural and functional investigation. *Journal of Agricultural and Food Chemistry*, 57(13), 5956-5964.

Kundu, S., Chinchalikar, A. J., Das, K., Aswal, V. K., & Kohlbrecher, J. (2013). Fe^{+3} ion induced protein gelation: Small-angle neutron scattering study. *Chemical Physics Letters,* 584, 172-176.

Lai, S. K., Wang, Y., & Hanes, J. (2009). Mucus-penetrating nanoparticles for drug and gene delivery to mucosal tissues. *Advanced Drug Delivery Reviews,* 61(2), 158-171.

Liberek, K., Lewandowska, A., & Zietkiewicz, S. (2008). Chaperones in control of protein disaggregation RID F-5812-2011. *Embo Journal,* 27(2), 328-335.

Librizzi, F., Carrotta, R., Spigolon, D., Bulone, D., & San Biagio, P. L. (2014). alpha-Casein inhibits insulin amyloid formation by preventing the onset of secondary nucleation processes. *Journal of Physical Chemistry Letters,* 5(17), 3043-3048.

Machida, S., Ogawa, S., Shi, X. H., Takaha, T., Fujii, K., & Hayashi, K. (2000). Cycloamylose as an efficient artificial chaperone for protein refolding. *FEBS Letters,* 486(2), 131-135.

Maltais, A., Remondetto, G. E., Gonzalez, R., & Subirade, M. (2005). Formation of soy protein isolate cold-set gels: Protein and salt effects. *Journal of Food Science,* 70(1), C67-C73.

Marangoni, A. G., Barbut, S., McGauley, S. E., Marcone, M., & Narine, S. S. (2000). On the structure of particulate gels - the case of salt-induced cold gelation of heat-denatured whey protein isolate. *Food Hydrocolloids,* 14(1), 61-74.

Martins, J. T., Ramos, O. L., Pinheiro, A. C., Bourbon, A. I., Silva, H. D., Rivera, M. C., Cerqueira, M. A., Pastrana, L., Xavier Malcata, F., Gonzalez-Fernandez, A., & Vicente, A. A. (2015). Edible

bio-based nanostructures: Delivery, absorption and potential toxicity. *Food Engineering Reviews*, 7(4), 491-513.

McClements, D. J. (2015). Nanoscale nutrient delivery systems for food applications: Improving bioactive dispersibility, stability, and bioavailability. *Journal of Food Science*, 80(7), N1602-N1611.

Miti, T., Mulaj, M., Schmit, J. D., & Muschol, M. (2015). Stable, metastable, and kinetically trapped amyloid aggregate phases. *Biomacromolecules,* 16(1), 326-335.

Nicolai, T. & Durand, D. (2013). Controlled food protein aggregation for new functionality. *Current Opinion in Colloid & Interface Science,* 18(4), 249-256.

Remondetto, G. E. & Subirade, M. (2003). Molecular mechanisms of Fe^{2+}-induced beta-lactoglobulin cold gelation. *Biopolymers,* 69(4), 461-469.

Schwenke, K. D., Dahme, A., & Wolter, T. (1998). Heat-induced gelation of rapeseed proteins: Effect of protein interaction and acetylation. *Journal of the American Oil Chemists Society,* 75(1), 83-87.

Singh, P. K., Kotia, V., Ghosh, D., Mohite, G. M., Kumar, A., & Maji, S. K. (2013). Curcumin modulates alpha-synuclein aggregation and toxicity. *Acs Chemical Neuroscience,* 4(3), 393-407.

Smart, J. D. (2005). The basics and underlying mechanisms of mucoadhesion. *Advanced Drug Delivery Reviews,* 57(11), 1556-1568.

USDA, United States Department of Agriculture,
http://apps.fas.usda.gov/psdonline/circulars/oilseeds.pdf, (accessed December, 2013).

Visschers, R. W. & de Jongh, H. H. J. (2005). Disulphide bond formation in food protein aggregation and gelation. *Biotechnology Advances,* 23(1), 75-80.

Wan, Z., Guo, J., & Yang, X. (2015). Plant protein-based delivery systems for bioactive ingredients in foods. *Food & Function,* 6(9), 2876-2889.

Wanasundara, J. P. D. (2011). Proteins of *Brassicaceae* oilseeds and their potential as a plant protein source. *Critical Reviews in Food Science and Nutrition*, 51(7), 635-677.

Wang, J., Ho, L., Zhao, W., Ono, K., Rosensweig, C., Chen, L., Humala, N., Teplow, D. B., & Pasinetti, G. M. (2008). Grape-derived polyphenolics prevent A beta oligomerization and attenuate cognitive deterioration in a mouse model of Alzheimer's disease. *Journal of Neuroscience,* 28(25), 6388-6392.

Wu, J., Aluko, R. E., & Muir, A. D. (2008). Purification of angiotensin I-converting enzyme-inhibitory peptides from the enzymatic hydrolysate of defatted canola meal. *Food Chemistry,* 111(4), 942-950.

Wu, J. & Muir, A. D. (2008). Comparative structural, emulsifying, and biological properties of 2 major canola proteins, cruciferin and napin. *Journal of Food Science,* 73(3), C210-C216.

Yong, Y. H. & Forgeding, E. A. (2010). Caseins: Utilizing molecular chaperone properties to control protein aggregation in foods. *Journal of Agricultural and Food Chemistry*, 58(2), 685-693.

CHAPTER 2-Literature review

2.1. Canola

Canola plants belong to the Brassicaceae (Cruciferae) family, consisting of numerous species such as *Brassica napus* and *Brassica rapa*, commonly known as rapeseed (Aachary and Thiyam, 2012). Canola/rapeseed, with annual worldwide production of 70 million metric tons, ranks as the second most abundant source of seed oil (USDA, 2013; Aider and Barbana, 2011). Canola industry adds $ 19.3 billion to Canadian economy which has a great impact on the economy; more than 43,000 Canadian farmers are involved in this industry. The export of 75% of annual production brings over $ 9 billion to the economy (Saskatchewan canola development commission). The term "canola" specifically denotes rapeseed varieties containing less than 2% erucic acid in fatty acid profile of oil and less than 30 μmol/g glucosinolates in air-dried oil-free meal (Tan et al., 2011). Canola seeds contain over 40% oil, 17-26% protein, 20% carbohydrates and 16% miscellaneous low molecular weight compounds (Pinterits and Arntfield, 2008). The main applications of canola oil are cooking oil and margarine (Aachary and Thiyam, 2012). The by-product of oil extraction is a protein rich canola meal with up to 40% protein on a dry basis (Aider and Barbana, 2011). Canola proteins have high protein efficiency ratio with well-balanced amino acid composition (Tan et al., 2011; Wu and Muir, 2008). However, despite the high biological value, canola meal is currently used as livestock and aquaculture feed (Tan et al., 2011).

2.1.1. Canola proteins

Canola protein fraction is mainly composed of cruciferin and napin, constituting 60-65 and 20-25% of total protein, respectively (Wanasundara, 2011; Aachary and Thiyam, 2012). Cruciferin, a 12S legumin-type globulin, is soluble in dilute salt solutions and napin is a water soluble 2S albumin. In addition to cruciferin and napin, canola also contains some minor structural and metabolic proteins. Oleosins, basic proteins with low molecular weight (15-26 kDa), are structural proteins associated with oil bodies and constitute 2-8% of the total canola seed proteins (Huang, 1992; Ghodsvali et al., 2005). Several metabolic proteins such as lipid transfer proteins (LTP), protease inhibitors and Ca^{2+} dependant-calmodulin binding proteins have been also reported (Wanasundara, 2011).

Similar to other legumin proteins, cruciferin, with a well-organized level of primary, secondary, tertiary and quaternary structures, shows the most similarity to soy glycinin (Wanasundara, 2011).

Cruciferin is a 300 kDa glycoprotein with arabinose, glucosamine, mannose, galactose and inositol as the sugar moieties (Gill and Tung, 1978). Cruciferin is composed of 6 subunits, each containing a heavy α- (acidic, approximate Mw of 30 kDa) and a light β- (basic, approximate Mw of 20 kDa) chain which are linked by a disulfide bond (Figure 2.1) (Wanasundara, 2011).

The primary structure of cruciferin includes a hydrophilic zone of amino acids, rich in glutamic and aspartic acids and dominated by Gly-Gln repeats (Wanasundara, 2011; Schwenke et al., 1981). Canola cruciferin has a high content of non-polar side chains, which is responsible for its hydrophobicity compared to other seed storage 11/12S globulins including soy glycinin (Schwenke et al., 1981). Prakash and Rao (1986) reported that native globulin structure is mostly stabilized by hydrophobic interactions. Cruciferin isoelectric point (pI) of 7.2 indicates that this protein is a "neutral" protein while the other seed storage proteins are acidic in nature (Schwenke et al., 1981). The secondary structure of cruciferin is characterized by a noticeable content of random coils (58%), a low content of α-helix (11%) and a relatively high content of β-sheet (31%) conformations (Uruakpa and Arntfield, 2006). At the quaternary level, it is assumed that twelve acidic and basic subunits form six α-β pairs which assemble into two hexagonal rings (Badley et al., 1975; Derbyshire et al., 1976). The hexameric structure of cruciferin shows reversible dissociation/association phenomena due to changes in pH and ionic strength (Wanasundara, 2011). When ionic strength decreases to lower that 0.5 M, the hexameric structure of cruciferin reversibly dissociates into trimers (Schwenke et al., 1981). Oligomeric cruciferin dissociates into 50 kDa α-β pairs in the presence of 8M urea and further to monomeric peptides if SDS is also present (Schwenke et al., 1981). However, high pressure treatments can denature and associate cruciferin, and form soluble aggregates which might be responsible for better gelling properties compared to the heat-denatured protein (He et al., 2014).

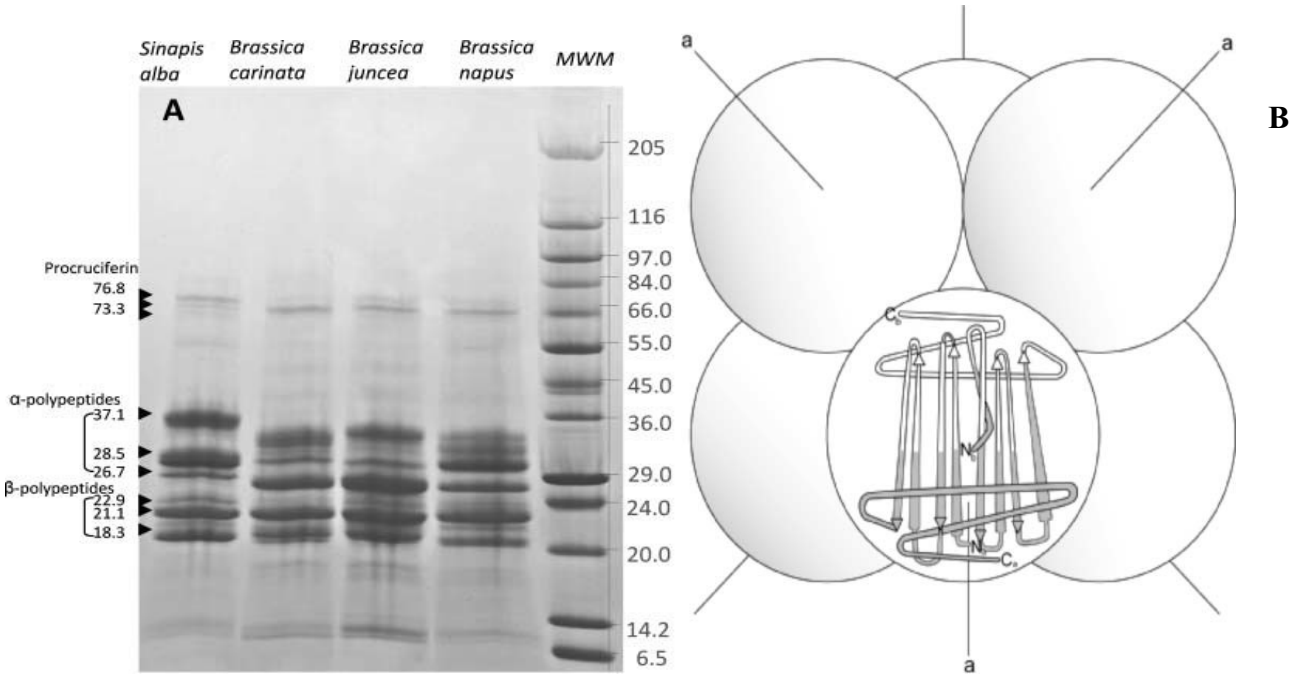

Figure 2.1. SDS PAGE pattern (under reducing conditions) of cruciferin extracted from four species of *Brassicaceae* (A) and pseudoradial-symmetrical arrangement of cruciferin (B). Hypothetical arrangement of α and β chains in each subunit within the hexameric molecule is shown. N and C designate the N- and C- terminal regions, respectively, of α and β chains (e.g., Nα, Nβ, Cα, and Cβ). (Reprinted from Wanasundara, 2011 with permission)

Napin is an alkaline protein with an isoelectric point of ~11. It is a 2S albumin protein composed of two subunits with MW of 4.5 (small) and 10 (large) kDa, respectively (Barciszewski et al., 2000). The polypeptide chains in napin are stabilized by two inter-chain disulfide bonds and two intra-chain disulfide bridges, formed by the eight cysteine residues (Shewry et al., 1995). Napin, in its secondary structure, contains 40-46% α-helices, 11-16% β-sheets and 41-43% random coil structures (Figure 2.2) (Prakash and Rao, 1986). Its three dimensional structure is composed of three α-helices of large subunit form a cleft in which two helices of small subunit fit properly (Barciszewski et al., 2000).

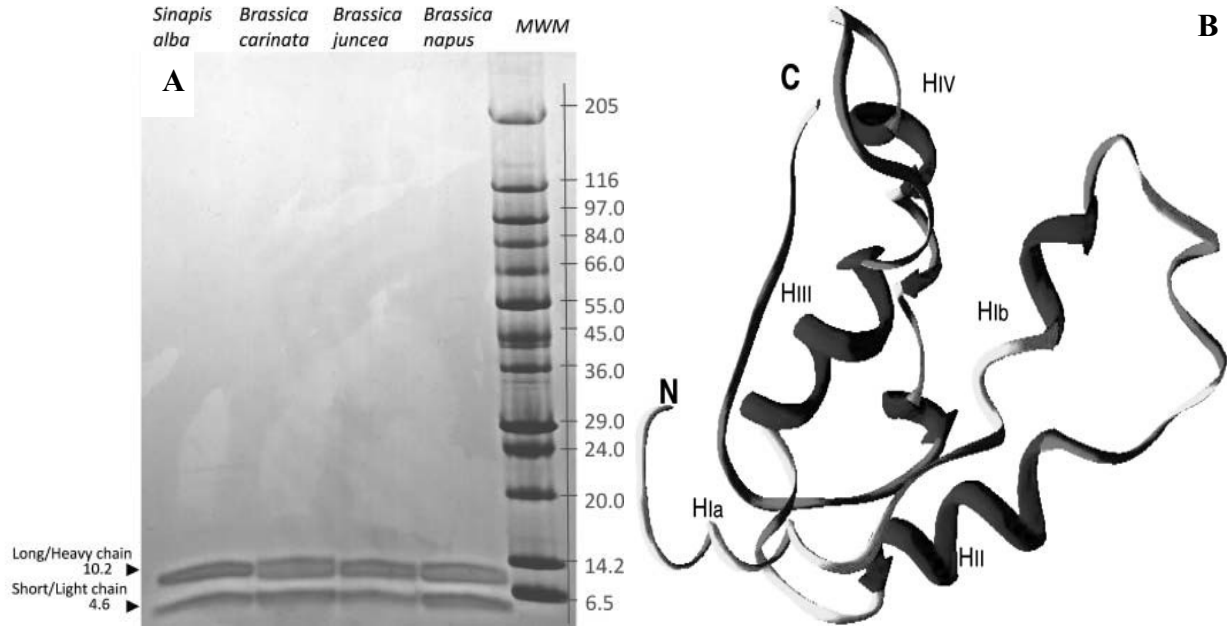

Figure 2.2. SDS PAGE pattern (under reducing conditions) of napin extracted from four species of *Brassicaceae* (A) and schematic ribbon representation of *B. napus* napin (B). The N indicates NH2- and C indicates COOH terminal. The HIa and HIb, HII, HIII and HIV indicate Helix I, Helix II, Helix III and Helix IV, respectively. (Reprinted from Wanasundara, 2011 with permission)

As the major canola proteins, both cruciferin and napin have good functional properties. Cruciferin, with good emulsifying, gelling and binding properties, can be used in meat, dressing and baked products (Mejia et al., 2009). Emulsification capacity of canola protein isolate is comparable to egg proteins (Yoshie-Stark et al., 2008). For instance, canola protein and its hydrolysates have been used as egg yolk substitutions in salad dressings (Aluko and McIntosh, 2005). The functional properties of canola proteins can be further improved by enzymatic hydrolysis (Cumby et al., 2008), succinylation (Paulson and Tung, 1988), acylation (Gruener and Ismond, 1997), or adding hydrocolloids (Arntfield and Cai, 1998). Their application has also extended to non-food uses such as natural adhesives, bio-foams and bio-plastics (Wu and Muir, 2008; Yoshie-Stark et al., 2008; Marczak et al., 2003; Xu and Diosady, 2000). However, the wide range of isoelectric points (pH 4 to 11) and molecular weights (13 to 320 kDa) decrease the efficiency and yield of protein extraction (Aachary and Thiyam, 2012). Furthermore, the presence

of antinutritional compounds such as glucosinolates, phenolics and phytic acid has restricted the utilization of canola protein isolate (Lacki and Duvnjak, 1998).

2.1.2. Removal of antinutritional compounds

Removing the undesirable compounds from canola protein extracts is challenging. In canola meal, phenolics are mainly present as free sinapic acid and sinapic acid esters that form complexes with proteins by hydrogen, covalent and ionic bonding, and hydrophobic interactions (Xu and Diosady, 2000). Phenolic compounds contribute to dark color and unpleasant bitter taste as well as reduced nutritional availability of essential amino acids. To remove phenolic compounds from canola meal, different methods have been employed including organic solvent, reducing and oxidizing agents, dilute alkali or acids condition, insoluble polyvinylpolypyrrolidone (PVP), activated carbon and ion exchange extraction methods. Most of these methods have drawbacks that might lead to protein loss, increase in phytic acid content and traces of organic solvents in protein product (Xu and Diosady, 1997). As an example, treatment of canola with methanol/ammonia/water mixture removed 70-80% of phenolic acids and 67-96% of condensed tannins originally present in the seeds, but the phytate content of extracted protein increased due to the dissolution of some polar constituents of the seed into methanol/ammonia (Shahidi et al., 1990).

Phytic acid, as an antinutritional compound, can bind mineral ions and reduce their bioavailability. Treatment with $CaCl_2$ and phytase (in acidic condition), chelating agents such as EDTA (in basic pH) and using variable pHs are some methods proposed to remove phytic acid from canola meal. Serraino and Thompson (1984) and Newkirk and Classen (1998) reported that phytase treatment totally removed phytic acid with negligible protein loss (Serraino and Thompson, 1984; Newkirk and Classen, 1998). Gillberg and Tornell (1976) showed that pH could play a key role in removing phytic acid from the meal (Gillberg and Tornell, 1976). However, the influence of pH on extractability of phytic acid is complicated. In an acidic medium, as both proteins and metal ions are positively charged, there is a competition between proteins and metal ions to form phytate complexes. Around neutral pH range (from 5 to 9), a ternary phytic acid-cation-protein complex is formed, leading to increased extractability of both protein and phytic acid (Tzeng et al., 1990); adding chelating agents, however, can remove cations, disrupt the complex, and therefore prevent the formation of the protein-phytate complex (Serraino and Thompson, 1984). At increasing pHs from 10 to 12, protein-phytic acid complexes become instable and the solubility of phytic acid

decreases because the number of positive charges in protein molecules decreases substantially (Gillberg and Tornell, 1976).

Glucosinolates, a group of antinutritional compounds, also present in rapeseeds; and nine different glucosinolates have been identified in two varieties of *B. napus* and *B. rapa* (Bell, 1993). Glucosinolates have displayed goitrogenic effect in animal studies (Sorensen, 1990). Canola meal contains 18-30 µmol glucosinolates /g meal (Tan et al., 2011). A two-phase solvent extraction method removed the majority of glucosinolates (Naczk et al., 1985). Since these antinutritional compounds have lower molecular weights compared to canola proteins, ultrafiltration can substantially remove them from protein isolates (Ser et al., 2008).

2.1.3. Canola protein extraction

2.1.3.1. Alkali extraction

Canola oil is extracted from crushed canola seeds by mechanical extraction in combination with solvent extraction (Wanasundara, 2011). The defatted meal is dried and then ground to small particles. Grinding increases the interaction of the meal with solvent to enhance protein release (Aluko and McIntosh, 2001). Alkaline extraction is the most common method used for canola proteins. In this method, defatted canola meal is stirred with an alkaline solution and then centrifuged to recover the solubilized proteins (Tan et al., 2011). The pH of supernatant is adjusted by dilute acid and then centrifuged to separate the precipitated proteins. The most typical alkaline solution used for protein extraction is sodium hydroxide (NaOH) which produces strong alkaline condition (pH 11 to 12) to ensure high protein solubilization. Although NaOH solution results in high extraction yield, the protein isolate has a dark color due to oxidation of phenolic compounds. Tzeng et al. (1990) reported that addition of 10% sodium sulphite (Na_2SO_3) inhibit oxidation of phenolic compound and reduce the dark color. Other alkaline solutions such as sodium hexametaphosphate have also been reported. It improves the product color and taste but a lower extraction yield was obtained compared to NaOH extraction (Tzeng et al., 1990). Isoelectric precipitation is conducted by using hydrochloric or acetic acid solution to reach to isoelectric point (Klockeman et al., 1997; Tzeng et al., 1990). Ghodsvali et al. (2005) precipitated canola proteins in a wide pH range (3.5 to 7.5) and concluded that optimum pH range for extraction is 4.5-5.5. Calcium chloride also increased the protein content by reducing phytates in the final product; the

higher yield of soluble proteins was due to the salting in effect (Tzeng et al., 1990; Tan et al., 2011; Ghodsvali et al., 2005; Aluko and McIntosh, 2005).

2.1.3.2. Protein Micellar Mass (PMM) method

Canola seed proteins are globulins which have high solubility in dilute salt solutions. Increasing ionic strength improves the solubility of cruciferin and napin due to the salting in effect (Wanasundara, 2011). In the PMM method, canola proteins are first solubilized by salt solution (Tan et al., 2011) and then antinutritional compounds are removed from the protein slurry using ultrafiltration (Tzeng et al., 1990). Membrane filters with 50 kDa MW cutoff effectively separated antinutritional compounds from canola proteins (Wanasundara, 2011). The retentate, which contains purified canola proteins, are diluted with cold water. Dilution reduces the ionic strength resulting in protein precipitation and thus protein micelles are formed (Tan et al., 2011; Wanasundara, 2011). The last step is to recover proteins by centrifugation. Despite reducing the content of antinutritional compounds in the protein isolate, the overall protein yield of the PMM method is lower than the alkaline extraction (Owen et al., 1971; Ismond and Welsh, 1992).

Therefore, canola proteins can be extracted with high purity and low cost, and due to the appropriate functional properties and abundance, they have great potential in various new food/non-food applications. Cruciferin, a resistant canola protein to gastric enzymes (Bos et al., 2007), can be used as a biopolymer-based carrier for encapsulation and delivery of bioactive compounds.

2.2. Encapsulation of bioactive/nutraceutical compounds

2.2.1. Importance of encapsulation

In recent years, there has been considerable interest in improving human health and wellbeing. Bioactive compounds including vitamins, probiotics, bioactive peptides and antioxidants play important roles in human metabolism making them essential for health. Most bioactive compounds are susceptible to pH, oxygen, light, high temperature and pro-oxidants in food processing and storage, and also digestive conditions in gastrointestinal tract. Encapsulation, as a protective method, can prevent degradation of the compounds and maintain their natural functional form and bioactivity (McClements, 2012a; McClements, 2015).

Poor solubility of some bioactive compounds restricts their direct incorporation into aqueous food products. Some examples of these compounds are ω-3 oils, phytosterols, carotenoids, curcumin, and oil-soluble vitamins. Many lipophilic compounds have low bioavailability due to poor solubility in biological fluids which results in poor bio-accessibility, a low absorption rate and transformation in body fluids. Particle matrix, encapsulating oil-soluble compounds, should have water soluble functional groups on the surface to ensure good water dispersability (McClements, 2015). Interaction of bioactive compounds with other food components might lead to instability and lower nutritional value of the whole product. Furthermore, some of the nutraceutical compounds such as omega-3 fatty acids have an unpleasant off-flavor which needs to be masked when incorporated in food formulations (McClements, 2013). Unpleasant appearance and mouthfeel, which could result from the high melting point of the components, also restrict their incorporation into food products (McClements, 2012b). For all these reasons, encapsulation is finding increasing utilization in functional food industry to protect, deliver and release susceptible bioactive compounds (Joye et al., 2014).

Over the past decade, significant progress has been made using encapsulation of bioactive compounds to improve their stability and bioavailability (Sagalowicz and Leser, 2010; Velikov and Pelan, 2008). For instance, oral bioavailability of encapsulated folic acid in casein particles increased 50% compared to its free form (Penalva et al., 2015). Similarly, relative bioavailability of curcumin increased by 47.7 times when it was encapsulated in the artificial oil bodies (Chang et al., 2013). Apparent permeation rate of encapsulated epigallocatechin gallate in chitosan particles was also ~ 4 times higher than that of unencapsulated form (Hu and Huang, 2013). Controlled-release encapsulation systems are able to improve absorption rate and ensure safe transfer to the target tissues (McClements and Xiao, 2014).

2.2.2. Nano-carrier systems

Among various encapsulation and delivery systems, nanostructure-based systems have attracted the most attention. The main advantages of the nano-based delivery systems include significant increase in surface area and improved stability and bioavailability of the encapsulated compound. Larger surface area might improve drug solubility. For instance, orally administered 120-nm nanoparticles showed 5-fold higher bioavailability in comparison with 5.5-μm particles (Wu et al., 2004). In a similar way, solid lipid nanoparticles (SLN) improved the stability of poorly soluble

compounds by 2- to 25-fold (Harde et al., 2011). Nanocarriers have also the advantage of improving drug uptake via different routes which will be explained in detail in following sections.

2.2.3. Nanoparticle fabrication methods

Nanoparticles can be prepared using a wide range of methods which can be classified in two general approaches; top-down and bottom-up approach. Some methods are a combination of these two approaches (McClements, 2015).

2.2.3.1. Bottom-up approach

In bottom-up approach, small particles are formed by spontaneous assembly of molecules under proper conditions. Micelles and microemulsions are some examples of bottom-up approach (Patel and Velikov, 2011; Garti and Aserin, 2012). In biopolymer-based systems, particle-forming biopolymers are dissolved in an appropriate solvent and then injected in an anti-solvent (in which the biopolymer has poor solubility). The biopolymer molecules interact each other to form small particles. In case of protein nanoparticles, a solution of globular proteins is heated up to a temperature higher than its denaturation temperature. The thermal treatment dissociates the quaternary structure of globular proteins and unfolds the secondary and tertiary structures facilitating hydrophobic association and cross-linking which lead to particle formation. The solution conditions such as pH and ionic strength should be precisely controlled to obtain proper electrostatic interactions between molecules (Jones and McClements, 2010). Small hydrogels composed of cross-linked proteins and polysaccharides may be also formed through these bottom-up approaches (Jones and McClements, 2011).

2.2.3.2. Top-down approach

Nanoemulsions and solid lipid nanoparticles are some examples of nanoparticles prepared by the top-down approach. Emulsions are initially formed in macroscopic scale and then broken down to nano-scale particles using homogenizers. Strong shearing force is applied during homogenization to disrupt large-sized emulsions and form new surfaces which are immediately covered by emulsifier molecules (McClements and Rao, 2011).

2.2.4. Nanoparticle composition

Along with recent developments in nanotechnology, nanoparticles have also found applications in food industry. Nanoparticle-based colloidal delivery systems have been reported for many nutraceutical compounds (McClements et al., 2009).

Nanoparticles are fabricated from various food components such as lipids, proteins and polysaccharides individually or in combinations (Joye et al., 2014). Each component has unique physicochemical properties and thereby, forms particular interactions with the micronutrient. Nanoemulsions and solid lipid nanoparticles are mainly composed of oil and water which form emulsion in the presence of an emulsifier (McClements and Rao, 2011; McClements, 2012a). Micelles are fabricated spontaneously from small surfactants in aqueous solutions (Garti and Aserin, 2012). To achieve a successful delivery system, proper selection of particle-forming food component and understanding the possible interactions with the nutraceutical compound are important (Joye et al., 2014).

2.2.5. Protein-based nanoparticles

Food proteins have been widely used as nanoparticle-forming biopolymers due to their exceptional properties, e.g. biodegradability, nutritional value and gel-forming capacity (Chen et al., 2006; Elzoghby et al., 2012b). Proteins possess various functional groups which can form a wide range of interactions with the core compound (nutraceutical or vitamins) to hold, protect and release it under proper conditions (Elzoghby et al., 2011). Furthermore, multiple functional groups on protein surface can be modified to enable specific binding and responsive release at target site (Elzoghby et al., 2012a).

One of the most important functional properties of food proteins in particle formation is gelation. Proteins can form gel networks with diverse mechanical and physicochemical properties (Chen et al., 2006). Recent studies have revealed that protein nanoparticles can protect susceptible encapsulated compounds and release them slowly, thus enhancing their bioavailability. Some protein-based nanoparticles also successfully delivered the drug to brain, macrophages and liver cells. For example, collagen nanoparticles improved transdermal drug delivery. Gliadin and lectin-coated nanoparticles are proved to have mucoadhesive property (Elzoghby et al., 2012b; Maham et al., 2009).

Protein hydrogels are the most common protein-based nanodelivery systems (Chen et al., 2006). Their unique characteristics, such as soft tissue biocompatibility, well-dispersability of drugs in gel matrix and high degree of responsive release, have made them very efficient in drug delivery studies (Elzoghby et al., 2011).

2.2.5.1. Animal proteins

Animal proteins such as casein and whey protein have been widely studied as hydrogel matrix. These proteins have several advantages over synthetic biopolymers, such as high nutritional value, higher absorption rate and lower toxicity of the intact protein and its degradation products (Elzoghby et al., 2011; Leo et al., 1997). Casein was used in encapsulation of hydrophobic micronutrients such as vitamin D and polyunsaturated fatty acids, while β-lactoglobulin nanoparticles showed promising results for curcumin and resveratol (Wan et al., 2015).

2.2.5.2. Plant proteins

Although plant-based food products have been the main part of our diet for thousands years, plant proteins have attracted more attention in last decades as a substitute for animal proteins. Plant proteins are mostly the by-product of oil, starch or other plant-based valuable compounds (Wan et al., 2015). Recent studies have revealed excellent functional properties of some plant proteins such as soybean and wheat proteins. Additionally, plant proteins have been utilized in fabrication of carriers for nutraceutical compounds (Reddy and Yang, 2011; Nesterenko et al., 2013). In contrast to hydrophilic nature of animal proteins, plant proteins are relatively more hydrophobic which makes them a potential matrix for delivery of hydrophobic micronutrients. Owing to their hydrophobic nature, the plant-based nanoparticles do not require further hardening step using chemical cross-linkers (Chen et al., 2006; Reddy and Yang, 2011; Ezpeleta et al., 1996; Elzoghby et al., 2012b). Furthermore, the plant protein-based nanoparticles provide a great opportunity for production of functional food for vegan diets (Tergesen, 2010).

2.2.6. Protein hydrogels

Hydrogel is an infinite network of hydrophilic biopolymer that holds a large amount of water in its three-dimensional structure (Qiu and Park, 2001). The network is formed and stabilized by cross-linking chains. Covalent bonds, hydrogen bonding, hydrophobic interactions and physical entanglements might be involved in biopolymer cross-linking (Kamath and Park, 1993). The gel network is able to entrap sensitive molecules in its open structure and protect them from severe

surrounding environment. Protein gels can be formed through different mechanisms. Heat gelation is the traditional way of gel formation in which a thermal treatment unfolds the polypeptide chain and exposes the buried hydrophobic residues (Aguilera, 1995; Twomey et al., 1997). The newly-exposed groups encourage self-aggregation of unfolded chains that leads to a three-dimensional network holding capillary water in its micro-structure (Aguilera, 1995; Twomey et al., 1997).
Despite its simplicity in preparation, thermal gel is restricted to encapsulate heat-stable compounds (Lefevre and Subirade, 2000). In order to entrap heat-sensitive compounds in a gel structure, cold gelation method is preferable to avoid heat damage to the encapsulated compounds.

2.2.6.1. Cold gelation

In cold gelation method, protein solution is preheated and then gelation is triggered by promoting attractive forces either by adjusting pH or adding multivalent ions (Chen et al., 2006). Heating the protein solution above its thermal denaturation temperature unfolds the protein to form soluble aggregates (Duval et al., 2015). Preheating step should be performed at low ionic strength and pH away from isoelectric point. In this condition, strong repulsion forces between the proteins molecules keep them separated in a linear conformation (McClements and Keogh, 1995). In the second step, gelation is induced by increasing attractive forces between protein chains. It can be carried out by adding multivalent ions or other biopolymers with opposite charges to the protein. Multivalent ions shield the surface charges and act as cross-linkers to form a network of soluble protein aggregates (Figure 2.3) (Maltais et al., 2008). The heat-sensitive nutraceutical compound is added before the gel network is set. In the cold gelation method, nanoparticles are formed without organic solvents and thermal treatment which reduces the risk of heat destruction of micronutrients. Additionally, the size of nanoparticles can be precisely controlled by different conditions of pH, ionic strength and temperature (McClements, 2013).
Cold gelation was first applied in preparation of whey protein gels (Barbut and Foegeding, 1993). Further studies were conducted to study the effect of different salts, pHs, ageing time and additives such as sucrose on gelation rate and gel strength of whey proteins (Bryant and McClements, 2000; Kulmyrzaev et al., 2000; Cavallieri and Da Cunha, 2008). Bryant and McClements (2000) introduced calcium chloride as a more effective salt in forming stronger gels compared to sodium chloride. It was attributed to the greater shielding power of divalent calcium ions compared to monovalent sodium ions. Positive ions are able to shield the negative charges on protein chains and reduce the repulsive forces between chains (Yasuda et al., 1986). More importantly, calcium

ions form salt bridge cross-links among negatively charged carboxylic acid groups on protein chains (Bryant and McClements, 2000).

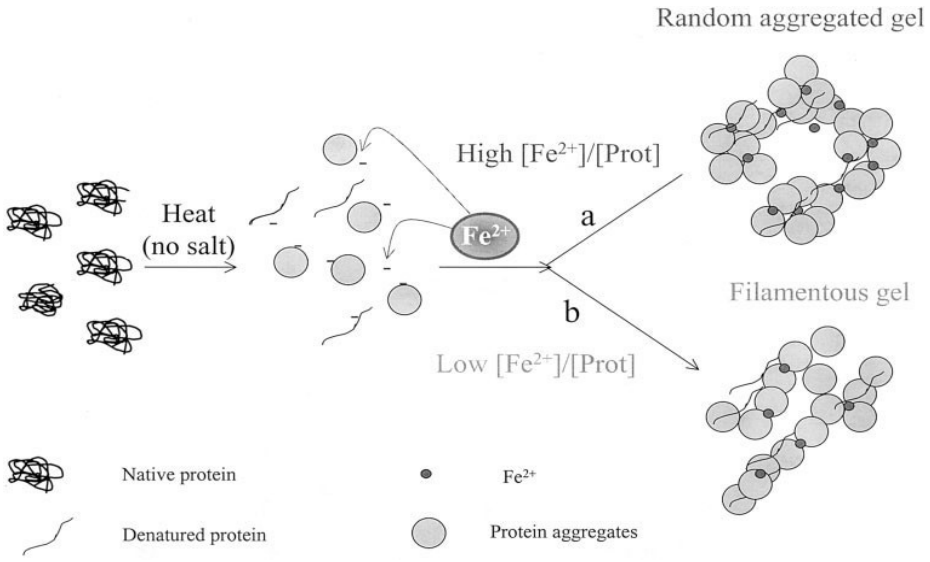

Figure 2.3. Mechanisms of denaturation/aggregation and cold-gelation of proteins (Reprinted from Remondetto and Subirade, 2003 with permission)

To study the effect of pH on whey protein gelation, Cavallieri and Da Cunha (2008) have shown that acidification rate influences the development of gel network through bond enforcing and chain re-arrangements. Slow acidification gives enough time to protein chains to interact and organize into a network. However, under fast acidification rate, molecular interactions are delayed until the final pH is achieved (Cavallieri and Da Cunha, 2008). Effect of sucrose before adding $CaCl_2$ was studied in cold gelation of whey proteins. At low concentrations of sucrose, gelation rate was decreased due to the increasing viscosity. But at higher concentrations of sucrose, protein-protein aggregation was facilitated because sucrose molecules compete for the hydration water with protein chains (Kulmyrzaev et al., 2000).

Cold gelation mechanism of soy protein was also investigated by Maltais et al. (2005). Soy proteins are globular proteins which are denatured and aggregated by preheating. In the second step, calcium ions induce gel network formation by cross-linking the protein chains. Concentration of calcium ions is the key factor which determines the gel type and its mechanical properties. At a concentration of calcium (10 mM), the protein surface charge is not totally shielded by calcium ions, thus, aggregation occurs with linear proteins leading to filamentous gels. However, at a

higher concentration of calcium ions (20 mM), all surface charges are neutralized by calcium ions which results in random aggregation of proteins and a particulate gel is formed. This method has also been used for preparing gel-like soy protein emulsions (Tang and Liu, 2013), whey protein micro-beads for delivery of probiotics (Doherty et al., 2011), ion-induced whey protein aerated gels (Tomczynska-Mleko, 2013), and whey protein/alginate hydrogel microparticles for oral delivery of insulin (Deat-Laine et al., 2013).

2.2.6.2. Protein-Polysaccharide complex hydrogels

One of the main advantages of the cold gelation method is that proteins can form cold-set gel individually or in combination with other biopolymers. Fabrication of complexes between proteins and polysaccharides provides more opportunities for controlling nanoparticles characteristics. Proteins and polysaccharides have electrostatic charges at various pHs. Protein net charge varies from positive to negative when pH increases from below to above its isoelectric point. Polysaccharides have more uniform monomers which can be anionic, cationic or non-ionic depending on the pKa value of the ionizable groups (Jones and McClements, 2010). At pHs above its pK_a value, the polysaccharide has negative charges, but it loses its negative charge as the pH decreases to below the pK_a value. Each polysaccharide has one type of ionizable group which could be anionic (carboxylate and sulfates) or cationic (amines) (Ridley et al., 2001). Pectins and carrageenans are anionic polysaccharides (containing carboxylates and sulfates, respectively) and chitosan is a cationic polysaccharide (contains amines) (Piculell, 1995; Kurita, 2006; Rinaudo, 2006).

Association of proteins and polysaccharides may occur at the pH range where these biopolymers have opposite charges. Thus, at pHs well above pI, protein and polysaccharide do not associate due to strong repulsion forces between chains. As the pH decreases to slightly above pI, although the protein net charge is negative, soluble complexes are formed by electrostatic attraction between cationic residues on protein and anionic groups of polysaccharide molecule (Gao et al., 1997; Jones et al., 2010). Further pH reduction leads to stronger complex formation due to coacervation or precipitation (de Kruif and Tuinier, 2001; Schmitt et al., 1998; Turgeon et al., 2003; Turgeon et al., 2007). Physicochemical characteristics of the complex and its formation depend on the protein and polysaccharide molecular properties as well as the solution condition such as temperature and ionic strength (Hattori et al., 2000; Seyrek et al., 2003; Aachary and Thiyam, 2012; Wang et al., 2007). When a protein is associated with a polysaccharide, its thermal features such as unfolding

and aggregation kinetics might be influenced. For example, a complex of a globular protein, ovalbumin, with a cationic polysaccharide, chitosan, resulted in nanoparticles with higher stability to pH changes (Yu et al., 2006). Similar results were obtained for β–lactoglobulin/chitosan and β–lactoglobulin/pectin complexes formed at pH 5 (Jones et al., 2009).

Chitosan is a derivative of chitin, a biopolymer of N-acetylglucosamine which can be found abundantly in nature. Chitosan is a positively charged biopolymer (pK_a 6.2-7.0) at low pHs where amino groups (NH_3^+) are protonated (Shahidi and Abuzaytoun, 2005). Owing to its biocompatibility, biodegradability, non-toxicity, low immunogenicity and mucoadhesive property, its application in nanoparticles fabrication is remarkably increasing (Chuah et al., 2009). However, it degrades in acidic condition of stomach restricting its application in oral delivery. Therefore, chitosan has been successfully used in complexation with various negatively charged biopolymers such as β-lactoglobulin (Chen and Subirade, 2005), carboxymethyl cellulose (Ichikawa et al., 2005), lecithin (Sonvico et al., 2006) and dextran sulfate (Schatz et al., 2004). Lee et al. (2012) coated the chitosan nanoparticles with denatured β-lactoglobulin and reported improved resistance to acid condition and pepsin digestion of stomach. The coated-nanoparticles were degraded by intestinal pancreatin leading to sustained release of the encapsulated compound (Aachary and Thiyam, 2012; Lee et al., 2012). Similar release pattern was obtained from complex nanoparticles developed from carboxymethyl chitosan and soy protein isolate (Teng et al., 2013). After encapsulation of bioactive compounds, release and absorption of the compounds in the body, as the main objectives of delivery systems, should be studied.

2.3. Oral administration of bioactive compounds- Delivery challenges in GI Tract

Oral administration is the most predominant route of drug delivery due to its non-invasive nature. It offers many advantages over injection such as being painless and self-administrable resulting in more patient compliance (Bernkop-Schnuerch, 2013). Additionally, it reduces the risk of contamination (des Rieux et al., 2006). In oral administration, gastrointestinal (GI) tract is in direct contact with the ingested material. GI tract, with a large surface area, is particularly important in drug delivery because of its high potential to absorb micronutrients and bioactive compounds (Thanki et al., 2013). In addition to the above advantages, site-specific delivery to certain locations of GI tract can be used for treatment of some GI tract disorders such as gastric and duodenal ulcers, GI infections and gastric and colon cancers (Martins et al., 2015).

2.3.1. Harsh conditions of GI tract

Nanocarriers encounter different physiological and morphological barriers in their passage through GI tract. These barriers include the harsh acidic condition in stomach, digestive enzymes in gut lumen and brush border membrane, the mucus layer and particles transport across epithelial cells (Ensign et al., 2012). In the upper part of GI tract, nanostructures enter the stomach where they are mixed with gastric lipase and protease which trigger the digestion. Strong acidic condition changes the physicochemical characteristics of nanostructures such as their charge and ionic composition (McClements and Xiao, 2012). The gastric digestion also includes peristalsis moves arising from wall contractile waves which force the stomach contents to move forward (Kong and Singh, 2010). As the structures reach to small intestine, they meet a mixture of pancreatin, bile salts, phospholipids and bicarbonates which increase the pH of lumen content. Pancreatic lipases release free fatty acids from triacylglycerols and produce monoacylglycerols. Proteases hydrolyze proteins into peptides and amino acids. In addition to the enzymatic digestion, nanostructures may experience aggregation due to the changes in pH and ionic strength (Martins et al., 2015).

2.3.2. Transit time in GI tract

In oral administration of encapsulated bioactive compounds, the majority of particle carriers associate with chyme and transit directly through GI tract and then fecal elimination. However, 2-6 hours transit time in small intestine might be inadequate for some particles to release their encapsulated compounds. The low release of bioactive compounds leads to poor absorption and low bioavailability. To overcome the negative effect of the short transit time, many studies focused on improving particles association to mucus. This phenomenon, known as mucoadhesion, increases the ability of the particles to adhere to the mucus layer. Mucoadhesion slows the particle transit and prolongs particle residence time to the time scale of mucus renewal; as a result, the concentration of released compounds and their absorption increases. Coating nanoparticles with bioadhesive materials can improve the mucoadhesion property of the carrier system (Mikos et al., 1991; Lai et al., 2009b; Smart, 2005).

2.3.3. Mucus barrier

Mucus is a semipermeable barrier, providing protection over a broad surface of living cells in the epithelia. Mucus exchanges nutrients, water, gases, odorants and hormones, but hinders most

bacteria and pathogens from entry into the body. Mucus contains mainly water (>95%) and mucins (Cone, 2009). Mucus viscoelasticity, an important factor in delivery of drugs through mucus, is influenced by pH, mucin to water ratio, and varying lipid and ion contents (Lai et al., 2009b). Mucus layer protects the GI epithelium against hydrochloric acid, proteases, exogenous pathogens and toxins (Cone, 2009). Additionally, mucus facilitates the passage of chyme (partially digested food) through GI tract by lubricating the GI epithelium (Boegh and Nielsen, 2015).

Although mucoadhesion is a promising approach to increase the bioavailability of bioactive compounds, the transit time of these systems is determined by the physiological turnover time of the mucus layers. Since the intestinal mucus turnover time is between 50 and 270 minutes, mucoadhesive nanoparticles are not expected to adhere for more than 4-5 hours (Galindo-Rodriguez et al., 2005; Lai et al., 2009a). As a result, although mucoadhesion systems are relatively effective approaches in increasing particle residence time and release, the penetration of the particles through the mucus layers and reach to epithelia cells are limited.

Using mucus-penetrating nanoparticles is a relatively new strategy to overcome the mucus barrier. To penetrate through mucus layer, nanoparticles must be small enough to avoid steric hindrance by the dense fiber mesh and they should not adhere to mucin fibers (Cone, 2009; Lai et al., 2009a). Lai et al. (2007) revealed that 500-nm particles, if coated with a muco-inert polymer, can quickly traverse the mucus layer with diffusivity as much as 4-fold reduction compared to their rates in pure water. The particles were actually synthesized by mimicking the surface properties of viruses which allow them to avoid mucoadhesion. The viruses are densely coated with both positively and negatively charged functional groups, leading to a densely charged yet net neutral surface (Lai et al., 2007; Lai et al., 2009a). Comparison between conventional mucoadhesive particles and mucus-penetrating particles showed that penetrating particles readily penetrate the luminal mucus layer (LML) and enter the underlying adherent mucus layer (AML) while mucoadhesive particles are largely immobilized in the LML(Lai et al., 2009a) (Figure 2.4).

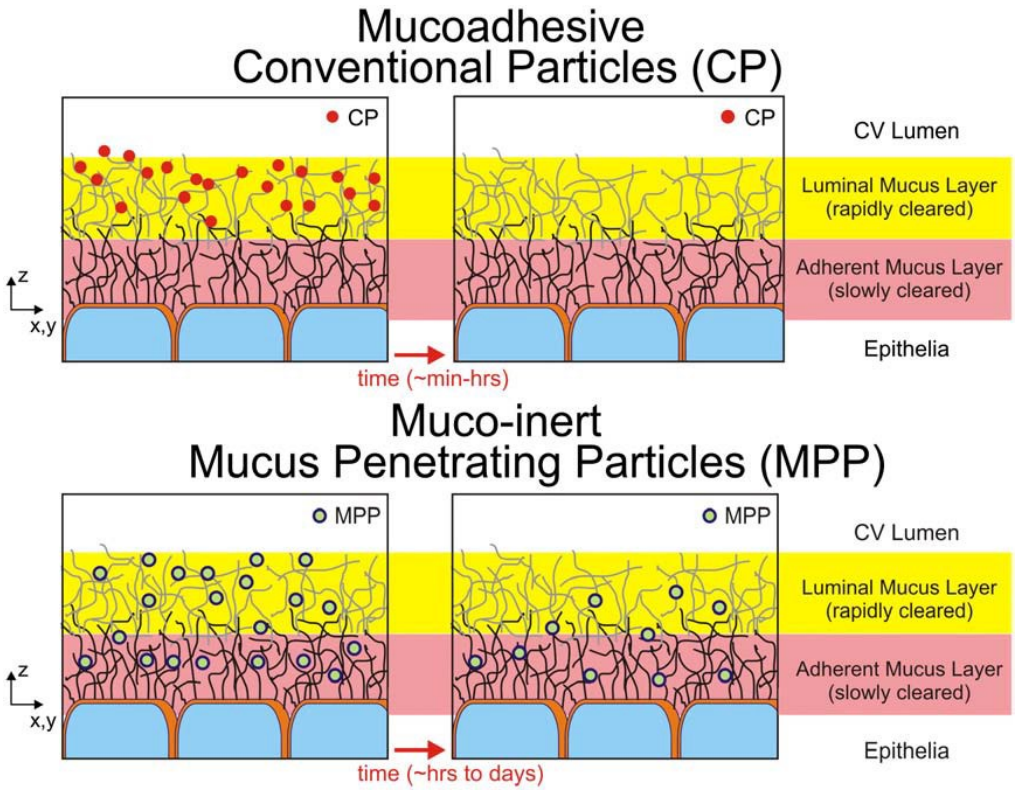

Figure 2.4. Summary schematic illustrating the fate of mucus-penetrating particles and conventional mucoadhesive particles administered to a mucosal surface (Reprinted from Lai et al., 2009a with permission)

2.3.4. Transport across intestinal epithelial cells

Intestinal mucosa includes several layers: a thin layer of smooth muscle cells (muscularis mucosae), connective tissue (lamina propria) and the epithelium (Shen, 2009). Encapsulated compounds have to cross the epithelium to reach the capillary network in the lamina propria and then enter the circulation system. The epithelium is a cell monolayer covered by mucus and located into crypts and villi with microvilli. The tight junctions between the epithelial cells are responsible for the tightness of the epithelium. The absorptive enterocytes is the major cell type in the epithelium; goblet cells, the second abundant epithelial cell type, secrete the mucus (Shen, 2009). Due to the absence of goblet cells in the stomach, stomach mucus is secreted by mucous cells. Less abundant cell types of the small intestine include Paneth cells, enteroendocrine cells and phagocytotic M cells (Boegh and Nielsen, 2015).

Since macro- and microparticles are too large to pass through epithelium, these structures must release their encapsulated bioactive compounds in the GI tract. However, nanoparticles can be taken up and traverse the intestinal barrier (Martins et al., 2015).

A macromolecule or a nanoparticle can theoretically cross the intestinal epithelium through paracellular and/or transcellular routes. Transport by paracellular route is mainly passive infusion across tight junctions, whereas transcellular pathway includes passive diffusion and active endocytosis transport mechanisms. Endocytosis pathways include clathrin–mediated endocytosis, caveolae-mediated endocytosis, macropinocytosis, and clathrin-, caveolin-independent endocytosis (Figure 2.5) (Sahay et al., 2010; Wang et al., 2015).

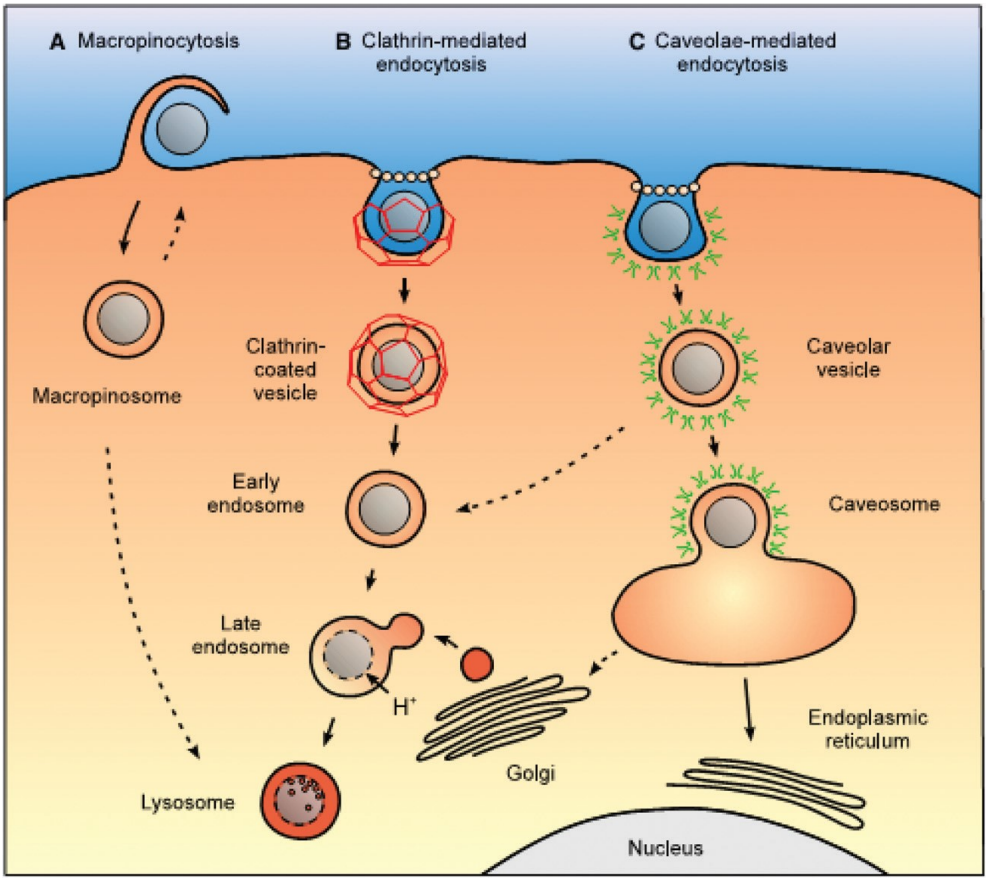

Figure 2.5. Intracellular nanocarrier trafficking following macropinocytosis, clathrin-mediated endocytosis and caveolae-mediated endocytosis (Reprinted from Hillaireau and Couvreur, 2009 with permission)

Clathrin–mediated endocytosis is the "classical route" of cellular entry, which is present and inherently active in all mammalian cells. It is the main uptake route for essential nutrients such as cholesterol and iron which are carried into cells through low density lipoprotein (LDL) and transferrin receptors, respectively. Caveolae-mediated endocytosis is primarily due to caveolin protein. The ability of caveolin to oligomerize due to their oligomerization domains is necessary for formation of caveolar endocytic vesicles (Sahay et al., 2010).

Macropinocytosis is an uptake route initiated by transient activation of receptor tyrosine kinases by growth factors. The receptor activation mediates a signaling cascade that leads to changes in the actin cytoskeleton and triggers membrane ruffles formation. Clathrin- and caveolae-independent pathways are four major processes of pinocytosis involving different types of receptor–ligand interactions: Arf6-dependent, flotillin-dependent, Cdc42-dependent and RhoA-dependent (Wang et al., 2015; Mao et al., 2013).

2.4. Chaperone like activity of proteins

Although protein aggregation is desirable and necessary for many applications, it should be prevented in some cases. Canola contains two major proteins with two distinct properties; while cruciferin aggregates could be used for development of delivery systems, napin, might show an anti-aggregation activity due to its thermal-resistance property (Wu and Muir, 2008).

2.4.1. Protein aggregation

Newly synthesized proteins have to form a three-dimensional conformation consisting of proper interactions and folding to ensure protein techno- and bio-functionality (Hartl et al., 2011). Protein denaturation, due to changes in environmental condition, results in unfolded polypeptide chains. These unfolded structures may adopt different conformations through numerous possible interactions between interactive residues (Bukau et al., 2006; Hartl et al., 2011). However, only the proper native interactions lead to a functional conformation. Therefore, non-native interaction might cause protein misfolding, leading to soluble oligomeric structures, amorphous aggregates and amyloid fibrils. The soluble aggregates induce oxidative stress and deposition of fibrillar aggregates in neuronal cells which are reported as the major risk factor in amyloid-related diseases (Ghadami et al., 2011; Morshedi et al., 2010). Therefore, a protective mechanism is required to

shield the residues from environmental conditions and prevent non-native interactions (Liberek et al., 2008).

Food proteins experience denaturation and aggregation during food processing and storage. These changes may result in improved or impaired functional properties (Bartlett and Radford, 2009). For example, protein aggregation is essential for gelation, thickening and stabilizing emulsions and foams. However, aggregation causes undesirable texture and sensory attributes by forming large particles and precipitates in protein-rich products (Nicolai and Durand, 2013).

2.4.2. Molecular chaperones

Molecular chaperones assist in folding or refolding of the unfolded polypeptides by minimizing the mis-matched interactions (Liberek et al., 2008). According to Liberek et al. (2008) and Ellis (2006), chaperones are a diverse group of proteins that share the functional property of assisting the non-covalent folding/unfolding and the assembly/disassembly of other macromolecular structures, but are not permanent components of these structures when they are performing their normal biological functions(Liberek et al., 2008; Ellis, 2006). Since chaperones act under stress conditions to help unfolded chains re-acquire their functional conformation, they are also known as heat-shock proteins (Hsps) (Hartl et al., 2011).

2.4.3. Food proteins with chaperone-like activity

Among food proteins, caseins have been reported to act like a chaperone (Chen and Subirade, 2005; Lodhia et al., 2010; McClements, 2013; He et al., 2011; Koudelka et al., 2009a; Morgan et al., 2005). Phosphorylation of serine residues in α_s- and β-caseins brings negative charges in proximity to high proportion of hydrophobic residues that provide an amphiphilic nature for the casein monomers. Hydrophobic interactions, proposed as the driving force for the self-assembly of caseins, are considered as the first interaction between chaperones and their target chains (Tanaka et al., 2008). Additionally, phosphate groups impart negative charges to the protein, in which, repulsive forces and the bulky nature of the phosphate groups hinder the chain folding and induce a flexible and dynamic conformation with low secondary structure in casein. A high proportion of proline residues also provide an open structure with more flexibility for β-casein due to bending of polypeptide chain (Yong and Forgeding, 2010). Therefore, both amphiphilicity and flexibility, two important elements of chaperone activity, is lost upon dephosphorylation

(Koudelka et al., 2009b). In brief, hydrophobic interaction between exposed hydrophobic regions of casein and partially unfolded chains are proposed to facilitate binding of caseins to the target proteins while repulsive electrostatic interactions, due to phosphorylated serine residues, maintain the flexibility of partially folded chain to find the proper conformation (Koudelka et al., 2009b; Treweek et al., 2011). A proposed model for chaperone activity of casein under heat-stress is shown in Figure 2.6. This model explains the chaperone function of α_s-casein towards a target protein (N). Fast and reversible unfolding pathway results in folded intermediates (I_1 and I_2) which are transiently present. However, the intermediately folded states on the slower off-folding pathway are present for a longer time. The more disordered states (I_2) are highly dynamic and possess more exposed hydrophobic regions, therefore, aggregate along the off-folding pathway leading to precipitation. The natively unfolded subunits of α_S-casein are shown by spheres (dark and light grey for α_{S1}- and α_{S2}-casein, respectively). α_s-Casein interacts with highly disordered intermediates (I_2) to form a high molecular weight (HMW) complex which prevents further aggregation and precipitation of the target protein.

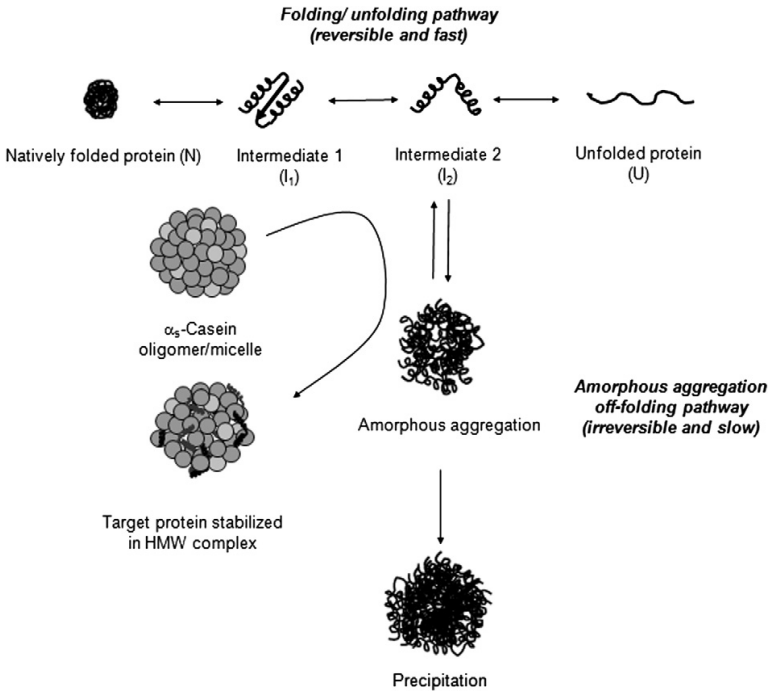

Figure 2.6. Schematic illustration of the chaperone function of α_s-casein towards a target protein (Reprinted from Treweek et al., 2011 with permission)

In addition to caseins, other food proteins were also investigated for their chaperone activity. Heme-containing proteins, such as hemoglobin and some enzymes (e.g. peroxidase and catalase), are proposed to prevent amyloid formation and aggregation. Khodarahmi et al. (2009) studied chaperone–like activity of heme group against amyloid fibril formation in heated egg ovalbumin. They suggested that a combination of hydrophobic and heme iron-histidine interactions are effective in anti-aggregatory property of heme (Khodarahmi et al., 2009). Peptide fragments were also reported to possess the ability to bind to partly unfolded proteins and prevent irreversible aggregation. Evidence provided by Artemova et al. (2010) demonstrated that some opioid peptides derived from wheat gluten, spinach, and bovine hemoglobin are able to assist endogenous defense mechanisms through refolding of stressed proteins and preventing aggregation. Opioid peptides are characterized by the presence of Tyr-Pro in their primary structures, which showed a positive correlation with their binding potential to exposed groups of unfolded chains.

2.4.4. Comparison of casein and heat-shock proteins

In order to understand the common features of molecular chaperones, some specifications of α-crystalline, a small Hsp in eye lens reported as molecular chaperone, are considered: (i) monomer molecular weight of 12-43 kDa, (ii) tendency to form oligomeric complex, (iii) chaperone activity under stress conditions, and (iv) a specific sequence in the functional domain of primary structure (Yong and Forgeding, 2010). In comparison with crystalline, the molecular weight of casein proteins is in the same range as small Hsps (Koudelka et al., 2009b). Monomers of caseins (β-casein and α_s-caseins) are amphiphilic, dynamic and able to form homo-oligomeric micelles (Koudelka et al., 2009b; Yong and Forgeding, 2010). Further investigations by Treweek et al. (2011) revealed that caseins, similar to small Hsps, have a relatively globular hydrophobic domain and clustered phosphoserine residues in polar domains (Treweek et al., 2011).

Although the significance of chaperones in preventing protein aggregation including amyloid fibril formation has been extensively documented in biological field, there is limited research on the potential effect of chaperone-like molecules on food protein functionality and food quality. Therefore, the potential application of chaperone-like molecules in the food products where aggregation and fibril formation are undesired such as protein-fortified beverages is at infancy.

2.4.5. Conclusions

Cruciferin and napin, two major canola proteins, possess distinct characteristics; cruciferin is resistant to gastric digestion and has excellent functional properties, and napin is an extremely thermal-resistant protein with an amphiphilic property. Therefore, cruciferin and napin have potential for encapsulation of bioactive compounds and chaperone-like activity, respectively. Our study on the potential applications not only could introduce new food-besed materials as a carrier and a chaperone-like molecule, but also might suggest new value-added products from canola proteins.

2.5. References

Aachary, A. A. & Thiyam, U. (2012). A pursuit of the functional nutritional and bioactive properties of canola proteins and peptides. *Critical Reviews in Food Science and Nutrition*, 52(11), 965-979.

Aguilera, J. M. (1995). Gelation of whey proteins. *Food Technology*, 49(10), 83-89.

Aider, M. & Barbana, C. (2011). Canola proteins: Composition, extraction, functional properties, bioactivity, applications as a food ingredient and allergenicity - A practical and critical review. *Trends in Food Science & Technology*, 22(1), 21-39.

Aluko, R. & McIntosh, T. (2005). Limited enzymatic proteolysis increases the level of incorporation of capola proteins into mayonnaise. *Innovative Food Science & Emerging Technologies*, 6(2), 195-202.

Aluko, R. & McIntosh, T. (2001). Polypeptide profile and functional properties of defatted meals and protein isolates of canola seeds. *Journal of the Science of Food and Agriculture*, 81(4), 391-396.

Arntfield, S. D. & Cai, R. (1998). Protein polysaccharide interactions during network formation: Observations involving canola protein. *Paradigm for Successful Utilization of Renewable Resources*, 108-122.

Artemova, N. V., Bumagina, Z. M., Kasakov, A. S., Shubin, V. V., & Gurvits, B. Y. (2010). Opioid peptides derived from food proteins suppress aggregation and promote reactivation of partly unfolded stressed proteins. *Peptides, 31*(2), 332-338.

Badley, R. A., Atkinson, D., Hauser, H., Oldani, D., Green, J. P., & Stubbs, J. M. (1975). Structure, physical and chemical properties of soy bean protein glycinin. *Biochimica Et Biophysica Acta*, 412(2), 214-228.

Barbut, S. & Foegeding, E. A. (1993). Ca^{2+}-Induced gelation of pre-heated whey-protein isolate. *Journal of Food Science*, 58(4), 867-871.

Barciszewski, J., Szymanski, M., & Haertle, T. (2000). Minireview: Analysis of rape seed napin structure and potential roles of the storage protein. *Journal of Protein Chemistry*, 19(4), 249-254.

Bartlett, A. I. & Radford, S. E. (2009). An expanding arsenal of experimental methods yields an explosion of insights into protein folding mechanisms. *Nature Structural & Molecular Biology*, 16(6), 582-588.

Bell, J. M. (1993). Factors affecting the nutritional-value of canola-meal - A review. *Canadian Journal of Animal Science*, 73(4), 679-697.

Bernkop-Schnuerch, A. (2013). Nanocarrier systems for oral drug delivery: Do we really need them? *European Journal of Pharmaceutical Sciences*, 49(2), 272-277.

Boegh, M. & Nielsen, H. M. (2015). Mucus as a barrier to drug delivery - understanding and mimicking the barrier properties. *Basic & Clinical Pharmacology & Toxicology*, 116(3), 179-186.

Boon, C. S., McClements, D. J., Weiss, J., & Decker, E. A. (2010). Factors influencing the chemical stability of carotenoids in foods. *Critical Reviews in Food Science and Nutrition*, 50(6), 515-532.

Bos, C., Airinei, G., Mariotti, F., Benamouzig, R., Berot, S., Evrard, J., Fenart, E., Tome, D., & Gaudichon, C. (2007). The poor digestibility of rapeseed protein is balanced by its very high metabolic utilization in humans. *Journal of Nutrition,* 137(3), 594-600.

Bryant, C. M. & McClements, D. J. (2000). Influence of NaCl and $CaCl_2$ on cold-set gelation of heat-denatured whey protein. *Journal of Food Science*, 65(5), 801-804.

Bukau, B., Weissman, J., & Horwich, A. (2006). Molecular chaperones and protein quality control. *Cell*, 125(3), 443-451.

Carver, J. A., Rekas, A., Thorn, D. C., & Wilson, M. R. (2003). Small heat-shock proteins and clusterin: Intra- and extracellular molecular chaperones with a common mechanism of action and function? *IUBMB Life*, 55(12), 661-668.

Cavallieri, A. L. F. & Da Cunha, R. L. (2008). The effects of acidification rate, pH and ageing time on the acidic cold set gelation of whey proteins. *Food Hydrocolloids*, 22(3), 439-448.

Chang, M., Tsai, T., Lee, C., Wei, Y., Chen, Y., Chen, C., & Tzen, J. T. C. (2013). Elevating bioavailability of curcumin via encapsulation with a novel formulation of artificial oil bodies. *Journal of Agricultural and Food Chemistry,* 61(40), 9666-9671.

Chen, L. Y., Remondetto, G. E., & Subirade, M. (2006). Food protein-based materials as nutraceutical delivery systems. *Trends in Food Science & Technology*, 17(5), 272-283.

Chen, L. Y. & Subirade, M. (2005). Chitosan/beta-lactoglobulin core-shell nanoparticles as nutraceutical carriers. *Biomaterials*, 26(30), 6041-6053.

Chuah, A. M., Kuroiwa, T., Ichikawa, S., Kobayashi, I., & Nakajima, M. (2009). Formation of biocompatible nanoparticles via the self-assembly of chitosan and modified lecithin. *Journal of Food Science*, 74(1), N1-N8.

Cone, R. A. (2009). Barrier properties of mucus. *Advanced Drug Delivery Reviews*, 61(2), 75-85.

Cumby, N., Zhong, Y., Naczk, M., & Shahidi, F. (2008). Antioxidant activity and water-holding capacity of canola protein hydrolysates. *Food Chemistry*, 109(1), 144-148.

de Kruif, C. G. & Tuinier, R. (2001). Polysaccharide protein interactions. *Food Hydrocolloids*, 15(4-6), 555-563.

Deat-Laine, E., Hoffart, V., Garrait, G., & Beyssac, E. (2013). Whey protein and alginate hydrogel microparticles for insulin intestinal absorption: Evaluation of permeability enhancement properties on Caco-2 cells. *International Journal of Pharmaceutics*, 453(2), 336-342.

Derbyshire, E., Wright, D. J., & Boulter, D. (1976). Legumin and vicilin, storage proteins of legume seeds. *Phytochemistry*, 15(1), 3-24.

des Rieux, A., Fievez, V., Garinot, M., Schneider, Y., & Preat, V. (2006). Nanoparticles as potential oral delivery systems of proteins and vaccines: A mechanistic approach. *Journal of Controlled Release*, 116(1), 1-27.

Doherty, S. B., Gee, V. L., Ross, R. P., Stanton, C., Fitzgerald, G. F., & Brodkorb, A. (2011). Development and characterisation of whey protein micro-beads as potential matrices for probiotic protection. *Food Hydrocolloids*, 25(6), 1604-1617.

Duval, S., Chung, C., & McClements, D. J. (2015). Protein-polysaccharide hydrogel particles formed by biopolymer phase separation. *Food Biophysics*, 10(3), 334-341.

Ecroyd, H. & Carver, J. A. (2009). Crystallin proteins and amyloid fibrils. *Cellular and Molecular Life Sciences*, 66(1), 62-81.

Ellis, R. J. (2006). Molecular chaperones: Assisting assembly in addition to folding. *Trends in Biochemical Sciences*, 31(7), 395-401.

Elzoghby, A. O., El-Fotoh, W. S. A., & Elgindy, N. A. (2011). Casein-based formulations as promising controlled release drug delivery systems. *Journal of Controlled Release*, 153(3), 206-216.

Elzoghby, A. O., Samy, W. M., & Elgindy, N. A. (2012a). Albumin-based nanoparticles as potential controlled release drug delivery systems. *Journal of Controlled Release*, 157(2), 168-182.

Elzoghby, A. O., Samy, W. M., & Elgindy, N. A. (2012b). Protein-based nanocarriers as promising drug and gene delivery systems. *Journal of Controlled Release*, 161(1), 38-49.

Ensign, L. M., Cone, R., & Hanes, J. (2012). Oral drug delivery with polymeric nanoparticles: The gastrointestinal mucus barriers. *Advanced Drug Delivery Reviews*, 64(6), 557-570.

Ezpeleta, I., Irache, J. M., Stainmesse, S., Chabenat, C., Gueguen, J., Popineau, Y., & Orecchioni, A. M. (1996). Gliadin nanoparticles for the controlled release of all-trans-retinoic acid. *International Journal of Pharmaceutics*, 131(2), 191-200.

Galindo-Rodriguez, S., Allemann, E., Fessi, H., & Doelker, E. (2005). Polymeric nanoparticles for oral delivery of drugs and vaccines: A critical evaluation of *in vivo* studies. *Critical Reviews in Therapeutic Drug Carrier Systems*, 22(5), 419-463.

Gao, J. Y., Dubin, P. L., & Muhoberac, B. B. (1997). Measurement of the binding of proteins to polyelectrolytes by frontal analysis continuous capillary electrophoresis. *Analytical Chemistry*, 69(15), 2945-2951.

Garti, N. & Aserin, A. (2012). Micelles and microemulsions as food ingredient and nutraceutical delivery systems. *Encapsulation Technologies and Delivery Systems for Food Ingredients and Nutraceuticals*, 239, 211-251.

Ghadami, S. A., Khodarahmi, R., Ghobadi, S., Ghasemi, M., & Pirmoradi, S. (2011). Amyloid fibril formation by native and modified bovine β-lactoglobulins proceeds through unfolded form of proteins: A comparative study. *Biophysical Chemistry*, 159(2-3), 311-320.

Ghodsvali, A., Khodaparast, M. H. H., Vosoughi, M., & Diosady, L. L. (2005). Preparation of canola protein materials using membrane technology and evaluation of meals functional properties. *Food Research International*, 38(2), 223-231.

Gill, T. A. & Tung, M. A. (1978). Chemistry and Ultrastructure of a Major Aleurone Protein of Rapeseed Meal. *Cereal Chemistry*, 55(2), 180-188.

Gillberg, L. & Tornell, B. (1976). Preparation of rapeseed protein isolates - dissolution and precipitation behavior of rapeseed proteins. *Journal of Food Science*, 41(5), 1063-1069.

Gruener, L. & Ismond, M. (1997). Effects of acetylation and succinylation on the functional properties of the canola 12S globulin. *Food Chemistry*, 60(4), 513-520.

Harde, H., Das, M., & Jain, S. (2011). Solid lipid nanoparticles: an oral bioavailability enhancer vehicle. *Expert Opinion on Drug Delivery*, 8(11), 1407-1424.

Hartl, F. U., Bracher, A., & Hayer-Hartl, M. (2011). Molecular chaperones in protein folding and proteostasis. *Nature*, 475(7356), 324-332.

Hattori, T., Hallberg, R., & Dubin, P. L. (2000). Roles of electrostatic interaction and polymer structure in the binding of beta-lactoglobulin to anionic polyelectrolytes: Measurement of binding constants by frontal analysis continuous capillary electrophoresis. *Langmuir*, 16(25), 9738-9743.

He, R., He, H., Chao, D., Ju, X., & Aluko, R. (2014). Effects of high pressure and heat treatments on physicochemical and gelation properties of rapeseed protein isolate. *Food and Bioprocess Technology,* 7(5), 1344-1353..

He, J., Zhu, S., Mu, T., Yu, Y., Li, J., & Azuma, N. (2011). Alpha(s)-Casein Inhibits the Pressure-Induced Aggregation of beta-lactoglobulin through its molecular chaperone-like properties. *Food Hydrocolloids*, 25(6), 1581-1586.

Heger, M., van Golen, R. F., Broekgaarden, M., & Michel, M. C. (2014). The molecular basis for the harmacokinetics and pharmacodynamics of curcumin and its metabolites in relation to cancers. *Pharmacological Reviews*, 66(1), 222-307.

Hillaireau, H. & Couvreur, P. (2009). Nanocarriers' entry into the cell: relevance to drug delivery. *Cellular and Molecular Life Sciences,* 66(17), 2873-2896.

Hu, B. & Huang, Q. (2013). Biopolymer based nano-delivery systems for enhancing bioavailability of nutraceuticals. *Chinese Journal of Polymer Science,* 31(9), 1190-1203.

Huang, A. H. C. (1992). Oil Bodies and Oleosins in Seeds. *Briggs, W.R.(Ed.).Annual Review of Plant Physiology and Plant Molecular Biology, Vol.43. 685p.Annual Reviews Inc.: Palo Alto, California, Usa.Illus,* 177-200.

Ichikawa, S., Iwamoto, S., & Watanabe, J. (2005). Formation of biocompatible nanoparticles by self-assembly of enzymatic hydrolysates of chitosan and carboxymethyl cellulose. *Bioscience Biotechnology and Biochemistry*, 69(9), 1637-1642.

Ismond, M. A. H. & Welsh, W. D. (1992). Application of new methodology to canola protein-isolation. *Food Chemistry*, 45(2), 125-127.

Jones, O. G., Decker, E. A., & McClements, D. J. (2009). Formation of biopolymer particles by thermal treatment of beta-lactoglobulin-pectin complexes. *Food Hydrocolloids*, 23(5), 1312-1321.

Jones, O. G. & McClements, D. J. (2011). Recent progress in biopolymer nanoparticle and microparticle formation by heat-treating electrostatic protein-polysaccharide complexes. *Advances in Colloid and Interface Science*, 167(1-2), 49-62.

Jones, O. G. & McClements, D. J. (2010). Functional biopolymer particles: Design, fabrication, and applications. *Comprehensive Reviews in Food Science and Food Safety*, 9(4), 374-397.

Jones, O., Decker, E. A., & McClements, D. J. (2010). Thermal analysis of beta-lactoglobulin complexes with pectins or carrageenan for production of stable biopolymer particles. *Food Hydrocolloids*, 24(2-3), 239-248.

Joye, I. J., Davidov-Pardo, G., & McClements, D. J. (2014). Nanotechnology for increased micronutrient bioavailability. *Trends in Food Science & Technology*, 40(2), 168-182.

Kamath, K. R. & Park, K. (1993). Biodegradable Hydrogels in Drug-Delivery. *Advanced Drug Delivery Reviews*, 11(1-2), 59-84.

Khodarahmi, R., Soori, H., & Karimi, S. A. (2009). Chaperone-like activity of heme group against amyloid-like fibril formation by hen egg ovalbumin: Possible mechanism of action. *International Journal of Biological Macromolecules*, 44(1), 98-106.

Klockeman, D. M., Toledo, R., & Sims, K. A. (1997). Isolation and characterization of defatted canola meal protein. *Journal of Agricultural and Food Chemistry*, 45(10), 3867-3870.

Kong, F. & Singh, R. P. (2010). A human gastric simulator (HGS) to study food digestion in human stomach. *Journal of Food Science*, 75(9), E627-E635.

Koudelka, T., Hoffmann, P., & Carver, J. A. (2009). Dephosphorylation of alpha(s)- and beta-caseins and its effect on chaperone activity: A structural and functional investigation. *Journal of Agricultural and Food Chemistry*, 57(13), 5956-5964.

Kulmyrzaev, A., Cancelliere, C., & McClements, D. J. (2000). Influence of sucrose on cold gelation of heat-denatured whey protein isolate. *Journal of the Science of Food and Agriculture*, 80(9), 1314-1318.

Kurita, K. (2006). Chitin and chitosan: Functional biopolymers from marine crustaceans. *Marine Biotechnology*, 8(3), 203-226.

Lacki, K. & Duvnjak, Z. (1998). Decrease of phenolic content in canola meal using a polyphenol oxidase preparation from *Trametes versicolor*: Effect of meal saccharification. *Biotechnology Techniques*, 12(1), 31-34.

Lai, S. K., Wang, Y., & Hanes, J. (2009a). Mucus-penetrating nanoparticles for drug and gene delivery to mucosal tissues. *Advanced Drug Delivery Reviews*, 61(2), 158-171.

Lai, S. K., Wang, Y., Wirtz, D., & Hanes, J. (2009b). Micro- and macrorheology of mucus. *Advanced Drug Delivery Reviews*, 61(2), 86-100.

Lai, S.K., O'Hanlon, D.E., Harrold, S., Man, S.T. Wang, Y.Y., Cone, R., & Hanes, J. (2007) Rapid transport of large polymeric nanoparticles in fresh undiluted human mucus, *Proceedings of the National Academy of Sciences U. S. A.* 104, 1482–1487.

Lee, P. S., Yim, S. G., Choi, Y., Thi Van Anh Ha, & Ko, S. (2012). Physiochemical properties and prolonged release behaviours of chitosan-denatured beta-lactoglobulin microcapsules for potential food applications. *Food Chemistry*, 134(2), 992-998.

Lefevre, T. & Subirade, M. (2000). Molecular differences in the formation and structure of fine-stranded and particulate beta-lactoglobulin gels. *Biopolymers*, 54(7), 578-586.

Leo, E., Vandelli, M. A., Cameroni, R., & Forni, F. (1997). Doxorubicin-loaded gelatin nanoparticles stabilized by glutaraldehyde: Involvement of the drug in the cross-linking process. *International Journal of Pharmaceutics*, 155(1), 75-82.

Liberek, K., Lewandowska, A., & Zietkiewicz, S. (2008). Chaperones in control of protein disaggregation RID F-5812-2011. *Embo Journal*, 27(2), 328-335.

Lindner, R. A., Carver, J. A., Ehrnsperger, M., Buchner, J., Esposito, G., Behlke, J., Lutsch, G., Kotlyarov, A., & Gaestel, M. (2000). Mouse Hsp25, a small heat shock protein - The role of its C-terminal extension in oligomerization and chaperone action. *European Journal of Biochemistry*, 267(7), 1923-1932.

Lodhia, J., Mandarano, G., Ferris, N., Eu, P., & Cowell, S. (2010). Development and use of iron oxide nanoparticles (Part 1): Synthesis of iron oxide nanoparticles for MRI. *Biomedical Imaging and Intervention Journal*, 6(2), e12-e12.

MaHam, A., Tang, Z., Wu, H., Wang, J. & Lin, Y. (2009). Protein-based nanomedicine platforms for drug delivery. *Small*, 5(15), 1706-1721.

Maltais, A., Remondetto, G. E., Gonzalez, R., & Subirade, M. (2005). Formation of soy protein isolate cold-set gels: Protein and salt effects. *Journal of Food Science*, 70(1), C67-C73.

Maltais, A., Remondetto, G. E., & Subirade, M. (2008). Mechanisms involved in the formation and structure of soya protein cold-set gels: A molecular and supramolecular investigation. *Food Hydrocolloids*, 22(4), 550-559.

Mao, Z., Zhou, X., & Gao, C. (2013). Influence of structure and properties of colloidal biomaterials on cellular uptake and cell functions. *Biomaterials Science*, 1(9), 896-911.

Marczak, E., Usui, H., Fujita, H., Yang, Y., Yokoo, M., Lipkowski, A., & Yoshikawa, M. (2003). New antihypertensive peptides isolated from rapeseed. *Peptides*, 24(6), 791-798.

Martins, J. T., Ramos, O. L., Pinheiro, A. C., Bourbon, A. I., Silva, H. D., Rivera, M. C., Cerqueira, M. A., Pastrana, L., Xavier Malcata, F., Gonzalez-Fernandez, A., & Vicente, A. A. (2015). Edible bio-based nanostructures: Delivery, absorption and potential toxicity. *Food Engineering Reviews*, 7(4), 491-513.

McClements, D. J. (2015). Nanoscale nutrient delivery systems for food applications: Improving bioactive dispersibility, stability, and bioavailability. *Journal of Food Science*, 80(7), N1602-N1611.

McClements, D. J. (2013). Edible lipid nanoparticles: Digestion, absorption, and potential toxicity. *Progress in Lipid Research*, 52(4), 409-423.

McClements, D. J. (2012a). Advances in fabrication of emulsions with enhanced functionality using structural design principles. *Current Opinion in Colloid & Interface Science*, 17(5), 235-245.

McClements, D. J. (2012b). Crystals and crystallization in oil-in-water emulsions: Implications for emulsion-based delivery systems. *Advances in Colloid and Interface Science*, 174, 1-30.

McClements, D. J. & Decker, E. A. (2000). Lipid oxidation in oil-in-water emulsions: Impact of molecular environment on chemical reactions in heterogeneous food systems. *Journal of Food Science*, 65(8), 1270-1282.

McClements, D. J., Decker, E. A., Park, Y., & Weiss, J. (2009). Structural design principles for delivery of bioactive components in nutraceuticals and functional foods. *Critical Reviews in Food Science and Nutrition*, 49(6), 577-606.

McClements, D. J. & Keogh, M. K. (1995). Physical-properties of cold-setting gels formed from heat-denatured whey-protein isolate. *Journal of the Science of Food and Agriculture*, 69(1), 7-14.

McClements, D. J. & Rao, J. (2011). Food-grade nanoemulsions: Formulation, fabrication, properties, performance, biological fate, and potential toxicity. *Critical Reviews in Food Science and Nutrition*, 51(4), 285-330.

McClements, D. J. & Xiao, H. (2014). Excipient foods: Designing food matrices that improve the oral bioavailability of pharmaceuticals and nutraceuticals. *Food & Function*, 5(7), 1320-1333.

McClements, D. J. & Xiao, H. (2012). Potential biological fate of ingested nanoemulsions: Influence of particle characteristics. *Food & Function*, 3(3), 202-220.

Mejia, L. A., Korgaonkar, C. K., Schweizer, M., Chengelis, C., Novilla, M., Ziemer, E., Williamson-Hughes, P. S., Grabiel, R., & Empie, M. (2009). A 13-week dietary toxicity study in

rats of a napin-rich canola protein isolate. *Regulatory Toxicology and Pharmacology*, 55(3), 394-402.

Mikos, A. G., Mathiowitz, E., Langer, R., & Peppas, N. A. (1991). Interaction of polymer microspheres with mucin gels as a means of characterizing polymer retention on mucus. *Journal of Colloid and Interface Science*, 143(2), 366-373.

Morgan, P., Treweek, T., Lindner, R., Price, W., & Carver, J. (2005). Casein proteins as molecular chaperones. *Journal of Agricultural and Food Chemistry*, 53(7), 2670-2683.

Morshedi, D., Ebrahim-Habibi, A., Moosavi-Movahedi, A. A., & Nemat-Gorgani, M. (2010). Chemical modification of lysine residues in lysozyme may dramatically influence its amyloid fibrillation. *Biochimica Et Biophysica Acta-Proteins and Proteomics*, 1804(4), 714-722.

Naczk, M., Diosady, L. L., & Rubin, L. J. (1985). Functional-properties of canola meals produced by a 2-phase solvent-extraction system. *Journal of Food Science*, 50(6), 1685-88.

Nesterenko, A., Alric, I., Silvestre, F., & Durrieu, V. (2013). Vegetable proteins in microencapsulation: A review of recent interventions and their effectiveness. *Industrial Crops and Products*, 42, 469-479.

Newkirk, R. & Classen, H. (1998). *In vitro* hydrolysis of phytate in canola meal with purified and crude sources of phytase. *Animal Feed Science and Technology*, 72(3-4), 315-327.

Nicolai, T. & Durand, D. (2013). Controlled food protein aggregation for new functionality. *Current Opinion in Colloid & Interface Science*, 18(4), 249-256.

Owen, D. F., Chichest. Co, Granadin.J, & Monckebe.F. (1971). Process for producing nontoxic rapeseed protein isolate and an acceptable feed by-product. *Cereal Chemistry*, 48(2), 91-98.

Patel, A. R. & Velikov, K. P. (2011). Colloidal delivery systems in foods: A general comparison with oral drug delivery. *Lwt-Food Science and Technology*, 44(9), 1958-1964.

Paulson, A., Tung, M., Aulson, A., & Tung, M. (1988). Emulsification properties of succinylated canola protein isolate. *Journal of Food Science*, 53(3), 817-820.

Penalva, R., Esparza, I., Agueeros, M., Gonzalez-Navarro, C. J., Gonzalez-Ferrero, C., & Irache, J. M. (2015). Casein nanoparticles as carriers for the oral delivery of folic acid. *Food Hydrocolloids,* 44, 399-406.

Piculell, L. (1995). Gelling carrageenans. Food Science and Technology (New York); *Food Polysaccharides and their Applications*, 67, 205-244.

Pinterits, A. & Arntfield, S. D. (2008). Improvement of canola protein gelation properties through enzymatic modification with transglutaminase. *Lwt-Food Science and Technology*, 41(1), 128-138.

Prakash, V. & Rao, M. S. N. (1986). Physicochemical properties of oilseed proteins. *CRC Critical Reviews in Biochemistry*, 20(3), 265-363.

Qiu, Y. & Park, K. (2001). Environment-sensitive hydrogels for drug delivery. *Advanced Drug Delivery Reviews*, 53(3), 321-339.

Reddy, N. & Yang, Y. (2011). Potential of plant proteins for medical applications. *Trends in Biotechnology*, 29(10), 490-498.

Remondetto, G.E. & Subirade, M. (2003). Molecular mechanisms of Fe^{2+} -induced β-lactoglobulin cold gelation. *Biopolymers*, 69, 461–469.

Ridley, B. L., O'Neill, M. A., & Mohnen, D. A. (2001). Pectins: Structure, biosynthesis, and oligogalacturonide-related signaling. *Phytochemistry*, 57(6), 929-967.

Rinaudo, M. (2006). Chitin and chitosan: Properties and applications. *Progress in Polymer Science*, 31(7), 603-632.

Sagalowicz, L. & Leser, M. E. (2010). Delivery systems for liquid food products. *Current Opinion in Colloid & Interface Science*, 15(1-2), 61-72.

Sahay, G., Alakhova, D. Y., & Kabanov, A. V. (2010). Endocytosis of nanomedicines. *Journal of Controlled Release*, 145(3), 182-195.

Saskatchewan Canola Development Commission. Online. 2016. Available from URL: http://saskcanola.com/industry/index.php.

Schatz, C., Lucas, J. M., Viton, C., Domard, A., Pichot, C., & Delair, T. (2004). Formation and properties of positively charged colloids based on polyelectrolyte complexes of biopolymers. *Langmuir*, 20(18), 7766-7778.

Schmitt, C., Sanchez, C., Desobry-Banon, S., & Hardy, J. (1998). Structure and technofunctional properties of protein-polysaccharide complexes: A review. *Critical Reviews in Food Science and Nutrition*, 38(8), 689-753.

Schwenke, K. D., Raab, B., Linow, K. J., Pahtz, W., & Uhlig, J. (1981). Isolation of the 12 S globulin from rapeseed (*Brassica napus* L) and characterization as a neutral protein on seed proteins .13. *Nahrung-Food*, 25(3), 271-280.

Ser, W. Y., Arntfield, S. D., Hydamaka, A. W., & Slorninski, B. A. (2008). Use of diabetic test kits to assess the recovery of glucosinolates during isolation of canola protein. *Lwt-Food Science and Technology*, 41(5), 934-941.

Serranio, M. & Thompson, L. (1984). Removal of phytic acid and protein phytic acid interactions in rapeseed. *Journal of Agricultural and Food Chemistry*, 32(1), 38-40.

Seyrek, E., Dubin, P. L., Tribet, C., & Gamble, E. A. (2003). Ionic strength dependence of protein-polyelectrolyte interactions. *Biomacromolecules*, 4(2), 273-282.

Shahidi, F. & Abuzaytoun, R. (2005). Chitin, chitosan, and co-products: Chemistry, production, applications, and health effects. *Advances in Food and Nutrition Research*, Vol 49, 49, 93-135.

Shahidi, F., Gabon, J. E., Rubin, L. J., & Naczk, M. (1990). Effect of methanol ammonia water-treatment on the fate of glucosinolates. *Journal of Agricultural and Food Chemistry*, 38(1), 251-255.

Shen, L. (2009). Functional morphology of the gastrointestinal tract. *Molecular Mechanisms of Bacterial Infection Via the Gut*, 337, 1-35.

Shewry, P., Napier, J., & Tatham, A. (1995). Seed storage proteins - Structures and biosynthesis. *Plant Cell*, 7(7), 945-956.

Smart, J. D. (2005). The basics and underlying mechanisms of mucoadhesion. *Advanced Drug Delivery Reviews*, 57(11), 1556-1568.

Sonvico, F., Cagnani, A., Rossi, A., Motta, S., Di Bari, M. T., Cavatorta, F., Alonso, M. J., Deriu, A., & Colombo, P. (2006). Formation of self-organized nanoparticles by lecithin/chitosan ionic interaction. *International Journal of Pharmaceutics*, 324(1), 67-73.

Sorensen, H. (1990). Glucosinolates: Structure, properties, function. In F. Shahidi (Ed.), Canola and Rapeseed: Production, Chemistry, Nutrition, and Processing Technology (149-172). *New York: Von Nostrand Reinhold*.

Tan, S. H., Mailer, R. J., Blanchard, C. L., & Agboola, S. O. (2011). Extraction and characterization of protein fractions from Australian canola meals. *Food Research International*, 44(4), 1075-1082.

Tanaka, N., Tanaka, R., Tokuhara, M., Kunugi, S., Lee, Y., & Hamada, D. (2008). Amyloid fibril formation and chaperone-like activity of peptides from alpha A-Crystallin. *Biochemistry*, 47(9), 2961-2967.

Tang, C. & Liu, F. (2013). Cold, gel-like soy protein emulsions by microfluidization: Emulsion characteristics, rheological and microstructural properties, and gelling mechanism. *Food Hydrocolloids*, 30(1), 61-72.

Teng, Z., Luo, Y., & Wang, Q. (2013). Carboxymethyl chitosan-soy protein complex nanoparticles for the encapsulation and controlled release of vitamin D-3. *Food Chemistry*, 141(1), 524-532.

Tergesen, J. F. (2010). Sustainability points to plant proteins. *Food Technology*, 64(11), 88-88.

Thanki, K., Gangwal, R. P., Sangamwar, A. T., & Jain, S. (2013). Oral delivery of anticancer drugs: Challenges and opportunities. *Journal of Controlled Release*, 170(1), 15-40.

Tomczynska-Mleko, M. (2013). Structure and stability of ion induced whey protein aerated gels. *Czech Journal of Food Sciences*, 31(3), 211-216.

Treweek, T. M., Thorn, D. C., Price, W. E., & Carver, J. A. (2011). The chaperone action of bovine milk alpha(S1)- and alpha(S2)-caseins and their associated form alpha(S)-casein. *Archives of Biochemistry and Biophysics*, 510(1), 42-52.

Turgeon, S. L., Beaulieu, M., Schmitt, C., & Sanchez, C. (2003). Protein-polysaccharide interactions: Phase-ordering kinetics, thermodynamic and structural aspects. *Current Opinion in Colloid & Interface Science*, 8(4-5), 401-414.

Turgeon, S. L., Schmitt, C., & Sanchez, C. (2007). Protein-polysaccharide complexes and coacervates. *Current Opinion in Colloid & Interface Science*, 12(4-5), 166-178.

Twomey, M., Keogh, M. K., Mehra, R., & OKennedy, B. T. (1997). Gel characteristics of beta-lactoglobulin, whey protein concentrate and whey protein isolate. *Journal of Texture Studies*, 28(4), 387-403.

Tzeng, Y. M., Diosady, L. L., & Rubin, L. J. (1990). Production of canola protein materials by alkaline extraction, precipitation, and membrane processing. *Journal of Food Science*, 55(4), 1147-1156.

Uruakpa, F. & Arntfield, S. (2006). Structural thermostability of commercial canola protein-hydrocolloid mixtures. *Lwt-Food Science and Technology*, 39(2), 124-134.

Uruakpa, F. & Arntfield, S. (2005). The physico-chemical properties of commercial canola protein isolate-guar gum gels. *International Journal of Food Science and Technology*, 40(6), 643-653.

USDA. (2013). Major oilseeds: world supply and distribution. United States Department of Agriculture. Available from URL: http://apps.fas.usda.gov/psdonline/circulars/oilseeds.pdf.

Velikov, K. P. & Pelan, E. (2008). Colloidal delivery systems for micronutrients and nutraceuticals. *Soft Matter*, 4(10), 1964-1980.

Wan, Z., Guo, J., & Yang, X. (2015). Plant protein-based delivery systems for bioactive ingredients in foods. *Food & Function*, 6(9), 2876-2889.

Wanasundara, J. P. D. (2011). Proteins of *Brassicaceae* oilseeds and their potential as a plant protein source. *Critical Reviews in Food Science and Nutrition*, 51(7), 635-677.

Wang, X., Lee, J., Wang, Y., & Huang, Q. (2007). Composition and rheological properties of beta-lactoglobulin/pectin coacervates: Effects of salt concentration and initial protein/polysaccharide ratio. *Biomacromolecules*, 8(3), 992-997.

Wang, J., Ma, W., & Tu, P. (2015). The mechanism of self-assembled mixed micelles in improving curcumin oral absorption: In vitro and in vivo. *Colloids and Surfaces B-Biointerfaces*, 133, 108-119.

Waraho, T., McClements, D. J., & Decker, E. A. (2011). Mechanisms of lipid oxidation in food dispersions. *Trends in Food Science & Technology*, 22(1), 3-13.

Wu, J. & Muir, A. D. (2008). Comparative structural, emulsifying, and biological properties of 2 major canola proteins, cruciferin and napin. *Journal of Food Science*, 73(3), C210-C216.

Wu, Y., Loper, A., Landis, E., Hettrick, L., Novak, L., Lynn, K., Chen, C., Thompson, K., Higgins, R., Batra, U., Shelukar, S., Kwei, G., & Storey, D. (2004). The role of biopharmaceutics in the development of a clinical nanoparticle formulation of MK-0869: A Beagle dog model predicts improved bioavailability and diminished food effect on absorption in human. *International Journal of Pharmaceutics*, 285(1-2), 135-146.

Xu, L. & Diosady, L. (2000). Interactions between canola proteins and phenolic compounds in aqueous media. *Food Research International*, 33(9), 725-731.

Xu, L. & Diosady, L. (1997). Rapid method for total phenolic acid determination in rapeseed/canola meals. *Food Research International*, 30(8), 571-574.

Yasuda, K., Nakamura, R., & Hayakawa, S. (1986). Factors affecting heat-induced gel formation of bovine serum-albumin. *Journal of Food Science*, 51(5), 1289-1292.

Yong, Y. H. & Forgeding, E. A. (2010). Caseins: Utilizing molecular chaperone properties to control protein aggregation in foods. *Journal of Agricultural and Food Chemistry*, 58(2), 685-693.

Yoshie-Stark, Y., Wada, Y., & Waesche, A. (2008). Chemical composition, functional properties, and bioactivities of rapeseed protein isolates. *Food Chemistry*, 107(1), 32-39.

Yu, S. Y., Hu, J. H., Pan, X. Y., Yao, P., & Jiang, M. (2006). Stable and pH-sensitive nanogels prepared by self-assembly of chitosan and ovalbumin. *Langmuir*, 22(6), 2754-2759.

CHAPTER 3- An integrated method of isolating napin and cruciferin from defatted canola meal

A version of this chapter has been published: Akbari, A. & Wu, J. (2015). An integrated method of isolating napin and cruciferin from defatted canola meal. *LWT-Food Science and Technology,* 64, 308-315.

3.1. Introduction

With an annual production of 70 million metric tonnes, canola/rapeseed now ranks as the second most abundant oilseed in the world (USDA, 2013). As a farm-gate crop in Canada, its annual production is predicted to exceed 15 million tonnes by 2015 (Canola Council of Canada, 2007). After oil extraction, canola meal contains 35-40% protein while is used mainly as an animal feed or as a fertilizer (Wu et al., 2009). Canola proteins contain a well-balanced amino acid composition, especially a high content of lysine (6.0%) and sulfur-containing amino acids (3-4%), and a high protein efficiency ratio (2.64) compared to soy protein (2.19), making them favorable for human consumption (Wu and Muir, 2008; Tan et al., 2011). The emulsification capacity of canola protein isolates is comparable with egg proteins (Yoshie-Stark et al., 2008); for instance, canola protein and its hydrolysates were used as substitutions of egg yolk in mayonnaise preparation (Aluko and McIntosh, 2005). The functional properties of canola proteins can be further improved by enzymatic hydrolysis, succinylation, acylation, or adding hydrocolloids (Aider and Barbana, 2011). Recently, canola protein-derived bioactive peptides were also reported (Wu and Muir, 2008; Wu et al., 2009; Yoshie-Stark et al., 2008; Marczak et al., 2003; Yamada et al., 2010).

Canola contains two major proteins, cruciferin (12S globulin) and napin (2S albumin), accounting for 65 and 25% of total canola proteins, respectively. Cruciferin, with an isoelectric point (pI) of around 7.2, is composed of six subunits, each subunit containing one acidic 30 kDa α-chain and one basic 20 kDa β-chain which are linked by a disulfide bond (Wanasundara, 2011); the molecular weight of cruciferin was reported to range from 230 to 300 kDa (Wu and Muir, 2008). Napin, a strongly basic protein (isoelectric point around 11), is composed of a 4.5 kDa (40 amino acids) chain and a 9.5 kDa (90 amino acids) chain with a molecular mass of approximately 12-14.5 kDa. The polypeptide chains in napin are stabilized by two inter-chain disulfide bonds and two intra-chain disulfide bridges, formed by eight cysteine residues. These two major proteins (cruciferin and napin) have very unique functional properties due to their structural differences. While cruciferin has emulsifying, gelling and binding properties and is suitable for uses in meat substitutes, sauces, and baked goods, napin has good foaming property for uses in confectionary, beverages, and aerated desserts (Aider and Barbana, 2011; Wanasundara, 2011). In addition to the food applications, there is an increasing attention for their non-food uses such as industrial bio-

adhesives, bio-foams and bio-plastics (Wanasundara, 2011). It is desirable to develop an environmentally friendly method to extract canola protein. Due to the presence of a wide range of molecular weights (13-320 kDa) and isoelectric points (pH 4-11), as well as the presence of various undesirable compounds such as glucosinolates, phenols, and phytic acid, extraction of canola proteins remains a challenge (Xu and Diosady, 2000; Wu and Muir, 2008; Tan et al., 2011). The objectives of the study were to determine the effects of different treatments on removing antinutritional compounds and to develop a simple and scalable method to extract and isolate two major canola proteins, cruciferin and napin.

3.2. Materials and Methods

3.2.1. Materials

Hexane-defatted, air-dried commercial canola meal, obtained from Richardson Oilseed Company (Lethbridge, AB, Canada) was ground, passed through a 0.5-mm screen and stored at -20 °C for further use. Folin-Ciocalteu's phenol reagent, sinapic acid, 2, 2-bipyridyl, thioglycollic acid, sodium phytate, SDS (sodium dodecyl sulfate**)** and pyronin Y were purchased from Sigma-Aldrich (St. Louis, MO, USA). Ready-to-use mini-protean gels (4-20% gradient gels), and protein standard markers were obtained from Bio-Rad (Bio-Rad Laboratories Inc., Hercules, CA, USA).

3.2.2. Effect of various parameters on protein extraction

Effects of various parameters, such as pHs ranging from 8 to 12.5 at increment of 0.5 unit, time of extraction (1 and 2 h), meal:solvent ratio (1:10 and 1:20, g:mL), NaCl concentrations (0.03, 0.0625, 0.125, 0.25, 0.5, and 1M), SDS concentrations (0.1, 0.5, 1, and 2%), and sodium sulfite concentrations (0.1, 0.25, 0.5, and 1%) on protein extraction were evaluated. For the first step, 1 g of defatted canola meal was mixed with 10 mL of NaOH solution at different basic pH values, and the mixture was agitated on a Forma orbital shaker (Model 416, Thermo Electron Corporation, Ohio, USA) at 300 rpm for one hour at room temperature (during agitation the pH decreased about 0.3-0.4 unit). The slurry was centrifuged (Beckman-Coulter, Brea, CA, USA) at 15000 ×g and 5°C for 20 min, and the supernatant was filtered through Whatman No 1 filter papers. The filtrate was freeze-dried, and protein purity and yield were determined. The pH with the highest protein content and yield was selected for the study of other parameters such as shaking time, meal:solvent ratio and the various concentrations of different chemicals.

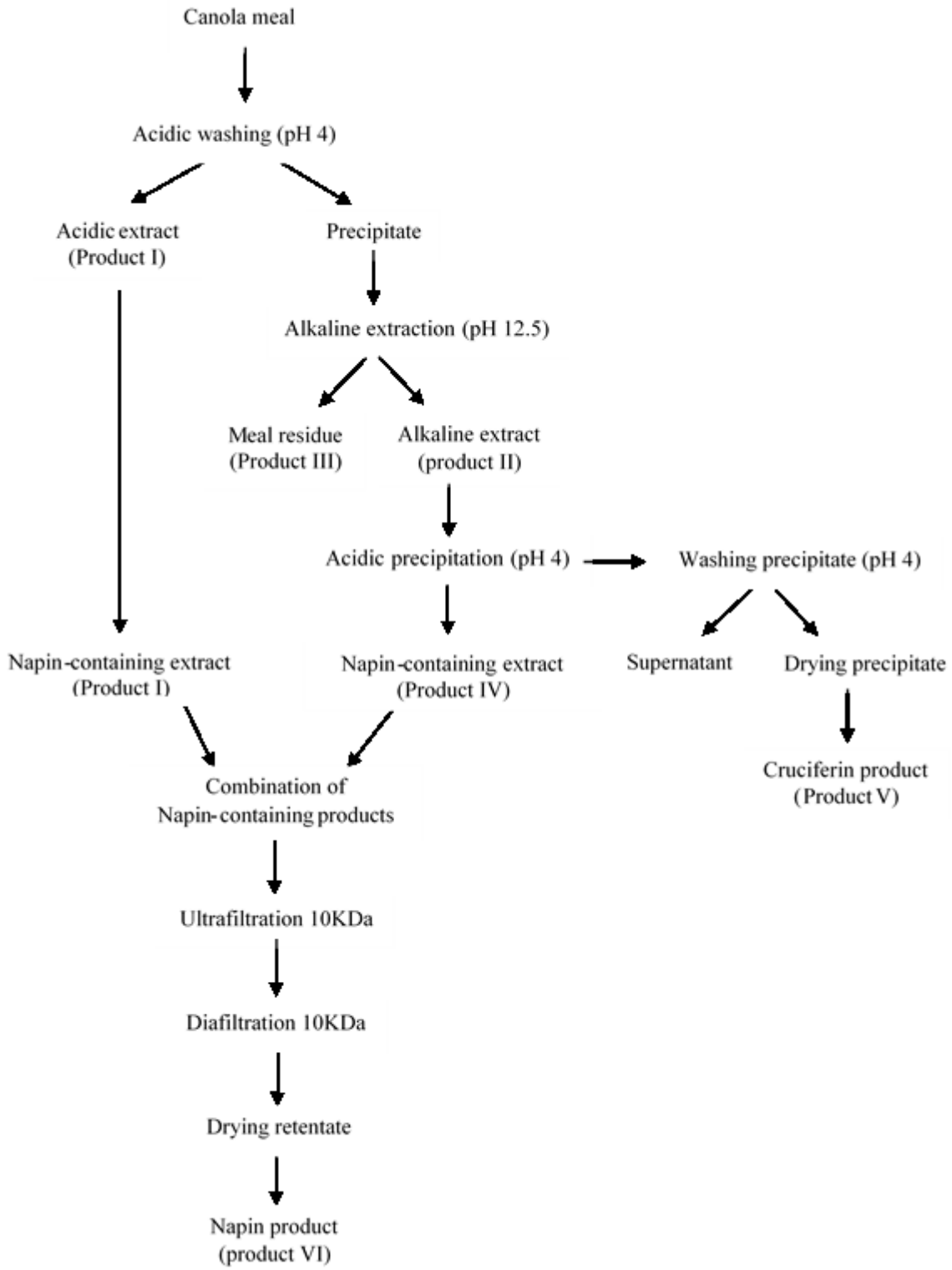

Figure 3.1. Proposed flowchart of canola protein extraction

3.2.3. Effect of acidic washing (different acidic pH values)

In the second experiment, the effect of acidic washing before alkaline extraction was evaluated. 1 g of defatted canola meal was mixed with 10 mL of HCl solutions at different pH values between 2.5 and 5 at increments of 0.5 unit and the mixture was agitated on the orbital shaker at 300 rpm for two hours at room temperature. The slurry was centrifuged at 15000 ×g and 5°C for 20 min, and the supernatant was filtrated through Whatman No 1 filter paper. The filtrate was freeze-dried. Residue was used for alkaline extraction at the condition established above. Protein purity and yield of the products were determined.

3.2.4. Effect of precipitation pHs on product purity and yield

After acidic washing (at pH 4) and alkaline extraction (at pH 12.5, agitation time 1h, and meal: solvent ratio 1:10), the filtrated extract was adjusted gradually (in 15 min) to pH values 4 and 4.5 with 0.1M HCl solution, and the resultant slurry was centrifuged (at 15000 ×g and 5°C for 20 min). The precipitates were washed (three times with 150 ml acidified water-pH 4) to remove remaining salts, then centrifuged (at 15000 ×g and 5°C for 20 min), and the washed precipitates were freeze-dried as isolate. Figure 3.1 shows a schematic representation of protein extraction.

3.2.5. Membrane separation of napin

The two napin-containing extracts obtained after acidic washing and precipitation were combined, adjusted to pH 4, and then subjected to an ultrafiltration system (Millipore, Bedford, MA, US). The spiral-wound membrane had a nominal molecular weight cut-off of 10 kDa and a membrane area of 0.2 m^2. Two concentration factors (CF), 10 and 20, and two diavolumes (DV), 5 and 10, were used in the ultrafiltration and diafiltration operations, respectively. The resultant retentate containing napin was freeze dried.

3.2.6. Chemical analysis

The nitrogen content of canola meal and protein extracts was determined by TruSpec CN carbon/nitrogen determinator (Leco Corp., St. Joseph, MI) and then converted to protein content using protein factor (N × 6.25). Protein yield was calculated using the following formula:

$$Protein\ yield\ (\%) = \frac{Wp \times Product\ protein\ content(g/100g, dry\ basis)}{Wm \times Starting\ meal\ protein\ content(g/100g, dry\ basis)} \times 100$$

Where, Wp = Weight of freeze-dried product; Wm = Weight of starting meal.

The amount of non-digestible fiber (NDF), ash, and moisture were measured by the AOAC methods (AOAC, 2000). Oil content was estimated by Goldfish extraction unit using diethyl ether. Total phenolic acid content was determined using the method developed by Xu and Diosady (1997). The method described by Haug and Lantzsch (1983) with some modifications was used for measuring phytic acid content in samples. Phytic acid was extracted by shaking 1 gram sample for 1 h in the presence of 80 ml 3% trichloroacetic acid (TCA). After extraction, the suspension was centrifuged (4000 ×g, 22°C, and 15 min) and the supernatant was collected. The supernatant (1 ml) was mixed with 19 ml of 0.02% ferric ammonium sulfate solution in 3% TCA and boiled for 30 min. After cooling and centrifuging, 2 ml of the supernatant was treated with 3 ml bipyridine-thioglycollic acid reagent and the absorbance was read at 519 nm. The concentration of phytic acid was calculated from a similarly prepared standard curve.

3.2.7. SDS-PAGE of proteins

SDS-PAGE was carried out as described by Uruakpa and Arntfield (2006). Gel electrophoresis of reduced and non-reduced canola protein samples were run on Mini-Protean gels (4-20% gradient gels). The loaded amount of proteins was 25 µg for napin sample and 90 µg for canola meal and cruciferin samples.

3.2.8. Functional properties

The emulsifying property of cruciferin and napin products was determined according to the method of Aluko and McIntosh (2001). Cruciferin was solubilized at pH 12 at a concentration of 2% and then the pH of the solution was adjusted to 7.5. The cruciferin solution was further diluted to 1% using 0.01M sodium phosphate buffer (pH 7.0). However, napin solution (1%) was directly prepared in the buffer. A mixture containing 5 mL protein solution and 1 mL pure commercial canola oil was homogenised at 24000 rpm for 1 min using an Ultra-turrax T25 homogenizer (IKA-Works, Inc., Cincinnati, OH) equipped with a 108 mm × 8 mm generator. The mean oil droplet size ($d_{3,2}$) and specific surface area (m^2/mL) of the emulsions were determined using a Mastersizer 2000S Particle Size Analyzer (Malvern Instruments Ltd., Malvern, U.K.) at 0 min and after 30 min standing at room temperature. The stability of emulsion was calculated by the ratio of the specific surface area between the time 0 and 30 min standing. To determine the emulsifying activity index (EAI), a 50 µL emulsion sample was immediately diluted with 7.5 mL of the buffer containing

0.1% SDS, and the absorbance of the mixture was measured at 500 nm (Karaca et al., 2011). EAI was calculated using the following equation:

$$EAI\ \left(m^2/g\right) = \frac{2 \times 2.303 \times A\ \times N}{C \times \varphi \times 10000}$$

Where A is the absorbance of the diluted emulsion immediately after homogenization, N is the dilution factor (×150), C is protein concentration (g/mL) and φ is the oil volume fraction of the emulsion.

The foaming capacity and stability of cruciferin and napin were determined at a concentration of 1.5% in 0.01M sodium phosphate buffer (pH 7.0) according to Chabanon et al. (2007). A 20 mL above solution was homogenised in 50 mL tubes at 18000 rpm for 5 min using the homogenizer. The volume of formed foam was recorded immediately after homogenisation and after 30, 60 and 120 min standing at room temperature. The foaming capacity was calculated as the ratio of the volume of formed foam and the initial volume of the protein solution and expressed as percentage. The foaming stability was expressed as the percentage of foam remaining after 30, 60 and 120 min at room temperature (Chabanon et al., 2007).

3.2.9. Statistical analysis

Experiments were carried out in triplicates and results were statistically analyzed using ANOVA. The multiple range test of Duncan ($p < 0.05$) (version 9.2, SAS Institute Inc., Cary, NC, USA) was used for comparing the results means.

3.3. Results and Discussion

3.3.1. Effect of various parameters on protein extraction

Proximate analysis showed taht defatted canola meal contained 10.8% moisture, 40.6% protein, 2.1% oil, 6.6% ash, 21.7% total fiber, 1.7% total phenolic compounds, and 2.8% phytic acid. Effects of pH, time, meal:solvent ratio, and different chemicals on protein extraction were performed. As shown in Figure 3.2a, the protein content of the extracts increased gradually from 38 to 56.4%, at increasing pH from 8 to 12.5. A similar trend existed for protein yield; however a dramatic increase was seen from pH 11.5 to 12.5. Therefore, pH 12.5 was selected for future study. While increasing agitation time did not affect protein extraction, a lower meal: solvent ratio decreased protein content but increased protein yield (Figure 3.2b). Since salt-soluble globulin proteins account for approximately 70% of total canola proteins (Tan et al., 2011), effect of NaCl

addition on protein extraction was also studied. Increase of salt concentration (from 0 to 2 M) decreased both protein content (56±1.1 to 13.6±0.6%) and yield (56.1±0.3 to 36.6±1.0%) (*Supplementary Figure 3.1*); this could be due to the salting out effect of added NaCl. Although globulin proteins are soluble in both salt and strong alkaline solutions (Tan et al., 2011), adding salt to high-pH solutions could have a salting out effect on the extracted proteins. Deak et al. (2006) also showed that the solubility of glycinin, 11S globulin soy protein, decreased at increasing salt concentration. Cruciferin, 12S globulin protein, is the main portion of canola protein extracted at pH 12.5; as a result, increasing salt concentration decreased the protein solubility and yield.

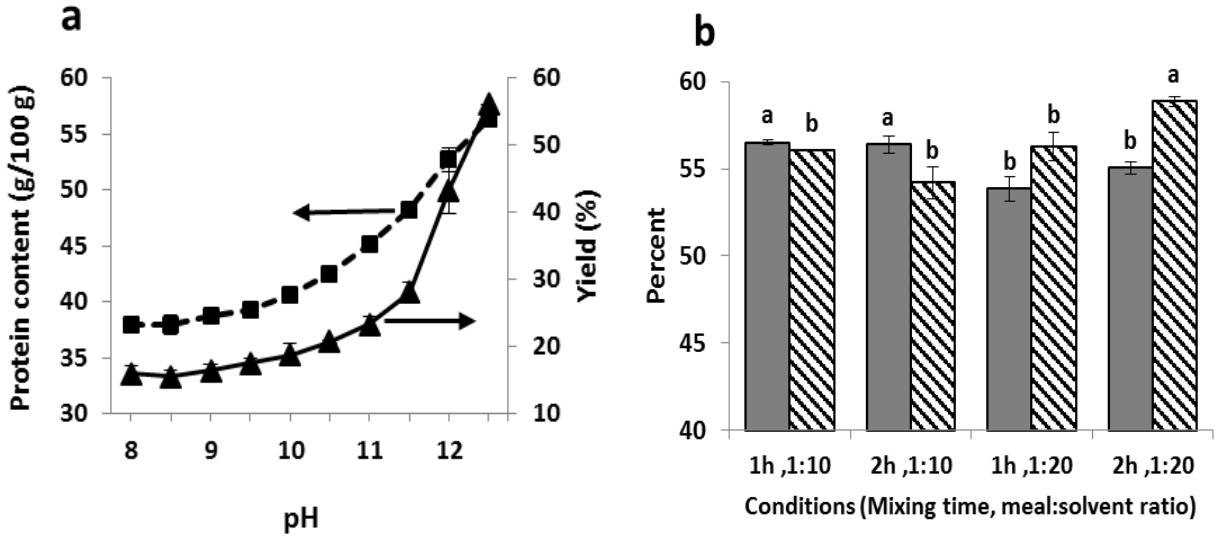

Figure 3.2. Effect of pH (a), shaking time and meal: solvent ratio (b) on protein extraction from canola meal. In part a: protein content (■) and yield (▲); in part b: protein content (gray) and yield (patterned). Columns with different lowercase letters are significantly ($p<0.05$) different. Error bars represent standard deviations, n=3.

SDS (sodium dodecyl sulfate), an anionic detergent, has ability to dissociate proteins hydrophobic bonds and as a result, solubilizes proteins through forming protein detergent complex. The protein content of our extracts decreased from 55.8±0.1 to 47±0.2% at increasing SDS concentrations from 0 to 2% (*Supplementary Figure 3.2*). This might be due to the binding ability of SDS to non-protein compounds which increased non-protein impurities. However, protein solubility was also

increased in the presence of SDS and as a result, more proteins were extracted and protein yield was increased from 56.1±0.6% to 73.3±2.1%. As a reducing agent, sodium sulfite might increase the solubility of canola proteins due to their less-compact structure after reduction. Our results showed that both protein content and yield decreased from 56±0.4 to 42.8±0.5% and 56.1±0.7 to 48.3±0.3%, respectively at increasing sodium sulfite concentrations from 0 to 1% (*Supplementary Figure 3.3*), which was in agreement with the results of Blaicher et al. (1983). Therefore, the optimal conditions for protein extraction from canola meal were determined at pH 12.5, 1 hour mixing time and meal: solvent ratio of 1:10.

3.3.2. Effect of acidic washing on protein extraction

The main purpose of acid washing prior to alkali extraction is to remove phenolic compounds and phytic acid from canola meal (Serraino and Thompson, 1984; Zhou et al., 1990). Phenolic compounds contribute to dark colour and unpleasant taste such as bitterness while phytic acid can bind with metal ions and make them unavailable for human body. Canola meal was first acid washed followed by alkaline extraction, resulting in an acidic extract (product I), alkaline extract (product II) and meal residue (product III) as shown in Figure 3.1. Figure 3.3a shows that the content of phytic acid in product I increased from 1.5% at pH 2.5 to 3% at pH 4.5 but decreased to 2.5% at pH 5. As expected, the content of phytic acid in the product II was decreased from 2.5% at pH 3 to 1.25% at pH 5. The phytic acid content in product III was almost constant around 0.5%. Acid washing at pH 2.5 removed 28% of total phytic acid compared to 47% at pH 4.5. Zhou, He, Yu, and Mukherjee (1990) reported that acidic washing at pH 4-5 could remove 50% of phytate. Gillberg and Tornell (1976) reported that pH could play a key role in removing phytic acid from the meal. However, the influence of pH on extractability of phytic acid is complicated. In an acidic medium, as both proteins and metal ions are positively charged, there is a competition between proteins and metal ions to form phytate complexes. At intermediate pH values (from 5 to 9), a ternary phytic acid-cation-protein complex is formed, leading to increased extractability of both protein and phytic acid (Tzeng et al., 1990); adding chelating agents however can remove metal ions, disrupt the complex, and therefore prevent the formation of the protein-phytate complex (Serraino and Thompson, 1984). At increasing pHs (from 10 to 12), since the number of positive charges in protein molecules decreases substantially, protein-phytic acid complexes become instable and the solubility of phytic acid decreases (Gillberg and Tornell, 1976). Therefore,

removing phytic acid in the acidic washing prevented the formation of protein-phytic acid complexes in the following alkaline extraction.

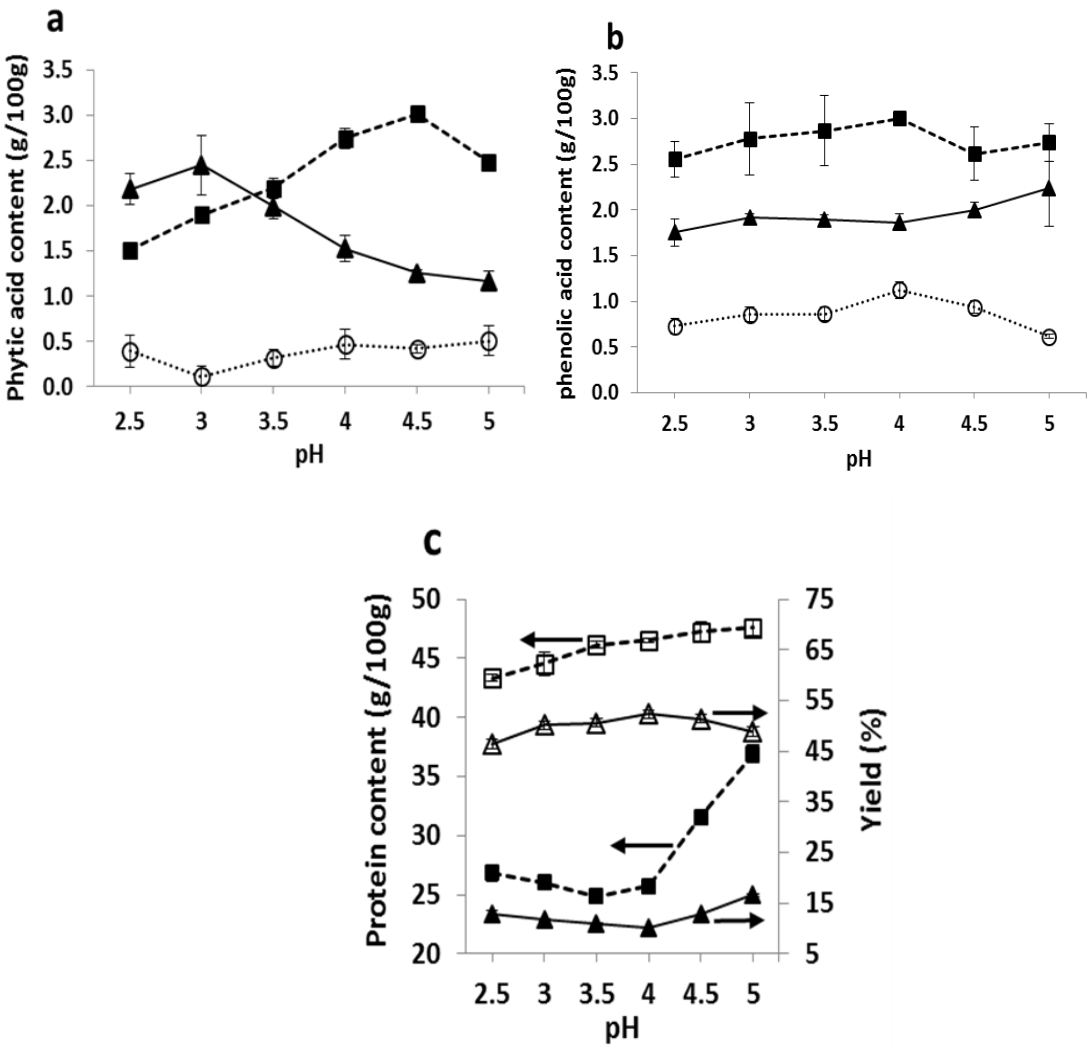

Figure 3.3. Effect of pH in acidic washing on phytic acid content (a) and phenolic compounds content (b) of different products (product I (■), product II (▲), product III (○)), and the protein content (product I (■) and product II (□)) and protein yield (product I (▲) and product II (Δ)) of the products(c). Error bars represent standard deviations, n=3.

Our results showed that the phenolic acid contents of the acidic extracts, alkaline extracts, and residuals were not affected by pHs from 2.5 to 4.0 (Figure 3.3b). During the acidic washing, 33-40% of total phenolic compounds were removed from the meal before protein extraction. As the amount of phenolic compounds removed by the acidic washing was not affected by changing pH,

the acidic washing just removed free phenolic compounds. Xu and Diosady (2000) suggested that phenolics in canola meal are mainly present in free forms and also phenolic-protein complexes formed through hydrogen, covalent and ionic bonding, and hydrophobic interactions. Since the high pH used in the following alkaline extraction enhances dark colour of the protein extract by increasing electrostatic interactions between positively charged sinapine and negatively charged proteins (Xu and Diosady, 2000), removing the free phenolics in the acidic washing could improve the quality of the final protein extract.

Due to the different isoelectric points of these two major proteins, acid washing could solubilize napin but keep cruciferin insoluble in the residue (Aluko and McIntosh, 2001; Wanasundara, 2011). As shown in Figure 3.3c, the protein content and yield of product I were almost constant from pH 2.5 to 4 but increased at pHs 4.5 and 5. SDS-PAGE of products I at different pHs were shown in Figure 3.4. Two major bands with estimated molecular weights of 10 and 15 kDa, representing napin polypeptides, were observed in the extracts of pHs 2.5 to 4. At increasing pH to 4.5 and 5, the intensity of 20, 25, 30 and 50 kDa bands, showing cruciferin subunits, remarkably increased. The increased protein content and yield of product I at these pHs were due to the presence of cruciferin protein in the extracts of pH 4.5 and 5 (Figure 3.3c).

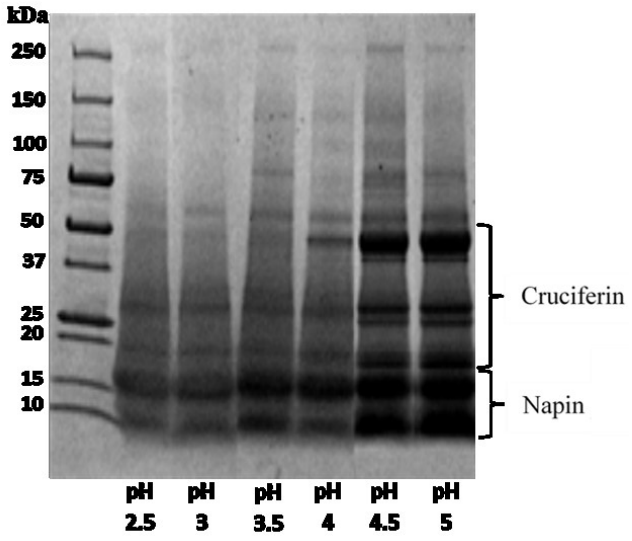

Figure 3.4. SDS-PAGE of products I extracted at different pHs

The protein content of product II after acid washing increased at increasing pHs from 2.5 to 5; similar trend existed for the yield but started to decrease from pH 4 to 5 (Figure 3.3c). Considering phytic acid and phenolic compounds removal, as well as cruciferin extractability and yield, pH 4 was determined for acid washing prior to alkaline extraction. Using this pH, in addition to removing phenolic compounds and phytic acid, cruciferin was separated from extracted napin in the acidic washing.

3.3.3. Preparation of cruciferin and napin

Based on above results, an approach including acid precipitation was proposed for cruciferin extract (product V). Acid precipitation at pH 4.0 showed higher protein content (91%) and yield (38.6%) than those of pH 4.5 (85.7 and 35%, respectively). Using alkaline extraction of commercial canola meal followed by acid precipitation, canola protein extracts were reported to contain 82.6 and 83.5% protein contents and yields of 22 and 18% by Tzeng et al. (1990) and Tan et al. (2011), respectively. Our results are favourably comparable to previous results. Resultant supernatant after centrifuging the precipitated cruciferin (product IV) and product I both contained napin. Products I and IV were combined and subjected to membrane processing to prepare napin product (Figure 3.1). Concentration factor (CF) and diavolume (DV) are two factors affecting the concentration of compounds in retentate and permeate in ultrafiltration and diafiltration, respectively. CF is defined as the degree of increasing the concentration of components in a membrane operation whereas DV is total buffer volume introduced to the operation during diafiltration divided by the initial retentate volume. The results indicated that using higher CF is more effective to increase protein content and yield than higher DV (Table 3.1). CF=20 and DV=10 were used in the membrane processing to prepare napin product (product VI) with a protein content of 82% and a yield of 12.5%. Proximate analysis of cruciferin and napin products and residue (products V, VI and III, respectively) were shown in Table 3.2. In summary, more than 51% of total canola meal protein was recovered in the two products of cruciferin and napin. This showed a remarkable increase in protein extractability compared to the previously reported protein yields of 33 and 27%, obtained using an alkaline extraction and Osborn method, respectively (Tzeng et al., 1990; Tan et al., 2011). In addition to its high protein recovery, another advantage of the proposed method is the removal of as high as 90 and 82% of initial phytic acid and phenolic

compounds, respectively; phytic acid and phenolic compounds are known to impair protein digestibility and functionalities.

Table 3.1. Effect of different concentration factors (CF) and diavolume (DV) on purification of products I and IV (mean ± standard deviations, n=3). Values with different lowercase letters in the same row are significantly ($p<0.05$) different.

	CF=10, DV=5	CF=20, DV=5	CF=20, DV=10
Protein content (%)	68.5±1.1[b]	78.6±2.0[a]	81.9±1.2[a]
Protein yield (%)	13.5±0.6[b]	15.7±0.8[a]	12.4±0.4[b]

Table 3.2. Proximate analysis of napin and cruciferin products and meal residue (mean ± standard deviations, n=3).

	Protein		Phytic acid	Phenolic	Ash	Fiber	Fat
	content %	yield %	content %	Content %	content %	content %	content %
Napin product	81.9±1.2	12.4±0.4	0.9±0.2	0.6±0.3	7.8±0.9	0.10±0.05	0.5±0.1
Cruciferin product	91.2±2.0	38.6±1.1	1.5±0.3	1.8±0.2	2.7±0.1	0.10±0.04	1.0±0.1
Meal residue	35.7±3.0	38.7±2.2	0.5±0.2	1.1±0.3	9.5±0.8	52.3±1.9	1.5±0.2

3.3.4. SDS-PAGE analysis of canola proteins

SDS-PAGE of canola meal, cruciferin and napin fractions in the presence and absence of 2-mercaptoethanol (ME) were shown in Figure 3.5. There are five major bands with estimated molecular weights of 15, 18, 27, 30 and 50 kDa in canola meal (lane 2, in the absence of ME); similar four major bands of 16, 18, 30 and 53 kDa in canola meal by Aluko and McIntosh (2001). Wu and Muir (2008) reported eight major bands with molecular weights ranging from 14 to 59 kDa. The characteristic bands for cruciferin are in the range of ~18-50 kDa, while for napin ranging from 5 to ~15 kDa. In the presence of reducing agent (lane 3), the band at 50 kDa was dissociated and a new band at ~20 kDa appeared and the intensity of ~27 and 30 kDa bands increased. Similar results were reported by Aluko and McIntosh (2001). Wanasundara (2011) showed that cruciferin in reducing conditions is dissociated to α-polypeptides and β-polypeptides chains with molecular weights ranging from 26.7 to 37.1 kDa and 18.3-22.9 kDa, respectively. The band of 15 kDa (lane

2) was also dissociated to two bands at ~5 and 10 kDa (lane 3); similar results were reported by Wu and Muir (2008) and Wanasundara (2011). The polypeptide compositions of cruciferin products with and without ME were shown in lanes 4 and 5, respectively. The smeared bands in lane 4 revealed that cruciferin polypeptides were partially unfolded in the alkaline extraction and then aggregated on SDS-PAGE gel. Band smearing in SDS-PAGE was also previously reported for alkaline protein extraction from rapeseed (Rommi et al., 2015), triticale (Bandara et al., 2011) and corn (Cookman and Glatz, 2009). Adding ME (lane 5) improved the separation as also reported by Rommi et al. (2015). The polypeptides bands in lane 5 are similar to those in lane 3 (reduced canola meal), suggesting this extract is cruciferrin. The napin fraction showed a major band at ~15 kDa (lane 6) and was dissociated into two bands at ~5 and 10 kDa in the presence of ME (lane 7). Berot et al. (2005) confirmed that napin, with a molecular weight of ~15 kDa, is composed of two polypeptides with molecular weights of ~10 and 5 kDa, and linked by four disulphide bonds.

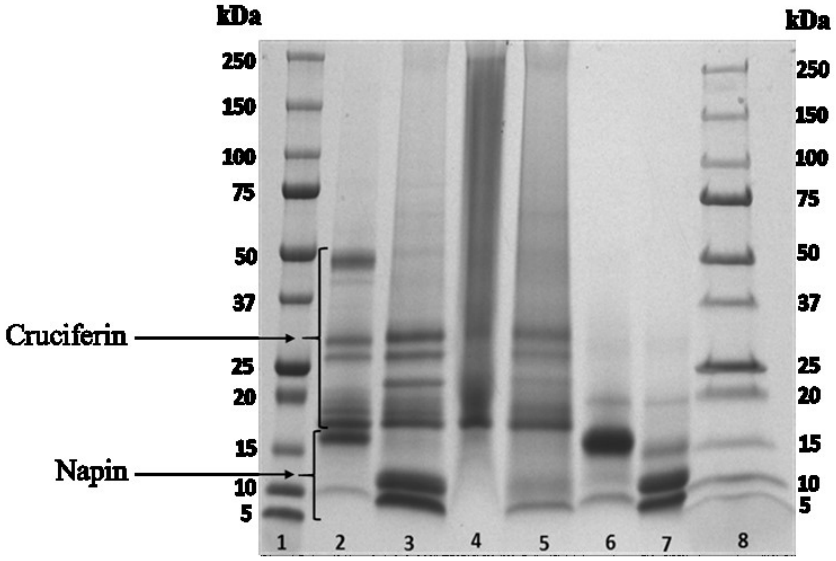

Figure 3.5. SDS-PAGE of canola meal (lanes 2 and 3), cruciferin (lanes 4 and 5) and napin products (lanes 6 and 7). Lanes 1 and 8: molecular weight markers, lanes 2, 4 and 6: in the absence of β-mercaptoethanol, while lanes 3, 5 and 7: in the presence of β-mercaptoethanol.

3.3.5. Functional properties

Emulsion prepared by cruciferin had a mean particle size of 1.4 (±0.05) μm and stability of 98.7%, which was close to our previous results showing mean droplet size and emulsion stability of 1.4

μm and 97.7%, respectively (Wu and Muir, 2008). In comparison, emulsion prepared by napin had a mean particle size of 8.9 (±0.07) μm and the aqueous and oil phases were separated after 5 min standing at room temperature. Napin is a strongly basic protein; the low emulsifying property of napin might be due to the abundance of basic amino acids which are not favourable for hydrophobic groups of oil phase. Wu and Muir (2008) showed that napin had deteriorating effect on the emulsifying property of canola proteins. EAI value of our cruciferin product (32.3 m^2/g) was also comparable with that of calcium-precipitated (35.1 m^2/g) and isoelectric-precipitated canola protein (15.0 m^2/g) (Karaca et al., 2011) and was in the range of 22 - 41.8 m^2/g for isoelectric-precipitated protein of different canola varieties (Aluko and McIntosh, 2001). As shown in Table 3.3, the foaming capacity and stability of cruciferin and napin products were better than the protein isolate extracted by Chabanon et al. (2007). The foaming capacity and foaming stability of napin were higher than those of cruciferin; Chabanon et al. (2007) reported similar results. The functional properties studies revealed that the properties of cruciferin and napin products were conserved in our developed method.

Table 3.3. Foaming capacity* and stability** of cruciferin and napin products (mean ± standard deviations, n=3).

Product	Foaming capacity (%)	Foaming stability (%)		
		30 min	60 min	120 min
Cruciferin	97±11	84±4	77±4	69±5
Napin	134 ±14	89±6	85±5	79±6

*The foaming capacity was calculated as the ratio of formed foam volume to initial protein solution volume (expressed as percentage). **The foaming stability was expressed as the percentage of foam remaining after 30, 60 and 120 min at room temperature.

3.4. Conclusions

Extraction of canola proteins has been a long-existing challenge due to the complexity of the canola proteins and the presence of various undesirable compounds. Therefore, removing undesirable compounds while obtaining canola proteins at satisfactory purity and yield are important considerations during canola protein extraction process. Unlike previous extraction methods, acidic washing was applied to remove phytic acid and phenolic compounds from the meal prior to protein extraction; the application of acidic washing increased the extractability of proteins in following alkaline extraction otherwise might form complexes with proteins at alkaline

pH during extraction. Since no organic solvent or toxic chemical was used, the method represents an environment friendly process. In addition to the favourable purity and yield of the cruciferin and napin, they showed good emulsifying and foaming properties. Canola proteins have unique functional and biological properties; the development of a simple and scalable method of isolation will facilitate our further research on their food and non-food applications.

3.5. References

Aider, M. & Barbana, C. (2011). Canola proteins: composition, extraction, functional properties, bioactivity, applications as a food ingredient and allergenicity - a practical and critical review. *Trends in Food Science & Technology,* 22(1), 21-39.

Aluko, R. & McIntosh, T. (2005). Limited enzymatic proteolysis increases the level of incorporation of canola proteins into mayonnaise. *Innovative Food Science & Emerging Technologies,* 6(2), 195-202.

Aluko, R. & McIntosh, T. (2001). Polypeptide profile and functional properties of defatted meals and protein isolates of canola seeds. *Journal of the Science of Food and Agriculture,* 81(4), 391-396.

AOAC. (2000). Official Methods of Analysis. (17th ed). Washington, DC: Association of Official Analytical Chemists.

Bandara, N., Chen, L., & Wu, J. (2011). Protein extraction from triticale distillers grains. *Cereal Chemistry*, 88(6), 553-559.

Berot, S., Compoint, J., Larre, C., Malabat, C., & Gueguen, J. (2005). Large scale purification of rapeseed proteins (*Brassica Napus L.*). *Journal of Chromatography B-Analytical Technologies in the Biomedical and Life Sciences,* 818(1), 35-42.

Blaicher, F., Elstner, F., Stein, W., & Mukherjee, K. (1983). Rapeseed protein isolates - effect of processing on yield and composition of protein. *Journal of Agricultural and Food Chemistry,* 31(2), 358-362.

Canola Council of Canada. (2007). Canola, growing great 2015. URL http://www.canolacouncil.org/media/502091/growing_great_pdf.pdf. Accessed December 12, 2013).

Chabanon, G., Chevalot, I., Framboisier, X. Chenu, S., & Marc, I. (2007). Hydrolysis of rapeseed protein isolates: Kinetics, characterization and functional properties of hydrolysates. *Process Biochemistry,* 42, 1419-1428.

Cookman, D. J. & Glatz, C. E. (2009). Extraction of protein from distiller's grain. *Bioresource Technology*, 100, 2012-2017.

Deak, N. A., Murphy, P. A., & Johnson, L. A. (2006). Effects of NaCl concentration on salting-in and dilution during salting-out on soy protein fractionation. *Journal of Food Science,* 71(4), C247-C254.

Gillberg, L. & Tornell, B. (1976). Preparation of rapeseed protein isolates - dissolution and precipitation behavior of rapeseed proteins. *Journal of Food Science,* 41(5), 1063-1069.

Haug, W. & Lantzsch, H. (1983). Sensitive method for the rapid-determination of phytate in cereals and cereal products. *Journal of the Science of Food and Agriculture,* 34(12), 1423-1426.

Karaca, A. C., Low, N., & Nickerson, M. (2011). Emulsifying properties of canola and flaxseed protein isolates produced by isoelectric precipitation and salt extraction. *Food Research International*, 44, 2991-2998.

Marczak, E., Usui, H., Fujita, H., Yang, Y., Yokoo, M., Lipkowski, A., & Yoshikawa, M. (2003). New antihypertensive peptides isolated from rapeseed. *Peptides,* 24(6), 791-798.

Rommi, K., Ercili-Cura, D., Hakala, T. K., Nordlund, E., Poutanen, K., & Lantto, R. (2015). Impact of total solid content and extraction pH on enzyme-aided recovery of protein from defatted rapeseed (*Brassica rapa L.*) press cake and physicochemical properties of the protein fractions. *Journal of Agricultural and Food Chemistry*, 63, 2997-3003.

Serraino, M. & Thompson, L. (1984). Removal of phytic acid and protein phytic acid interactions in rapeseed. *Journal of Agricultural and Food Chemistry,* 32(1), 38-40.

Tan, S. H., Mailer, R. J., Blanchard, C. L., & Agboola, S. O. (2011). Extraction and characterization of protein fractions from Australian canola meals. *Food Research International,* 44(4), 1075-1082.

Tzeng, Y., Diosady, L., & Rubin, L. (1990). Production of canola protein materials by alkaline extraction, precipitation, and membrane processing. *Journal of Food Science,* 55(4), 1147-1156.

Uruakpa, F. & Arntfield, S. (2006). Impact of urea on the microstructure of commercial canola protein-carrageenan network: A research note. *International Journal of Biological Macromolecules,* 38(2), 115-119.

USDA. (2013). Major oilseeds: World supply and distribution. United States Department of Agriculture. URL http://apps.fas.usda.gov/psdonline/circulars/oilseeds.pdf. Accessed December 13, 2013.

Wanasundara, J. P. D. (2011). Proteins of *Brassicaceae* oilseeds and their potential as a plant protein source. *Critical Reviews in Food Science and Nutrition,* 51(7), 635-677.

Wu, J. & Muir, A. D. (2008). Comparative structural, emulsifying, and biological properties of 2 major canola proteins, cruciferin and napin. *Journal of Food Science,* 73(3), C210-C216.

Wu, J., Aluko, R. E., & Muir, A. D. (2009). Production of angiotensin I-converting enzyme inhibitory peptides from defatted canola meal. *Bioresource Technology,* 100(21), 5283-5287.

Xu, L. & Diosady, L. (2000). Interactions between canola proteins and phenolic compounds in aqueous media. *Food Research International,* 33(9), 725-731.

Xu, L. & Diosady, L. (1997). Rapid method for total phenolic acid determination in rapeseed/canola meals. *Food Research International,* 30(8), 571-574.

Yamada, Y., Iwasaki, M., Usui, H., Ohinata, K., Marczak, E. D., Lipkowski, A. W., & Yoshikawa, M. (2010). Rapakinin, an anti-hypertensive peptide derived from rapeseed protein, dilates mesenteric artery of spontaneously hypertensive rats via the prostaglandin IP receptor followed by CCK1 receptor. *Peptides,* 31(5), 909-914.

Yoshie-Stark, Y., Wada, Y., & Waesche, A. (2008). Chemical composition, functional properties, and bioactivities of rapeseed protein isolates. *Food Chemistry,* 107(1), 32-39.

Zhou, B., He, Z., Yu, H., & Mukherjee, K. (1990). Proteins from double-zero rapeseed. *Journal of Agricultural and Food Chemistry,* 38(3), 690-694.

3.6. Appendix A: Supplementary Information

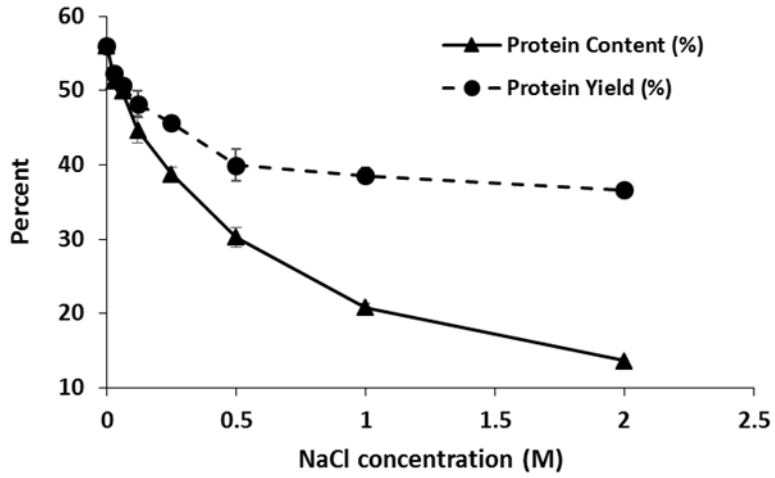

Supplementary Figure 3.1. Effect of NaCl concentration on canola protein extraction at pH 12.5

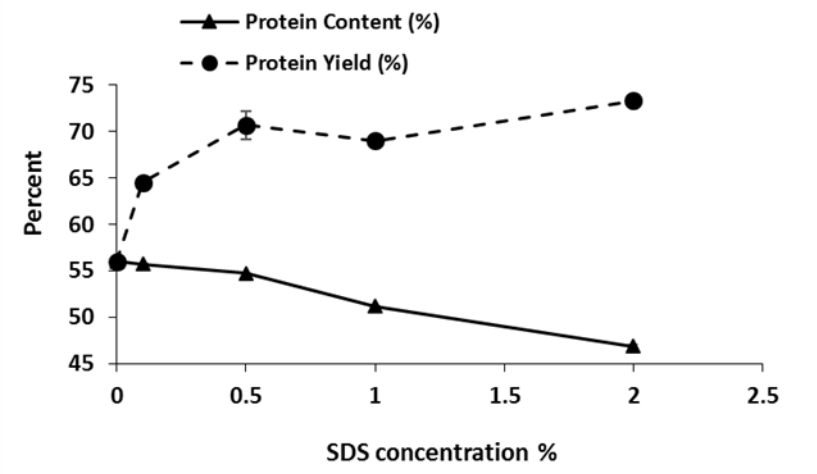

Supplementary Figure 3.2. Effect of SDS concentration on canola protein extraction at pH 12.5

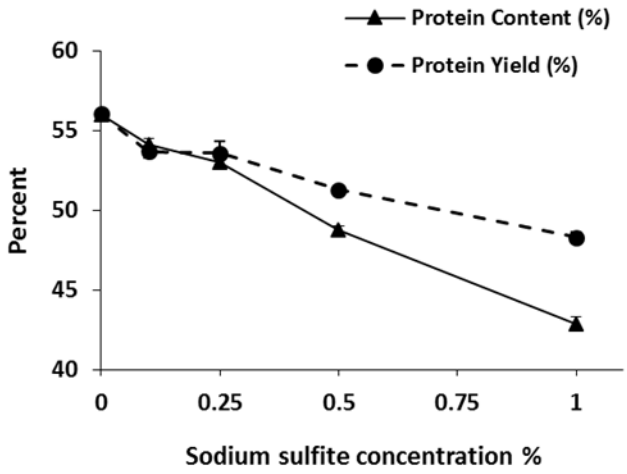

Supplementary Figure 3.3. Effect of sodium sulfite concentration on canola protein extraction at pH 12.5

CHAPTER 4-Cruciferin nanoparticles: preparation, characterization and their potential application in delivery of bioactive compounds

A version of this chapter has been published: Akbari, A. & Wu, J. (2016). Cruciferin nanoparticles: Preparation, characterization and their potential application in delivery of bioactive compounds. *Food Hydrocolloids,* 54, 107-118.

4.1. Introduction

Canola including rapeseed, with an annual production of 70 million metric tonnes, now ranks as the second most abundant oilseed in the world (USDA, 2013). The meal after oil extraction contains 35-40% proteins; canola proteins are potential food proteins due to its well-balanced amino acid composition, high amount of lysine (6.0%) and sulfur-containing amino acids (3 to 4%), and high protein efficiency ratio (2.64) (Tan et al., 2011; Wu and Muir, 2008). Furthermore, canola proteins were reported to show good emulsifying and gelling properties, or can be used as a precursor for bioactive peptides (Wu and Muir, 2008; Wu et al., 2009; Yamada et al., 2010; Yoshie-Stark et al., 2008). Canola contains two major proteins, cruciferin (12S globulin) and napin (2S albumin), accounting for 65% and 25% of total canola proteins, respectively. Cruciferin, with an isoelectric point (pI) of around 7.2 and a molecular weight of 300 kDa is composed of six subunits. Napin, a strongly basic protein (isoelectric point around 11), is composed of two subunits of 4.5 and 9.5 kDa (Wanasundara, 2011).

Proteins showing good emulsifying and gelling properties might also be used in delivery system. Food proteins are generally recognized as safe (GRAS), biocompatible, and biodegradable natural polymers. In addition to their ability to interact with different drug or nutraceutical compounds via multiple functional groups, proteins have capacity to protect the compounds within their three-dimension gel networks (Elzoghby et al., 2012). To the best of our knowledge, the potential use of canola proteins in delivery systems has not been explored. Most of food proteins form heat-set hydrogels where different compounds can be entrapped and slowly be released. However, heat-set gels may not be suitable for encapsulation of heat-sensitive compounds. An alternative method is protein cold gelation where protein solution is preheated and then a network of the soluble protein aggregates is formed using multivalent ions; the bioactive compounds are added before forming the network. This method was first explored with whey protein (Barbut and Foegeding, 1993) and then effects of different salts (Bryant and McClements, 2000), sucrose (Kulmyrzaev et al., 2000) and pH and ageing time on the gelation (Cavallieri and Da Cunha, 2008) were studied. This method was further applied to study other proteins such as β-lactoglobulin (Remondetto and Subirade, 2003), soy protein (Maltais et al., 2005; Maltais et al., 2008), and bovine serum albumin (Kundu et al., 2013). Using this method, proteins can form gel individually or in combination with other polymers. This method has been used for preparing cold, gel-like soy protein emulsions (Tang and Liu, 2013) , delivery of probiotics using whey protein micro-beads (Doherty et al., 2011), forming

ion-induced whey protein aerated gel (Tomczynska-Mleko, 2013), and whey protein/alginate hydrogel microparticles for oral delivery of insulin (Deat-Laine et al., 2013).

Due to resistance of cruciferin to gastric enzymes (Bos et al., 2007), it was hypothesized that cruciferin particles can protect bioactive compounds in the gastric conditions. The objectives of this study were to prepare canola proteins nanoparticles using the cold gelation method and to evaluate their potential for encapsulation and protection of model compounds. We showed that calcium-induced cruciferin (Cru/Ca) particles are promising carriers for delivery of nutraceutical compounds.

4.2. Materials and methods

4.2.1. Materials

Commercial canola meal, obtained from Richardson Oilseed Company (Lethbridge, AB, Canada) was ground, passed through a 35-mesh screen and stored at -20 °C for further use. Caco-2 cells (HTB37) were obtained at passage 19 from the American type culture collection (Manassas, VA). Dulbecco's modified eagle medium (DMEM), 0.25% (w/v) trypsin-0.53 mM EDTA, 4-(2-hydroxyethyl)-1-piperazineethanesulfonic acid (HEPES), fetal bovine serum, 1% nonessential amino acids, and 1% antibiotics were all procured from Gibco Invitrogen (Burlington, ON, Canada). 3-(4,5-dimethylthiazol-2-yl)-2,5-diphenyltetrazolium bromide (MTT), dimethyl sulfoxide (DMSO), 1-anilinonaphthalene-8-sulfonic acid (ANS), coomassie brilliant blue G-250, β-carotene, urea, sodium dodecyl sulfate (SDS), dithiothreitol (DTT), pepsin, pancreatin, Coumarin 6 and 4',6-diamidino-2-phenylindole (DAPI) were obtained from Sigma (Oakville, ON, Canada).

4.2.2. Canola protein extraction

Canola proteins, cruciferin and napin, were extracted using the method we previously developed (Akbari and Wu, 2015). A slurry of canola meal:water (1:10, w/v) was acidified to pH 4, stirred for 2 h and centrifuged at 10,000 rpm for 20 min at 4°C. The resultant pellet was mixed with 10X volume of water, and the pH was adjusted to 12 while stirring at room temperature for 1h. After centrifugation, the supernatant was adjusted to pH 4 to precipitate proteins. The collected precipitate was washed twice with acidified water (pH 4), centrifuged and freeze-dried as cruciferin isolate. The supernatants obtained from acidic washing and protein precipitation were combined (pH 4) and subjected to an ultrafiltration system (Millipore, Bedford, MA, US) to

remove salts and anti-nutritional compounds using a 10 kDa membrane; the protein solution was concentrated and filtered at the concentration factor of 20 and diavolume of 10, respectively. The obtained retentate was freeze dried as napin.

4.2.3. Preparation of particles

Canola protein nanoparticles were prepared using the cold gelation method used by Barbut and Foegeding (1993), Marangoni et al. (2000), Maltais et al. (2005), Remondetto and Subirade (2003) and Zhang et al. (2012) with some modifications. Effects of preheating temperatures, pHs and calcium concentrations on cold gelation of cruciferin and napin were studied. In brief, 18 mL cruciferin and napin dispersions (10 mg/mL) in MQ-water were stirred for 1h at 500 rpm and then the pH was adjusted to 12 using 1M NaOH. After stirring for 1h, the protein solutions were heated at 95°C and 120°C for 30 min in tightly closed tubes. After 0.5h cooling at room temperature, the protein solutions were diluted with 12 mL water containing 0.06% w/v sodium azide and the pH was adjusted to 7, 8, 9 and 10 using 1M HCl. Afterward, 6 mL of 9, 18, 27 and 36 mM $CaCl_2$ was added drop by drop to the protein solutions (at final $CaCl_2$ concentrations of 1.5, 3, 4.5 and 6 mM, respectively) while stirring to induce particle formation. The stability and turbidity of the particle suspensions were assessed to determine the appropriate conditions for particles formation. The stability of the particles was studied for a period of 3 weeks stored at 4°C. The turbidity was measured at 600 nm using a UV/VIS spectrophotometer (V-530 Jasco, Japan). The dispersions containing stable particles with at least 50% increase in the turbidity compared to the initial protein solution turbidity were considered as appropriate particle dispersions. Effects of cruciferin concentrations (5, 10, 15, and 20 mg/mL), final $CaCl_2$ concentrations of 1.5 and 3 mM, and pHs 8, 9, 10 on the particle formation at preheating temperature of 120°C were also studied.

4.2.4. Particles characterization

4.2.4.1. Size, surface charge and morphology of particles

Size of the particles was determined by dynamic light scattering using Malvern Nanosizer ZS (Malvern, Worcestershire, UK). Zeta potential of the particles was also measured by laser doppler velocimetry using the Nanosizer. Prior the measurements, samples were diluted in 10 mM phosphate buffers (the same pH as particle suspensions) to obtain a slight opalescent dispersion and prevent multiple scattering effects. Morphology of the prepared particles was studied using a transmission electron microscopy (TEM, Philips Morgagni 268, FEI Company, The Netherlands)

at 80 kV. The particles were freshly prepared, put on Formvar-covered copper grids, negatively stained with phosphotungstic acid, and then air dried.

4.2.4.2. Protein conformation studies

The conformational changes of cruciferin before and after heating as well as after particle formation were characterized using Circular Dichroism (CD), Fourier transform infrared (FTIR) and fluorescence spectrophotometer. The far-UV CD spectra of the protein samples (1 mg/mL) at pH 9 were measured using Olis DSM 17 Circular Dichroism (GA, USA). The path length of the quartz cell was 0.2 cm and the spectra represented an average of five scans collected in 1-nm steps at a rate of 20 nm/min over the wavelength range of 190-250 nm.

For FTIR, the freeze-dried samples were dried in a vacuum desiccator using phosphorous pentoxide for 48 h. FTIR spectra of the milled samples in KBr pellets were recorded in the range of 4000–400 cm^{-1} using a Thermo Fisher Scientific Nicolet 8700 FTIR spectrophotometer (Madison, WI, USA). The recorded spectra were deconvoluted in amide I band region (1700-1600 cm^{-1}) using Omnic 8.1 software at a bandwidth of 25 cm^{-1} and an enhancement factor of 2.5. The detected amide I bands in the spectra were assigned to protein secondary structures using previously established wavenumber ranges reported by Kong and Yu (2007) and Pelton and McLean (2000).

The intrinsic fluorescence emissions of the samples were measured using a Shimadzu RF-5301PC spectrofluorophotometer (Kyoto, Japan) equipped with a 1-cm path length quartz cell. The protein concentration and pH of the samples were adjusted to 5 mg/mL and pH 9, respectively. The fluorescence measurements were performed using excitation wavelength of 295 nm (slit width=5 nm) and the emission spectra were recorded from of 300 to 650 nm wavelength (slit width=5 nm) (Perez et al., 2014).

4.2.4.3. Surface hydrophobicity

Surface hydrophobicity of cruciferin before and after heating as well as after particles formation were determined using ANS fluorescent probe (Alizadeh-Pasdar and Li-Chan, 2000). Briefly, the samples were diluted to six concentrations ranging from 0.0006% to 0.012% using 0.1 M phosphate buffers at pHs 8, 9 and 10. 20 µL of 8 mM ANS prepared in the same buffer was added to 4 mL of the diluted protein solutions and fluorescence intensity at emission wavelength of 470 nm was measured using the spectrofluorophotometer. Excitation wavelength was 390 nm and slit

widths were 5 nm for both excitation and emission. Buffers containing ANS and protein solutions in the absence of ANS were blanks which were subtracted from the measured fluorescence values. The slope of the linear plot of net fluorescence values versus protein concentrations was used as an index of the protein surface hydrophobicity.

4.2.4.4. Driving forces involving the particles formation

The importance of hydrophobic, hydrogen and disulfide interactions were evaluated using SDS, urea and DTT, respectively. The particles suspension was mixed with the same volume of the dissociating agents at different concentrations. The mixtures were adjusted to pH 9 and vortexed 10 s and after 6 h, their turbidity were measured at 600 nm using the UV/VIS spectrophotometer. The turbidity of the mixtures was compared to that of initial particles suspension. Decrease of the turbidity of the mixtures was considered as an indicator of the degree of particles dissociation (Schmitt et al., 2010).

4.2.5. Effect of the particles on cell viability

Toxicity of the prepared particles on Caco-2 cells was assessed using MTT method. The MTT test measures the activity of dehydrogenase enzyme, which can convert MTT to insoluble purple formazan in Caco-2 cells. The formazan is dissolved in DMSO and the intensity of formed purple color determines the enzymes activity and cell viability. Caco-2 cells were seeded (50,000 cell/mL) in high-glucose and L-glutamine DMEM medium supplemented with 10% FBS, 1% non-essential amino acids, 1% penicillin and streptomycin, and 2.5% HEPES in a 96-well plate (200 µL/cell) and incubated at 37°C in a humidified incubator with 5% CO_2 for 24h. After incubation, the media in the wells was replaced with freshly prepared particles suspended in the DMEM medium at different concentrations of 0.5, 1.5, and 2.5 mg/mL. DMEM without nanoparticles was used as control. After 24h incubation, the particles were gently washed three times with PBS from the cells. 15 µL MTT (5 mg/mL in PBS) and 185 µL medium were added to the cells and incubated for 4h. Medium was removed and the formed formazan crystals were dissolved in 150 µL DMSO. Absorbance was measured at 570 nm using a microplate reader (GENios, Tecan, Mannedorf, Switzerland). Relative cell viability (%) was calculated comparing the absorbance of particle cells with that of control cells (Slutter et al., 2009).

4.2.6. Cell uptake of particles

To study the cell uptake of nanoparticles in Caco-2 cells, coumarin 6 (C6), as a fluorescent marker, was encapsulated into the Cru/Ca nanoparticles. The cellular uptake of C6-loaded Cru/Ca was compared with free C6 (not encapsulated). In brief, 0.5 mL C6 solution in ethanol with concentrations ranging from 0.08 to 80 µg/mL was added to 9 mL of 10 mg/mL heated cruciferin solution (pH 9). After diluting the protein/C6 solution with 6 mL water (pH 9), 3 mL of 9 mM $CaCl_2$ was added dropwise to the solution while stirring. After 2 h stirring, the suspension was centrifuged at 40000 ×g and 4 °C for 30 min, and the loaded particles pellet was collected, washed twice with water and centrifuged to remove free C6. The labelled particles were re-suspended in DMEM medium at concentrations of 0.05 and 0.5 mg/mL. Caco-2 cells (10^5 cells/well) were seeded on cover glasses placed in 6-well plates (Costar, Corning, NY), and incubated until cells were about 80% confluent (Luo et al., 2013). 2.5 mL labelled-particles suspensions or free C6 solution in DMEM medium was added to each well and incubated for 6 h at 37 °C. Then, the cells were washed three times with PBS to remove free nanoparticles and C6. Cell membranes were stained with 10 µg/mL Alexa Fluor 594-Concanavalin A conjugate in PBS for 10 min. After three-time washing with PBS, the cells were fixed using ice-cold solution of 3.7% formaldehyde for 30 min. Cell nuclei were also stained with 0.3 µg/mL DAPI for 10 min and three times washing with PBS. The coverslips covered with fixed cells were removes from the wells, inverted on slides containing 40 µL of 90% glycerol in PBS, then dried overnight in dark and room temperature, and kept at 4 °C. The cells were observed with a CLSM 510 Meta confocal laser scanning microscope (Carl Zeiss Microscopy, Jena, Germany) using an oil immersion objective (63×) and wavelengths of 405, 561 and 488 nm to visualize cell nuclei, membranes and labelled particles, respectively. Images were processed with ZEN 2011 LE software (Carl Zeiss, AG, Oberkochen, Germany) (Gaumet et al., 2009; He et al., 2013).

4.2.7. Encapsulation of model compounds

Encapsulation capacity of the particles was assessed using both water-soluble and water-insoluble compounds.

4.2.7.1. Encapsulation of a water-soluble model compound

Brilliant Blue (BB) was used as a water-soluble model drug. BB encapsulated Cru/Ca particles were prepared by adding 12 mL BB solution (1 mg/mL) containing 0.06% (w/v) sodium azide to

18 mL cruciferin solution (10 mg/mL, pH 9), and then 6 mL 9 mM $CaCl_2$ was added (final concentration 1.5 mM) to induce BB-loaded Cru/Ca particles. After stirring for 30 min, the particle suspension was centrifuged at 40,000 ×g and 4 °C for 30 min, and the particle pellet was collected, washed twice with water (the same pH as suspension), and centrifuged to remove the adsorbed BB on the particle surface. The content of free BB in the combined supernatants was measured using the spectrophotometer at 590 nm. Encapsulation efficiency (EE) and loading capacity (LC) were calculated using the following equations.

$$EE(\%) = 100 \times (A-B)/A$$

$$LC(\%) = 100 \times (A-B)/C$$

where, *A* is mg of the model compound added to the initial suspension, *B* is mg of free compound (unencapsulated), and C is the weight of dried loaded particles (mg).

4.2.7.2. Encapsulation of a water-insoluble model compound

β-carotene was loaded in the particles using a solvent displacement technique (Chu et al., 2007). Due to its light sensitivity, all β-carotene-involved experiments were conducted in the dark. In preparing Cru/Ca particles, 6 mL β-carotene ethanol solution (0.5 mg/mL) was added to 18 mL cruciferin solution (10 mg/mL) at pH 9. The cruciferin solution was previously solubilized at pH 12 and heated at 120 °C. After diluting the protein/ β-carotene solution with 10 mL water (pH 9), 6 mL 9 mM $CaCl_2$ was added dropwise to the solution. After stirring 30 min, the suspension was concentrated to 30 mL using a rotary vacuum evaporator (Heidolph 2-Collegiate, Germany) at 50 °C. 1 mL of the concentrated suspension containing the loaded particles was mixed with 5 mL hexane, vortexed for 10 sec and then centrifuged at 10,000 rpm for 20 min at 4°C. The β-carotene extracted in the organic phase represented both unencapsulated and loosely-adsorbed β-carotene on the surface of particles. Absorbance of the organic phases was measured at 450 nm using the UV–VIS spectrometer and EE and LC were calculated (Mensi et al., 2013).

4.2.8. Simulated gastro-intestinal release study

Release experiments were performed in simulated gastric fluid (SGF) followed by simulated intestinal fluid (SIF) (Chen and Subirade, 2005; Mensi et al., 2013). BB- and β-carotene-encapsulated Cru/Ca particles separated from 18 mL particles suspensions (previously described) were re-suspended in 20 mL water pH 1.2 and 0.5 mg/mL pepsin. To study the effect of the enzyme on the release of encapsulated compounds in SGF, the release experiment was also performed in

the absence of pepsin. The release experiments were conducted at 37 °C in a water bath and under 100 rpm agitation. 0.5 mL-samples from the release media were withdrawn at predetermined intervals. 0.25 mL 1M sodium bicarbonate was added to the samples to increase pH to 7.4 and inactivate pepsin. BB-containing samples were centrifuged and released BB in supernatant was measured. β-carotene was extracted from the withdrawn samples using 2.5 mL hexane and quantified using the same method previously described. After 2 h incubation in SGF, pepsin was inactivated by raising pH to 7.4 using 10 mL 1M sodium bicarbonate and release study was followed in SIF medium by adding 5 ml 200 mM phosphate buffer pH 7.4 in the absence and presence of 0.5 mg/mL pancreatin. 0.5 mL samples were withdrawn at predetermined intervals. To stop pancreatin activity after sampling, BB-containing samples were heated at 90 °C for 5 min while for β-carotene samples, free β-carotene was immediately extracted using hexane. The concentrations of released BB and β-carotene in SGF and following SIF media were measured and their cumulative percentages were calculated based on the total amount of the initial loaded compounds.

4.2.9. Study of polypeptide profile of particles in release conditions

Sodium dodecyl sulphate polyacrylamide gel electrophoresis (SDS-PAGE) of unheated and heated cruciferin and Cru/Ca particles was carried out as described by Uruakpa and Arntfield (2006). Particles samples were withdrawn after 0.5, 2, 3, 5 and 7 h incubation in SGF and SIF (in the presence and absence of pepsin or cruciferin). The samples (50 µg protein) were run on Mini-Protean gels (4-20% gradient gels) and the gels were scanned using an Alpha Innotech gel scanner (Alpha Innotech Corp., San Leandro, CA) and the bands were analysed by FluorChem SP software.

4.2.10. Binding of β-carotene to particles

The interaction between encapsulated β-carotene and Cru/Ca particles was studied using the fluorescence quenching effect of β-carotene on the intrinsic fluorescence of tryptophan residue in cruciferin (Zimet and Livney, 2009). In brief, different concentrations of β-carotene, soluble in ethanol, were encapsulated in Cru/Ca particles as previously was explained. The intrinsic fluorescence of β-carotene-loaded particles, with β-carotene final concentration of 0.006 - 0.11 mg/mL, was measured using an excitation wavelength of 295 nm. The emission spectra were

recorded from of 300 to 600 nm wavelength. The emission intensities at 365 nm were also plotted as a function of β-carotene concentrations.

4.2.11. Stability of encapsulated β-carotene

The heat stability of encapsulated β-carotene in Cru/Ca particles was compared with free β-carotene. 6 mL of suspensions of free β-carotene or the β-carotene-encapsulated particles were adjusted to pH 7 or 4 using 3 mL 500 mM phosphate or citrate buffers, respectively. The mixtures were subjected to heat treatment at 75 °C for 30 min. β-carotene was extracted from the heated suspensions using the solvent extraction and then quantified using UV–visible spectroscopy method (Mensi et al., 2013; Saiz-Abajo et al., 2013).

4.2.12. Statistical analysis

Experiments were carried out in triplicates and results were statistically analysed using ANOVA and Duncan tests (version 9.2, SAS Institute Inc., Cary, NC, USA).

4.3. Results and discussion

4.3.1. Preparation of Cru/Ca particles

Since the denaturation temperatures of cruciferin and napin are 91 and 110°C, respectively (Wu and Muir, 2008), the preheating temperatures were performed at either 95 or 120°C. Our preliminary study showed that napin particles was not formed at all conditions tested, while preheating the cruciferin solution at 120°C, but not 95°C, followed by adding 1.5 and 3 mM $CaCl_2$ at pHs 8, 9 and 10 resulted in stable suspensions. As shown in Table 4.1, repulsion forces among particles due to the negative charges are responsible for the stable suspension. As will be explained later, soluble aggregates were first formed after heat treatment, due to the negative charge at pHs over 8, small networks were developed in the presence of Ca^{2+}, and, particles were formed resultant from aggregation of the networks. Since the charge of the soluble aggregates after 120°C preheating was higher than that after 95°C preheating (*Supplementary Table 4.1*), the formed particles at higher temperature were more stable due to enhanced repulsion forces compared to the particles after 95°C heat treatment. Since napin didn't form soluble aggregate after heating, no napin particle was formed in the presence of Ca^{2+} ions.

Further effects of cruciferin concentrations (5, 10, 15, and 20 mg/mL) on the particle formation were studied. The particles prepared from 20 mg/mL cruciferin were not stable and precipitated.

Since particles increased the turbidity of suspensions, a 50% increase in the suspension turbidity compared to initial protein solution was used as an indicator for an appropriate particles formation. Increased turbidity of the particles suspensions obtained from 5 mg/mL cruciferin was less, while those of 10 and 15 mg/mL cruciferin suspensions increased the turbidity more than 50%; therefore, concentrations of 10 and 15 mg/mL were chosen for measuring size and PDI.

Table 4.1. Effect of preheating (120°C) and adding $CaCl_2$ on zeta-potential (mV) of unheated, heated cruciferin and Cru/Ca particles (10 mg/mL) at different pH values. Values with different lowercase letters in the same column are significantly ($p<0.05$) different.

	Suspension pH			
Samples	8	9	10	12
Unheated	-24.2±1.9 ^{c}	-27.6±1.2 ^{c}	-29.5±1.6 ^{c}	-41.4±5.8 ^{b}
Heated (without $CaCl_2$)	-37.7±1.4 ^{a}	-40.4±2.0 ^{a}	-43.1±2.2 ^{a}	-69.8±2.9 ^{a}
Heating + 1.5 mM $CaCl_2$	-29.2±2.1 ^{b}	-33.0±2.1 ^{b}	-38.4±1.3 ^{b}	---
Heating + 3 mM $CaCl_2$	-21.3±1.4 ^{c}	-25.1±1.2 ^{d}	-26.8±1.2 ^{d}	---

4.3.2. Particle characterization

4.3.2.1. Zeta potential and particle size of particles

Surface charge of particles is an important parameter affecting their stability as well as their interactions with other particles. In this study, since the solubilising pH (pH 12) was higher than isoelectric point of cruciferin (7.1), unheated samples showed negative charge. Heat treatment of the cruciferin solutions at pH 12 increased deprotonation of amine and carboxylic groups (Sek, 2013) and exposed more charged groups leading to increasing negative charge. Ryan et al. (2012) also showed that negative charge of whey proteins and β-lacoglobulin increased after heating. As shown in Table 4.1, the negative charges of particles significantly increased at increasing pHs, due to the pH moved further away from the isoelectric point. Adding positively charged ions (Ca^{2+}) shielded the negatively charged carboxylic groups in the soluble aggregates and decreased their surface charge; therefore the negative charge of cruciferin particles significantly decreased at increasing $CaCl_2$ concentrations (Table 4.1). Multi-way ANOVA analysis also showed that there were significant interactions between pH and $CaCl_2$ concentrations in terms of influence on particles charge.

Depending on the pH, cruciferin and $CaCl_2$ concentrations, the size of particles ranged from 175 to 255 nm (Table 4.2). While no trend was observed in the size at various pHs, a higher $CaCl_2$ concentration tended to increase the particles size. Ca^{2+} ions played an important role in networking of soluble aggregates which eventually formed particles. Negative charge of the particles providing repulsion forces was the main force to prevent precipitation of the particles. As previously shown, the surface charge of soluble networks decreased with increasing Ca^{2+} concentration, leading to more aggregation and increased particle size. At a concentration to 15 mg/mL, the particle size was not affected by pH at 1.5 mM $CaCl_2$; however particles precipitated at 3 mM $CaCl_2$.

Table 4.2. Effect of cruciferin concentration, $CaCl_2$ concentration, and pH on the suspension turbidity, particle size and PDI of Cru/Ca nanoparticles. Values with different lowercase letters in the same column are significantly ($p<0.05$) different.

Cruciferin Conc. (mg/mL)	$CaCl_2$ concentration (mM)	pH	Increasing turbidity (%)	Size (nm)	PDI
10	1.5	8	56±0.6*	175±2 e	0.42±0.02 b
		9	79±0.1	207±5 d	0.27±0.01 e
		10	74±5	222±13 c	0.26±0.02 e
	3	8	99±4**	241±9 b	0.57±0.07 a
		9	100±0.8*	255±4 a	0.38±0.03 c
		10	26±0.5***	---	---
15	1.5	8	Precipitated particles****	---	---
		9	78±1.9	215±1 c	0.44±0.02 b
		10	76±5	218±3 c	0.31±0.02 d

* The particles were stable for less than 8 days; ** the particles were stable less than 2 days; *** Low turbidity of particles suspension **** Particles precipitated in 2 h.

In general, increasing pHs improved the stability of particles due to increasing particles surface charge. However, particles were less stable when 3 mM $CaCl_2$ was used (lower surface charge). PDI (polydispersity index), a parameter showing the "uniformity" of particles, is another important factor affecting particles physicochemical properties, biodistribution, bioavailability and potential biological fates in the body (Balogh et al., 2007; Lodhia et al., 2010; McClements, 2013). Since particles with lower PDI values are desirable, particles prepared at pHs 9 and 10 with lower PDI

were considered as appropriate pHs. Since pH 9 is relatedly mild for encapsulation of sensitive compounds, conditions were established at the pH of 9, concentration of 10 mg/mL cruciferin and 1.5 mM $CaCl_2$ to prepare stable (more than 3 weeks at 4°C) and uniform particles with ~200 nm diameter. Previous study suggested that M-cell rich layer in the small intestine, the most common route for particles uptake, can transfer particles in the range of 200-500 nm (He et al., 2012; Powell et al., 2010).

4.3.2.2. Conformational structures

Conformational changes of cruciferin structures (unheated, heated and particles) were studies using CD, FTIR and intrinsic fluorescence. Changes in CD spectra of the cruciferin samples were shown in Figure 4.1A. The presence of a zero-crossing spectrum at near 200 nm as well as a negative peak at 208 nm indicated that α-helix is the main secondary structure for the unheated cruciferin. After heat treatment, shift of the strong negative band from 208 nm to 200 nm suggested an increase in disordered structure (Nagano et al., 1995); this was complemented by a decreased α-helix indicated by increased negative ellipticity values at 208 nm. He et al. (2014) reported similar results for rapeseed protein isolate. Compared to the heated sample, in Cru/Ca particles, the disordered structure was increased slightly. Since the accuracy of CD for measuring turns and β-sheets are as low as 50 to 75% (compared to 97% for helices and 89% for other structures) (Ranjbar and Gill, 2009), secondary structures of the samples were also studied using FTIR. Deconvoluted FTIR spectra of amide I band region of the samples were compared with the previously established wavenumber ranges (Kong and Yu, 2007; Pelton and McLean, 2000). The strong absorption of IR at 1658 cm^{-1} indicated that α-helix was predominant in unheated cruciferin, although bands of 1637, 1692 and 1676 cm^{-1} presenting β-sheets and turns were also observed (Figure 4.1B). Due to using a high pH for cruciferin solubilisation, it is possible that some secondary structures might be lost; as a result, a few structures were detected in the spectra. In the heat treatment, α-helix peak was disappeared and two peaks at 1663 and 1610 cm^{-1} were appeared which have been assigned to 310–helices/unordered structured and β-sheet, respectively (Kong and Yu, 2007). In Cru/Ca particles spectrum, the intensity of the unordered structured peak increased and also two new structures of β-sheet (1623 cm^{-1}) and β-turn (1685 cm^{-1}) were appeared. The band of 1623 cm^{-1} is assigned to intermolecular β-sheets resulting from hydrogen bonds formed in the particle aggregation (Gilbert et al., 2005). Results from CD and FTIR analysis

suggested that α-helix was decreased and the predominant structures were disordered structure and β-sheets/turns in the heated samples and particles, respectively. Therefore, the denatured cruciferin structures (due to high pH and temperature) were reorganized during the heat treatment and the preparation of particles.

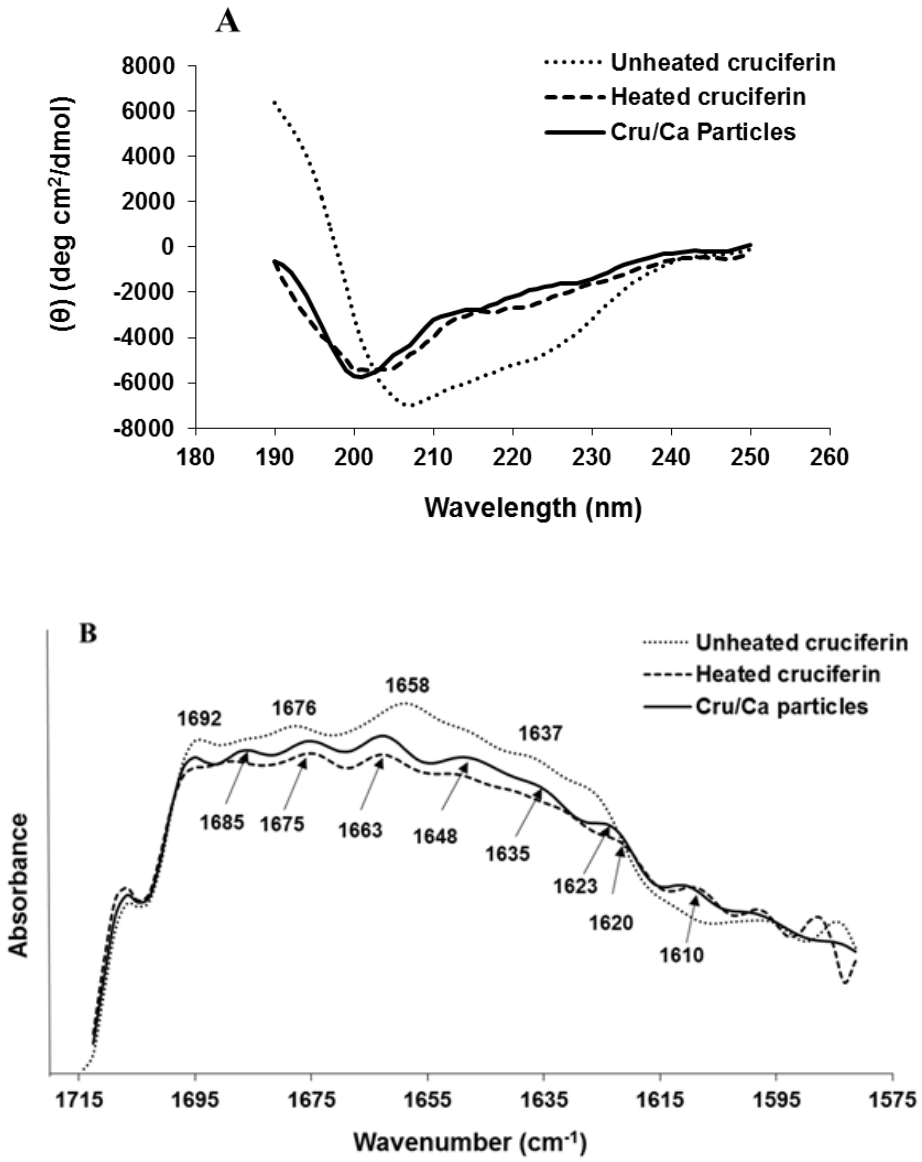

Figure 4.1. Far-UV CD spectra (A) and deconvoluted FTIR spectra (B) of unheated and heated cruciferin and Cru/Ca particles

The intrinsic fluorescence of a protein strongly depends on the conformations that the protein adopts in response to bulk solution conditions. Intrinsic fluorescence property of a protein is due to the presence of aromatic amino acids which can mostly be excited at 280 nm. Tryptophan, the dominant intrinsic fluorophore, is the only residue in the protein structure which can be excited at 295 nm (Gorinstein et al., 2000). The intrinsic fluorescence property of cruciferin solutions before and after heating and particle formation were studied using wavelengths of 280 and 295 nm (Figure 4.2A). Both unheated and heated cruciferin spectra showed the maximum emissions at 475 nm and the fluorescence intensity of heated sample was higher (using 295 nm). The increase of fluorescence intensity of tryptophan in the heated structures showed that the polarity of surrounding microenvironment changed to "less-polar" (Jiang et al., 2009). It means the structure of unheated samples, which was unfolded due to the high pH, started to refold after the heat treatment and cooling, and as a result, less tryptophan residues were exposed to aqueous media. The appearance of a shoulder at 360 nm in heated sample spectrum also showed that the emission λ_{max} started to switch to a smaller wavelength (blue shift) which is also an indicator for a less-polar environment. This shoulder might represent few tryptophan residues which were buried after refolding and before aggregation (Duy and Fitter, 2006). After particles formation, the fluorescence intensity of tryptophan dramatically increased and the emission λ_{max} switched to 365 nm. This revealed that more tryptophan residues were further buried in less-polar interior protein structures due to the aggregation process of the refolded cruciferin structures. The results of intrinsic fluorescence confirmed the conformational changes previously represented by CD and FTIR.

4.3.2.3. Surface hydrophobicity

The surface hydrophobicity (S_0) of unheated sample was more than four times higher than that of heated samples at different pHs (Figure 4.2B). Similar results were observed using another fluorescent probe (Rose Bengal) (*Supplementary Figure 4.1*). However, adding $CaCl_2$ in preparing particles did not affect S_0. Relkin (1998) showed that surface hydrophobicity of β-lactoglobulin increased in a thermal treatment. Ryan et al. (2012) also reported that adding NaCl didn't influence the S_0 of whey protein soluble aggregates. The dramatic decrease of S_0 in heated samples indicated that unheated proteins were already unfolded due to the high pH of protein solubilisation. After

the heat treatment and cooling, refolding and/or aggregation of the proteins happened and due to the buried hydrophobic residues in the interior structures, S_0 decreased.

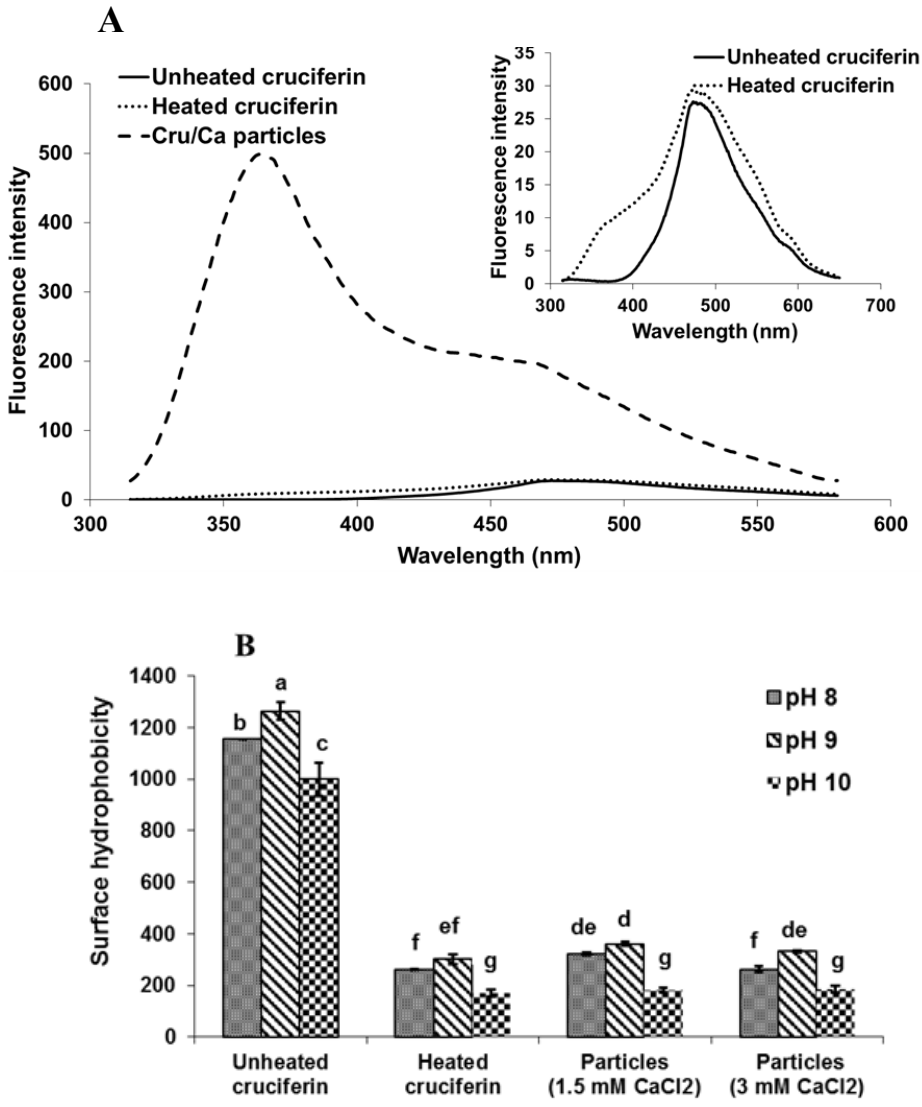

Figure 4.2. Intrinsic emission fluorescence spectra (excitation wavelength: 295 nm) (A) and changes in the surface hydrophobicity (probe: ANS) (B) of unheated and heated cruciferin and Cru/Ca particles. Values with different lowercase letters are significantly ($p<0.05$) different.

As we showed in intrinsic fluorescence study, the aggregation and/or conformational changes of proteins continued after adding $CaCl_2$; however, surface hydrophobicity didn't change significantly in the prepared particles. In other words, the surface hydrophobicity study showed

that most hydrophobic groups were buried after heating and cooling, but in intrinsic study, dramatic increase in tryptophan fluorescence happened after particle formation. This could be explained that the unheated proteins (with high S_0) formed soluble aggregates (with low S_0) after heat treatment mainly through hydrophobic interactions (Ryan et al., 2012). After adding $CaCl_2$, the soluble aggregates formed small networks using Ca^{2+} bridges. Although due to the formation of these small compacted protein networks, microenvironment of around tryptophan changed to less-polar and increased tryptophan fluorescence (Duy and Fitter, 2006); however, S_0 of the proteins forming the compact networks didn't change significantly compared to soluble aggregates since the hydrophobic residues were already buried in heated samples.

4.3.2.4. Morphology of particles

Morphology of cruciferin samples (before and after heating, as well as Cru/Ca particles) were assessed using TEM. No specific structure was observed in unheated cruciferin solution due to the high solubilising pH (Figure 4.3A). Soluble aggregates formed after heating are shown in Figure 4.3B. Cru/Ca nanoparticles (Figure 4.3C) were mostly observed in spherical shapes with ~ 200 nm diameter and smooth surface.

4.3.2.5. Driving forces involving the particles formation

Different interactions such as electrostatic, disulfide, hydrophobic and hydrogen bonding could affect the particles formation. As described before, formation of soluble aggregates from denatured proteins and preparation of networks from the aggregates using Ca^{2+} bridges were two main steps in the Cru/Ca particles formation. The 4-time decrease of the surface hydrophobicity of proteins after heating indicated that hydrophobic interaction is the major force for formation of soluble aggregates. Adding $CaCl_2$ to the soluble aggregates decreased the proteins zeta potentials due to formation of electrostatic interactions between positively charged calcium and negatively charged proteins. Particle size increased at increasing $CaCl_2$ concentrations suggested that electrostatic interaction is another force which plays an important role in the particles formation. To study the role of hydrophobic, disulfide and hydrogen interactions, the particles suspensions were dissociated using different concentrations of SDS, DTT and urea. Dissociation of the particles in the presence of the reagents decreased the suspensions turbidity. Comparison of the relative decreases of the turbidity could be an indicator to show the importance of the interactions in the

particles formation. The turbidity of the suspensions decreased 89, 36 and 24% using SDS, DTT and urea, respectively (Figure 4.3D-F). As it was expected, the results showed that hydrophobic interaction was the major driving force for the particle formation compared to disulfide and hydrogen forces. Although hydrophobic and electrostatic forces played the main roles in the particles formations, disulfide and hydrogen forces might influence the compactness and interior structures of the particles. Ren et al. (2009) reported that hydrophobic and hydrogen interactions are the major forces for soy protein particles.

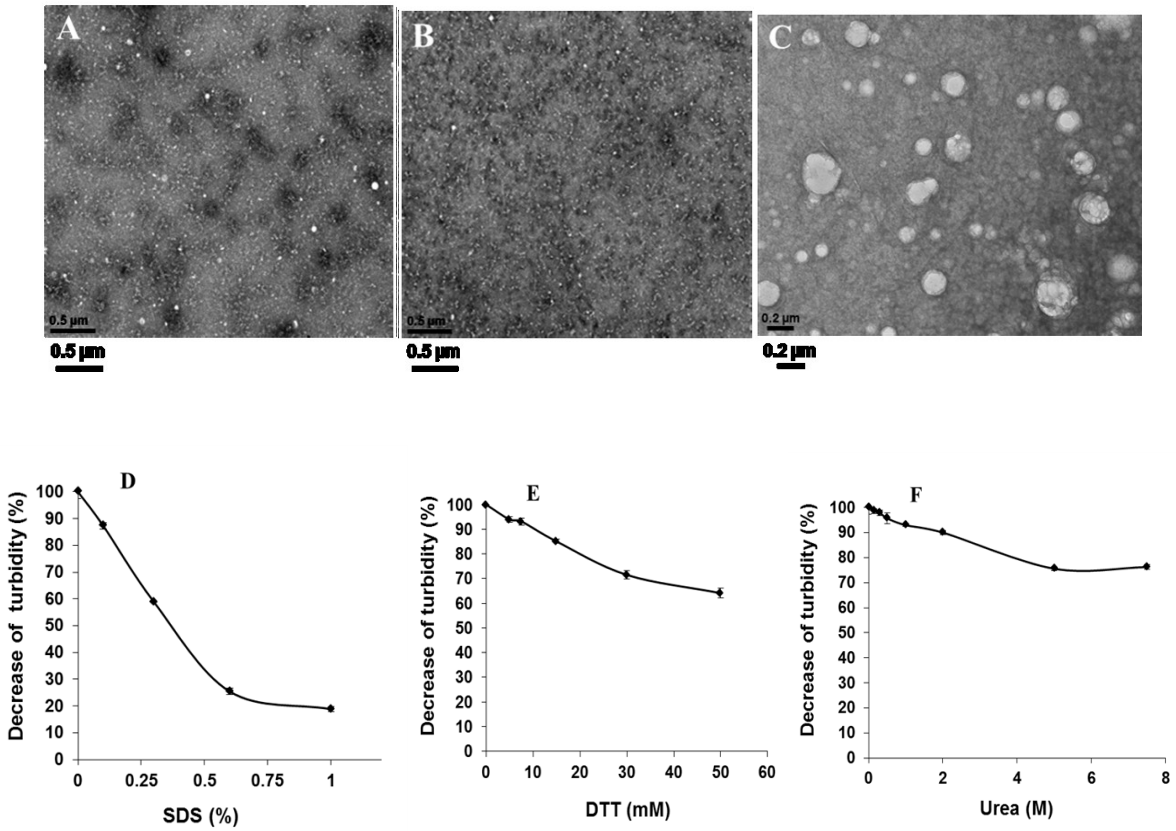

Figure 4.3. TEM images of unheated (A) and heated (B) cruciferin solutions (10 mg/mL) and Cru/Ca nanoparticles (10 mg/mL cruciferin and 1.5 mM $CaCl_2$) (C). Effect of SDS (D), DTT (E) and urea (F) on decrease of the turbidity of Cru/Ca particle dispersions.

4.3.3. In vitro cytotoxicity of particles

The potent cytotoxicity of the particles on Caco-2 cells was assessed using the MTT assay. Incubation of Cru/Ca particles at three concentrations of 0.5, 1.5, and 2.5 mg/mL for 24 h didn't

show any significant change in the cellular viability compared to control (Figure 4.4A). As cell viabilities values more than 80% are considered as non-toxic (Niamprem et al., 2014), the high-concentrated particle suspensions were not toxic.

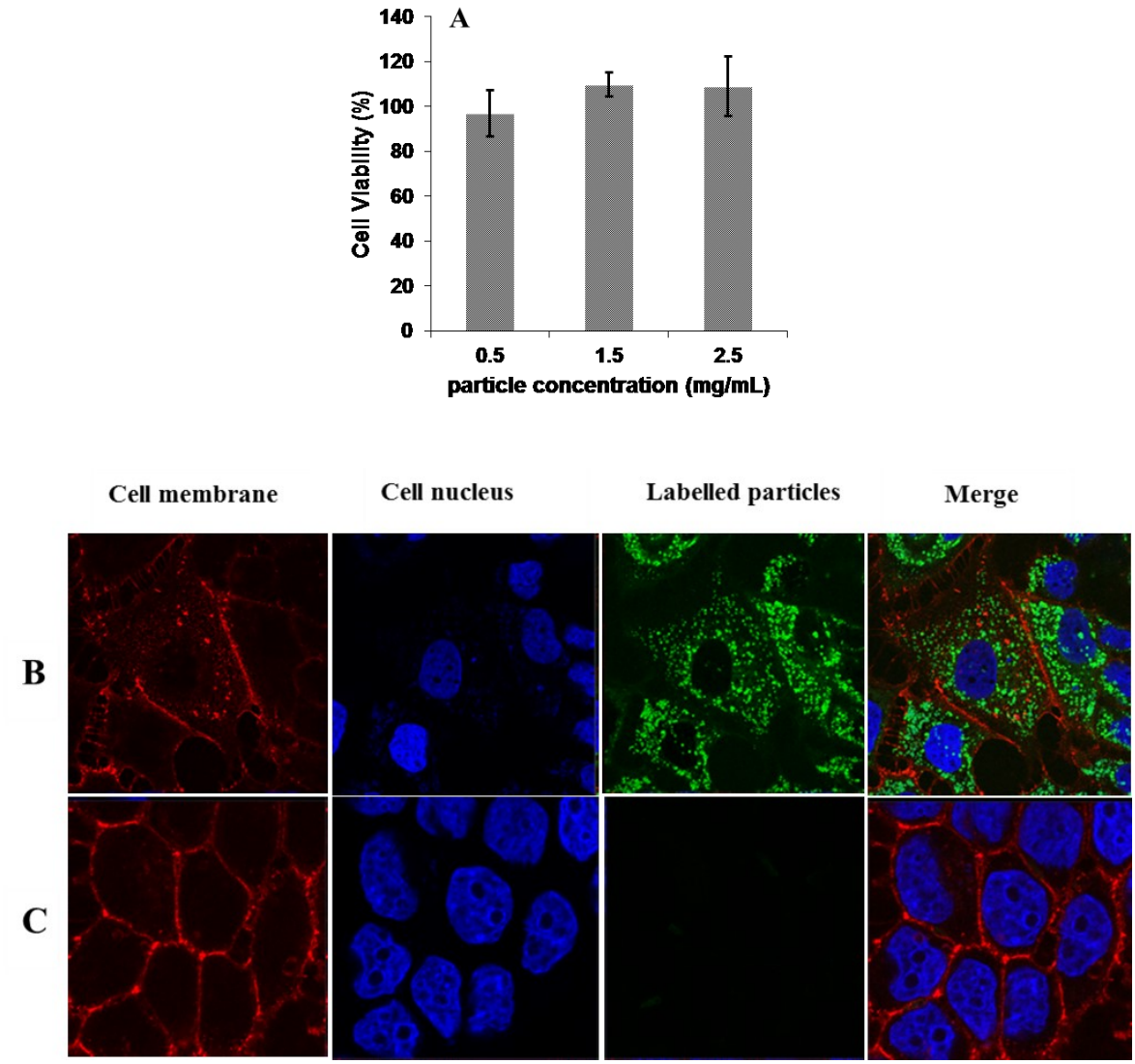

Figure 4.4. Effect of Cru/Ca nanoparticles on Caco-2 cells survival after 24 h incubation at 37°C (compared to control) (A). Confocal microscopic images of Caco-2 cells after 6 h incubation with coumarin 6-labelled Cru/Ca nanoparticles (green) (B) and free coumarin 6 (C). The cell membrane and nucleus were stained using Alexa 594 and DAPI, respectively.

4.3.4. Cell uptake of particles

Uptake of C6-labelled Cru/Ca particles into Caco-2 monolayer was shown in Figure 4.4. Nanoparticles at a concentration of 0.5 mg/mL in DMEM medium (final C6 concentration of 40 µg/mL) were internalised throughout the cytoplasm surrounding the nucleus (Figure 4.4B). The fluorescence intensity of loaded C6 showed that the particles successfully delivered C6 into cytoplasm whereas free C6 wasn't directly uptaken (Win and Feng, 2005) and the negligible detected fluorescence in control cells (Figure 4.4C) was due to leakage of free C6. The results showed that Cru/Ca particles have ability to internalise cell cytoplasm and deliver loaded compounds.

4.3.5. Encapsulation and *in vitro* release of the model compounds

4.3.5.1. Encapsulation of BB and β-carotene in particles

Encapsulation property and release behaviour, two important factors affecting the efficiency of a delivery system, were studied for Cru/Ca particles. BB and β-carotene, a hydrophilic and hydrophobic model compound, respectively, were encapsulated in the Cru/Ca particles. While EE and LC of BB were 19.4%±0.8 and 11.7%±0.4, those for β-carotene were 86.2%±2.3 and 14.7%±1.5, respectively. Chen and Subirade (2005) showed that BB with EE of 15-22% was encapsulated in chitosan-β-lactoglobulin nanoparticles. EE of β-carotene in chitosan-alginate beads and sodium caseinate sub-micelles were reported 54.7% and 87.6%, respectively (Chu et al., 2007; Donhowe et al., 2014). The high EE and LC of β-carotene in Cru/Ca particles might be due to the presence of hydrophobic residues in cruciferin providing high affinity of the particles toward β-carotene (Chu et al., 2007). Figure 4.5 shows a schematic illustration of the particle formation and encapsulation of model compounds.

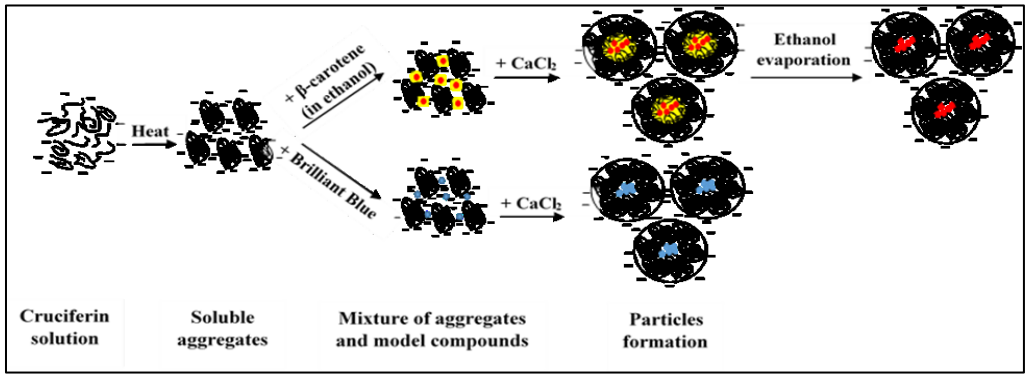

Figure 4.5. A scheme of Cru/Ca particle formation and encapsulation of model compounds

4.3.5.2. Binding of β-carotene to particles

Binding of β-carotene to Cru/Ca particles can be characterized by determination of intrinsic fluorescence of tryptophan in cruciferin structure. Changes in the fluorescence intensity of tryptophan could be resulted from binding-induced quenching of the intrinsic fluorescence (Perez et al., 2014; Zimet and Livney, 2009).

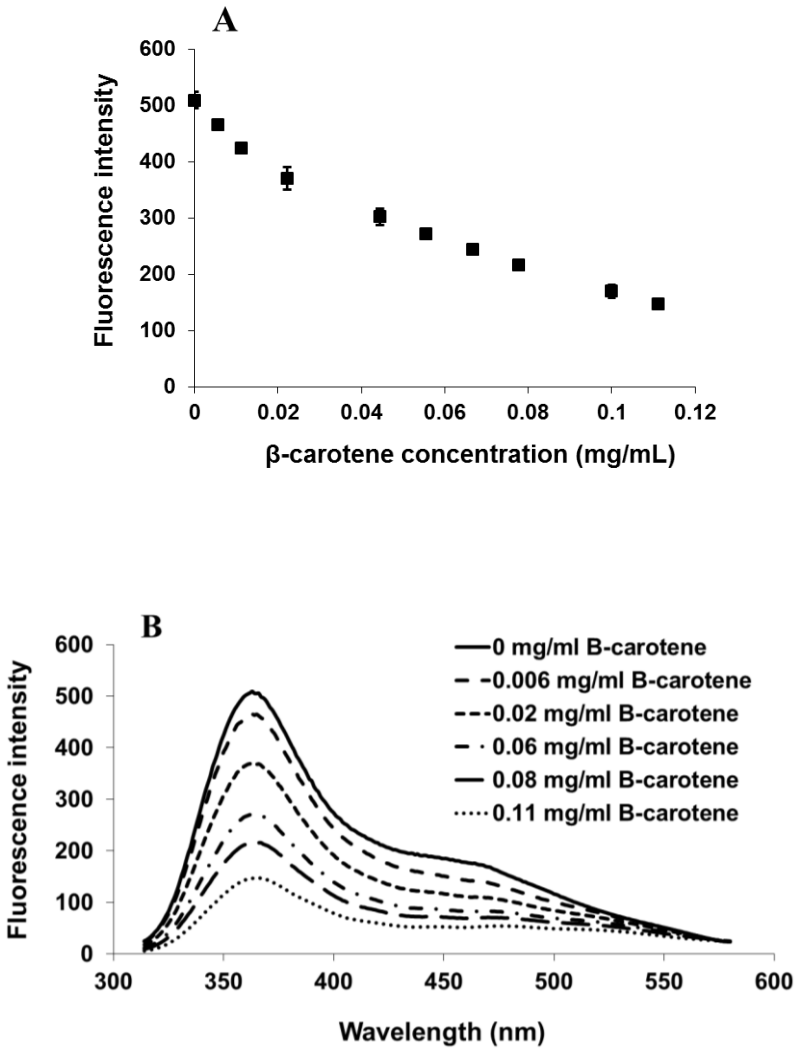

Figure 4.6. Effect of encapsulated β-carotene concentration on the fluorescence intensity (A) and shift of maximum emission wavelength (B) of cruciferin in Cru/Ca particles.

As in Figure 4.6A shown, the fluorescence intensity of β-carotene-loaded cruciferin particles decreased dose-dependently at increasing β-carotene concentrations, indicating that binding occurred. The fluorescence emission spectra of β-carotene-loaded cruciferin particles in different

β-carotene concentration showed that although the fluorescence intensity decreased but no red-shift occurred in the emission λ_{max} (Figure 4.6B). An emission λ_{max} red-shift (toward longer wavelength) happens upon unfolding of a protein structure and when tryptophan residues replace from the less-polar interior of the protein to polar environment. Since the red-shift was not observed in the spectra, the folded/aggregated forms the particles might be kept and β-carotene was trapped inside of the aggregates. Therefore, the decrease of fluorescence intensity of the particles proteins might be due to the quenching effect of β-carotene on tryptophan residues.

4.3.5.3. Release of BB and β-carotene from particles

In vitro release behaviour of BB and β-carotene from Cru/Ca particles was studied using 2h incubation in SGF followed by 6h in SIF with and without pepsin and pancreatin, respectively. In SGF, about 13% and 14% of encapsulated BB and β-carotene were rapidly released at the first 30 min which might be due to release of the weakly-attached compounds to the surface of the particles; prolonged incubation to 2 h did not change their release rates either in the presence or absence of pepsin (Figure 4.7A and B), which suggested the resistance of the particles to both low pH and pepsin. The particles resistance to the low pH revealed that particles have compact structures. Due to the low pH of 1.2 in SGF, cruciferin amine groups were protonated and formed strong electrostatic interactions with negatively charged carboxylic groups and as result, increased the compactness of the protein networks which were not affected in SGF. The pepsin resistance might be attributed to the presence of 30-35 % hydrophobic residues in cruciferin (Chabanon et al., 2007) which could block active peptide bonds hydrolysable by pepsin and as a result, Cru/Ca particles were not degraded by the enzyme. Bos et al. (2007) also reported that cruciferin was indigestible in the stomach and our results showed that the pretreatments before particle formation (high-pH solubilisation and heat treatment) also didn't decrease the resistance of the protein in SGF. Lee et al. (2012) showed that denatured β-lactoglobulin was pepsin resistant and was used for coating chitosan particles.

In SIF however, the release profiles showed different trends (Figure 4.7A and B). As the pH of the media was increased to 7.4, which was close to cruciferin isoelectric point (7.1), deprotonation of amine and carboxylic groups increased and due to decreased electrostatic interactions (Sek, 2013) the compact particles structures were unfolded. The unfolded particles structure allowed water to diffuse into the network and released the entrapped compounds.

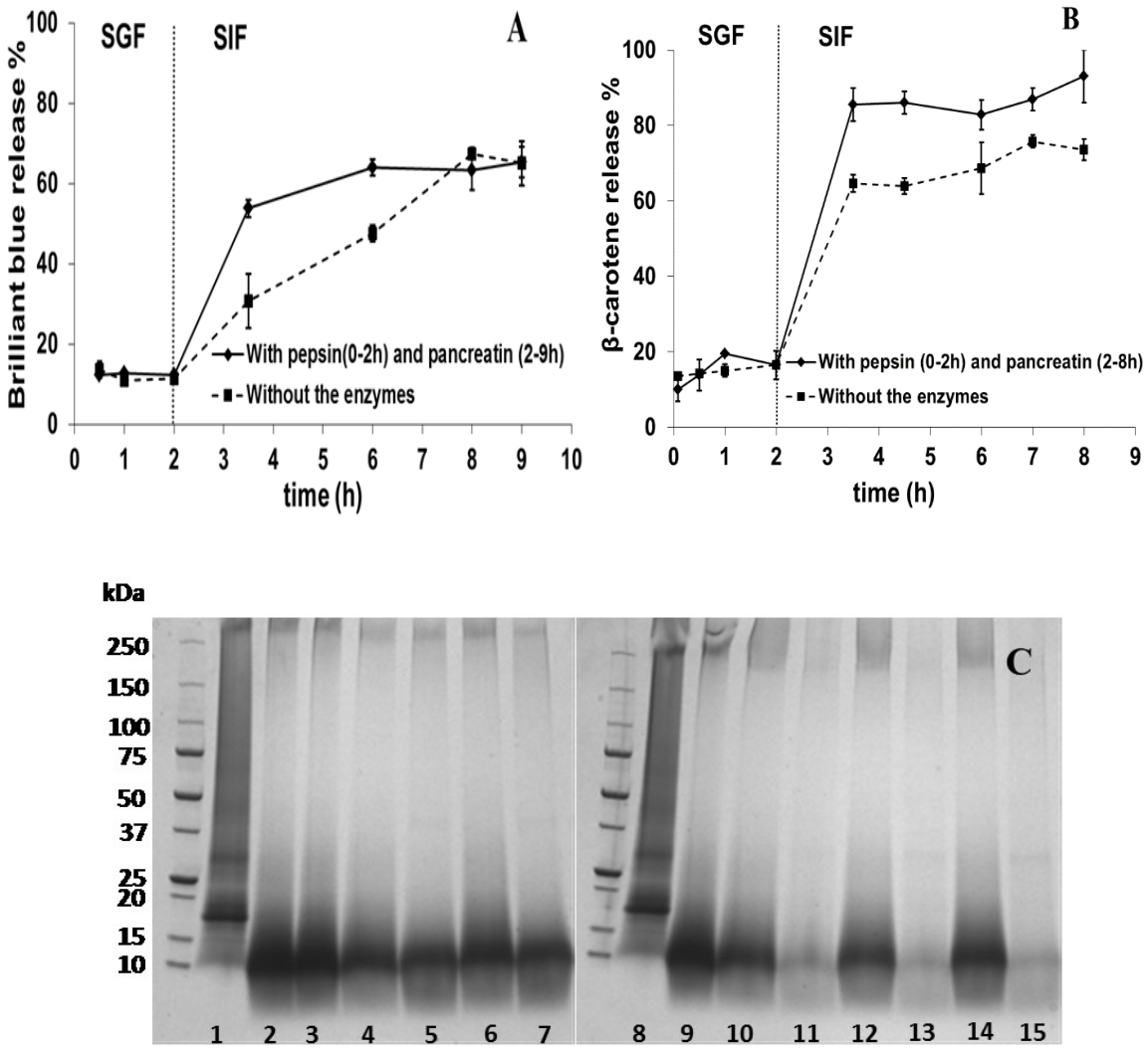

Figure 4.7. Release profiles of brilliant blue (A) and β-carotene (B) from Cru/Ca particles in simulated gastric fluid (SGF) followed by simulated intestinal fluid (SIF) in the presence and absence of pepsin and pancreatin, respectively. SDS-PAGE of cruciferin samples (lanes 1 and 8, unheated protein; lane 2, heated protein; lanes 3 and 9, Cru/Ca particles; lanes 4 and 6 after 0.5 and 2h incubation in SGF without pepsin; lanes 5 and 7 after 0.5 and 2h incubation in SGF with pepsin; lanes 10, 12 and 14 after 3, 5 and 7 h incubation in SIF without pancreatin; lanes 11, 13 and 15 after 3, 5 and 7 h incubation in SIF with pancreatin) (C)

The release was faster in the presence of pancreatin. For example, the particles released 54% of the encapsulated BB after 1.5 h incubation with the enzyme, compared to 31% in the absence of

enzyme. Almost similar trends were observed for β-carotene release study; while released β-carotene were 65% and 74% after 1 and 6 h incubation without the enzyme, those were 85% and 93% in the enzyme treatment. The faster release of the compounds in the presence of pancreatin indicated that cruciferin particles were degraded by the enzyme. The results revealed that Cru/Ca particles protected sensitive compounds in SGF and release them in SIF. In addition, the particles not only were appropriate for water-soluble compounds but also can carry water-insoluble molecules in an oil-free system.

4.3.5.4. Study of polypeptide profile of particles in release conditions

SDS-PAGE of unheated and heated cruciferin and incubated Cru/Ca particles in SGF and SIF were shown in Figure 4.7C. Two major polypeptide bands with estimated molecular weights of 18 and 30 kDa were detected in unheated sample (lanes 1 and 8). Wu and Muir (2008) reported four main polypeptides with MW of 20 to 50 kDa for cruciferin, while some bands in the unheated sample were disappeared or their intensities decreased due to the use of a high pH condition. Most bands were dissociated after heating the samples, leading to the appearance of a high-intense band around 10 kDa (lane 2). SDS-PAGE of Cru/Ca particles (lanes 3 and 9) showed that polypeptide profile didn't change significantly compared to the heated samples. Incubation of particles in the absence of pepsin in SGF (lanes 4 and 6) and in the presence of pepsin (lanes 5 and 7) showed that the particles were resistant to degradation by pepsin, which confirmed the results of our release studies. However, the particles were completely degraded in the presence of pancreatin after 3, 5 and 7 h incubation in the SIF (lanes 11, 13 and 15) compared to lanes 10, 12 and 14 (in the absence of pancreatin). The degradation of particles confirmed the release of 93% encapsulated β-carotene in the intestine (observed in release study). Bos et al. (2007) and Valette et al. (1993) also reported that cruciferin was resistant to pepsin but digestible by pancreatin.

4.3.6. Stability of encapsulated β-carotene

β-carotene, an unstable molecule, is sensitive to oxidation, pH and temperature (Courraud et al., 2013; Rodriguez-Amaya, 1999). Encapsulation is a feasible approach for protection of β-carotene in food processing which could be an important progress in fortification of foods and beverages. Cruciferin with denaturation temperature of as high as 91 °C could be an appropriate material for delivery of sensitive compounds in food heat processing. To study the potential of Cru/Ca particles

for protection of the compounds in food systems, β-carotene-loaded Cru/Cs particles were subjected to a heat treatment and the stability of encapsulated and free β-carotene were compared. The results showed that after heating at 75 °C for 30 min at pH 4 and 7, 20% to 25% of free β-carotene was degraded, while the degradation of encapsulated β-carotene was only 5% (Figure 4.8). Saiz-Abajo et al. (2013) showed that 14.1% of encapsulated β-carotene in re-assembled casein micelles was degraded after 30 min heating at 80 °C compared to 39% degradation of unencapsulated compound. Mensi et al. (2013) and Qian et al. (2012) reported that β-lactoglobulin aggregates and β-Lactoglobulin-coated lipid droplets stabilised β-carotene in different conditions.

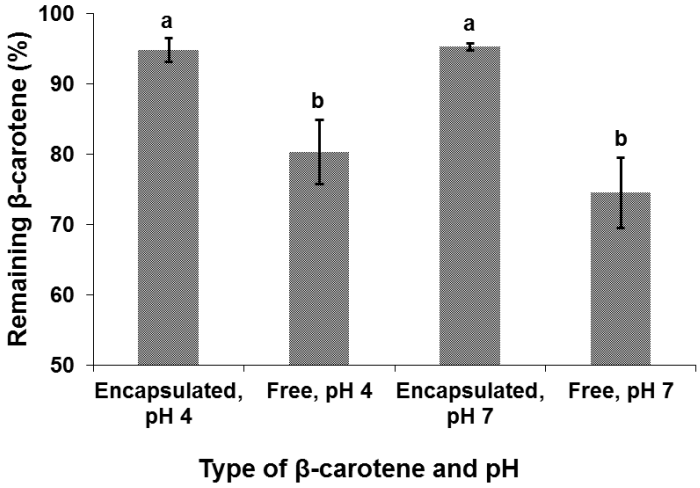

Figure 4.8. Heat stability of encapsulated β-carotene in Cru/Ca particles compared to its free form in a heat treatment (30 min heating at 75ºC and pHs 4 and 7). Values with different lowercase letters are significantly ($p<0.05$) different.

4.4. Conclusions

The main goals of encapsulation are to protect sensitive bioactive compounds in the harsh conditions such as food processing and GI tract, to increase their solubility in aqueous media, and to improve their bioavailability. In this study, cruciferin particles were successfully developed for the first time using the cold gelation method. The main driving forces for the particle formations were hydrophobic interaction and electrostatic forces. These Cru/Ca particles were not toxic at the concentrations of up to 2.5 mg/mL and could be up-taken by Caco-2 monolayer. The potential of using Cru/Ca particles for the delivery of bioactive compounds was demonstrated. Our results

suggested that cruciferin can be used as a material for preparing particles and delivery of bioactive food components.

4.5. References

Akbari, A. & Wu, J. (2015). An integrated method of isolating napin and cruciferin from defatted canola meal. *LWT-Food Science and Technology,* 64, 308-315.

Alizadeh-Pasdar, N. & Li-Chan, E. C. Y. (2000). Comparison of protein surface hydrophobicity measured at various pH values using three different fluorescent probes. *Journal of Agricultural and Food Chemistry,* 48(2), 328-334.

Balogh, L., Nigavekar, S. S., Nair, B. M., Lesniak, W., Zhang, C., Sung, L. Y., Kariapper, M. S. T., El-Jawahri, A., Llanes, M., Bolton, B., Mamou, F., Tan, W., Hutson, A., Minc, L., & Khan, M. K. (2007). Significant effect of size on the *in vivo* biodistribution of gold composite nanodevices in mouse tumor models. *Nanomedicine-Nanotechnology Biology and Medicine,* 3(4), 281-296.

Barbut, S. & Foegeding, E. A. (1993). Ca^{2+}-induced gelation of pre-heated whey-protein isolate. *Journal of Food Science,* 58(4), 867-871.

Bos, C., Airinei, G., Mariotti, F., Benamouzig, R., Berot, S., Evrard, J., Fenart, E., Tome, D., & Gaudichon, C. (2007). The poor digestibility of rapeseed protein is balanced by its very high metabolic utilization in humans. *Journal of Nutrition,* 137(3), 594-600.

Bryant, C. M. & McClements, D. J. (2000). Influence of NaCl and CaCl2 on cold-set gelation of heat-denatured whey protein. *Journal of Food Science,* 65(5), 801-804.

Cavallieri, A. L. F. & Da Cunha, R. L. (2008). The effects of acidification rate, pH and ageing time on the acidic cold set gelation of whey proteins. *Food Hydrocolloids,* 22(3), 439-448.

Chabanon, G., Chevalot, I., Framboisier, X., Chenu, S., & Marc, I. (2007). Hydrolysis of rapeseed protein isolates: Kinetics, characterization and functional properties of hydrolysates. *Process Biochemistry,* 42(10), 1419-1428.

Chen, L. Y. & Subirade, M. (2005). Chitosan/beta-lactoglobulin core-shell nanoparticles as nutraceutical carriers. *Biomaterials,* 26(30), 6041-6053.

Chu, B., Ichikawa, S., Kanafusa, S., & Nakajima, M. (2007). Preparation and characterization of beta-carotene nanodispersions prepared by solvent displacement technique. *Journal of Agricultural and Food Chemistry,* 55(16), 6754-6760.

Courraud, J., Berger, J., Cristol, J.P., & Avallone, S. (2013). Stability and bioaccessibility of different forms of carotenoids and vitamin A during *in vitro* digestion. *Food Chemistry,* 136, 871-877.

Deat-Laine, E., Hoffart, V., Garrait, G., & Beyssac, E. (2013). Whey protein and alginate hydrogel microparticles for insulin intestinal absorption: Evaluation of permeability enhancement properties on Caco-2 cells. *International Journal of Pharmaceutics,* 453(2), 336-342.

Doherty, S. B., Gee, V. L., Ross, R. P., Stanton, C., Fitzgerald, G. F., & Brodkorb, A. (2011). Development and characterisation of whey protein micro-beads as potential matrices for probiotic protection. *Food Hydrocolloids,* 25(6), 1604-1617.

Donhowe, E. G., Flores, F. P., Kerr, W. L., Wicker, L., & Kong, F. (2014). Characterization and *in vitro* bioavailability of beta-carotene: Effects of microencapsulation method and food matrix. *LWT-Food Science and Technology,* 57(1), 42-48.

Duy, C. & Fitter, J. (2006). How aggregation and conformational scrambling of unfolded states govern fluorescence emission spectra. *Biophysical Journal,* 90(10), 3704-3711.

Elzoghby, A. O., Samy, W. M., & Elgindy, N. A. (2012). Protein-based nanocarriers as promising drug and gene delivery systems. *Journal of Controlled Release,* 161(1), 38-49.

Gaumet, M., Gurny, R., & Delie, F. (2009). Localization and quantification of biodegradable particles in an intestinal cell model: The influence of particle size. *European Journal of Pharmaceutical Sciences,* 36(4-5), 465-473.

Gilbert, V., Rouabhia, M., Wang, H. X., Arnould, A. L., Remondetto, G., & Subirade, M. (2005). Characterization and evaluation of whey protein-based biofilms as substrates for *in vitro* cell cultures. *Biomaterials,* 26(35), 7471-7480.

Gorinstein, S., Goshev, I., Moncheva, S., Zemser, M., Weisz, M., Caspi, A., Libman, I., Lerner, H. T., Trakhtenberg, S., & Martin-Belloso, O. (2000). Intrinsic tryptophan fluorescence of human serum proteins and related conformational changes. *Journal of Protein Chemistry,* 19(8), 637-642.

He, B., Lin, P., Jia, Z., Du, W., Qu, W., Yuan, L., Dai, W., Zhang, H., Wang, X., Wang, J., Zhang, X., & Zhang, Q. (2013). The transport mechanisms of polymer nanoparticles in Caco-2 epithelial cells. *Biomaterials,* 34(25), 6082-6098.

He, C., Yin, L., Tang, C., & Yin, C. (2012). Size-dependent absorption mechanism of polymeric nanoparticles for oral delivery of protein drugs. *Biomaterials,* 33(33), 8569-8578.

He, R., He, H., Chao, D., Ju, X., & Aluko, R. (2014). Effects of high pressure and heat treatments on physicochemical and gelation properties of rapeseed protein isolate. *Food and Bioprocess Technology,* 7(5), 1344-1353.

Jiang, J., Chen, J., & Xiong, Y. L. (2009). Structural and emulsifying properties of soy protein isolate subjected to acid and alkaline pH-shifting Processes. *Journal of Agricultural and Food Chemistry,* 57(16), 7576-7583.

Kong, J. & Yu, S. (2007). Fourier transform infrared spectroscopic analysis of protein secondary structures. *Acta Biochimica Et Biophysica Sinica,* 39(8), 549-559.

Kulmyrzaev, A., Cancelliere, C., & McClements, D. J. (2000). Influence of sucrose on cold gelation of heat-denatured whey protein isolate. *Journal of the Science of Food and Agriculture,* 80(9), 1314-1318.

Kundu, S., Chinchalikar, A. J., Das, K., Aswal, V. K., & Kohlbrecher, J. (2013). Fe^{+3} ion induced protein gelation: Small-angle neutron scattering study. *Chemical Physics Letters,* 584, 172-176.

Lee, P. S., Yim, S. G., Choi, Y., Thi Van Anh Ha, & Ko, S. (2012). Physiochemical properties and prolonged release behaviours of chitosan-denatured beta-lactoglobulin microcapsules for potential food applications. *Food Chemistry,* 134(2), 992-998.

Lodhia, J., Mandarano, G., Ferris, N., Eu, P., & Cowell, S. (2010). Development and use of iron oxide nanoparticles (Part 1): Synthesis of iron oxide nanoparticles for MRI. *Biomedical Imaging and Intervention Journal,* 6(2), e12-e12.

Luo, Y., Teng, Z., Wang, T. T. Y., & Wang, Q. (2013). Cellular uptake and transport of zein nanoparticles: Effects of sodium caseinate. *Journal of Agricultural and Food Chemistry,* 61(31), 7621-7629.

Maltais, A., Remondetto, G. E., Gonzalez, R., & Subirade, M. (2005). Formation of soy protein isolate cold-set gels: Protein and salt effects. *Journal of Food Science,* 70(1), C67-C73.

Maltais, A., Remondetto, G. E., & Subirade, M. (2008). Mechanisms involved in the formation and structure of soya protein cold-set gels: A molecular and supramolecular investigation. *Food Hydrocolloids,* 22(4), 550-559.

Marangoni, A. G., Barbut, S., McGauley, S. E., Marcone, M., & Narine, S. S. (2000). On the structure of particulate gels - the case of salt-induced cold gelation of heat-denatured whey protein isolate. *Food Hydrocolloids,* 14(1), 61-74.

McClements, D. J. (2013). Edible lipid nanoparticles: digestion, absorption, and potential toxicity. *Progress in Lipid Research,* 52(4), 409-423.

Mensi, A., Choiset, Y., Haertle, T., Reboul, E., Borel, P., Guyon, C., de Lamballerie, M., & Chobert, J. (2013). Interlocking of beta-carotene in beta-lactoglobulin aggregates produced under high pressure. *Food Chemistry,* 139(1-4), 253-260.

Nagano, T., Akasaka, T., & Nishinari, K. (1995). Study on the heat-induced conformational-changes of beta-conglycinin by FTIR and CD analysis. *Food Hydrocolloids,* 9(2), 83-89.

Niamprem, P., Rujivipat, S., & Tiyaboonchai, W. (2014). Development and characterization of lutein-loaded SNEDDS for enhanced absorption in Caco-2 cells. *Pharmaceutical Development and Technology,* 19(6), 735-742.

Pelton, J. T. & McLean, L. R. (2000). Spectroscopic methods for analysis of protein secondary structure. *Analytical Biochemistry,* 277(2), 167-176.

Perez, A. A., Andermatten, R. B., Rubiolo, A. C., & Santiago, L. G. (2014). beta-Lactoglobulin heat-induced aggregates as carriers of polyunsaturated fatty acids. *Food Chemistry,* 158, 66-72.

Powell, J. J., Faria, N., Thomas-McKay, E., & Pele, L. C. (2010). Origin and fate of dietary nanoparticles and microparticles in the gastrointestinal tract. *Journal of Autoimmunity,* 34(3), J226-J233.

Qian, C., Decker, E. A., Xiao, H., & McClements, D. J. (2012). Physical and chemical stability of beta-carotene-enriched nanoemulsions: Influence of pH, ionic strength, temperature, and emulsifier type. *Food Chemistry,* 132(3), 1221-1229.

Ranjbar, B. & Gill, P. (2009). Circular dichroism techniques: Biomolecular and nanostructural analyses- A review. *Chemical Biology & Drug Design,* 74(2), 101-120.

Relkin, P. (1998). Reversibility of heat-induced conformational changes and surface exposed hydrophobic clusters of beta-lactoglobulin: Their role in heat-induced sol-gel state transition. *International Journal of Biological Macromolecules,* 22(1), 59-66.

Remondetto, G. E. & Subirade, M. (2003). Molecular mechanisms of Fe^{2+}-induced beta-lactoglobulin cold gelation. *Biopolymers,* 69(4), 461-469.

Ren, C., Tang, L., Zhang, M., & Guo, S. (2009). Structural characterization of heat-Induced protein particles in soy milk. *Journal of Agricultural and Food Chemistry,* 57(5), 1921-1926.

Rodriguez-Amaya, B. (1999). *A guide to carotenoid analysis in foods.* (1st ed.). Washington, D.C.: ILSI Press.

Ryan, K. N., Vardhanabhuti, B., Jaramillo, D. P., van Zanten, J. H., Coupland, J. N., & Foegeding, E. A. (2012). Stability and mechanism of whey protein soluble aggregates thermally treated with salts. *Food Hydrocolloids,* 27(2), 411-420.

Saiz-Abajo, M., Gonzalez-Ferrero, C., Moreno-Ruiz, A., Romo-Hualde, A., & Gonzalez-Navarro, C. J. (2013). Thermal protection of beta-carotene in re-assembled casein micelles during different processing technologies applied in food industry. *Food Chemistry,* 138(2-3), 1581-1587.

Schmitt, C., Moitzi, C., Bovay, C., Rouvet, M., Bovetto, L., Donato, L., Leser, M. E., Schurtenberger, P., & Stradner, A. (2010). Internal structure and colloidal behaviour of covalent whey protein microgels obtained by heat treatment. *Soft Matter,* 6(19), 4876-4884.

Sek, S. (2013). Review peptides and proteins wired into the electrical circuits: an SPM-based approach. *Biopolymers,* 100(1), 71-81.

Slutter, B., Plapied, L., Fievez, V., Alonso Sande, M., des Rieux, A., Schneider, Y., Van Riet, E., Jiskoot, W., & Preat, V. (2009). Mechanistic study of the adjuvant effect of biodegradable nanoparticles in mucosal vaccination. *Journal of Controlled Release,* 138(2), 113-121.

Tan, S. H., Mailer, R. J., Blanchard, C. L., & Agboola, S. O. (2011). Extraction and characterization of protein fractions from Australian canola meals. *Food Research International,* 44(4), 1075-1082.

Tang, C. & Liu, F. (2013). Cold, gel-like soy protein emulsions by microfluidization: Emulsion characteristics, rheological and microstructural properties, and gelling mechanism. *Food Hydrocolloids,* 30(1), 61-72.

Tomczynska-Mleko, M. (2013). Structure and stability of ion induced whey protein aerated gels. *Czech Journal of Food Sciences,* 31(3), 211-216.

Uruakpa, F. & Arntfield, S. (2006). Impact of urea on the microstructure of commercial canola protein-carrageenan network: A research note. *International Journal of Biological Macromolecules,* 38(2), 115-119.

USDA. Major oilseeds: world supply and distribution. United States Department of Agriculture. Online. 2013. Available from URL: http://apps.fas.usda.gov/psdonline/circulars/oilseeds.pdf.

Valette, P., Malouin, H., Corring, T., & Savoie, L. (1993). Impact of exocrine pancreatic adaptation on *in vitro* protein digestibility. *British Journal of Nutrition,* 69(2), 359-369.

Wanasundara, J. P. D. (2011). Proteins of *Brassicaceae* oilseeds and their potential as a plant protein source. *Critical Reviews in Food Science and Nutrition,* 51(7), 635-677.

Win, K. Y. & Feng, S. S. (2005). Effects of particle size and surface coating on cellular uptake of polymeric nanoparticles for oral delivery of anticancer drugs. *Biomaterials,* 26(15), 2713-2722.

Wu, J. & Muir, A. D. (2008). Comparative structural, emulsifying, and biological properties of 2 major canola proteins, cruciferin and napin. *Journal of Food Science,* 73(3), C210-C216.

Wu, J., Aluko, R. E., & Muir, A. D. (2009). Production of angiotensin I-converting enzyme inhibitory peptides from defatted canola meal. *Bioresource Technology,* 100(21), 5283-5287.

Yamada, Y., Iwasaki, M., Usui, H., Ohinata, K., Marczak, E. D., Lipkowski, A. W., & Yoshikawa, M. (2010). Rapakinin, an anti-hypertensive peptide derived from rapeseed protein, dilates mesenteric artery of spontaneously hypertensive rats via the prostaglandin IP receptor followed by CCK1 receptor. *Peptides,* 31(5), 909-914.

Yoshie-Stark, Y., Wada, Y., & Waesche, A. (2008). Chemical composition, functional properties, and bioactivities of rapeseed protein isolates. *Food Chemistry,* 107(1), 32-39.

Zhang, J., Liang, L., Tian, Z., Chen, L., & Subirade, M. (2012). Preparation and in vitro evaluation of calcium-induced soy protein isolate nanoparticles and their formation mechanism study. *Food Chemistry*, 133, 390–399.

Zimet, P. & Livney, Y. D. (2009). Beta-lactoglobulin and its nanocomplexes with pectin as vehicles for omega-3 polyunsaturated fatty acids. *Food Hydrocolloids,* 23(4), 1120-1126.

4.6. Appendix B: Supplementary Information

Supplementary Table 4.1. Effect of preheating (95°C) and adding $CaCl_2$ on zeta-potential (mV) of unheated, heated cruciferin and Cru/Ca particles (10 mg/mL) at different pH values

	Suspension pH			
Samples	8	9	10	12
Unheated	-24.2±1.9	-27.6±1.2	-29.5±1.6	-41.4±5.8
Heated (without $CaCl_2$)	-23.4±2.1	-30.8±1.8	-33.4±1.4	-51.7±3.2
Heating + 1.5 mM $CaCl_2$	-22.7±1.3	-28.7±1.4	-27.4±3.3	---
Heating + 3 mM $CaCl_2$	-19.3±2.5	-23.6±1.3	-25.5±1.9	---

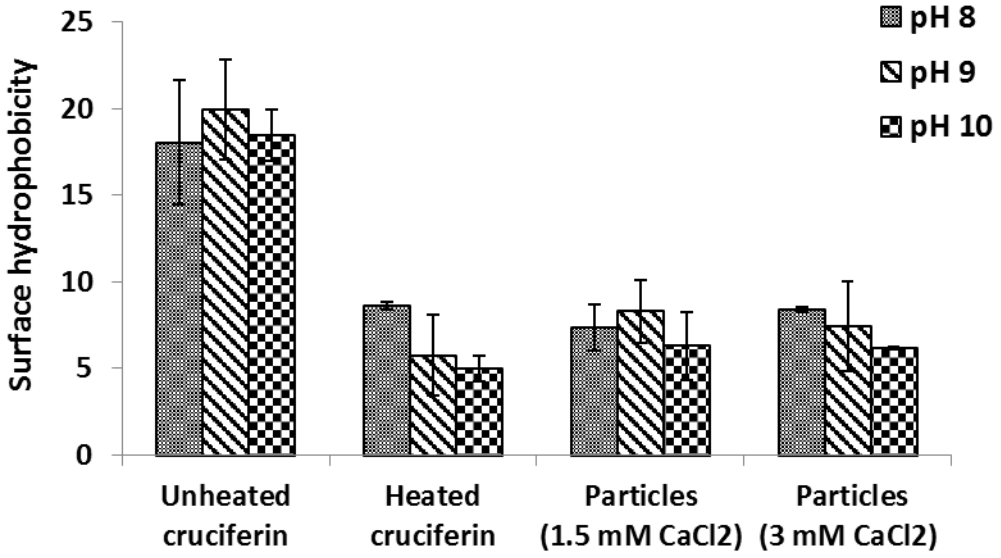

Supplementary Figure 4.1. Changes in the surface hydrophobicity (probe: Rose Bengal) of unheated and heated cruciferin, and Cru/Ca particles

CHAPTER 5- Cruciferin coating improves the stability of chitosan nanoparticles at low pHs

A version of this chapter has been accepted for publication in the *Journal of Materials Chemistry B* (DOI: 10.1039/c6tb00415f).

5.1. Introduction

Functional foods and nutraceuticals have great potential to improve human health and wellness; however the low bioavailability of many bioactive food compounds makes this potential health benefit impaired (Bouwmeester et al., 2009). Encapsulation of bioactive compounds is widely recognized as an effective approach to improve the bioavailability through providing protection against food processing and digestion in the gastrointestinal (GI) tract, improving their solubility and/or permeability in the GI tract (Teng et al., 2013). Chitosan, a cationic carbohydrate derived from chitin of fungi cell walls or exoskeleton of crabs and shrimps, has been extensively explored as wall material for preparing particles due to its unique mucoadhesive and permeation enhancing properties. However, degradation at low pH stomach is the main drawback of chitosan particles in oral delivery (Makhlof et al., 2011). To overcome this hurdle, chitosan particles are often coated with synthetic co-polymers like different types of Eudragits (Chourasia and Jain, 2003). However, in food uses, natural polymers such as food proteins, are more desirable compared to the synthetic ones (Elzoghby et al., 2012). Cruciferin is the major canola protein (12S globulin) accounting for ~65% of total canola proteins. Canola/rapeseed, with an annual production of 70 million metric tonnes, now ranks as the second most abundant oilseed in the world (USDA, 2013). The meal after oil extraction contains 35-40% proteins; canola proteins are potential food proteins as they contains a well-balanced amino acid composition, high contents of lysine (6.0%) and sulfur-containing amino acids (3 to 4%), and a high protein efficiency ratio (Wu and Muir, 2008; Tan et al., 2011). Furthermore, canola proteins were reported to show good emulsifying and gelling properties, and as a precursor of bioactive peptides (Wu and Muir, 2008; Wu et al., 2009; Yamada et al., 2010; Yoshie-Stark et al., 2008; Pinterits and Arntfield, 2008). Cruciferin, with an isoelectric point (pI) of around 7.2 and a molecular weight of 300 kDa, is composed of six subunits and is resistant to gastric digestion (Bos et al., 2007). We hypothesized that cruciferin coating would improve the stability of chitosan-nanoparticles at low pH.

To the best of our knowledge, the potential use of canola proteins in delivery systems has not been explored. Most food proteins form heat-induced aggregations at temperatures above 70°C where different compounds can be entrapped and slowly be released (Elzoghby et al., 2011). Since heat-set hydrogels may not be suitable for encapsulation of heat-sensitive compounds, an alternative method, cold gelation, in which proteins form gel using multivalent ions or in combination with other polymers, will be applied. The objective of this study was to prepare cruciferin-coated

chitosan particles with improved stability at low-pH. The particles were characterized, and their encapsulation and release properties were studied.

5.2. Materials and methods

5.2.1. Materials

Commercial canola meal, obtained from Richardson Oilseed Company (Lethbridge, AB, Canada) was ground, passed through a 35-mesh screen and stored at -20 °C for further use. Caco-2 cells (HTB37) were obtained at passage 19 from the American type culture collection (Manassas, VA). Dulbecco's modified eagle medium (DMEM), 0.25% (w/v) trypsin-0.53 mM EDTA, 4-(2-hydroxyethyl)-1-piperazineethanesulfonic acid (HEPES), fetal bovine serum, 1% nonessential amino acids, and 1% antibiotics were all procured from Gibco Invitrogen (Burlington, ON, Canada). (3-(4,5-dimethylthiazol-2-yl)-2,5-diphenyltetrazolium bromide) (MTT), dimethyl sulfoxide (DMSO), coomassie brilliant blue G-250, β-carotene, chitosan (molecular weight of 140-220 kDa and degree of acetylation ≤40%), urea, sodium dodecyl sulfate (SDS), dithiothreitol (DTT), pepsin, pancreatin, Coumarin 6 and 4',6-diamidino-2-phenylindole (DAPI) were obtained from Sigma (Oakville, ON, Canada).

5.2.2. Canola protein extraction

Cruciferin was extracted using the method we previously developed (Akbari and Wu, 2015). A slurry of canola meal:water (1:10, W:V) was acidified to pH 4, stirred for 2 h and centrifuged at 10,000 rpm for 20 min at 4°C. The resultant pellet was mixed with 10X volume of water, and the pH was adjusted to 12 while stirring at room temperature for 1h. After centrifugation, the supernatant was adjusted to pH 4 to precipitate proteins. The collected precipitate was washed twice with acidified water (pH 4), centrifuged and freeze-dried as cruciferin isolate.

5.2.3. Preparation of particles

Cruciferin was used to prepare nanoparticles based on the method developed by Makhlof et al. (2011) with some modifications. 18 mL of cruciferin solution at different protein concentrations (2, 3, 5, 7.5, and 10 mg/mL) and pH 12 was dropwise added to 18 mL chitosan solution (2 mg/mL in 0.1 M acetic acid) containing 0.04% w/v sodium azide while stirring. The pH of the suspensions was adjusted to 3.5, 4.5, 5.5, 6.5, and 7.5, and the suspensions were stirred for 1 h. The stability and turbidity of the particle suspensions were used to assess conditions for particles formation.

The stability of the particles was studied for a period of 3 weeks stored at 4°C. The turbidity was measured at 600 nm using a UV/VIS spectrophotometer (V-530 Jasco, Japan) (Lee et al., 2012). The dispersions containing stable particles with at least 50% increase in turbidity compared to initial protein solution turbidity were considered as appropriate dispersions.

5.2.4. Particles characterization

5.2.4.1. Size, surface charge and morphology of particles

Size of the particles was determined by dynamic light scattering (DLS) using Malvern Nanosizer ZS (Malvern, Worcestershire, UK). Zeta potential of the particles was also measured by laser doppler velocimetry using the Nanosizer. Prior to measurement, samples were diluted in 10 mM phosphate buffers (the same pH of particle suspensions) to obtain a slight opalescent dispersion to prevent multiple scattering effects. Morphology of the prepared particles was studied using a transmission electron microscopy (TEM, Philips Morgagni 268, FEI Company, The Netherlands) at 80 kV. The particles were freshly prepared at the cruciferin:chitosan ratio of 5:2 and pH 5.5, diluted 10 times, put on Formvar-covered copper grids, negatively stained with 2% phosphotungstic acid for 20 S, and then air dried.

5.2.4.2. Surface hydrophobicity

The surface hydrophobicity of cruciferin and the particles was determined using ANS fluorescent probe (Alizadeh-Pasdar and Li-Chan, 2000). Briefly, the samples were diluted to ten concentrations ranging from 0.0025 to 0.1 mg/mL using 0.1 M citrate buffers at pH 5. Then, 20 μL of 8 mM ANS solution prepared in the same buffer was added to 4 mL of the diluted samples and the fluorescence intensity was measured at emission and excitation wavelengths of 470 nm and 390 nm, respectively, at a slit width of 5 nm using a 1-cm path length quartz cell on Shimadzu RF-5301PC spectrofluorophotometer (Kyoto, Japan). The buffer containing ANS and diluted samples (in the absence of ANS), as blanks, was subtracted from the measured fluorescence values. The slope of the linear plot of net fluorescence values versus protein concentrations was used as an index of the protein surface hydrophobicity.

5.2.4.3. Intrinsic fluorescence study

The intrinsic fluorescence emissions of cruciferin and the particles were measured using a Shimadzu RF-5301PC spectrofluorophotometer (Kyoto, Japan) equipped with a 1-cm path length quartz cell. The protein concentration and pH of the samples were adjusted to 0.005 mg/mL and

pH 5.5 using 10 mM citrate buffer. The fluorescence measurements were performed using the excitation wavelength of 295 nm and the emission wavelengths of 300 to 650 nm, both at a slit width of 5 nm (Perez et al., 2014). The interactions between encapsulated β-carotene and the particles were also studied using the intrinsic fluorescence property (Zimet and Livney, 2009). In brief, different concentrations of β-carotene, soluble in ethanol, were encapsulated in the particles as will be explained in 2.7.2 section. The intrinsic fluorescence of the β-carotene-loaded particles, at final β-carotene concentrations of 0.002-0.06 mg/mL, was also measured using 295 nm excitation wavelength. The emission spectra were recorded from of 300 to 650 nm.

5.2.4.4. Driving forces involving the particles formation

The importance of hydrophobic, electrostatic, hydrogen and disulfide interactions in forming the particles were evaluated using SDS, NaCl, urea and DTT, respectively. The particles suspension was mixed with the same volume of each dissociating agent at different concentrations. The mixtures were adjusted to pH 5.5 and vortexed 10 s and after 6 h, their turbidity were measured at 600 nm using the UV/VIS spectrophotometer. The turbidity of the mixtures was compared to that of initial particles suspension. Decrease in the turbidity of the mixtures was considered as an indicator of the degree of particles dissociation (Schmitt et al., 2010).

5.2.4.5. Thermal property study

Freeze-dried samples were dried in a vacuum desiccator using phosphorous pentoxide for 48 h. The dried samples (~5 mg) were weighed in hermetically sealed aluminium pans, sealed and loaded into a differential scanning calorimeter (Q2000-DSC, TA Instruments, New Castle, DE, USA). The samples were heated at a scanning rate of 10°C /min from 15 to 300°C under inert nitrogen atmosphere. An empty aluminium pan was used as a reference.

5.2.4.6. FTIR study

Freeze-dried samples were dried in the vacuum desiccator before FTIR analysis. The milled samples in KBr (~10 mg) were loaded on a Thermo Nicolet 8700 FTIR spectrometer (Madison, WI, USA). A background spectrum in air was obtained before running the samples. The infrared spectra were collected from the wavenumber of 400 to 4000 cm^{-1} at a resolution of 4 cm^{-1}. Each sample was subjected to 64 repeated scans. The spectra were smoothed and standardized, and their baselines were calibrated using Omnic 8.1 software (Madison, WI, USA). The recorded spectra were also deconvoluted in amide I band region (1700-1600 cm^{-1}) using the software at a bandwidth

of 25 cm^{-1} and an enhancement factor of 2.5. The detected amide I bands in the spectra were assigned to protein secondary structures using previously established wavenumber ranges (Pelton and McLean, 2000; Kong and Yu, 2007).

5.2.5. Effect of the particles on cell viability

Toxicity of the prepared particles on Caco-2 cells was assessed using MTT method. The MTT test measures the activity of dehydrogenase enzyme, which can convert MTT to insoluble purple formazan in Caco-2 cells. The formazan is dissolved in DMSO and the intensity of formed purple color determines the enzyme activity and cell viability. Caco-2 cells were seeded (50,000 cell/mL) in high-glucose and L-glutamine DMEM medium supplemented with 10% FBS, 1% non-essential amino acids, 1% penicillin and streptomycin, and 2.5% HEPS in a 96-well plate (200 µl/cell) and incubated at 37°C in a humidified incubator with 5% CO_2 for 24h. After incubation, the media in the cells was replaced with freshly prepared particles suspended in the DMEM medium at different concentrations of 0.5, 1.5, and 2.5 mg/mL. DMEM without nanoparticles was used as control. After 24h incubation, the wells were gently washed three times with PBS from the cells, and then 15 µl MTT (5 mg/mL in PBS) and 185 µl medium were added to the cells and incubated for 4h. Medium was removed and the formed formazan crystals were dissolved in 150 µl DMSO. Absorbance was measured at 570 nm using a microplate reader (GENios, Tecan, Mannedorf, Switzerland). Relative cell viability (%) was calculated by comparing the absorbance of the particle samples with that of the control (Slutter et al., 2009).

5.2.6. Cell uptake of the particles

To study the cell uptake of nanoparticles in Caco-2 cells, coumarin-6, as a fluorescent marker, was encapsulated into the nanoparticles. The cellular uptake of coumarin-6-loaded nanoparticles was compared to free coumarin-6 (not encapsulated). In brief, 1 mL of coumarin-6 solution in ethanol at concentrations ranging from 10 to 400 µg/mL was mixed with 9 mL 2 mg/mL chitosan solution in 0.1 M acetic acid. 9 mL of 5 mg/mL cruciferin solution (solubilized at pH 12) was added dropwise to the solution while stirring. The pH of the suspension was adjusted to 5.5, stirred for 2 h and then was centrifuged at 40000 g and 4 °C for 30 min. Loaded particles pellet was collected, washed twice with water and centrifuged to remove free coumarin-6. The labelled particles were re-suspended in DMEM medium at concentrations of 0.1, 0.5 and 1 mg/mL. The size and zeta potential of the re-suspended particles were measured. Caco-2 cells (10^5 cells/well) were seeded

on cover glasses placed in 6-well plates (Costar, Corning, NY), and incubated until cells were about 80% confluence (Luo et al., 2013). 2.5 mL of labelled-particles suspensions or free coumarin-6 solution in DMEM medium was added to each well and incubated for 6 h at 37 °C. Then, the cells were washed three times with PBS to remove free nanoparticles and coumarin-6. Cell membranes were stained with 10 µg/mL Alexa Fluor 594-Concanavalin A conjugate in PBS for 10 min. After three washings with PBS, the cells were fixed using ice-cold solution of 3.7% formaldehyde for 30 min. Cell nuclei were also stained with 0.3 µg/mL DAPI for 10 min and then washed with PBS. The coverslips covered with fixed cells were removed from the wells, inverted on slides containing 40 µL (90% glycerol in PBS), then dried overnight in dark at room temperature, and kept at 4 °C. The cells were observed with a CLSM 510 Meta confocal laser scanning microscope (Carl Zeiss Microscopy, Jena, Germany) using an oil immersion objective (63×) at wavelengths of 405, 561 and 488 nm to visualize cell nuclei, membranes and labelled particles, respectively. Images were processed with ZEN 2011 LE software (Carl Zeiss, AG, Oberkochen, Germany) (He et al., 2013; Gaumet et al., 2009).

5.2.7. Encapsulation of model compounds

The encapsulation capacity of the particles was assessed using both water-soluble and water-insoluble compounds.

5.2.7.1. Encapsulation of a water-soluble model compound

Brilliant blue-loaded particles were prepared by adding dropwise 18 mL of cruciferin solution (pH 12) to 18 mL chitosan solution (2 mg/mL in 0.1 M acetic acid) containing brilliant blue (1 mg/mL) and 0.04% (w/v) sodium azide, and then the pH was adjusted to 5.5. After stirring for 30 min, the particle suspension was centrifuged at 40000 g, 4 °C for 30 min, and the particle pellet was collected, washed twice with water (the same pH as suspension), and centrifuged to remove the adsorbed brilliant blue on the particle surface. The content of free brilliant blue in the combined supernatants was measured using the spectrophotometer at 590 nm. Encapsulation efficiency (EE), loading capacity (LC), and particle preparation yield (PPY) were calculated using the following equations:

$$EE\ (\%) = 100 \times (A-B)/A$$

$$LC\ (\%) = 100 \times (A-B)/C$$

$$PPY\ (\%) = 100 \times C/D$$

Where, *A* is mg model compound added to the initial suspension, *B* is mg free compound (unencapsulated), C is the weight (mg) of dried loaded particles, and D is the total initial dry weight (mg) of all the compounds forming the particles.

5.2.7.2. Encapsulation of a water-insoluble model compound

Encapsulating β-carotene in particles was performed by slowly adding 2 mL β-carotene ethanol solution (0.5 mg/mL) to 18 mL chitosan (2 mg/mL in 0.1 M acetic acid), and then 18 mL of cruciferin solution (solubilized at pH 12) was added dropwise, the pH of the suspension was adjusted to 5.5, stirred for 30 min, and then concentrated to 30 mL using a rotary vacuum evaporator (Heidolph 2-Collegiate, Germany) at 50 °C. 1 mL of the concentrated suspension containing the loaded particles was mixed with 5 mL hexane, vortexed for 10 sec and then centrifuged at 10,000 rpm for 20 min at 4°C. The β-carotene extracted in the organic phase represented both unencapsulated and loosely-adsorbed β-carotene on the surface of particles. Absorbance of the organic phases was measured at 450 nm using the UV–VIS spectrometer and EE, LC and PPY were calculated (Mensi et al., 2013).

5.2.8. Simulated gastro-intestinal release study

Release experiments were performed in simulated gastric fluid (SGF) followed by simulated intestinal fluid (SIF) (Mensi et al., 2013; Chen and Subirade, 2005). Brilliant blue- and β-carotene-loaded particles were prepared using the previously described method. To simulate gastric condition, 20 mL of above suspensions was adjusted to pH 1.4 using 10 mL of 0.05M HCl containing 1 mg/mL pepsin and was agitated at 100 rpm and 37 °C in a water bath. Release studies were also performed at pH 1.4 and in the absence of pepsin. 0.5 mL samples were withdrawn from the release media at predetermined intervals. 0.25 mL of 1M sodium bicarbonate was added to the samples to increase pH to 7.4 and inactivate pepsin. Brilliant blue -containing samples were centrifuged (40000 g) and released brilliant blue in supernatant was measured. β-carotene was extracted from the withdrawn samples using 2.5 mL hexane and quantified using the same method previously described. After 2 h incubation in SGF, pepsin was inactivated by raising pH to 7.4 using 10 mL of 1M sodium bicarbonate and release studies were followed in SIF medium by adding 5 ml of 200 mM phosphate buffer pH 7.4 in the absence and presence of 2 mg/mL pancreatin. 0.5 mL samples were withdrawn at predetermined intervals. To stop pancreatin activity after sampling, brilliant blue -containing samples were heated at 90 °C for 5 min while for β-

carotene samples, free β-carotene was immediately extracted using hexane. The concentrations of released brilliant blue and β-carotene in SGF and following SIF media were measured and their cumulative percentages were calculated based on the total amount of the initial loaded compounds and the released compounds in recovery studies.

5.2.9. Statistical analysis

Experiments were carried out in triplicates and results were statistically analyzed using ANOVA and Duncan tests (version 9.2, SAS Institute Inc., Cary, NC, USA).

5.3. Results and discussion

5.3.1. Preparation of the particles

To prepare the particles, cruciferin and chitosan were solubilized at different concentrations at alkaline (pH 12) and acidic (pH 3) conditions, respectively, and then the cruciferin solution was dropwise added to the chitosan solution to achieve a pH ~ 4.5. The pH of the mixture was adjusted to different pHs and the formed particles suspensions were studied. Since the formation of particles would increase the turbidity of the suspensions, an indicator of 50% increase in the turbidity compared to initial protein solution was used to determine an appropriate particles formation. Our results showed that the mixtures didn't form particles at pHs 3.5 and 4.5 (low turbidity) due to high repulsive forces between positively-charged cruciferin and chitosan, likely formed at pHs 5.5 and 6.5 but depended on the ratio of cruciferin:chitosan, precipitated at pH 7.5. At pHs 5.5 and 6.5, in general, the appearance of the particles suspensions changed from clear to opaque at increasing cruciferin concentrations. Whereas the mixtures didn't form highly-turbid suspension at the ratio of 2:2, the particles prepared at the ratios of 7.5:2 and 10:2 were not stable and precipitated; the particles prepared at the ratios of 3:2 and 5:2 were stable and therefore used for further studies.

5.3.2. Particles characterization

5.3.2.1. Size, zeta potential and morphology of the particles

In general, the particle size increased at increasing pHs from 5.5 to 6.5 due to decreased protonation of chitosan (pKa~6.4) and cruciferin (pI ~7.2) (Table 5.1), which would decrease repulsion forces between chitosan and cruciferin, leading to particle aggregation and even precipitation at increasing cruciferin and chitosan ratio above 5:2. The zeta potential of particles

was not affected. Similar trend was reported for chitosan/tripolyphosphate and chitosan/hydroxypropyl methylcellulose phthalate by Makhlof et al. (2011). Polydispersity index (PDI) of the particles sizes was ~ 0.35, revealing satisfactory particles uniformity. Therefore, the particles prepared at the cruciferin:chitosan ratios of 3:2 and 5:2 at pH 5.5 were appropriate, and the ratio of 5:2 was chosen to prepare particles for further studies. Morphology of cruciferin and chitosan solutions and the particles were examined using TEM. The different structures observed in figure 1c compared to figures 1a and b, revealed that new spherical complexes formed through interaction between cruciferin and chitosan. The size of the structures was estimated in the range of 150-200 nm which is in aggrement with our results in particle size determination by DLS.

Table 5.1. Effect of cruciferin:chitosan ratio and pH of particles preparation on increasing the turbidity of particles suspension, and size and zeta potential of prepared particles. Values with different lowercase letters in the same column are significantly ($p<0.05$) different.

cruciferin:chitosan ratio	pH	Increasing turbidity (%)	Size (nm)	Zeta potential (mV)
3:2	5.5	190±4 ^{c}	157±8 ^{b}	+20±1.6 ^{a}
	6.5	281±1 ^{a}	175±10 ^{a}	+15.1±2.4 ^{a}
5:2	5.5	204±1 ^{b}	165±3 ^{ab}	+18.2±1.3 ^{a}
	6.5	Precipitated particles	---	---

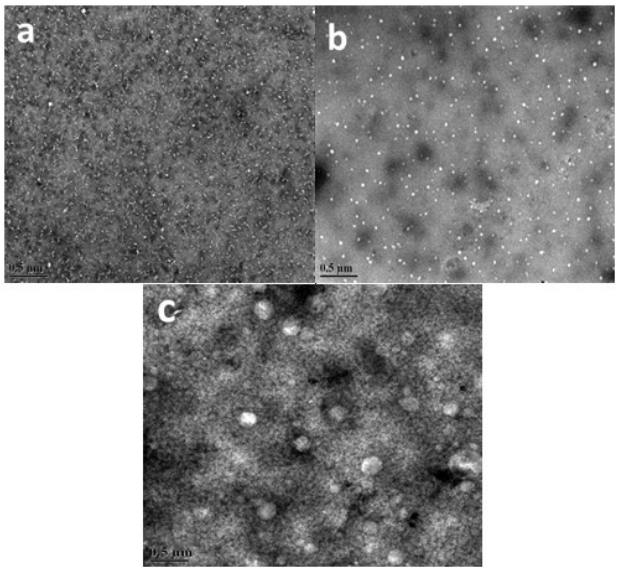

Figure 5.1. TEM images of cruciferin solution (5 mg/mL) (a); chitosan solution (2 mg/mL) (b); cruciferin/chitosan particles suspension (c). Samples were diluted 10 times before observation.

5.3.2.2. Surface hydrophobicity study

The surface hydrophobicity (S_0) of cruciferin was not affected before and after particle formation (8613±3 and 8421±34, respectively) (*Supplementary Figure 5.1)*, which indicated that the particle formation process didn't affect protein folding/unfolding and/or the availability of hydrophobic groups on the protein surface. Unlike Boeris et al. (2011) who reported chitosan decreased the S_0 of the pepsin/chitosan complex due to blocking the surface hydrophobic groups; the unchanged S_0 during particle formation suggested that either S_0 of cruciferin in the coating layer was not affected by chitosan, or the coating layer was just composed of cruciferin.

5.3.2.3. Intrinsic fluorescence study

The intrinsic fluorescence of a protein strongly depends on the conformation that the protein adopts in response to bulk solution conditions. Intrinsic fluorescence property of a protein is due to the presence of aromatic amino acids such as tryptophan and tyrosine (Gorinstein et al., 2000). The intensity of intrinsic fluorescence property of the particles at 594 nm was lower than that of cruciferin (Figure 5.2). Since no shift occurred in the emission λ_{max} of cruciferin before and after the complex formation, suggesting that the polarity of the environment surrounding tryptophan residues didn't change and therefore folding/unfolding process didn't happen in the particles formation process, which is in agreement with surface hydrophobicity results. There are two possibilities for the lower intrinsic fluorescence intensity of the particles: 1) the increased suspension turbidity resulting from the particles formation which could reduce the exciting and/or emitted radiations and 2) binding-induced quenching effect (van de Weert and Stella, 2011). However, the effect of the turbidity on emission intensity would be negligible due to the use of extensively diluted samples (×100 times). Therefore, binding-induced quenching effect resulted from interaction between chitosan and cruciferin might be responsible for the decreased intrinsic emission fluorescence of tryptophan during particle formation. Similar results were reported by van de Weert and Stella (2011) and Zimet and Livney (2009).

5.3.2.4. Driving forces involving the particles formation

As described in the materials and methods section, adding alkaline cruciferin solution (negatively-charged) into acidic chitosan solution (positively-charged) led to a pH value of ~ 4.5, which was lower than pI of cruciferin (~7.2) and pKa of chitosan (~6.4); therefore, both cruciferin and

chitosan polymers were positively-charged which would prevent the particle formation due to the presence of repulsive forces. At increasing pHs to 5.5-6, the decreased protonation of the polymers also decreased their repulsive forces, enabling them come closer to form different interactions.

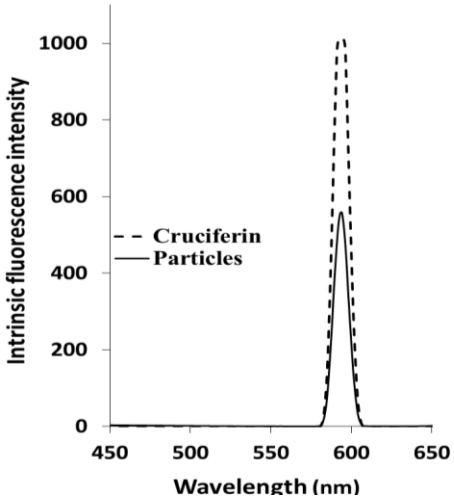

Figure 5.2. Intrinsic fluorescence intensity of cruciferin and cruciferi/chitosan particles.

The formation of particles could be affected by a number of interactions such as electrostatic, disulfide, hydrophobic and hydrogen bonding. To understand the responsible force for the particle formation, effects of dissociating agents, namely SDS, DTT, urea and NaCl, on the suspensions turbidity were determined. The suspension turbidity was decreased by 89 and 14% in the presence of urea and NaCl, respectively, but was not affected by DTT (Figure 5.3); SDS precipitated the particles due to the attractive interaction with the positively charged particles. The results showed that although electrostatic interaction could influence the particles formation due to the presence of amine and carboxyl groups in chitosan and cruciferin, hydrogen bonding was the major driving force for the particle preparation. Qin et al. (2011) and Xu and Du (2003) also reported that hydrogen bonding was the main force for chitosan particles formation (Qin et al., 2011; Xu and Du, 2003). As it was expected, disulfide bond and hydrophobic interactions were not important in the particles formation due to the absence of sulfhydryl and hydrophobic groups in chitosan. However, it was interesting to note that protein-protein interactions (i.e., hydrophobic forces) didn't play critical roles in the particles preparation.

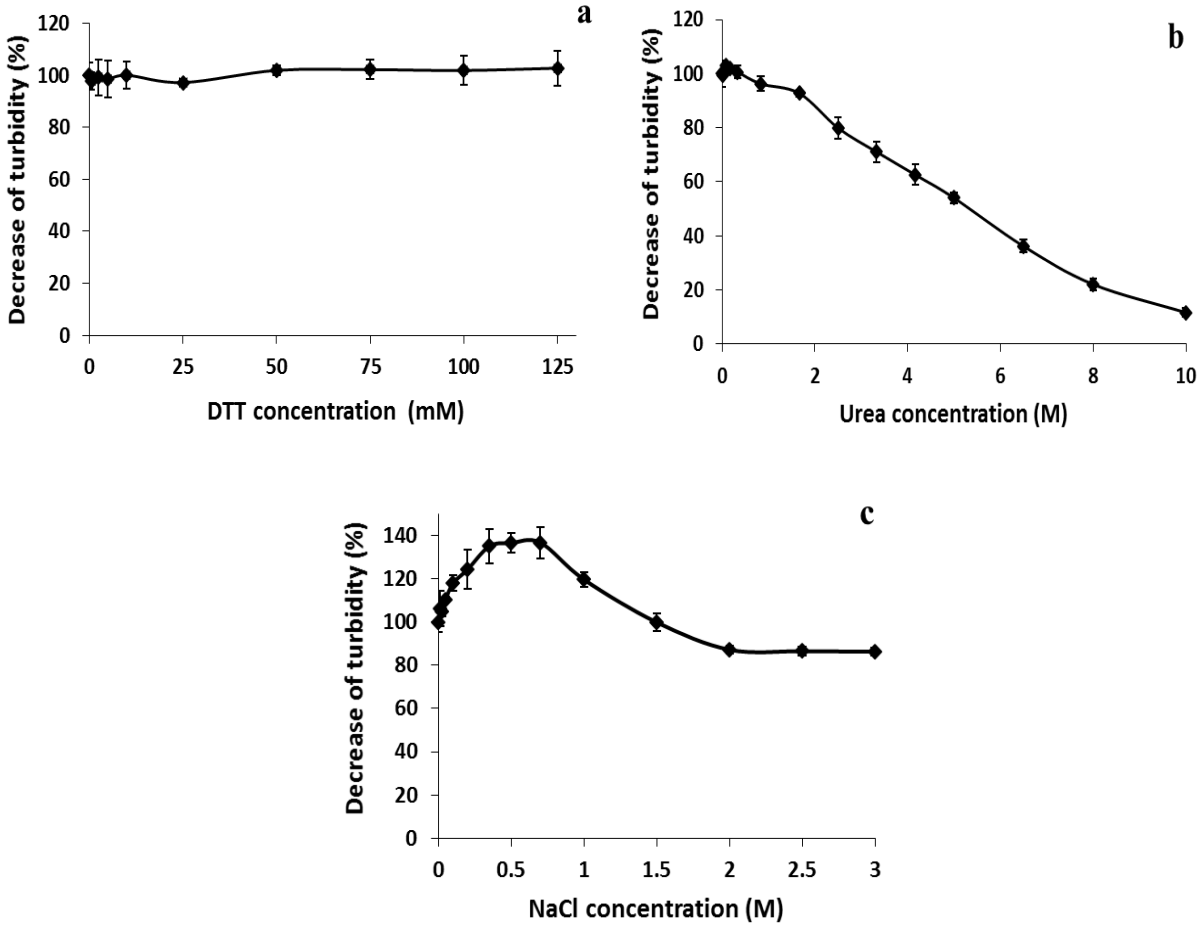

Figure 5.3. The effect of DTT (a), urea (b) and NaCl (c) on the turbidity of the nanoparticles dispersions

5.3.2.5. Thermal property study

The denaturation temperature of cruciferin powder was recorded at 174 °C (Figure 5.4) whereas it was previously reported 91 °C at 10% cruciferin solution (Wu and Muir, 2008). The presence of the moisture might be the reason for the difference observed in the thermal properties (Bier et al., 2014). Similar results were reported for dry sunflower protein isolate (181 °C) (Rouilly et al., 2001), lysozyme (200 °C), ovalbumin (208 °C) and bovine serum albumin (195 °C) (Carpenter et al., 2009) whereas the denaturation of these proteins occurred below 100 °C in aqueous solution. The midpoint of protein denaturation peaks is often called protein's melting temperature, drawing an analogy with melting points in solids (Bier et al., 2014). The melting points of chitosan and the particles were also observed at 159 and 209 °C, respectively (Figure 5.4a). The remarkable increase of melting point of the particles compared to cruciferin and chitosan suggested formation

of a new structure with enhanced thermal stability; the stability might be due to strong interactions between cruciferin and chitosan. Improvement in the thermal stability was also previously shown for the complexes of soy protein and chitosan (Huang et al., 2012) and carboxy methylcellulose and β-lactoglobulin (Capitani et al., 2007). The presence of a small peak at 166 °C in the particles thermogram could be attributed to the free form of cruciferin and/or chitosan which didn't contribute in the cruciferin-chitosan interactions.

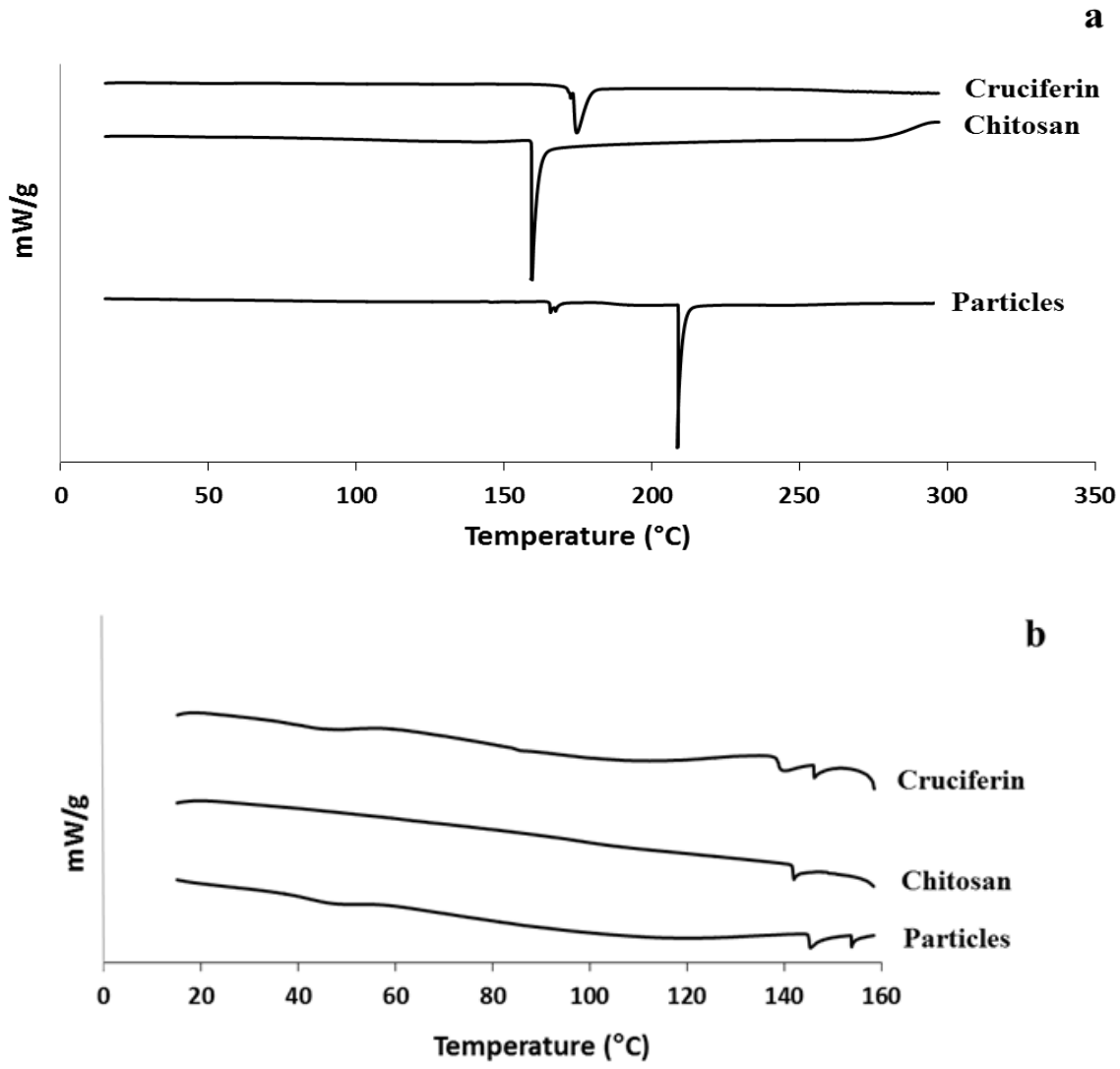

Figure 5.4. DSC thermograms of cruciferin, chitosan and cruciferin/chitosan particles: melting points (a) and water evaporation temperatures (b)

In the range of 15-160 °C (prior to the melting points), the DSC thermograms showed endothermic peaks corresponding to bound water evaporation temperatures from the polymer molecules (Figure 5.4b). While bound water was evaporated in the range of 139-142 °C from cruciferin and chitosan powders, the evaporation peak was recorded at 146 °C for the particles. Similar results were also reported for catechin-loaded chitosan particles (Dudhani and Kosaraju, 2010). The increased water evaporation temperature in the particles' thermograms might be due to the presence of more hydrophilic groups which strengthened the affinity of water binding to the particles (Luo et al., 2011).

5.3.2.6. FTIR study

In FTIR spectra, amide I (1600-1700 cm^{-1}) and amide II (1480-1545 cm^{-1}), corresponding respectively to C=O stretching and N−H bending, provide useful information about structural changes in polymers (Kong and Yu, 2007). In comparison with amide I, amide II has much less sensitivity to conformational changes but it is more sensitive to hydrogen-bonding changes in the environment of N-H groups (Almutawah et al., 2007; Ullah et al., 2011). In our study, while amide I band in the spectra of cruciferin, chitosan and the particles shifted in a small range of 1654-1656 cm^{-1}, amide II peak shifted from 1537 cm^{-1} wavenumber in cruciferin spectrum to 1558 cm^{-1} in the particles (Figure 5.5a). The blue shift of amide II peak indicated enhanced hydrogen bonding in the formation of cruciferin and chitosan particles, which was in agreement with our driving forces study showing that hydrogen bonding is the main driving force involved in the particles formation. However, the very small shift observed between the amide I bands of cruciferin and the particles revealed that the conformation of cruciferin didn't significantly change in particles formation. The result is also supported by our surface hydrophobicity and intrinsic fluorescence studies. The intensity of the peak at 1405 cm^{-1}, which is a joint contribution of vibration of –OH and –CH (Huang et al., 2012), increased in the particles spectrum compared to that in cruciferin spectrum. The increased intensity might be also due to formation of hydrogen bonding between cruciferin and chitosan. To study the small conformational changes, the secondary structure of cruciferin powder and the particles were also evaluated using deconvoluted FTIR spectra of amide I band, and were compared to the previously established wavenumber ranges (Kong and Yu, 2007; Pelton and McLean, 2000). The strong absorption at 1658 cm^{-1} indicated that α-helix was predominant in cruciferin, although the bands of 1637, 1692 and 1678 cm^{-1} representing β-sheets and turns were also observed (Figure 5.5b).

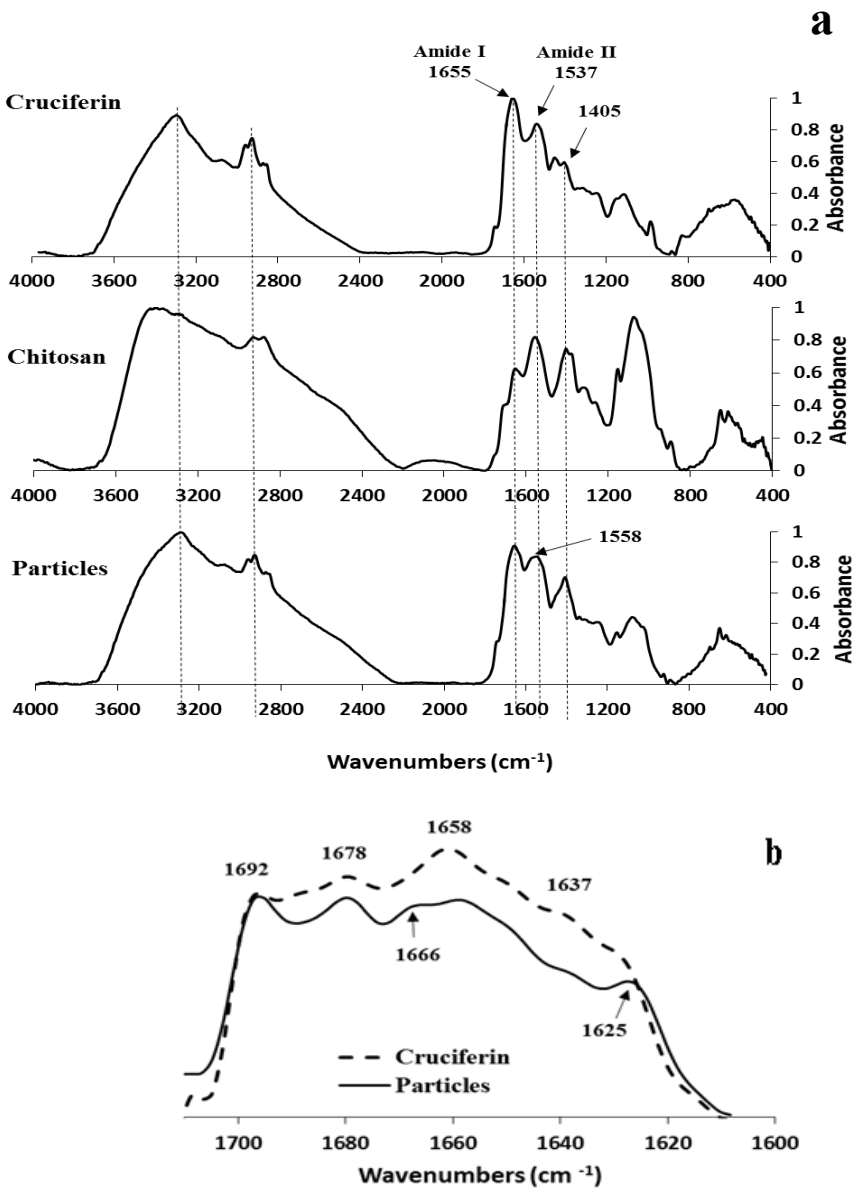

Figure 5.5. FTIR spectra (a) and deconvoluted FTIR spectra (b) of cruciferin, chitosan and cruciferin/chitosan particles

In complex with chitosan, the intensity of the β-turn peak (1678 cm^{-1}) increased and new peaks were appeared at 1625 and 1666 cm^{-1} assigning to the new structures of β-sheet and turns, respectively (Kong and Yu, 2007; Pelton and McLean, 2000) which are mainly formed through hydrogen bonding (Gilbert et al., 2005). The appearance of the new peaks indicated an ordered structure formed in the particles due mainly to enhanced hydrogen bonding.

5.3.3. In vitro cytotoxicity of the particles

The potential cytotoxicity of the particles on Caco-2 cells was assessed using the MTT assay. Incubation of the particles at three concentrations of 0.5, 1.5, and 2.5 mg/mL for 24 h didn't show any significant change in the cellular viability compared to the control (Figure 5.6), suggesting that the particles were not toxic to the cells.

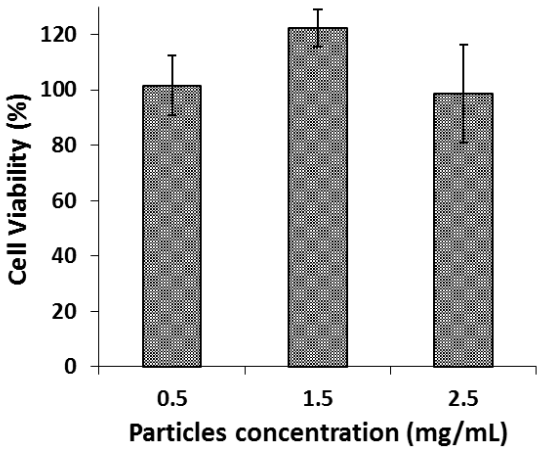

Figure 5.6. Effect of cruciferin/chitosan nanoparticles on Caco-2 cells survival after 24 h incubation at 37°C (compared to control).

5.3.4. Cell uptake of the particles

Confocal microscopy images of Caco-2 cells after 6h incubation with coumarin-6-loaded particles and free coumarin-6 were shown in figures 5.7A and B. The final concentration of the particles and coumarin-6 in the incubating DMEM medium were 0.5 mg/mL and 2.5 μg/mL, respectively. The size and zeta potential of the re-suspended particles were 304±41 nm and +7.9±2.2 mV, respectively. Since the pH of the suspension was close to cruciferin isoelectric point (pH 7.2), the zeta potential of the particles decreased, and probably due to the decrease of repulsive forces, the size of particles increased. While remarkable fluorescence intensity was observed within the cells treated with the loaded particles, no noticeable signal was detected in the cells incubated with free coumarin-6. The results showed that the particles were uptaken by cells and mostly delivered into the cells cytoplasm. This implied that the particles might be an appropriate carrier for delivery of encapsulated compounds to the cells.

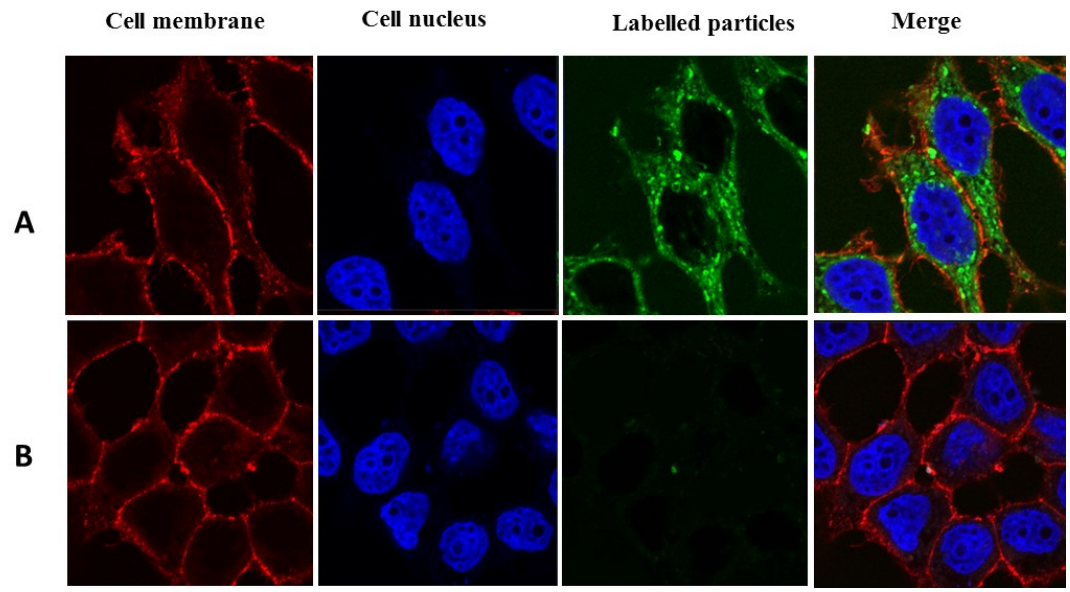

Figure 5.7. Confocal microscopic images of Caco-2 cells after 6 h incubation with coumarin 6-loaded cruciferin/chitosan nanoparticles (green) (A) and free coumarin-6 (B). The cell membrane and nucleus were stained using Alexa 594 and DAPI, respectively.

5.3.5. Encapsulation and *in vitro* release of the model compounds

Encapsulation property and release behaviour, two important factors affecting the efficiency of a delivery system, were studied for the particles. Brilliant blue and β-carotene, representing hydrophilic and hydrophobic model compounds, were encapsulated in the particles. While the encapsulation efficiency (EE), loading capacity (LC) and particle preparation yield (PPY) of brilliant blue were 72.4%±0.7, 16.3%±0.8 and 55.5%±2.6, those for β-carotene were 98.8%±0.2, 7.7%±0.2 and 44.5%±1.1, respectively. Previously the EE of β-carotene was reported to be 39.5%±0.3 in chitosan-β-lactoglobulin nanoparticles (Lee et al., 2012), 54.7% and 87.6%, respectively, in chitosan-alginate beads and sodium caseinate sub-micelles (Chu et al., 2007; Donhowe et al., 2014). The higher EE of the particles suggested that the particles are appropriate carriers for both water-soluble and -insoluble compounds. Figure 5.8 shows a schematic illustration of the particle formation and encapsulation of model compounds.

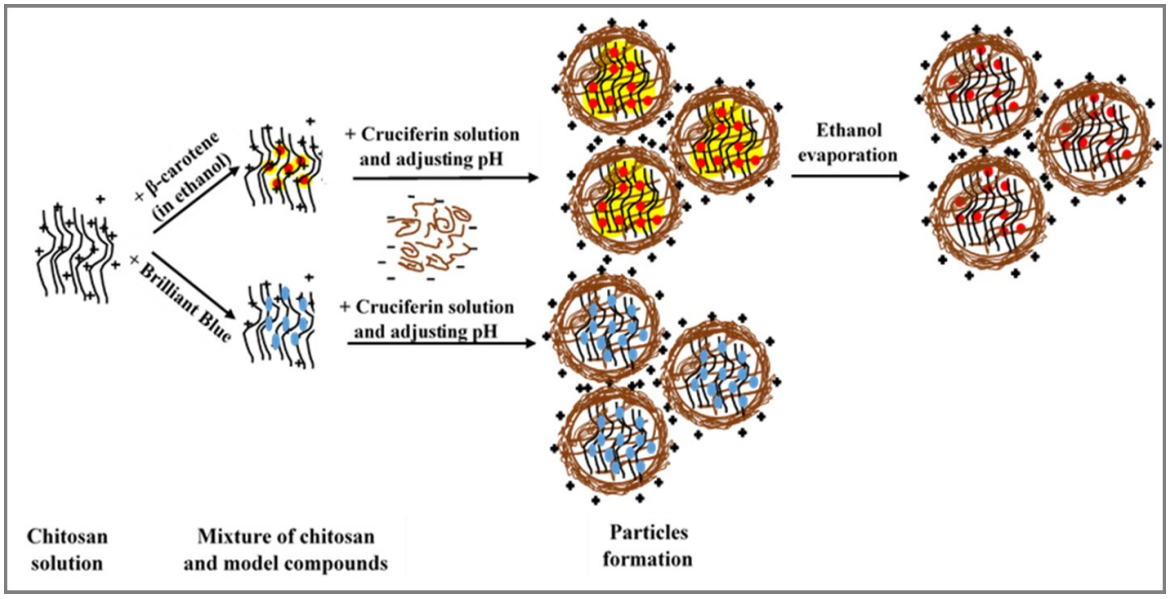

Figure 5.8. A scheme of Cru/Cs particle formation and encapsulation of model compounds

In vitro release of brilliant blue and β-carotene from the particles was studied using 2 h incubation in SGF followed by 6 h in SIF with and without pepsin and pancreatin, respectively (Figure 5.9). In SGF (in the presence or absence of pepsin), less than 10% and 5% of encapsulated brilliant blue and β-carotene were released in the first 2 h, due to the weakly attached compounds on the surface of the particles. These results suggested that the particles were resistant to both low pH and pepsin. Since chitosan is degraded at low pH (Makhlof et al., 2011), the particles resistance in the SGF further supported that chitosan was coated by cruciferin layers. The coating layer might be a monolayer of cruciferin but not a complex of cruciferin and chitosan since the complex can be degraded at pH 1.2 due to high protonation of chitosan (pKa~6.4) and cruciferin (pI ~7.2) and increased repulsive forces. This result further bolstered our previous surface hydrophobicity results showing the presence of a cruciferin layer on the particles surface. The indigestibility of cruciferin in the stomach was reported in our previous study (Akbari and Wu, 2016) and also by Bos et al. (2007). Our results suggested that cruciferin could be applied as a protective polymer for coating chitosan particles and its protection effect is comparable with other coating polymers such as hydroxypropyl methylcellulose phthalate (a pH-sensitive polymer); where, 25% of encapsulated insulin was released from chitosan/hydroxypropyl methylcellulose phthalate particles (Makhlof et al., 2011).

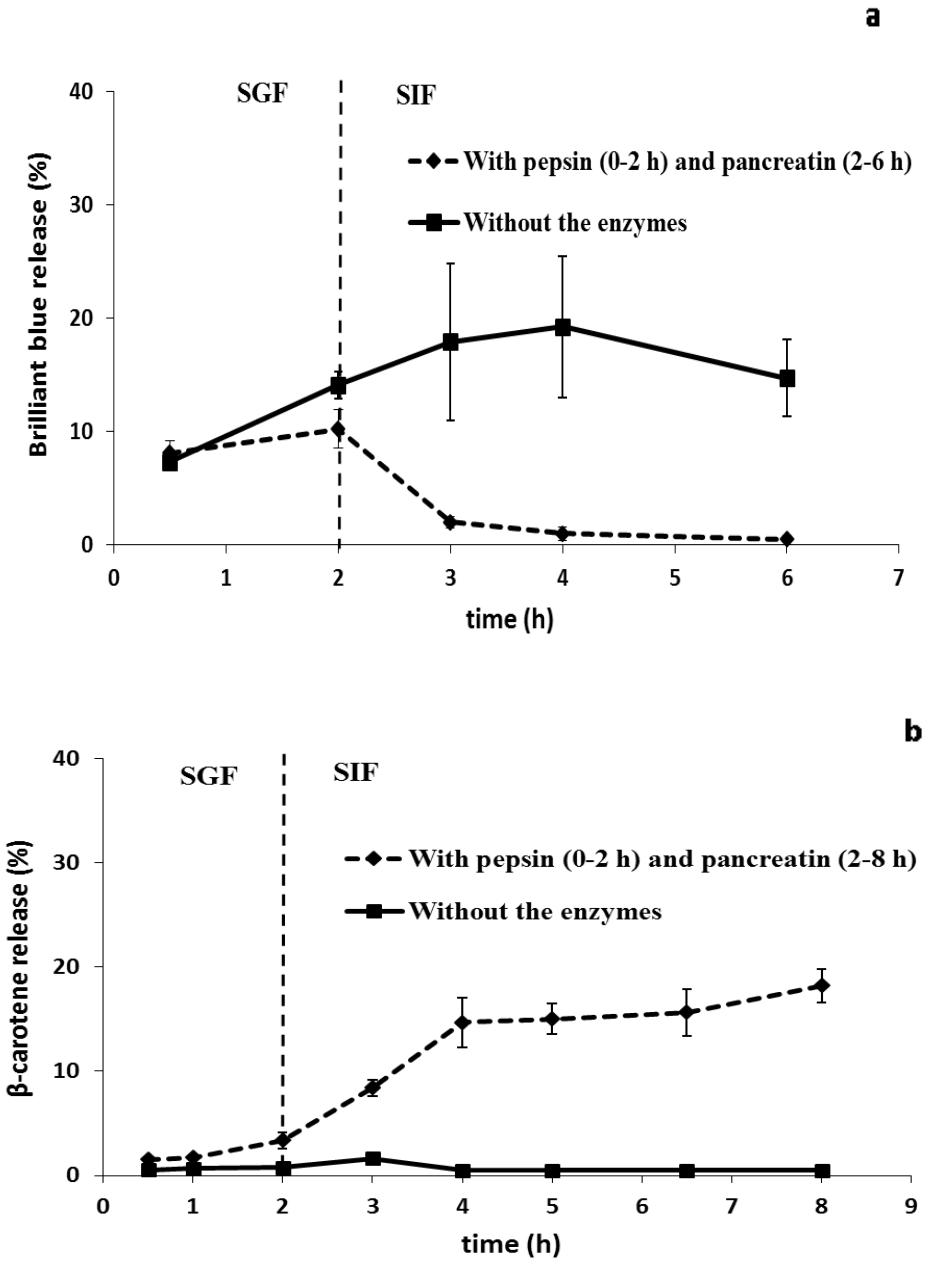

Figure 5.9. Release profiles of brilliant blue (a) and β-carotene (b) from cruciferin/chitosan particles in simulated gastric fluid (SGF) followed by simulated intestinal fluid (SIF) in the presence and absence of pepsin and pancreatin, respectively

In SIF (pH 7.4) and in the absence of pancreatin, the particles stayed resistant and only less than 5-10% of encapsulated brilliant blue and B-carotene were released (Figure 5.9). However, in the presence of pancreatin, the previously released brilliant blue (during in SGF) was re-adsorbed by

the particles and precipitated along with particles after centrifugation. The reason might be due to the degradation of the cruciferin layer by pancreatin which released positively-charged amine groups of chitosan and then bound to the previously released negatively-charged brilliant blue. Similar results were reported by Chen and Subirade (2005).

However, unlike brilliant blue-loaded particles, degradation of the cruciferin layer by pancreatin released ~15% of β-carotene in SIF. The released β-carotene from enzymatic-hydrolyzed particles might be related to the β-carotene which was entrapped in the cruciferin coating layer. Afterward, the remaining encapsulated β-carotene, entrapped in the chitosan-based core, was not released since the used chitosan was resistant in SIF. The release profile of encapsulated compounds from chitosan particles depends on chitosan characteristics such as molecular weight and degree of deacetylation. For instance, the release rate of the compounds from high-molecular weight chitosan (HMC) is lower than that of low-molecular weight chitosan (LMC) (Xu and Du, 2003). Since the chitosan core in this study didn't release the compounds, the release profile was not affected by cruciferin coating. However, if LMC is used as a particle core, the composition of coating layers might influence the release rate from whole particles. Similar results were reported in a chitosan dispersed system coated with aminoalkyl methacrylate copolymer RS (Eudragit RS) (Shimono et al., 2002) and lactose-sodium alginate-chitosan composite particles (Takeuchi et al., 2005). Therefore, the particles are promising carriers for delivery of sensitive compounds to both gastric and intestinal conditions such as protein-based bioactive compounds.

5.3.6. Interaction between β-carotene and the particles

The encapsulated β-carotene might affect the thermal property and structure of the particles. In the study of the DSC thermograms, pure crystalline β-carotene showed two melting peaks at 168 and 176 °C (Figure 5.10a).

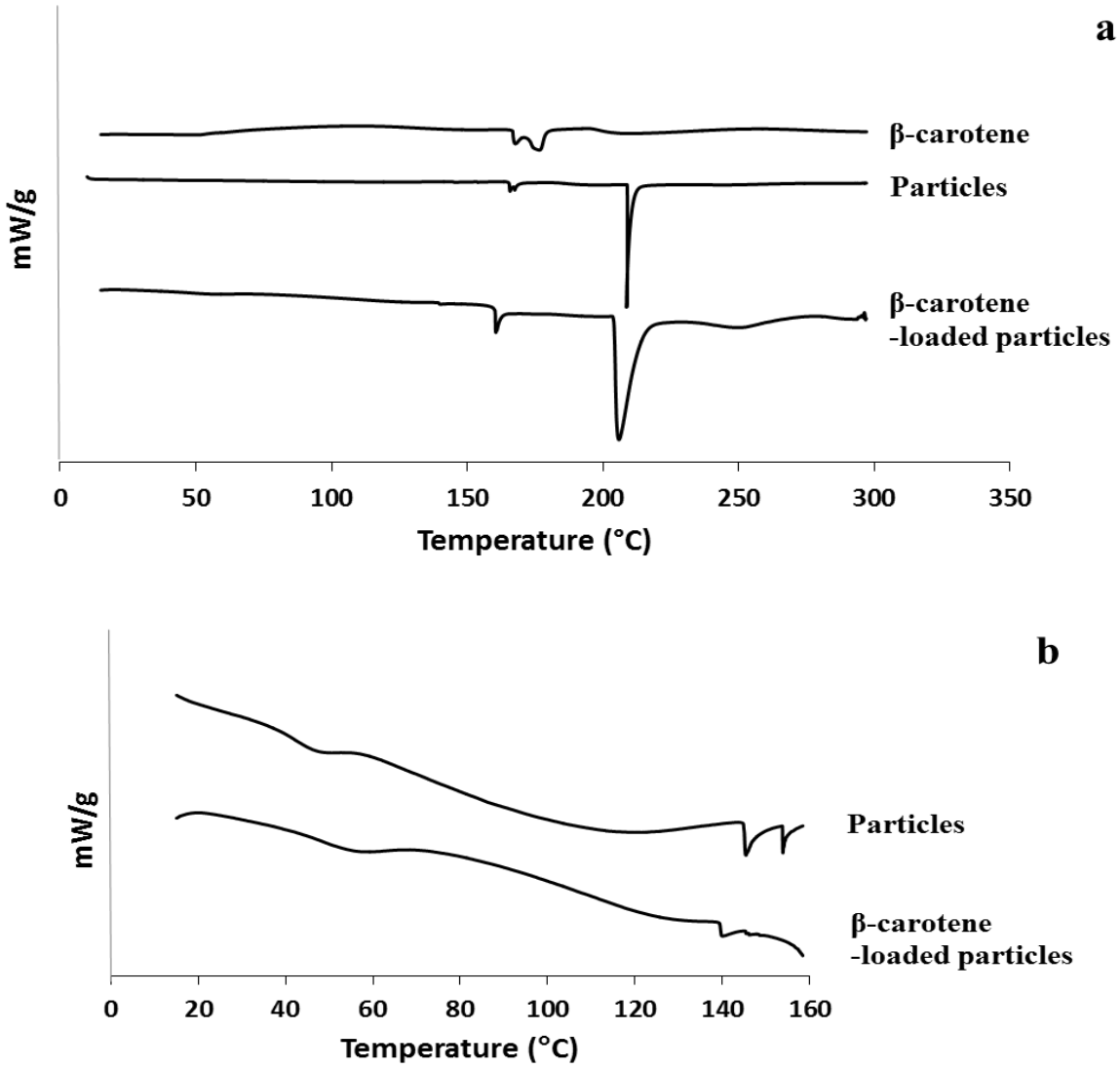

Figure 5.10. DSC thermograms of β-carotene, cruciferin/chitosan particles and β-carotene-loaded particles: melting points (a) and water evaporation temperatures (b)

After dissolving β-carotene in ethanol and encapsulation in the particles, its melting point decreased to 160 °C. The melting point of loaded particles was 205 °C compared to 209 °C of empty particles indicating less crystalline structure in the loaded particles. Transition of β-carotene molecules from crystalline powder to its amorphous form during encapsulation process might be the reason for the decreased melting point. Similar melting points of 178-180 °C and 150-160 °C were also reported by Coronel-Aguilera and Martín Gonzalez (2015) and de Paz et al. (2012) for pure (crystalline) and encapsulated (amorphous) forms of β-carotene, respectively.

At the temperature range of 15-160 °C (prior to the melting points), endothermic water evaporation peaks were presented at 146 °C and 140 °C for empty and β-carotene-loaded particles, respectively (Figure 5.10b). The decrease in the water evaporation temperature might be due to the presence of β-carotene aliphatic chain and its hydrophobic groups which had less affinity to water and decreased the evaporation temperature. Similar observations were also reported by Luo et al. (2011) and Paula et al. (2011) in encapsulation of vitamin D3 and essential oils, respectively.

To study the effect of the encapsulation on the structure of the particles, the FTIR spectra of β-carotene, particles and β-carotene-loaded particles were compared in Figure 5.11. Two strong peaks were observed at 965 and 2925 cm^{-1} in the β-carotene spectrum representing trans conjugated alkene CH and CH stretching vibration, respectively (Yi et al., 2015; Schlucker et al., 2003). The disappearance of 965 and 1724 cm^{-1} peaks in the β-carotene-loaded particles spectrum indicated successful encapsulation of β-carotene in the particles. Similar result was shown by Teng et al. (2013) in encapsulation of D_3 in chitosan/soy protein complex. Evaluation of the spectrum of β-carotene-loaded particles also showed that no shift was observed in the amide I peak compared to that of particles, indicating that the incorporation of β-carotene didn't affect the conformation of the protein. However, a redshift of amide II band of loaded-particles compared to that of empty particles (from 1558 to 1537 cm^{-1}) revealed that the environment of N-H groups changed favouring weaker hydrogen bonding. The intensity of 1405 cm^{-1} peak was also decreased after β-carotene incorporation, further supporting decreased hydrogen bonding. The decreased hydrogen bonding in the loaded particles might be due to the presence of long aliphatic chain of β-carotene which weakened the initial hydrogen interactions present in the particles. Luo et al. (2011) also reported that amide I and II in the spectrum of α-tocopherol-loaded zein particles redshifted to lower frequencies compared to those in zein spectrum. They suggested that electrostatic interaction is involved in the α-tocopherol encapsulation. However, Yi et al. (2015) showed that the incorporation of β-carotene in casein, whey and soy protein particles shifted amide I and amide II respectively to lower and higher frequencies compared to empty particles.

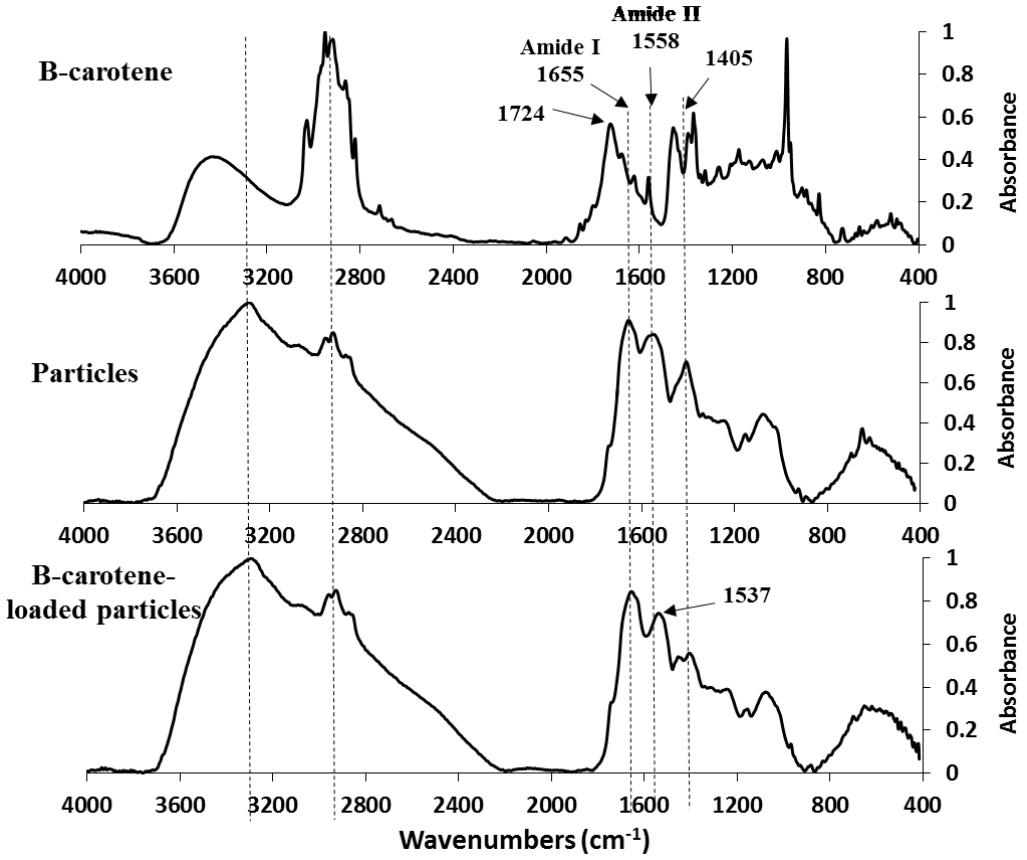

Figure 5.11. FTIR spectra of cruciferin/chitosan particles, β-carotene and β-carotene -loaded particles

Binding of β-carotene to the particles can also be characterized by determination of intrinsic fluorescence of tryptophan residues in cruciferin structure. The intensity of particles was initially decreased after encapsulation of 100 mg/mL β-carotene (Figure 5.12). However, unlike the results reported by Perez et al. (2014) and Zimet and Livney (2009) showing that the fluorescence intensity of loaded particles decreased does-dependently at increasing loaded compounds concentrations due to the quenching effect, the emission intensity of β-carotene-loaded particles didn't change at increasing concentrations of loaded β-carotene. The initial decrease observed in the intensity after adding β-carotene suggested that a small part of β-carotene was bound to cruciferin coating and led to quenching effect; while, most of loaded β-carotene didn't interact with cruciferin and the binding occurred in chitosan core part and in other words, β-carotene was loaded in chitosan-based core of the particles. This confirms that the 15% released β-carotene in

SIF (with enzyme) was released from cruciferin coating layer and the remaining 80-85% β-carotene was entrapped in chitosan core which was not affected by the enzyme and/or pH 7.4.

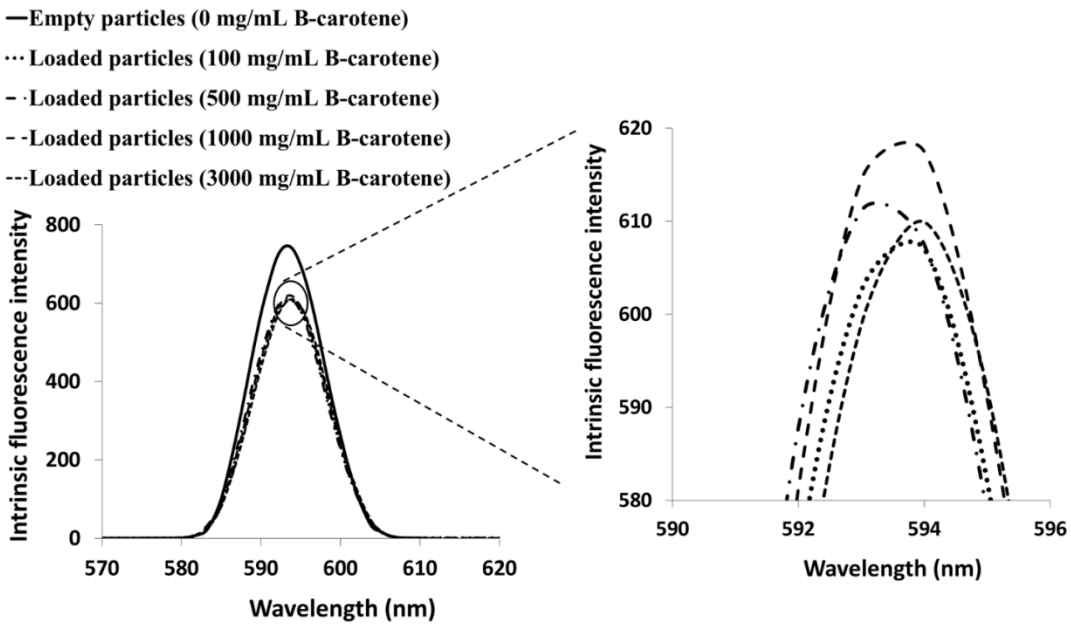

Figure 5.12. Effect of encapsulation of different β-carotene concentrations on intrinsic fluorescence intensity of cruciferin/chitosan particles

5.4. Conclusion

Cruciferin/chitosan nanoparticles with average size of 165 nm were prepared at pH of 5.5 and a cruciferin: chitosan ratio of 5:2. The particles were not toxic to Caco-2 cells and were uptaken after 6 h of incubation. The particles had ability to encapsulate both hydrophilic and hydrophobic model compounds. Our study demonstrated that chitosan particles coated with a single cruciferin layer have enhanced stability at low pH, thus circumventing the common degradation of uncoated-chitosan particles at low pH stomach and strengthening their applicability in food uses. Therefore, the nanoparticles would be promising carriers for sensitive compounds to stomach and intestine conditions. The nano-sized particles might be also absorbed directly by cells with improved bioavailability due to the mucoadhesive and paracellular permeation enhancing properties of chitosan. Moreover, the complex might act as colon targeting delivery systems since chitosan is degraded in the colon and release the encapsulated compounds in the target sites. Since cruciferin is a GRAS natural polymer, bioactive-loaded particles might be used for food fortification; this is

the advantage of the particles compared to synthetic polymers-coated chitosan particles which are applicable for drugs.

5.5. References:

Akbari, A. & Wu, J. (2016). Cruciferin nanoparticles: Preparation, characterization and their potential application in delivery of bioactive compounds. *Food Hydrocolloids,* 54, 107-118.

Akbari, A. & Wu, J. (2015). An integrated method of isolating napin and cruciferin from defatted canola meal. *Lwt-Food Science and Technology,* 64(1), 308-315.

Alizadeh-Pasdar, N. & Li-Chan, E. C. Y. (2000). Comparison of protein surface hydrophobicity measured at various pH values using three different fluorescent probes. *Journal of Agricultural and Food Chemistry,* 48(2), 328-334.

Almutawah, A., Barker, S. A., & Belton, P. S. (2007). Hydration of gluten: A dielectric, calorimetric, and fourier transform infrared study. *Biomacromolecules,* 8(5), 1601-1606.

Bier, J. M., Verbeek, C. J. R., & Lay, M. C. (2014). Thermal transitions and structural relaxations in protein-based thermoplastics. *Macromolecular Materials and Engineering,* 299(5), 524-539.

Boeris, V., Micheletto, Y., Lionzo, M., da Silveira, N. P., & Pico, G. (2011). Interaction behavior between chitosan and pepsin. *Carbohydrate Polymers,* 84(1), 459-464.

Bos, C., Airinei, G., Mariotti, F., Benamouzig, R., Berot, S., Evrard, J., Fenart, E., Tome, D., & Gaudichon, C. (2007). The poor digestibility of rapeseed protein is balanced by its very high metabolic utilization in humans. *Journal of Nutrition,* 137(3), 594-600.

Bouwmeester, H., Dekkers, S., Noordam, M. Y., Hagens, W. I., Bulder, A. S., de Heer, C., ten Voorde, S. E. C. G., Wijnhoven, S. W. P., Marvin, H. J. P., & Sips, A. J. A. M. (2009). Review of health safety aspects of nanotechnologies in food production. *Regulatory Toxicology and Pharmacology,* 53(1), 52-62.

Capitani, C., Perez, O. E., Pacheco, B., Teresa, M., & Pilosof, A. M. R. (2007). Influence of complexing carboxymethylcellulose on the thermostability and gelation of alpha-lactalbumin and beta-lacto globulin. *Food Hydrocolloids,* 21(8), 1344-1354.

Carpenter, J., Katayama, D., Liu, L., Chonkaew, W., & Menard, K. (2009). Measurement of T-g in lyophilized protein and protein excipient mixtures by dynamic mechanical analysis. *Journal of Thermal Analysis and Calorimetry,* 95(3), 881-884.

Chen, L. Y. & Subirade, M. (2005). Chitosan/beta-lactoglobulin core-shell nanoparticles as nutraceutical carriers. *Biomaterials,* 26(30), 6041-6053.

Chourasia, M. K. & Jain, S. K. (2003). Pharmaceutical approaches to colon targeted drug delivery systems. *Journal of Pharmacy and Pharmaceutical Sciences,* 6(1), 33-66.

Chu, B., Ichikawa, S., Kanafusa, S., & Nakajima, M. (2007). Preparation and characterization of beta-carotene nanodispersions prepared by solvent displacement technique. *Journal of Agricultural and Food Chemistry,* 55(16), 6754-6760.

Coronel-Aguilera, C. P. & Martin-Gonzalez, M. F. S. (2015). Encapsulation of spray dried beta-carotene emulsion by fluidized bed coating technology. *Lwt-Food Science and Technology,* 62(1), 187-193.

de Paz, E., Martin, A., Estrella, A., Rodriguez-Rojo, S., Matias, A. A., Duarte, C. M. M., & Jose Cocero, M. (2012). Formulation of beta-carotene by precipitation from pressurized ethyl acetate-on-water emulsions for application as natural colorant. *Food Hydrocolloids,* 26(1), 17-27.

Donhowe, E. G., Flores, F. P., Kerr, W. L., Wicker, L., & Kong, F. (2014). Characterization and in vitro bioavailability of beta-carotene: Effects of microencapsulation method and food matrix. *Lwt-Food Science and Technology,* 57(1), 42-48.

Dudhani, A. R. & Kosaraju, S. L. (2010). Bioadhesive chitosan nanoparticles: Preparation and characterization. *Carbohydrate Polymers,* 81(2), 243-251.

Elzoghby, A. O., El-Fotoh, W. S. A., & Elgindy, N. A. (2011). Casein-based formulations as promising controlled release drug delivery systems. *Journal of Controlled Release,* 153(3), 206-216.

Elzoghby, A. O., Samy, W. M., & Elgindy, N. A. (2012). Protein-based nanocarriers as promising drug and gene delivery systems. *Journal of Controlled Release,* 161(1), 38-49.

Gaumet, M., Gurny, R., & Delie, F. (2009). Localization and quantification of biodegradable particles in an intestinal cell model: The influence of particle size. *European Journal of Pharmaceutical Sciences,* 36(4-5), 465-473.

Gilbert, V., Rouabhia, M., Wang, H. X., Arnould, A. L., Remondetto, G., & Subirade, M. (2005). Characterization and evaluation of whey protein-based biofilms as substrates for in vitro cell cultures. *Biomaterials,* 26(35), 7471-7480.

Gorinstein, S., Goshev, I., Moncheva, S., Zemser, M., Weisz, M., Caspi, A., Libman, I., Lerner, H. T., Trakhtenberg, S., & Martin-Belloso, O. (2000). Intrinsic tryptophan fluorescence of human serum proteins and related conformational changes. *Journal of Protein Chemistry,* 19(8), 637-642.

He, B., Lin, P., Jia, Z., Du, W., Qu, W., Yuan, L., Dai, W., Zhang, H., Wang, X., Wang, J., Zhang, X., & Zhang, Q. (2013). The transport mechanisms of polymer nanoparticles in Caco-2 epithelial cells. *Biomaterials,* 34(25), 6082-6098.

Huang, G., Sun, Y., Xiao, J., & Yang, J. (2012). Complex coacervation of soybean protein isolate and chitosan. *Food Chemistry,* 135(2), 534-539.

Kong, J. & Yu, S. (2007). Fourier transform infrared spectroscopic analysis of protein secondary structures. *Acta Biochimica Et Biophysica Sinica,* 39(8), 549-559.

Lee, P. S., Yim, S. G., Choi, Y., Thi Van Anh Ha, & Ko, S. (2012). Physiochemical properties and prolonged release behaviours of chitosan-denatured beta-lactoglobulin microcapsules for potential food applications. *Food Chemistry,* 134(2), 992-998.

Luo, Y., Teng, Z., Wang, T. T. Y., & Wang, Q. (2013). Cellular uptake and transport of zein nanoparticles: Effects of sodium caseinate. *Journal of Agricultural and Food Chemistry,* 61(31), 7621-7629.

Luo, Y., Zhang, B., Whent, M., Yu, L., & Wang, Q. (2011). Preparation and characterization of zein/chitosan complex for encapsulation of alpha-tocopherol, and its *in vitro* controlled release study. *Colloids and Surfaces B-Biointerfaces,* 85(2), 145-152.

Makhlof, A., Tozuka, Y., & Takeuchi, H. (2011). Design and evaluation of novel pH-sensitive chitosan nanoparticles for oral insulin delivery. *European Journal of Pharmaceutical Sciences,* 42(5), 445-451.

Mensi, A., Choiset, Y., Haertle, T., Reboul, E., Borel, P., Guyon, C., de Lamballerie, M., & Chobert, J. (2013). Interlocking of beta-carotene in beta-lactoglobulin aggregates produced under high pressure. *Food Chemistry,* 139(1-4), 253-260.

HSDA 2013

Paula, H. C. B., Sombra, F. M., Cavalcante, R. d. F., Abreu, F. O. M. S., & de Paula, R. C. M. (2011). Preparation and characterization of chitosan/cashew gum beads loaded with Lippia sidoides essential oil. *Materials Science & Engineering C-Materials for Biological Applications,* 31(2), 173-178.

Pelton, J. T. & McLean, L. R. (2000). Spectroscopic methods for analysis of protein secondary structure. *Analytical Biochemistry,* 277(2), 167-176.

Perez, A. A., Andermatten, R. B., Rubiolo, A. C., & Santiago, L. G. (2014). Beta-Lactoglobulin heat-induced aggregates as carriers of polyunsaturated fatty acids. *Food Chemistry,* 158, 66-72.

Pinterits, A. & Arntfield, S. D. (2008). Improvement of canola protein gelation properties through enzymatic modification with transglutaminase. *Lwt-Food Science and Technology,* 41(1), 128-138.

Qin, Y., Chen, L., Wang, X., Zhao, X., & Wang, F. (2011). Enhanced mechanical performance of poly(propylene carbonate) via hydrogen bonding interaction with o-lauroyl chitosan. *Carbohydrate Polymers,* 84(1), 329-334.

Rouilly, A., Orliac, O., Silvestre, F., & Rigal, L. (2001). DSC study on the thermal properties of sunflower proteins according to their water content. *Polymer,* 42(26), 10111-10117.

Schlucker, S., Szeghalmi, A., Schmitt, M., Popp, J., & Kiefer, W. (2003). Density functional and vibrational spectroscopic analysis of beta-carotene. *Journal of Raman Spectroscopy,* 34(6), 413-419.

Schmitt, C., Moitzi, C., Bovay, C., Rouvet, M., Bovetto, L., Donato, L., Leser, M. E., Schurtenberger, P., & Stradner, A. (2010). Internal structure and colloidal behaviour of covalent whey protein microgels obtained by heat treatment. *Soft Matter,* 6(19), 4876-4884.

Shimono, N., Takatori, T., Ueda, M., Mori, M., Higashi, Y., & Nakamura, Y. (2002). Chitosan dispersed system for colon-specific drug delivery. *International Journal of Pharmaceutics,* 245(1-2), 45-54.

Slutter, B., Plapied, L., Fievez, V., Alonso Sande, M., des Rieux, A., Schneider, Y., Van Riet, E., Jiskoot, W., & Preat, V. (2009). Mechanistic study of the adjuvant effect of biodegradable nanoparticles in mucosal vaccination. *Journal of Controlled Release,* 138(2), 113-121.

Takeuchi, H., Thongborisute, J., Matsui, Y., Sugihara, H., Yamamoto, H., & Kawashima, Y. (2005). Novel mucoadhesion tests for polymers and polymer-coated particles to design optimal mucoadhesive drug delivery systems. *Advanced Drug Delivery Reviews,* 57(11), 1583-1594.

Tan, S. H., Mailer, R. J., Blanchard, C. L., & Agboola, S. O. (2011). Extraction and characterization of protein fractions from Australian canola meals. *Food Research International,* 44(4), 1075-1082.

Teng, Z., Luo, Y., & Wang, Q. (2013). Carboxymethyl chitosan-soy protein complex nanoparticles for the encapsulation and controlled release of vitamin D-3. *Food Chemistry,* 141(1), 524-532.

Ullah, A., Vasanthan, T., Bressler, D., Elias, A. L., & Wu, J. (2011). Bioplastics from feather quill. *Biomacromolecules,* 12(10), 3826-3832.

van de Weert, M. & Stella, L. (2011). Fluorescence quenching and ligand binding: A critical discussion of a popular methodology. *Journal of Molecular Structure,* 998(1-3), 144-150.

Wu, J. & Muir, A. D. (2008). Comparative structural, emulsifying, and biological properties of 2 major canola proteins, cruciferin and napin. *Journal of Food Science,* 73(3), C210-C216.

Wu, J., Aluko, R. E., & Muir, A. D. (2009). Production of angiotensin I-converting enzyme inhibitory peptides from defatted canola meal. *Bioresource Technology,* 100(21), 5283-5287.

Xu, Y. M. & Du, Y. M. (2003). Effect of molecular structure of chitosan on protein delivery properties of chitosan nanoparticles. *International Journal of Pharmaceutics,* 250(1), 215-226.

Yamada, Y., Iwasaki, M., Usui, H., Ohinata, K., Marczak, E. D., Lipkowski, A. W., & Yoshikawa, M. (2010). Rapakinin, an anti-hypertensive peptide derived from rapeseed protein, dilates mesenteric artery of spontaneously hypertensive rats via the prostaglandin IP receptor followed by CCK1 receptor. *Peptides,* 31(5), 909-914.

Yi, J., Lam, T. I., Yokoyama, W., Cheng, L. W., & Zhong, F. (2015). Beta-carotene encapsulated in food protein nanoparticles reduces peroxyl radical oxidation in Caco-2 cells. *Food Hydrocolloids,* 43, 31-40.

Yoshie-Stark, Y., Wada, Y., & Waesche, A. (2008). Chemical composition, functional properties, and bioactivities of rapeseed protein isolates. *Food Chemistry,* 107(1), 32-39.

Zimet, P. & Livney, Y. D. (2009). Beta-lactoglobulin and its nanocomplexes with pectin as vehicles for omega-3 polyunsaturated fatty acids. *Food Hydrocolloids,* 23(4), 1120-1126.

5.6. Appendix C: Supplementary Information

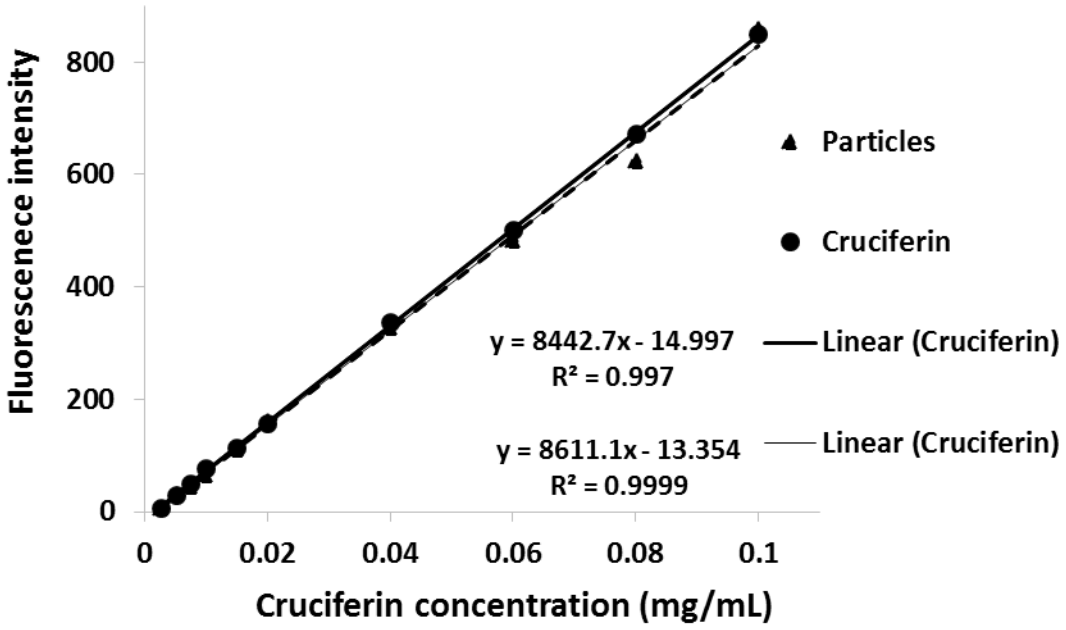

Supplementary Figure 5.1. Surface hydrophobicity (S_0) of cruciferin and cruciferin/chitosan particles

CHAPTER 6- Cellular uptake and trans-cellular transport of cruciferin-based nanoparticles in Caco-2 and its co-culture with /HT29-MTX cells

6.1. Introduction

In addition to providing protection to bioactive compounds from harsh conditions of processing and gastrointestinal (GI) tract, encapsulation is a promising strategy to improve absorption and bioavailability (McClements, 2015; MaHam et al., 2009). Absorption is affected by the composition of the delivery systems and their physicochemical properties such as size, shape, charge and surface hydrophobicity (Martins et al., 2015). In the case of size, whereas Chithrani et al. (2006) revealed that within 1-100 nm range, 50 nm gold particles show the maximum uptake in HeLa cells, Roger et al. (2009) showed no significant difference in Caco-2 cellular uptake of lipid particles at size of 25-130 nm. Zhang et al. (2015a) also demonstrated that the uptake of 100 nm soy protein particles in Caco-2 cells was higher than that of 30 and 180 nm. Win and Feng (2005) reported that 100 nm polystyrene particles had 2.3-folds greater uptake in Caco-2 cells compared to that of 50 nm particles, 1.3-folds to that of 500 nm particles, about 1.8 folds that of 1000 nm particles. They concluded that nanoparticles of 100-200 nm size acquired the best properties for cellular uptake. He et al. (2012) and Thorek and Tsourkas (2008) demonstrated that the uptake of carboxylated chitosan and superparamagnetic iron oxide particles with size < 300 nm was higher than larger particles in Caco-2 and T cells, respectively. Awaad et al. (2012) also showed that in the range of 50-500 nm thiol-organosilica particles, 95-200 nm is the ideal size for increased uptake in M cells.

However, the influence of surface charge on cellular uptake of particles is highly controversial. While some researchers concluded that positively-charged particles, due to attractive forces to negatively-charge cell membrane have higher cellular uptake (Karlsson et al., 1999; Foged et al., 2005), others believed that negatively-charged particles showed greater cellular uptake due to formation of particle clusters at some positive sites present on the cell membrane (He et al., 2010; Patil et al., 2007). In terms of surface hydrophobicity of particles, a balance between hydrophobic and hydrophilic groups is important; Zhang et al. (2015b) and Han et al. (2014) revealed that the increased hydrophobicity could improve cellular uptake of particles. Han et al. (2006) and Chithrani et al. (2006) reported that spherical particles internalized substantially faster than asymmetrically shaped particles.

In addition to the physicochemical properties of particles, study of the mechanisms by which the particles are uptaken into the cells is also important. When nanoparticles place in cell external milieu, they might enter inside the cells through different endocytosis mechanisms. In general,

membrane-bound vesicles (endosomes) are formed surrounding the particles. Cells contain various endosomes which deliver the particles to specialized vesicular structures to sort towards different destinations. Finally, different intracellular compartments either recycle the particles to the extracellular milieu or deliver them across cells (transcytosis). Generally, endocytosis can be classified into two broad categories of phagocytosis and pinocytosis. Phagocytosis is specific for macrophages, neutrophils, monocytes and dendritic cells, pinocytosis is present in all types of cells and has multiple forms (Sahay et al., 2010). To transport particles through intestinal epithelial cells, in addition to the transcellular delivery mechanisms, paracellular pathway might be used in which particles pass through tight junctions, the spaces between adjacent cells. Paracellular, a passive transport, is an appropriate route for hydrophilic molecules which are not able to pass through the cell bilayer membrane (Murugan et al., 2015).

To simulate the cellular uptake and transcellular delivery of particles through intestinal epithelial cells, Caco-2 cells, derived from intestinal absorptive cell, are widely employed. The use of only Caco-2 cells however is criticized for the lack of mucus-secreting goblet cells. Mucus, a semi-permeable barrier, hinders entry of bacteria and pathogens into the body, but allows exchange of nutrients, water, gases, odorants and hormones (Chen et al., 2010; Lai et al., 2009b). Co-culture of Caco-2 and HT29-MTX cell, derived from intestinal goblet cells, has been applied to study the influence of presence of mucus on absorption of peptide drugs, Glucagon like peptide-1 and insulin (Antunes et al., 2013; Araújo et al., 2014; Jin et al., 2012).

Mucus might have both positive and negative effects on the efficiency of delivery systems. Mucoadhesion is a phenomenon in which the micro- and nano-based delivery systems adhere to mucus and as a result, the residence and release time of the systems are prolonged, leading to increased concentration of the released compounds. Otherwise, along with intestinal chyme, the delivery systems would pass the intestine and have no sufficient time to release bioactive compounds. However, due to the mucoadhesion property, the particle residence time is limited to mucus turnover time. Use of mucus-penetrating nanoparticle is a new strategy which could overcome this limitation (Lai et al., 2009a). Although the mucoadhesion and mucus-penetrating property have been studied for synthetic polymers, very few researches have been performed on the properties of edible biopolymer-based delivery systems.

Among different edible biopolymers, food proteins, in addition to appropriate biocompatibility, biodegradability, emulsifying and gelling properties, possess different functional groups to bind

with encapsulated compounds (Elzoghby et al., 2012). In our previous studies, for the first time, cruciferin, a major canola protein, was used to prepare cruciferin/calcium (Cru/Ca) and cruciferin/chitosan (Cru/Cs) nanoparticles. Cruciferin's resistance to gastric enzymes (Bos, et al., 2007) may find its unique application to encapsulate bioactive compounds against gastric harsh conditions and also coat and protect chitosan material against degradation at low stomach pH (Makhlof et al., 2011). Cru/Ca particles released encapsulated compounds in intestinal conditions while Cru/Cs particle were stable in both stomach and intestine (Akbari and Wu, 2016; Chapter 5).

Therefore, the objective of this study was to compare the *in vitro* cellular uptake and trans-cellular transport of Cru/Ca and Cru/Cs particles which are approximately similar in size (165-200nm diameter), spherical shape and the composition of particle surface (cruciferin protein), but different in surface charge (negatively-charged Cru/Ca and positively-charged Cru/Cs particles). Two cell systems of Caco-2 and Caco-2/HT29 co-culture were used to simulate the effect of mucus on the intestinal cellular uptake and transport of the undigested and digested particles.

6.2.Materials and methods

6.2.1. Materials

Defatted canola meal, obtained from Richardson Oilseed Company (Lethbridge, AB, Canada) was ground, passed through a 35-mesh screen and stored at -20 °C for further use. Caco-2 (HTB37) and HT29-MTX-E12 cells were obtained from the American type culture collection (Manassas, VA) and Sigma-Aldrich (Oakville, ON, Canada), respectively. Dulbecco's modified eagle medium (DMEM), 0.25% (w/v) trypsin-0.53 mM EDTA, 4-(2-hydroxyethyl)-1-piperazineethanesulfonic acid (HEPES), Hanks' balanced salt solution (HBSS), phosphate buffer saline (PBS), fetal bovine serum (FBS), 1% nonessential amino acids, and 1% antibiotics were all procured from Gibco Invitrogen (Burlington, ON, Canada). Alcian blue, sodium dodecyl sulfate (SDS), dithiothreitol (DTT), pepsin, pancreatin, coumarin 6, basic fuchsin, periodic acid, sodium meta-bisulphite, triton X-100, trypan blue, sodium azide, chlorpromazine, quercetin, indomethacin, β-cyclodextrin and amiloride were obtained from Sigma-Aldrich (Oakville, ON, Canada).

6.2.2. Preparation of coumarin 6-loaded particles

To study the cellular uptake and transport, coumarin-6, a fluorescent marker, was loaded in the particles. 1 mL coumarin-6 solution in ethanol (at concentrations of 2- 400 μg/mL) was added to

9 mL of 10 mg/mL heated cruciferin solution (pH 9). After diluting the protein/coumarin-6 solution with 6 mL water (pH 9), 3 mL of 9 mM $CaCl_2$ was added dropwise while stirring to prepare coumarin 6-loaded Cru/Ca particles (Akbari and Wu, 2016). To load coumarin 6 in Cru/Cs particles, 1 mL of the coumarin-6 solution was added to 9 mL of 2 mg/mL chitosan solution in 0.1 M acetic acid. 9 mL of 5 mg/mL cruciferin solution (solubilized at pH 12) was added dropwise while stirring and pH of the suspension was adjusted to 5.5. (Chapter 5). The Cru/Ca and Cru/Cs particles were centrifuged (40000 g and 4 °C for 30 min) and washed twice to remove free coumarin-6.

6.2.3. *In vitro* digestion of particles

The coumarin 6-loaded particles, undigested forms or after digestion in simulated gastric and intestinal fluids, were used for uptake or transport studies. To simulate gastric conditions, the loaded particles were re-suspended at 20 mL water (pH 1.2) containing pepsin (10% of protein concentration) and was agitated at 100 rpm and 37 °C for 2 h in a water bath. Then, pepsin was inactivated by raising pH to 7.4 using 10 mL of 1M sodium bicarbonate and digestion was followed in simulated intestinal medium by adding 5 ml of 200 mM phosphate buffer pH 7.4 containing pancreatin (10% of protein concentration). After 4 h intestinal digestion, pancreatin was inactivated using trypsin inhibitors. Therefore, a portion of the particles was dissociated after the digestion, and a mixture of encapsulated and free coumarin-6 was obtained in the digested particles, while coumarin-6 remained encapsulated in the undigested particles.

6.2.4. Size and surface charge particles

Size of the particles was determined by dynamic light scattering using Malvern Nanosizer ZS (Malvern, Worcestershire, UK). Zeta potential of the particles was also measured by laser doppler velocimetry using the Nanosizer. Prior to measurement, samples were diluted in 10 mM phosphate buffers (the same pH of particle suspensions) to obtain a slight opalescent dispersion to prevent multiple scattering effects.

6.2.5. Cell cultures

Caco-2 (passage #25-64) and HT29-MTX (passage #30-67) cells were separately cultured at a density of 0.5×10^{-5} in 75 cm^2 flasks using high-glucose and L-glutamine DMEM medium supplemented with 10% FBS, 1% non-essential amino acids, 1% penicillin and streptomycin, and

2.5% HEPS. The cells were incubated at 37°C in a humidified incubator with 5% and the culture medium was refreshed every other day.

6.2.6. Mucus staining

Caco-2 cells and Caco-2/HT29 co-culture (8:2 ratio) were seeded at a density of 0.8×10^{-5} cells/mL on 6-well plates and incubated for 4, 7, 14 and 21 days. To visualize secreted mucus, it was stained using Alcian blue. In brief, culture media were aspirated and the cells were washed once by PBS; 1% Alican blue in 3% acetic acid was added to the cell cultures. After 20 min incubation at room temperature, extra Alician blue was removed by three-time washing using PBS. The stained mucus was observed by an inverted microscope (Primo Vert, Zeiss, Oberkochen, Germany) (Leonard et al., 2010).

6.2.7. Mucus quantification

Secreted mucus in the cultures was quantified using the periodic acid/Schiff reagent method modified by Leonard et al. (2010). Schiff reagent was prepared by dissolving 0.1% fuchsin in boiling water; 20 mL of 1M HCl was added to 50 °C-fuchsin solution. Before experiment, 1.66 g sodium meta-bisulphite was added to the solution and incubate at 37 °C until the solution was colorless or pale red. Periodic acid solution was also prepared by adding 10 µL of 50% of periodic acid to 10 mL of 7% acetic acid. The media were carefully removed from the cell cultures, and the cells were lysed using 1 mL of 1% Triton-X in PBS. The samples were then incubated with 100 μL of the periodic acid solution at 37 °C for 2 h. Afterward, 100 µL of the schiff reagent was added and samples were incubated at room temperature for 30 min. Absorbance of the samples was measure at 555 nm using Spectramax M3. Porcine mucin was used to prepare a standard curve (Leonard et al., 2010).

6.2.8. Cell uptake of particles

Cellular uptake of undigested and digested Cru/Ca and Cru/Cs particles was studied using Caco-2 culture and Caco-2/HT29 co-culture. Two methods of uptake efficiency and fluorescence intensity of the cells uptaking the particles were used to quantify cellular uptake.

6.2.8.1. Uptake efficiency of particles

Caco-2 and Caco-2/HT29 (8:2 ratio) cells were seeded at density of 0.8×10^{-5} cells/mL on black 96-well plates and incubated to be confluent (A clear 96-well plate was used to visualize the cell

confluency). Culture media were replaced with 200 µL/well HBSS (buffered with 30 mM HEPES) and the cells were incubated at 37 °C for 30 min and then HBSS was removed. The pre-incubated cells were incubated with 100 µL/well HBSS containing 10, 40 and 100 µg/mL undigested and digested particles for 4 h at 37 °C. After three-time washing the particles using HBSS, extra-cellular fluorescence was quenched with 100 µL/well 0.2% Trypan blue in HBSS for 10 min. HBSS was used for three-time washing and then cell membrane was permeabilized and the particles were dissociated using 100 µL/well of 1% Triton X-100/1% SDS in 0.4N NaOH. After 3h, the fluorescence intensity of the cellular uptaken particles was measured at excitation and emission wavelength of 467 and 502 nm using Spectramax M3. The fluorescence intensity of the cells along with all loaded particles (without washing) was measured and the uptake efficiency was calculated compared to the total fluorescence intensity of the cells and loaded particles. Control experiment was carried out for the cells without the particles. Free coumarin-6 (equivalent to loaded coumarin-6 in 40 µg/mL particles) was also loaded on the cells and cellular uptake was measured (Win and Feng, 2005).

6.2.8.2. Flow cytometry of the cells uptaking particles

Caco-2 and Caco-2/HT29 cells were cultured on 6-well plates and incubated up to confluence. The cells were incubated with 2 mL/well HBSS containing 1.2 and 2.5 µg/mL undigested and digested particles for 4 h at 37 °C. After three-time washing the particles and treatment with the Trypan blue solution, the cells were detached from the plate using 1 mL of 0.25% Trypsine-EDTA. Trypsin was inactivated using 3 mL cold DMEM containing 10% FBS and the cells were transferred to centrifuge tubes and centrifuged at 500 g for 5min. The cell pellet was washed with FCS buffer (PBS containing 2mM EDTA, 0.05 sodium azide and 0.5% FBS) and centrifuged. The cells were fixed using 4% cold formaldehyde for 20 min and centrifuged. The cell pellet was re-suspended in 0.5-0.8 mL flow cytometry standard (FCS) buffer and transferred to FACS tubes. Mean fluorescence intensity (MFI) and % positive cells were measured using BD FACS Canto II flow cytometry (Becton Dickinson, San Jose, CA, USA) (Li et al., 2011).

6.2.9. Mechanism of the particle cell uptake

The possible pathways of cellular uptake of the particles were studied using specific endocytosis inhibitors and then fluorescence intensity was measured by flow cytometry. Caco-2 cells were seeded at a density of 0.8×10^{-5} cells/mL on 6-well plates and incubated to be confluent. The cells

were pre-incubated with chlorpromazine (20 μg/mL), quercetin (20 μg/mL), indomethacin (100 μg/mL), β-cyclodextrin (2 mg/mL), amiloride (40 μg/mL) and sodium azide (100 mM) for 1 h at 37◦C. Afterward, 1 mL HBSS containing 2.5 μg/mL digested and undigested particles was added to the cells and incubated at 37 °C for 4 h (the concentration of the inhibitors was constant). To study the uptake mechanism at 4 °C, Caco-2 cells were also pre-incubated at 4 °C for 1 h and then incubated with the particles at 4 °C for 4 h. After washing the particles and inhibitors, extra-cellular fluorescence was quenched, the cells were harvested and fixed, and MFI was measured by flow cytometry as described previously (Wang et al., 2015).

6.2.10. Transport studies

Transport of the undigested and digested particles through intestinal epithelial cells were simulated by seeding Caco-2 and Caco-2/HT29 (8:2 ratio) cells at density of 2.5×10^{-5} cells/mL on Corning trans-well plates (pore size 3 μm, surface area 1.12 cm^2). The cells were incubated at 37 °C for 21 days. Cell medium was refreshed every other day in the first week, and then every day in the second and third weeks. The integrity of the cell monolayers was determined by measuring trans-epithelial electrical resistance (TEER) using epithelial tissue voltohmmeter (EVOM2, World Precision Instruments, Saratosa, FL, USA). Transport studies were performed on the cell monolayers with TEER values starting 750 Ω cm^2. Prior transport studies, cell medium was replaced with HBSS (buffered with 30 mM HEPES) at pH 7.4 and incubated at 37 °C for 30 min. The HBSS in the apical side of the trans-wells was removed and 0.5 mL HBSS containing 40 μg/mL coumarin-6 loaded particles was loaded on the surface of the cell monolayers. Transport study was conducted at 37 °C for 6 h, and then samples were drawn from basolateral side. Transferred particles were dissociated and fluorescence intensity was measured as described previously. The apparent permeability coefficient (P_{app}) was calculated as:

$$P_{app} = dQ/dt \times 1/AC_0$$

where, dQ/dt is the permeability rate, A is the surface area of the membrane filter, and C_0 is the initial concentration of coumarin-6 in the apical compartment (He et al., 2013; Luo et al., 2013).

6.2.11. Statistical analysis

Experiments were performed in triplicate and are represented as mean ± standard deviation (SD). One-way analysis of variance (ANOVA) and Duncan test (version 9.2, SAS Institute Inc., Cary,

NC, USA) were used to analyse the data. The level of significance was set at probabilities of *p < 0.05, **p < 0.01, and ***p < 0.001.

6.3. Results and discussion

6.3.1. Mucus staining and quantitation

To confirm the secretion of mucus on the surface of the Caco-2 culture and Caco-2/HT29 co-culture, the mucus was stained by Alcian blue over different incubation times. Co-culture cells showed a higher intensity of resultant blue than that of Caco-2 cells, indicating the secretion of mucus by HT29 cells (Figure 6.1). Using this method, Antunes et al. (2013) and Chen et al. (2010) also showed that HT29 cells produced mucus in co-culture with Caco-2 cells.

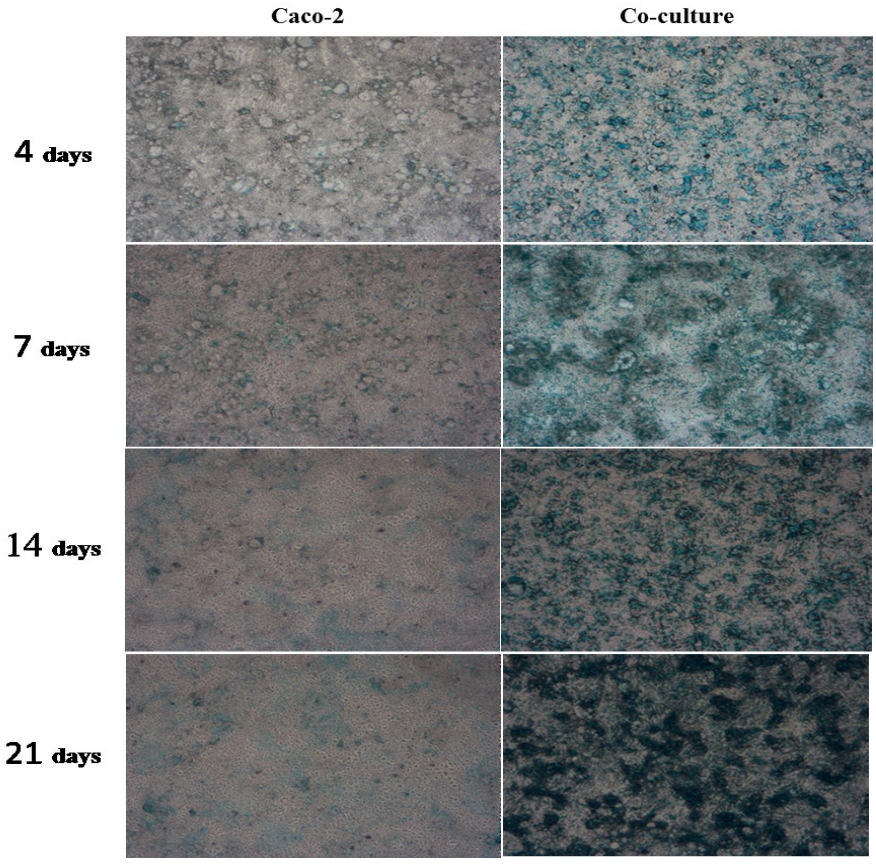

Figure 6.1. Caco-2 and Caco-2/HT29 co-culture cells stained with Alcian blue after different cell incubation times

The periodic acid/Schiff reagent method was used to measure the aldehyde groups of carbohydrates present in mucus glycoprotein (Leonard, et al., 2010). Although mucin was detected in Caco-2 line, the concentration of mucin in the Caco-2/HT29 co-culture was significantly higher than that of Caco-2 culture, and it increased over cell incubation (Figure 6.2).

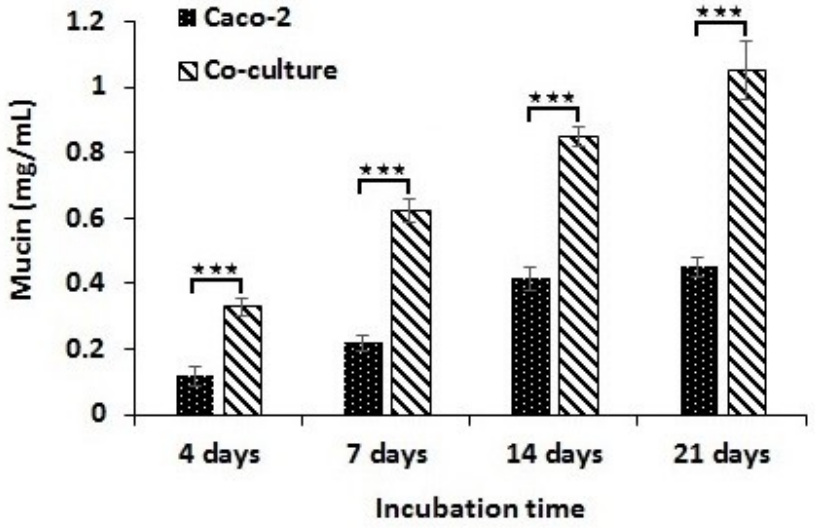

Figure 6.2. Mucus quantification in Caco-2 and Caco-2/HT29 co-culture cells using periodic acid/Schiff stain colorimetric assay. Data shown as means ± SD (n = 3-5). *: $P < 0.05$, **: $P < 0.01$, ***: $P < 0.001$.

6.3.2. Cell uptake of particles

Cell internalization of particles was observed using confocal microscopy (Akbari and Wu, 2016); cell uptake of coumarin 6-loaded particles was quantified using fluorescence and flow cytometry methods with/out simulated gastrointestinal (GI) digestion.

6.3.2.1. Uptake efficiency of the particles

The size of the re-suspended Cru/Ca and Cru/Cs particles in HBSS increased from 207±5 and 165±3 to 280±34 and 334±41 nm, while that of the surface charge were decreased from -33.0±2.1 and +18.2±1.3 to -14.3±1.8 mV and +7.9±2.2 mV, respectively. Since the pH of the suspensions was close to cruciferin isoelectric point (pH 7.2), the zeta potential of the particles decreased. The increased particles size might be due to the decreased surface charges, which led to reduced

repulsive forces between the particles. The reduced repulsive forces resulted in association of the particles and formation of larger particles.

The results of cellular uptake efficiency of Cru/Ca and Cru/Cs particles (Figure 6.3) showed that at increasing particles concentrations, their uptake efficiency decreased. This revealed that the uptake of the particles was a saturable process.

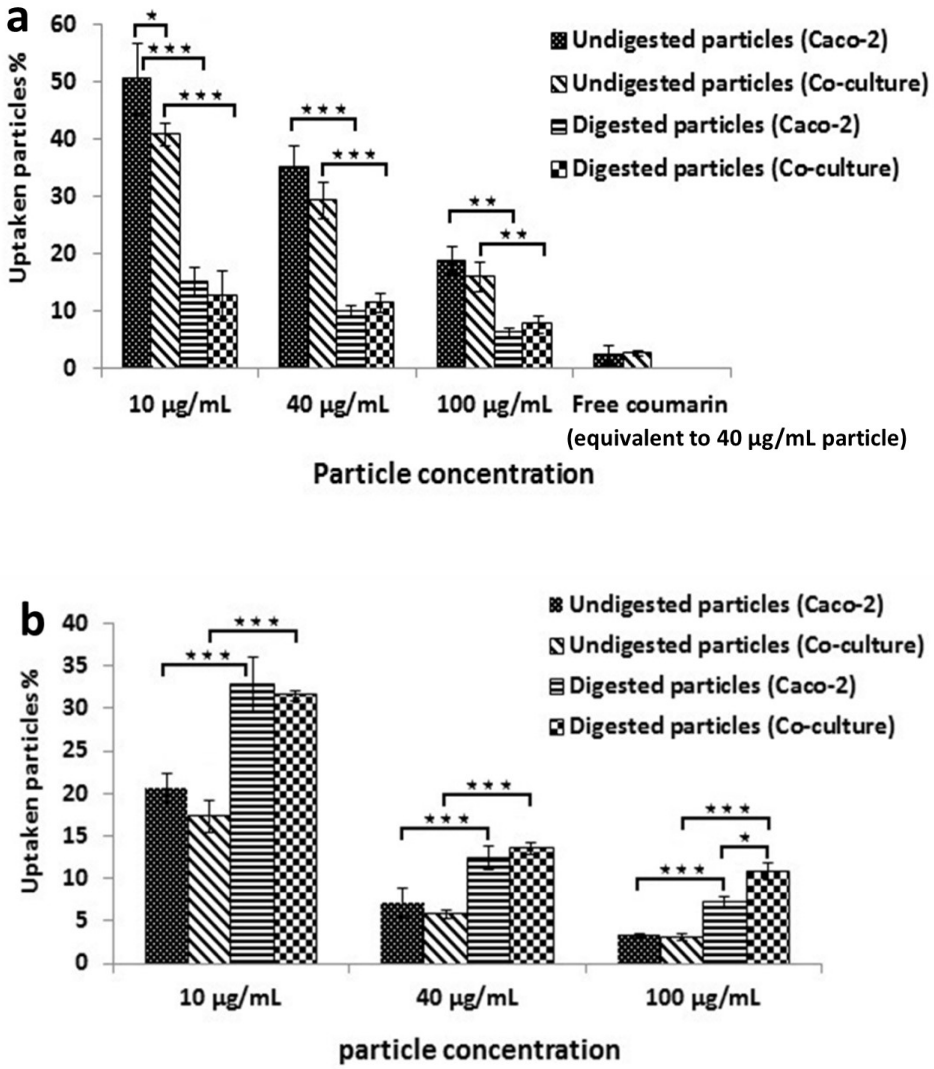

Figure 6.3. Cellular uptake efficiency of Cru/Ca (a) and Cru/Cs (b) particles in Caco-2 and Caco-2/HT29 co-culture cells. Data shown as means ± SD (n = 3-5). *: $P < 0.05$, **: $P < 0.01$, ***: $P < 0.001$.

As shown in Figure 6.3a, the uptake efficiency of digested Cru/Ca particles in both Caco-2 and Caco-2/HT29 co-culture cells were significantly lower ($p < 0.001$) compared to their undigested forms. Digestion of Cru/Ca particles led to release of ~ 84% encapsulated coumarin-6; since the cell uptake of released coumarin-6, in the free form, was negligible (Figure 6.3a), MFI of the cells treated with digested Cru/Ca particles decreased. This confirmed our previous results revealing that 70-90% of Cru/Ca particles were degraded in simulated intestinal fluid (SIF) (Akbari and Wu, 2016). Win and Feng (2005) also reported that free coumarin-6 is not directly uptaken by cells.

Although the uptake efficiency of 10 μg/mL undigested Cru/Ca particles in Caco-2 cells was higher ($p < 0.05$) than that in the co-culture, no difference was observed between the two cell cultures at particle concentrations of 40 and 100 μg/mL (Figure 6.3a). The results revealed that the presence of mucus secreted by HT29 cells in the co-culture system did not affect the cell update of the particles.

The uptake efficiency of digested Cru/Cs particles was higher ($p < 0.001$) than that of undigested Cru/Cs particles, which was in contrast with that of Cru/Ca particles (Figure 6.3). As shown in chapter 5, cruciferin coating of the particles was digested in SIF, but the chitosan core, entrapping encapsulated compound, was not degraded and encapsulated compounds were not released. Therefore, compared to undigested particles, a higher proportion of digested Cru/Cs particles was internalized to the cells in both Caco-2 and Caco-2/HT29 co-culture. The increase of the uptake efficiency of digested particles might be due to decreases size of particles to 58±11 nm (compared to 165 nm diameter of undigested particles). However, similar to Cru/Ca particles, there was no difference between the two cell culture systems to uptake undigested Cru/Cs particles (Figure 6.3b) revealing that the particles were not hindered by secreted mucus in Caco-2/HT29 co-culture.

Since the cellular uptake of both Cru/Ca and Cru/Cs particles was not affected by the presence of mucus in the co-culture, it can be proposed that the particles traversed the mucus layers and reached the underlying epithelial cells. In general, particles with ability to pass across mucus layers are known as mucus-penetrating particles. To improve delivery of bioactive compounds to epithelial cells and increase their absorption, two particle types are prepared: mucoadhesive particles and mucus-penetrating particles. Conventional mucoadhesive particles are mostly immobilized in luminal mucus layer, the surface layer which is rapidly cleared, while mucus-penetrating particles easily penetrate the luminal layer and enter the underlying adherent mucus layer where is slowly cleared. Therefore, mucus-penetrating particles have higher chance to reach

the underlying epithelial cells to be uptaken and/or efficiently release their encapsulated compounds close to absorptive cells (Lai et al., 2009a).

Lai et al. (2007) reported that large nanoparticles (200 and 500 nm in diameter) densely coated with polyethylene glycol showed near-neutral surface charge and negligible mucoadhesion property. The particles penetrated through mucus with an effective diffusion coefficient (Deff) only 6- and 4-fold lower than that in water (Lai et al., 2007). The particles were actually synthesized by mimicking the surface properties of viruses which allow them to avoid mucoadhesion. The viruses are densely coated with both positively and negatively charged functional groups, leading to a densely charged yet net neutral surface (Lai et al., 2009a). Therefore, the proposed mucus-penetrating property of our particles might also follow the same phenomenon. This property might be due to the presence of a high number of amino and carboxyl groups in the structure of cruciferin covering the particles surface. In addition, the presence of slight negative (-14.3 mV) and positive (+7.9 mV) charges in Cru/Ca and Cru/Cs respectively, didn't cause significant mucoadhesion for the particles.

In the case of undigested particles, the uptake efficiency of Cru/Ca particles was 2.5-6 times higher than that of Cru/Cs particles. Since the secretion of mucus had negligible effect on the cell uptake of the particles, therefore, the difference observed might be due to the difference in the cell internalisation of the particles. Since the size and shape of the particles were similar, the surface charge of the particles should play a key role for the different cellular internalisation. Although negatively-charged particles might be repelled by large negatively-charged domains of cell membranes, there are a few cationic sites for adsorption of the negatively charged particles. There is an assumption suggesting that the negatively charged particles bind at the cationic sites in the form of clusters. The presence of the particle clusters and non-specific adsorption process might be the driving forces for particle adsorption (He, et al., 2010; Patil, et al., 2007). Therefore, the negatively-charged undigested Cru/Ca particles showed higher cellular uptake compared to positively-charged undigested Cru/Cs particles. He et al. (2010) and Patil et al. (2007) also reported that the particles with slight negative charge were uptaken more efficiently than positively-charged particles.

6.3.2.2. Flow cytometry of cells uptaking particles

Flow cytometry can directly quantify particle uptake. The mean fluorescence intensity (MFI) of the cells uptaking digested Cru/Ca particles was dramatically lower than that of undigested particles (Figure 6.4a). The results were in agreement with our particle uptake efficiency study, confirming degradation of the particles in SIF (chapter 5). In addition, the presence of mucus in the co-culture system did not affect the uptake of undigested Cru/Ca and Cru/Cs particles (Figure 6.4 a & b). This confirmed our previous results in the uptake efficiency study, and also supported the possible mucus-penetrating property of the undigested particles.

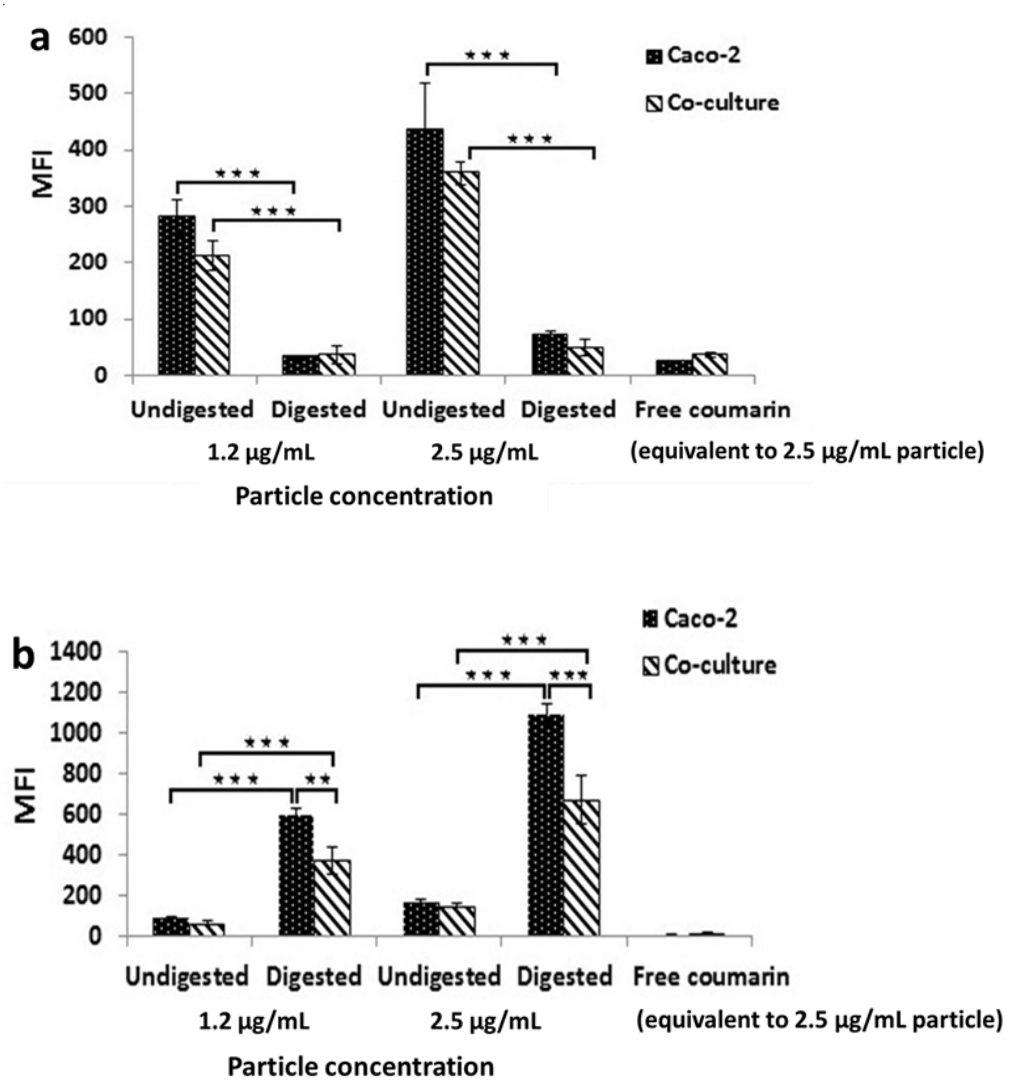

Figure 6.4. Mean fluorescence intensity (MFI) of the cells uptaking Cru/Ca (a) and Cru/Cs (b) particles in Caco-2 and Caco-2/HT29 co-culture cells (measured by flow cytometry). Data shown as means ± SD (n = 3-5). *: $P < 0.05$, **: $P < 0.01$, ***: $P < 0.001$.

Interestingly, the MFI of the cells uptaking digested Cru/Cs particles was six times higher than that of undigested particles, similar to the results of uptake efficient study. It should be noted that the MFI of digested Cru/Cs particles in the co-culture was lower than that of Caco-2 cultur, which suggested that the presence of mucus in co-culture system hindered the update of the digested particles, which might be due to mucoadhesive property of exposed chitosan-based core after digestion of cruciferin coating. Although the chitosan core was small in size, because of mucoadhesion property of chitosan, their ability to pass mucus layers was reduced. The difference in uptake was not detected between Caco-2 and Caco-2/HT29 in uptake efficiency study (Figure 6.3b). The reason might be related to the method of washing un-uptaken particles. In uptake efficiency study, even after washing, a part of mucus along with some particles might remain with Caco-2/HT29 cells and the particles were considered as uptaken particles. However, three-time centrifugation in flow cytometry method completely removed mucus and un-uptaken attached particles.

The MFI of negatively-charged undigested Cru/Ca particles was 3-time higher than that of positively-charged Cru/Cs particles, confirming the previous uptake efficiency study.

The percentage of positive cells is another parameter to show the proportion of the cells uptaking particles to total measured cells. In Figure 6.5, the percentages of positive Caco-2 cells uptaking 2.5 μg/mL undigested/digested Cru/Ca and Cru/Cs particles are compared. These results confirmed that the two particles had completely different stability in GI tract; while Cru/Ca particles were dissociated, degradation of coating of Cru/Cs particles increased their cellular uptake. In addition, these results showed that the number of the cells uptaking the particles was also very effective in the particle uptake.

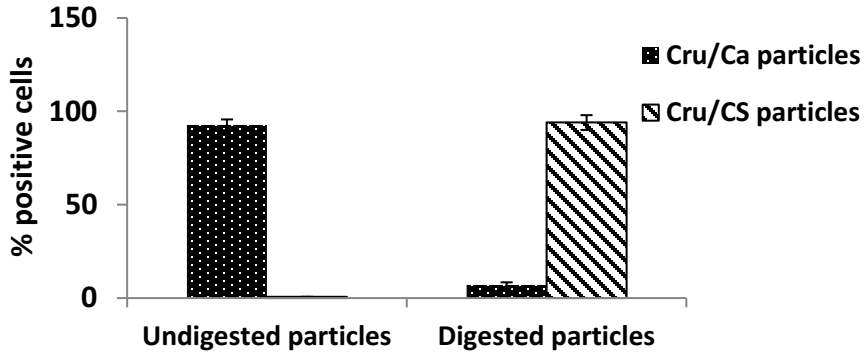

Figure 6.5. The percentage of positive cells (cells uptaking the particles). Data shown as means ± SD (n = 3-5).

6.3.3. Mechanism of cell uptake of particles

Potential endocytosis pathways including active endocytosis, clathrin–mediated endocytosis, caveolae-mediated endocytosis, lipid raft/caveolae-dependent endocytosis, clathrin- and caveolin–independent endocytosis, and micropinocytosis were studied using their respective blockers such as sodium azide, chlorpromazine, indomethacin, β-cyclodextrin, quercetin, and amiloride, respectively. The cell uptake of particles incubated at 4 °C was also compared with that of 37 °C to study the effect of energy-mediated pathways.

Clathrin-mediated endocytosis is the main uptake route for essential nutrients such as cholesterol and iron which are carried into cells through low density lipoprotein (LDL) and transferrin receptors, respectively (Sahay et al., 2010). Caveolae-mediated endocytosis is mainly due to the presence of caveolin proteins which form caveolar endocytic vesicles through oligomerization of their domains (Sahay et al., 2010). Unlike clathrin–mediated endocytosis, the uptaken compounds in the caveolar vesicles are not degraded which is important for protection of bioactive compounds (del Pozo-Rodriguez et al., 2009). Particles can also be regulated by lipid rafts/caveolaes endocytosis, cholesterol/sphingolipids-rich membrane-bound microdomains, and then enter a specific vesicle named as caveosome (He et al., 2013). Like caveolae-dependent endocytosis, lipid raft-mediated endocytosis avoids the lysosomal pathway and its consequent vector degradation. The presence of caveolin-1 in caveolaes, which stabilizes these domains in the plasma membrane, is the only difference between caveolaes and lipid rafts. Whereas some researchers consider caveolae-mediated endocytosis as a subclass of lipid raft-mediated endocytosis, others use the same categorization for both mechanisms (caveolae/raft-dependent endocytosis) (del Pozo-Rodriguez et al., 2009). In clathrin- and caveolin-independent endocytosis, four different types of receptor-ligand interactions of Arf6-dependent, flotillin-dependent, Cdc42-dependent and RhoA-dependent are involved (Mao et al., 2013; Wang et al., 2015). Macropinocytosis, an actin-dependent process initiated from surface membrane ruffles, is a non-selective uptake of solute molecules, nutrients and particles. Either degradation at the late endosome/lysosome or recycling back to the plasma membrane are two possible fates of the content uptaken by macropinosomes (Lim and Gleeson, 2011).

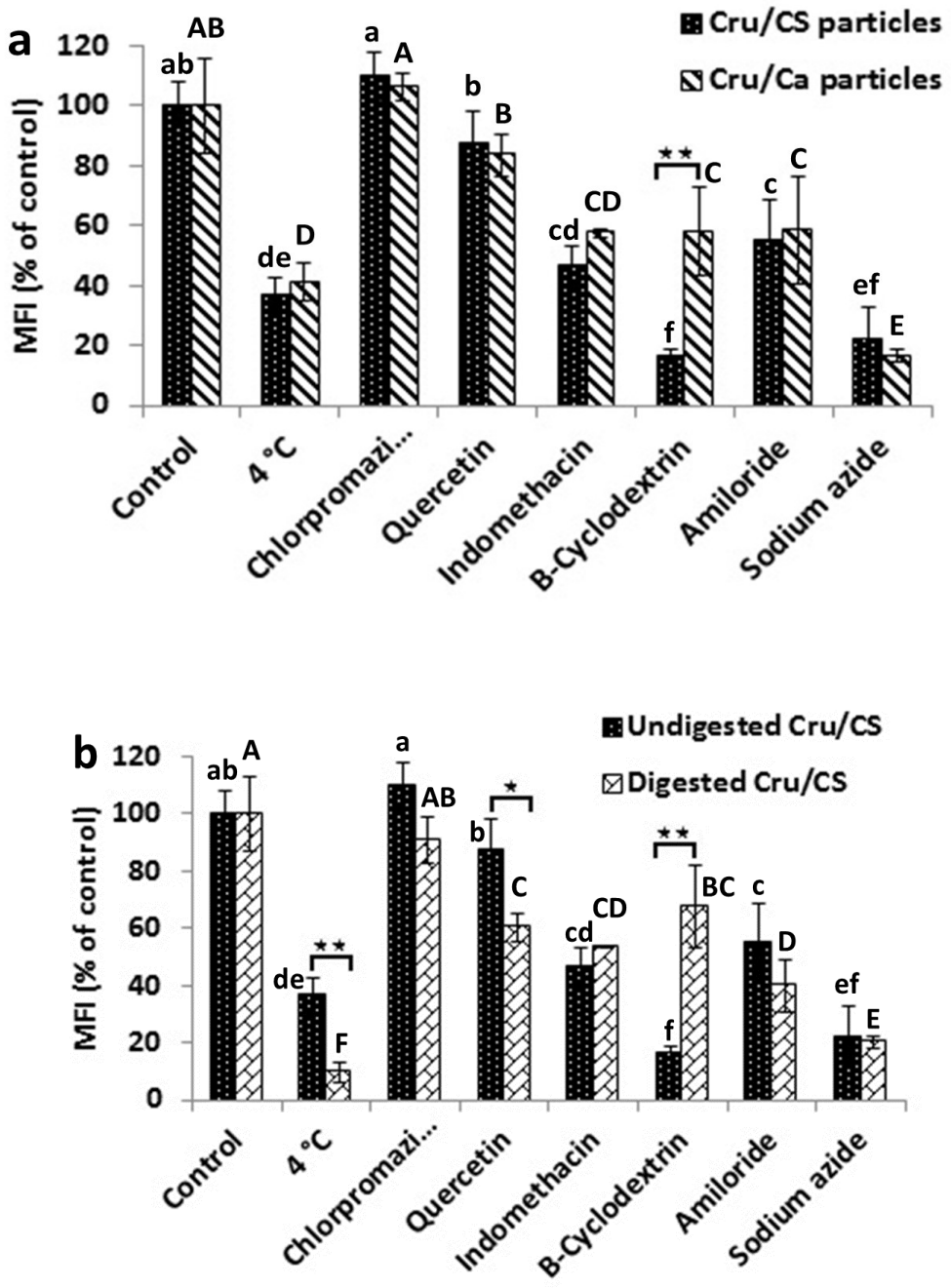

Figure 6.6. Mean fluorescence intensity (MFI) of the cells uptaking undigested Cru/Ca and Cru/Cs particles (a) and undigested and digested Cru/Cs particles (b) after 4 h incubation in the presence of different uptake mechanism inhibitors. In comparison of the treatments using Duncan test, values with different letters are significantly ($p<0.05$) different. Data shown as means ± SD (n = 3-5). *: $P < 0.05$, **: $P < 0.01$, ***: $P < 0.001$.

The cellular uptake of Cru/Ca and Cru/CS particles was not affected when the cells were treated with chlorpromazine and quercetin, revealing that clathrin-mediated endocytosis and clathrin- and caveolin-independent endocytosis mechanisms were not involved or had negligible effect on the uptake of the particles (Figure 6.6a). However, sodium azide, a metabolic inhibitor blocking ATP production in cells, decreased 80-85% of the uptake of both Cru/Ca and Cru/Cs particles, which implied that active- or energy-mediated mechanisms are the major endocytosis pathways for uptake of the particles. Incubation of the cells at 4 °C, which limits cell metabolisms and decreases the fluidity of the cell membrane, led to 60-65% decrease in the uptake of Cru/Ca and Cru/Cs particles, further supporting the active-mediated mechanisms of uptake. The presence of uptake at 4 °C was possibly due to limited active-based mechanisms or passive diffusion.

Caveolin-, and lipid raft/caveolae-dependent endocytosis, as well as micropinocytosis, three energy-mediated mechanisms, were further studied using their respective blockers, indomethacin, β-cyclodextrin, and amiloride, respectively. Whereas there was no difference between the uptake of Cru/Ca and Cru/Cs particles by caveolin-dependent endocytosis and micropinocytosis (42-55% of the control uptake), lipid raft/caveolae endocytosis played a greater role in uptaking of Cru/Cs particles. The higher surface hydrophobicity of Cru/Cs particles compared to that of Cru/Ca particles (Akbari and Wu, 2016; Chapter 5), might be the reason for the greater role of lipid raft in uptaking of Cru/Cs particles. Lipid raft/caveolae pathway was previously reported as the major mechanism for uptake of lipid nano-carriers (Roger et al., 2009).

The mechanisms involved in the uptake of digested Cru/Cs particles were also studied and compared with undigested particles (Figure 6.6b). Like undigested particles, energy-mediated mechanisms were the major pathways for uptake of the digested particles, whereas clathrin–mediated endocytosis was not involved. Blocking lipid raft/caveolae endocytosis resulted in 84% reduction of uptake for undigested particles, in comparison to 30% reduction for digested particles. As previously mentioned, the greater role of the lipid raft in uptaking of undigested Cru/Cs particles might be due to their high surface hydrophobicity, but after digestion and expose of the chitosan core, surface hydrophobicity dramatically decreased leading to lowering the role of the lipid raft for uptake of digested particles. These results revealed that energy-dependent mechanisms were dominated in digested Cru/Cs particle uptake.

6.3.4. Transport studies

Transcellular delivery of particles through intestinal epithelial monolayers of Caco-2 and Caco-2/HT29 co-culture was studied. The initial TEER values of both cell monolayers ranged from 750 to 1000 Ω cm^2. Chen et al. (2010) also showed that the ratio of Caco-2 to HT29 had no significant influence on TEER. TEER of the cell monolayers decreased 5-15% after 6 h incubation with undigested and digested particles, implying the integrity of the monolayer cells during the transport study. Transport studies showed that undigested Cru/Ca particles had higher permeability compared to the digested particles (Figure 6.7a); these results confirmed our cellular uptake studies. The decrease was due to the degradation of 75-90% of the particles which released the encapsulated coumarin-6 (Akbari and Wu, 2016). Free coumarin-6 showed negligible permeability compared to its encapsulated form.

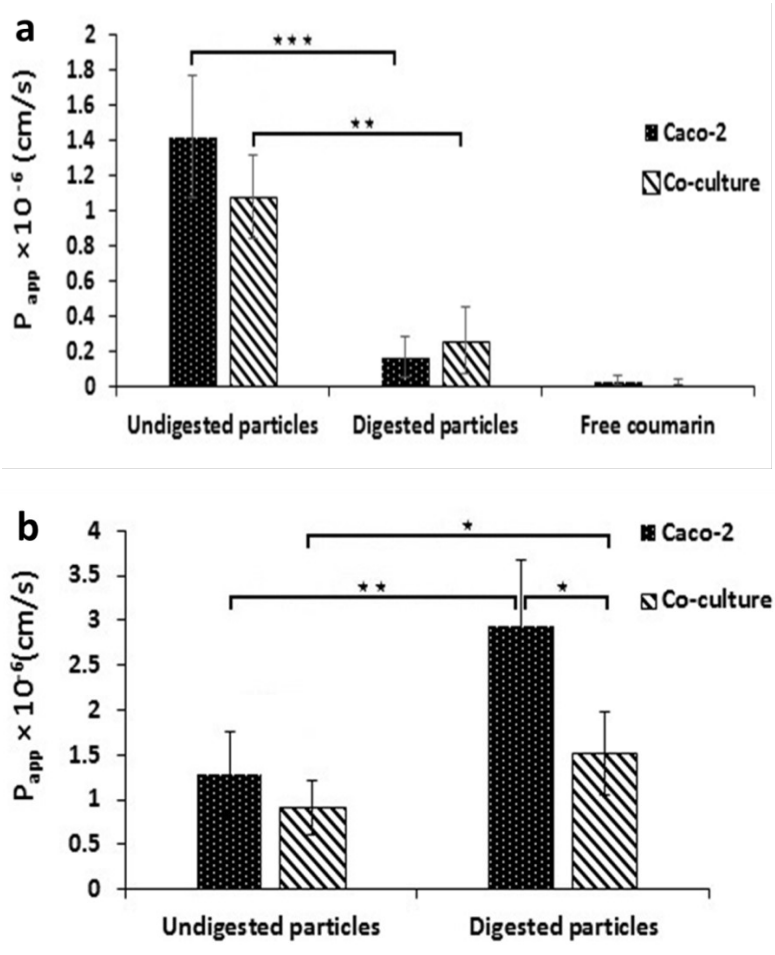

Figure 6.7. Transport of Cru/Ca (a) and Cru/Cs (b) particles through Caco-2 and Caco-2/HT29 co-culture cells. Data shown as means ± SD (n = 3-5). *: $P < 0.05$, **: $P < 0.01$, ***: $P < 0.001$.

There was no difference in the transport of undigested Cru/Ca and Cru/Cs particles across Caco-2 and co-culture cells (Figure 6.7), which implied that the secretion of mucus in co-culture cells had no effect on transport of the particles through mucus and the cell monolayer. These results, in agreement with our uptake studies, supporting our proposed mucus-penetrating property of undigested Cru/Ca and Cru/Cs particles. The transport of digested Cru/Cs particles across Caco-2 and co-culture cells significantly increased compared to undigested Cru/Cs particles, which may be due to decreased size after digestion (decreased from 165 nm to ~58 nm; this result was in agreement with our particle uptake studies. However, the transport of digested Cru/Cs particles across co-culture cells significantly decreased compared to that of Caco-2 culture. As previously described in flow cytometry study, this might be due to the mucoadhesion property of the chitosan-based core particles which were exposed to mucus. Since our transport and uptake studies were performed in static systems, the adhesion of digested Cru/Cs particles to mucus decreased the uptake and transport of the particles. However, in dynamic or *in vivo* systems, where the particles are quickly transported along with intestinal chyme in the intestine, the mucoadhesion property could prolong the residence time of the particles in the intestine and increase the concentration of released encapsulated compounds on the surface if intestinal epithelial cells, and as result, improve the absorption and bioavailability of the compounds.

6.4. Conclusions

Our results showed that the cellular uptake and transport of the cruciferin-based particles were not affected in the presence of mucus in the Caco-2/HT29 co-culture, compared to those in Caco-2 cells. These results revealed that mucus had negligible influence on particles uptake, implying that the particles might have mucus-penetrating property which is important for delivery of bioactive compounds through mucus layers. Since the mucus-penetrating property is lost after digestion of the particles in GI tract, these particles might be appropriate carriers for drug delivery in non-digestive mucosal tissues.

The cell internalisation of negatively-charged Cru/Ca particles was higher than positively-charged Cru/Cs particles. The cellular uptake and transport of digested Cru/Ca particles decreased compared to undigested form due to dissociation in the simulated digestion. Digested Cru/Cs particles, however, enhanced their cellular uptake and transport compared to undigested form, due

to reduced size of chitosan-based particle core. Digested Cru/Cs particles also showed mucoadhesion property resulted from exposed chitosan core of the particles. Due to an increasing interest to use edible biopolymer-based particles in delivery systems, study their cellular uptake and intra-cellular transport is a necessary step to develop these systems.

6.5. References

Akbari, A. & Wu, J. (2016). Cruciferin nanoparticles: Preparation, characterization and their potential application in delivery of bioactive compounds. *Food Hydrocolloids,* 54, 107-118.

Antunes, F., Andrade, F., Araujo, F., Ferreira, D., & Sarmento, B. (2013). Establishment of a triple co-culture *in vitro* cell models to study intestinal absorption of peptide drugs. *European Journal of Pharmaceutics and Biopharmaceutics,* 83(3), 427-435.

Araujo, F., Shrestha, N., Shahbazi, M., Fonte, P., Makila, E. M., Salonen, J. J., Hirvonen, J. T., Granja, P. L., Santos, H. A., & Sarmento, B. (2014). The impact of nanoparticles on the mucosal translocation and transport of GLP-1 across the intestinal epithelium. *Biomaterials,* 35(33), 9199-9207.

Awaad, A., Nakamura, M., & Ishimura, K. (2012). Imaging of size-dependent uptake and identification of novel pathways in mouse Peyer's patches using fluorescent organosilica particles. *Nanomedicine-Nanotechnology Biology and Medicine,* 8(5), 627-636.

Bos, C., Airinei, G., Mariotti, F., Benamouzig, R., Berot, S., Evrard, J., Fenart, E., Tome, D., & Gaudichon, C. (2007). The poor digestibility of rapeseed protein is balanced by its very high metabolic utilization in humans. *Journal of Nutrition,* 137(3), 594-600.

Chen, X., Elisia, I., & Kitts, D. D. (2010). Defining conditions for the co-culture of Caco-2 and HT29-MTX cells using Taguchi design. *Journal of Pharmacological and Toxicological Methods,* 61(3), 334-342.

Chithrani, B. D., Ghazani, A. A., & Chan, W. C. W. (2006). Determining the size and shape dependence of gold nanoparticle uptake into mammalian cells. *Nano Letters,* 6(4), 662-668.

del Pozo-Rodriguez, A., Pujals, S., Delgado, D., Solinis, M. A., Gascon, A. R., Giralt, E., & Pedraz, J. L. (2009). A proline-rich peptide improves cell transfection of solid lipid nanoparticle-based non-viral vectors. *Journal of Controlled Release,* 133(1), 52-59.

Elzoghby, A. O., Samy, W. M., & Elgindy, N. A. (2012). Protein-based nanocarriers as promising drug and gene delivery systems. *Journal of Controlled Release,* 161(1), 38-49.

Foged, C., Brodin, B., Frokjaer, S., & Sundblad, A. (2005). Particle size and surface charge affect particle uptake by human dendritic cells in an *in vitro* model. *International Journal of Pharmaceutics,* 298(2), 315-322.

Han, S., Wan, H., Lin, D., Guo, S., Dong, H., Zhang, J., Deng, L., Liu, R., Tang, H., & Dong, A. (2014). Contribution of hydrophobic/hydrophilic modification on cationic chains of poly(epsilon-caprolactone)-graft-poly(dimethylamino ethylmethacrylate) amphiphilic co-polymer in gene delivery. *Acta Biomaterialia,* 10(2), 670-679.

Han, Y., Alsayed, A. M., Nobili, M., Zhang, J., Lubensky, T. C., & Yodh, A. G. (2006). Brownian motion of an ellipsoid. *Science,* 314(5799), 626-630.

He, B., Lin, P., Jia, Z., Du, W., Qu, W., Yuan, L., Dai, W., Zhang, H., Wang, X., Wang, J., Zhang, X., & Zhang, Q. (2013). The transport mechanisms of polymer nanoparticles in Caco-2 epithelial cells. *Biomaterials,* 34(25), 6082-6098.

He, C., Hu, Y., Yin, L., Tang, C., & Yin, C. (2010). Effects of particle size and surface charge on cellular uptake and biodistribution of polymeric nanoparticles. *Biomaterials,* 31(13), 3657-3666.

He, C., Yin, L., Tang, C., & Yin, C. (2012). Size-dependent absorption mechanism of polymeric nanoparticles for oral delivery of protein drugs. *Biomaterials,* 33(33), 8569-8578.

Jin, Y., Song, Y., Zhu, X., Zhou, D., Chen, C., Zhang, Z., & Huang, Y. (2012). Goblet cell-targeting nanoparticles for oral insulin delivery and the influence of mucus on insulin transport. *Biomaterials,* 33(5), 1573-1582.

Karlsson, J., Ungell, A. L., Grasjo, J., & Artursson, P. (1999). Paracellular drug transport across intestinal epithelia: Influence of charge and induced water flux. *European Journal of Pharmaceutical Sciences,* 9(1), 47-56.

Lai, S. K., O'Hanlon, D. E., Harrold, S., Man, S. T., Wang, Y., Cone, R., & Hanes, J. (2007). Rapid transport of large polymeric nanoparticles in fresh undiluted human mucus. *Proceedings of the National Academy of Sciences of the United States of America,* 104(5), 1482-1487.

Lai, S. K., Wang, Y., & Hanes, J. (2009a). Mucus-penetrating nanoparticles for drug and gene delivery to mucosal tissues. *Advanced Drug Delivery Reviews,* 61(2), 158-171.

Lai, S. K., Wang, Y., Wirtz, D., & Hanes, J. (2009b). Micro- and macrorheology of mucus. *Advanced Drug Delivery Reviews,* 61(2), 86-100.

Leonard, F., Collnot, E., & Lehr, C. (2010). A Three-dimensional coculture of enterocytes, monocytes and dendritic cells to model inflamed intestinal mucosa *in vitro*. *Molecular Pharmaceutics,* 7(6), 2103-2119.

Li, X., Chen, D., Le, C., Zhu, C., Gan, Y., Hovgaard, L., & Yang, M. (2011). Novel mucus-penetrating liposomes as a potential oral drug delivery system: Preparation, *in vitro* characterization, and enhanced cellular uptake. *International Journal of Nanomedicine,* 6, 3151-3162.

Lim, J. P. & Gleeson, P. A. (2011). Macropinocytosis: An endocytic pathway for internalising large gulps. *Immunology and Cell Biology,* 89(8), 836-843.

Luo, Y., Teng, Z., Wang, T. T. Y., & Wang, Q. (2013). Cellular uptake and transport of zein nanoparticles: Effects of sodium caseinate. *Journal of Agricultural and Food Chemistry,* 61(31), 7621-7629.

MaHam, A., Tang, Z., Wu, H., Wang, J. & Lin, Y. (2009). Protein-based nanomedicine platforms for drug delivery. *Small*, 5(15), 1706-1721.

Makhlof, A., Tozuka, Y., & Takeuchi, H. (2011). Design and evaluation of novel pH-sensitive chitosan nanoparticles for oral insulin delivery. *European Journal of Pharmaceutical Sciences,* 42(5), 445-451.

Mao, Z., Zhou, X., & Gao, C. (2013). Influence of structure and properties of colloidal biomaterials on cellular uptake and cell functions. *Biomaterials Science,* 1(9), 896-911.

Martins, J. T., Ramos, O. L., Pinheiro, A. C., Bourbon, A. I., Silva, H. D., Rivera, M. C., Cerqueira, M. A., Pastrana, L., Xavier Malcata, F., Gonzalez-Fernandez, A., & Vicente, A. A. (2015). Edible bio-based nanostructures: Delivery, absorption and potential toxicity. *Food Engineering Reviews*, 7(4), 491-513.

McClements, D. J. (2015). Nanoscale nutrient delivery systems for food applications: Improving bioactive dispersibility, stability, and bioavailability. *Journal of Food Science*, 80(7), N1602-N1611.

Murugan, K., Choonara, Y. E., Kumar, P., Bijukumar, D., du Toit, L. C., & Pillay, V. (2015). Parameters and characteristics governing cellular internalization and trans-barrier trafficking of nanostructures. *International Journal of Nanomedicine,* 10, 2191-2206.

Patil, S., Sandberg, A., Heckert, E., Self, W., & Seal, S. (2007). Protein adsorption and cellular uptake of cerium oxide nanoparticles as a function of zeta potential. *Biomaterials,* 28(31), 4600-4607.

Roger, E., Lagarce, F., Garcion, E., & Benoit, J. (2009). Lipid nanocarriers improve paclitaxel transport throughout human intestinal epithelial cells by using vesicle-mediated transcytosis. *Journal of Controlled Release,* 140(2), 174-181.

Sahay, G., Alakhova, D. Y., & Kabanov, A. V. (2010). Endocytosis of nanomedicines. *Journal of Controlled Release,* 145(3), 182-195.

Thorek, D. L. J. & Tsourkas, A. (2008). Size, charge and concentration dependent uptake of iron oxide particles by non-phagocytic cells. *Biomaterials,* 29(26), 3583-3590.

Wang, J., Ma, W., & Tu, P. (2015). The mechanism of self-assembled mixed micelles in improving curcumin oral absorption: In vitro and in vivo. *Colloids and Surfaces B-Biointerfaces,* 133, 108-119.

Win, K. Y. & Feng, S. S. (2005). Effects of particle size and surface coating on cellular uptake of polymeric nanoparticles for oral delivery of anticancer drugs. *Biomaterials,* 26(15), 2713-2722.

Zhang, J., Field, C. J., Vine, D., & Chen, L. (2015a). Intestinal uptake and transport of vitamin B-12-loaded soy protein nanoparticles. *Pharmaceutical Research,* 32(4), 1288-1303.

Zhang, Z., Van Steendam, K., Maji, S., Balcaen, L., Anoshkina, Y., Zhang, Q., Vanluchene, G., De Rycke, R., Van Haecke, F., Deforce, D., Hoogenboom, R., & De Geest, B. G. (2015b). Tailoring cellular uptake of gold nanoparticles via the hydrophilic-to-hydrophobic ratio of their (co)polymer coating. *Advanced Functional Materials,* 25(22), 3433-3439.

CHAPTER 7- Napin shows a chaperone-like activity through limiting fibril formation

7.1. Introduction

Napin, a major canola protein, belongs to 2S albumin family with a molecular mass of 14-15 kDa (Tan et al., 2011). Napin is a disulfide-linked complex of two subunits; a small 4.5-kDa and a large 10-kDa subunit (Barciszewski et al., 2000). Napin, with a high denaturation temperature of 110 °C (Wu and Muir, 2008), is thermal stabile against thermal-induced aggregation. In terms of secondary structure, napin has a high content of α-helical structure (40-46%) and a low content of β–sheet conformation (12%) (Tan et al., 2011; Barciszewski, et al., 2000). Napin, a basic protein with isoelectric point around 11, contains a large proportion of glutamine, lysine and cysteine residues (Jyothi et al., 2007). Although napin is hydrophilic protein, its core is formed by hydrophobic interactions between α-helical structures (Wanasundara, 2011). In addition, Folawio and Apenten (1996) showed that heating at pH ≤ 7 increased napin surface hydrophobicity more than that of pH ≤ 4. Highly positive charge and the increased hydrophobicity during heating could provide an amphiphilic property for napin. As a result, the high charge density and low hydrophobicity lead to a weakly folded structure which is mostly held by disulfide linkages (Jyothi et al., 2007; Wanasundara, 2011). Napin, also contains 6.4% proline (Aider and Barbana, 2011), a hydrophobic residue, which provides great flexibility to protein structures (Yong and Foegeding, 2010). Therefore, the loosely folded and relatively flexible structure of napin, along with highly positive charge and presence of surface hydrophobic groups can facilitate its interaction with other proteins through electrostatic and/or hydrophobic forces. Napin, due to its high thermal stability, has an ability to increase the resistance to aggregation. This property could be similar to anti-aggregation activity of chaperones.

Chaperones are a large group of proteins that prevent aggregation and fibrillation of intrinsically disordered or partially unfolded proteins (Ellis, 2006; Liberek et al., 2008). Amyloid fibrils, morphologically similar to β-sheet-rich protein aggregates, are formed through self-assembly of different proteins with various sequence, structure and functional properties (Ehrnhoefer et al., 2008). The formation of amyloid fibrils is recognized as a major contributing factor in amyloid-related diseases such as Alzheimer's and Huntington's (Ghadami et al., 2011; Khodarahmi et al., 2009). Amyloid fibrillization is a thermodynamically favored process to form stable structures with the lowest free energy level (Liao et al., 2012). Although there are many studies aimed to characterize protein aggregation and amyloid formation, our knowledge about the mechanisms is limited (Oboroceanu et al., 2010; Ghadami et al., 2011). At least two distinct competitive pathways

were proposed: one is reversible non-nucleation growth in which oligomers and worm-like (semi-flexible) fibrils are rapidly assembled, while the 2nd one is nucleation-dependent, where rigid long-straight fibrils (amyloids) are formed through lag-phased nucleation and growth. The competing pathways can produce a heterogeneous mixture of the fibrils in which the population of each fibril type depends on the assembly rate and stability of the fibril in solution conditions (Gosal et al., 2005; Miti et al., 2015).

Although protein aggregation is required for some functional properties such as gelling, thickening and stabilizing emulsions and foams, they may result in undesirable consequences due to the formation of large clusters and precipitates in some high-protein products, in particular beverage products (Nicolai and Durand, 2013). As protein has stronger satiety feeling than carbohydrate and fat (Bertenshaw et al., 2008), demands for high-protein products for obesity control and body-weight management are increasing. The high protein beverage products are also used for the patients who suffer from developing impaired function in the organs and muscles due to long-term hospitalisation (Potter et al., 2001; Saglam et al., 2014). Therefore, protein aggregation should be prevented to improve appearance and flow behaviour in high protein beverage products. Ingested pre-formed aggregates might also act as fibrillization seeds to trigger extensive aggregation in the body (Chiti and Dobson, 2006). Thus, process-induced unfolding, misfolding and aggregation need to be controlled in some high protein food products where the presence of aggregates or amyloid fibrils is not desired.

Chaperone-like activity was reported for some protein/non-protein molecules such as casein (Librizzi et al., 2014; Kehoe and Foegeding, 2014), poly phenols (Hudson et al., 2009; Singh et al., 2013; Wang et al., 2008), cyclodextrin (Machida et al., 2000), Heme-containing proteins (Khodarahmi et al., 2009). Librizzi et al. (2014) showed that α-casein sequestered initial oligomers of insulin before they can trigger the secondary nucleation to form amyloid fibrils. Kehoe and Foegeding (2014) reported that β-casein-β-lactoglobulin heterogeneous aggregates were less prone to growth and/or to secondary aggregation.

Our objective in this research was to study the potential chaperone-like activity of napin. For this purpose, the ability of napin to suppress heat aggregation of ovotransferrin (OT) was investigated. OT is the most heat-labile protein in egg white proteins which aggregates at lower temperature near 60 °C (Matsudomi et al., 2004). The possible mechanism by which napin might limit OT aggregation will also be discussed.

7.2. Material and methods

7.2.1. Materials

Napin isolate was prepared as we previously reported (Akbari and Wu, 2015). Ovotransferrin, Thioflavin T and 1-anilinonaphthalene-8-sulfonic acid (ANS) were obtained from Sigma (Oakville, ON, Canada).

7.2.2. Sample preparation, Thioflavin T fluorescence and turbidity studies

Ovotransferrin (OT) solutions (0.5, 1 and 2 mg/mL) were prepared at pH 10, and then adjusted to pH 7 using 0.1 M HCl. Napin was solubilised at pH 7 and then mixed with OT solutions at ratios 1:1 and 1:0.5 (OT:napin). OT and napin solutions and their mixtures were heated at 85 °C and 100 rpm shaking for 30 min in a water bath. After cooling to room temperature, the turbidity and thioflavin T (Th T) fluorescence intensity of the solutions were determined to monitor protein aggregation. The turbidity was measured at 400 nm using a microplate reader (Spectramax M3, Molecular Devices, Sunnyvale, CA). Th T fluorescence intensity was determined using the method developed by Nielsen et al. (2001) with some modification. In brief, 1 mM Th T stock solution was prepared and stored at 4 °C protected from light to prevent quenching until usage. 200 µL sample was diluted with 3700 µL water (pH 7), and then 80 µL 1 mM Th T was added and incubated for 2 min. Fluorescence intensity was measured at emission wavelength of 482 nm using RF-5301PC spectrofluorophotometer (Shimadzu, Kyoto, Japan) equipped with a 1-cm path length quartz cell. Excitation wavelength was 450 nm and slit widths were 5 nm for both excitation and emission. In addition to the Th T fluorescence property of the protein solutions (before and after heating), the fluorescence of dissolving water (with and without Th T) was also measured as blank.

7.2.3. Zeta potential

Zeta potential of the solutions was measured by laser doppler velocimetry using a Zetasizer NanoS (ZEN1600, Malvern Instruments Ltd., Worcestershire, UK). Prior the measurements, samples were diluted to obtain a slight opalescent dispersion and prevent multiple scattering effects.

7.2.4. Surface hydrophobicity

Surface hydrophobicity of the protein solutions before and after heating was determined using ANS fluorescent probe (Alizadeh-Pasdar and Li-Chan, 2000). Briefly, the samples were diluted to eight concentrations ranging from 0.006 to 0.14 mg/mL using water pH 7. After adding 20 µL of

8 mM ANS to 4 mL of the diluted protein solutions, fluorescence intensity at emission wavelength of 470 nm was measured using the spectrofluorophotometer. Excitation wavelength was 390 nm and slit widths were 5 nm for both excitation and emission. The fluorescence intensity of blank solution (without protein) and protein solutions without ANS were subtracted from the measured fluorescence value of samples. The slope of the linear plot of net fluorescence values versus protein concentrations was used as an index of the protein surface hydrophobicity.

7.2.5. Intrinsic fluorescence

Intrinsic fluorescence emission of unheated and heated samples was measured using the spectrofluorophotometer equipped with a 1-cm path length quartz cell. The protein concentration and pH of the samples were adjusted to 1 mg/mL OT and pH 7, respectively. The fluorescence measurements were performed using excitation wavelength of 280 nm (slit width=5 nm), and emission spectra were recorded from of 290 to 500 nm wavelength (slit width=5 nm) (Perez et al., 2014).

7.2.6. CD spectroscopy

Conformational change of the protein samples before and after heating was characterized using Circular Dichroism (CD). The far-UV CD spectra of the protein samples (1 mg/mL) at pH 7 was measured using DSM 17 Circular Dichroism (Olis, Bogart, GA, USA). The path length of the quartz cell was 0.2 cm and the spectra represented an average of five scans collected in 1-nm steps at a rate of 20 nm/min over the wavelength range of 190-250 nm.

7.2.7. FTIR

Attenuated total reflectance Fourier-transform infrared (ATR-FTIR) (Nicolet-IS50, Thermo Scientific, Waltham, MA, USA) was also used to study the conformational changes in the secondary structure of the protein samples. Freeze-dried samples were dried in a vacuum desiccator using phosphorous pentoxide for 72 h. FTIR spectrum of the samples was recorded in the range of 4000-400 cm^{-1} using 128 scans at 4 cm^{-1} resolution. The recorded spectra were deconvoluted in amide I band region (1700-1600 cm^{-1}) using Omnic 8.1 software at a bandwidth of 25 cm^{-1} and an enhancement factor of 2.5. The detected amide I bands in the spectra were assigned to protein secondary structures using previously established wavenumber ranges reported by Kong and Yu (2007) and Pelton and McLean (2000).

7.2.8. Statistical analysis

The experiments were carried out in triplicates and results were statistically analysed using ANOVA and Duncan tests (version 9.2, SAS Institute Inc., Cary, NC, USA).

7.3. Results and discussion

7.3.1. Th T fluorescence and turbidity studies

To study the chaperone-like activity of napin, OT solution alone and OT/napin mixture were heated at 85 °C for 0.5-6 h. Thioflavin T (ThT) fluorescence and turbidity methods were used to monitor fibrillation and random aggregation of the protein solutions, respectively. The fluorescence property of Th T, a specific fluorescence probe for detection of protein β-structures, has been widely used to study the formation of fibrils (Khodarahmi et al., 2009).

The fluorescence intensity of the protein solutions at different concentrations was measured before and after the heat treatment. Heating OT solution increased fibril concentration ~ 28 times more than unheated form (Figure 7.1).

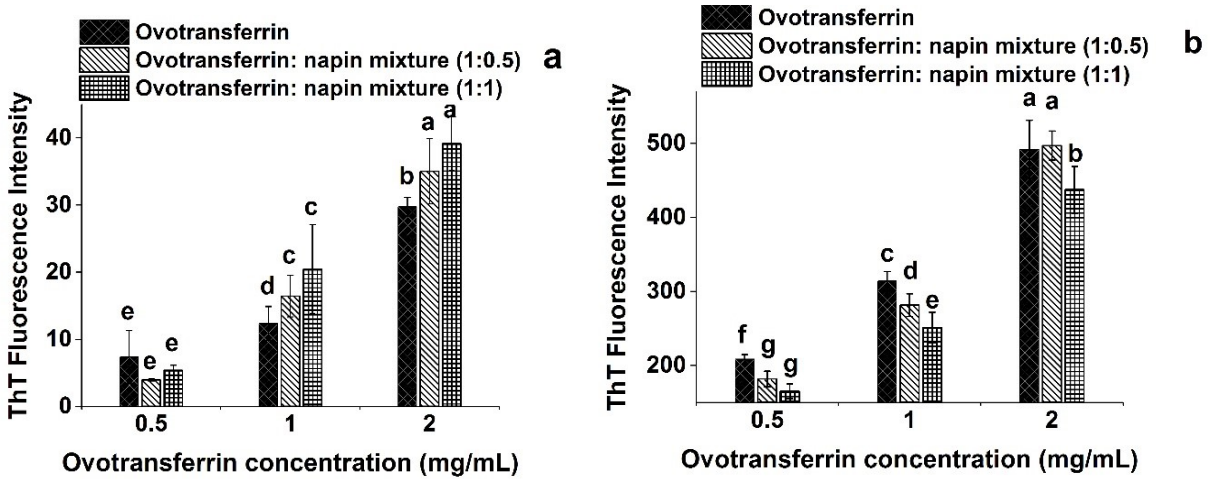

Figure 7.1. Thioflavin T fluorescence intensity of ovotransferrin solution in the absence and presence of different ratio of napin before (a) and after heating (b) at 85 °C for 30min.

However, the Th T fluorescence intensity of heated OT/napin mixture was significantly lower than heated OT solution. The chaperone-like activity of napin also depended on the heating temperature. Napin decreased ~50% of OT fibril formation after heating at 65 °C (*Supplementary*

Figure 7.1) compared to 20% decrease of 85 °C heating. The reason might be due to formation of different intermediates at 85 °C which were not properly suppressed by napin. The decreasing effect of napin on OT fibril formation increased over the heating period (Figure 7.2). However, no significant difference was observed in the Th T florescence of napin solution before and after heating. The resistance of napin to aggregation and/or fibril formation is due to its high denaturation temperature at 110 °C (Wu and Muir, 2008).

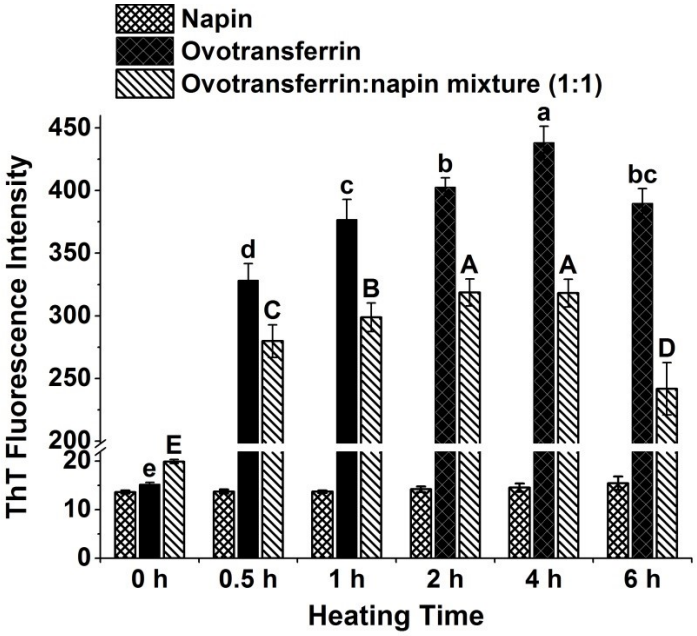

Figure 7.2. Thioflavin T fluorescence intensity of ovotransferrin solution (1 mg/mL) with and without napin over the heat treatment (85 °C)

However, adding napin did not decrease the turbidity of the mixture after heating, but even increased the turbidity at low napin concentrations (Figure 7.3). The results indicated that fibril formation, but not amorphous aggregation, was inhibited by napin; similar chaperone-like activities were reported for polyphenolic compounds (Borana et al. 2014; Ehrnhoefer et al., 2008; Porat et al., 2006) and gold nanoparticles (Liao et al., 2012). It was thought that non-covalent interactions between aromatic rings of polyphenolic compounds and exposed hydrophobic residues of amyloidogenic cores could interfere with the fibril growth and as a result, suppressed fibril formation (Porat et al., 2006). Similar non-covalent interactions might also develop between napin and OT fibril cores which resulted in decreased fibril formation.

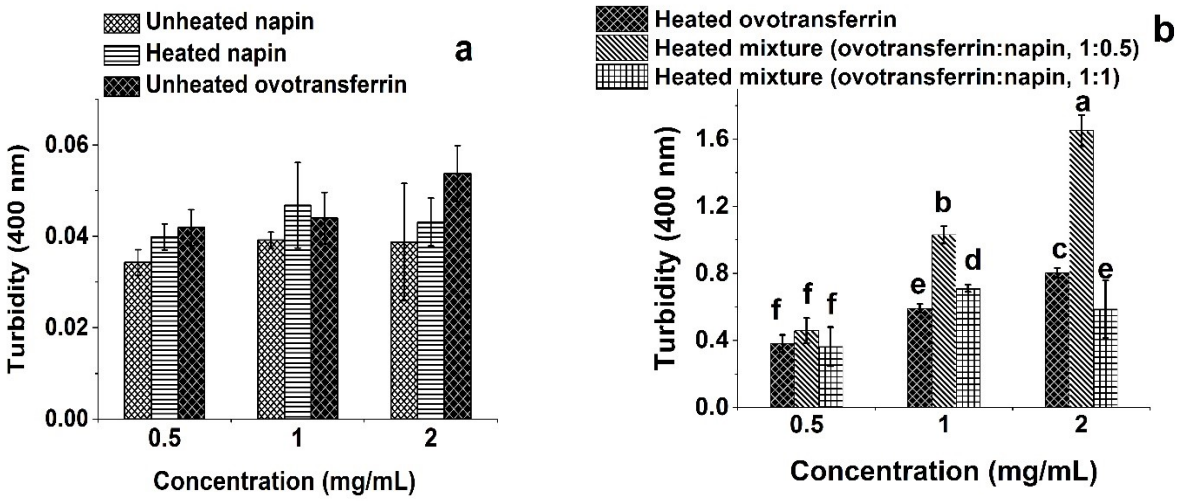

Figure 7.3. Turbidity of ovotransferrin and napin solutions and their mixture before and after the heat treatment.

Heat denatured OT with a zeta potential of -28.1±0.8 mV tended to form fibrils while at decrease of the surface charge of heated mixture to -19.3±1.6 mV, random amorphous aggregates formed. With adding positively-charged napin, zeta potential of the mixture decreased and formation of random amorphous aggregation increased due to weakened repulsive forces.

The influence of the attractive and repulsive forces on protein aggregation was previously reported by van der Linden and Venema (2007), who reported that protein fibrillar structures are formed at low ionic strengths, and pH values far from the protein isoelectric point (PI) while amorphous aggregates are more favorable structures at pHs close to protein PI and high ionic strengths (van der Linden and Venema, 2007). Formation of amorphous aggregates in the presence of high concentration of salts was also reported by Miti et al. (2015) and Foley et al. (2013). However, unlike Miti et al. (2015) who showed fibrils are the prevailing aggregate phase at low salt concentrations, and sharply switched to amorphous fibril formation at increased salt concentration, our results revealed that at increasing napin concentrations, amorphous fibril formation decreased compared to that at low napin concentrations. Epigallocatechin gallate, the most important polyphenolic compound in green tea extract, also prevented fibril formation through stabilising fibril-forming proteins in their native form instead of reordering formed fibrils to disordered/amorphous structures (Hudson et al., 2009).

7.3.2. Surface hydrophobicity

The surface hydrophobicity of napin was not affected while that of OT was dramatically increased after heating (Figure 7.4); the rapid increased surface hydrophobicity of OT was due to exposure of more hydrophobic groups to surface after denaturation. The increase in surface hydrophobicity accrued simultaneously with fibril formation after heating. This similar trend in increase of surface hydrophobicity and fibril formation indicated that OT conformation completely changed in the aggregation/fibril formation process; and also the aggregates/fibrils possessed more exposed hydrophobic groups compared to native OT. Vetri et al. (2007) also showed that the aggregation process and in particular formation of amyloid aggregates exposed new hydrophobic regions to the protein surface.

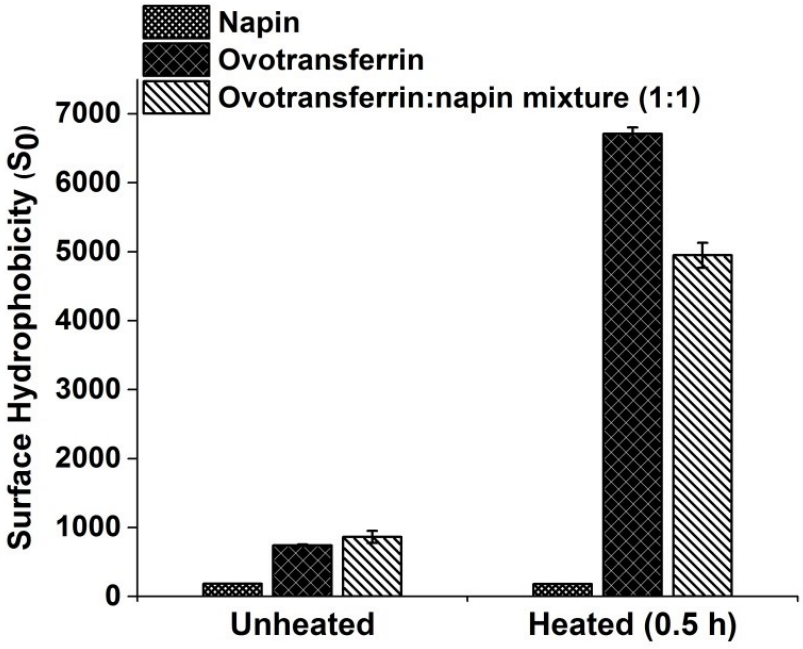

Figure 7.4. Surface hydrophobicity of ovotransferrin and napin solutions and their mixture before and after the heat treatment.

After heating, although the surface hydrophobicity of the mixture increased compared to the unheated form, it was lower than that of heated OT solution alone. This indicated that less

hydrophobic groups were available on the surface of the aggregates, due probably to partial re-folding of the denatured OT structure in the presence of napin, hydrophobic interaction between napin and OT, and/or formation of new aggregate with lower surface hydrophobicity. Curcumin, a chaperone-like poly phenolic compound, also decreased the surface hydrophobicity of aggregates through interaction with amyloid fibrils (Singh et al., 2013).

7.3.3. Intrinsic fluorescence

The intrinsic fluorescence of a protein strongly depends on the conformations that the protein adopts in response to bulk solution conditions. Intrinsic fluorescence property of a protein is due to the presence of aromatic amino acids (especially tryptophan) which can mostly be excited at 280 nm (Gorinstein et al., 2000; Duy and Fitter, 2006). As shown in Figure 7.5, no significant change was observed in the position of emission λ_{max} and also in the fluorescence intensity of napin before and after heating. This confirmed that the conformation of napin didn't change over the heat treatment. However, the red shift in emission λ_{max} (330 to 339 nm), and increased fluorescence intensity of denatured OT revealed that OT structure unfolded, and surrounding microenvironment changed to "more-polar". The presence of napin, however, had no effect on the emission spectrum of heated OT.

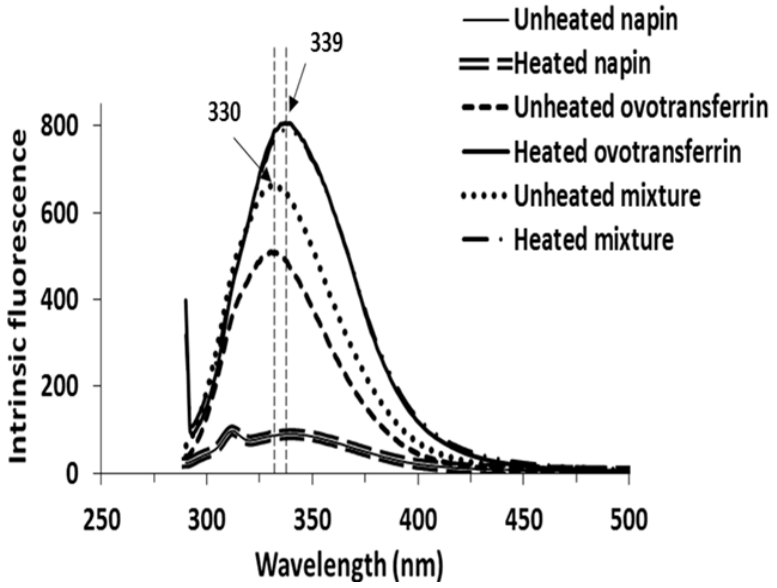

Figure 7.5. Intrinsic fluorescence intensity of ovotransferrin and napin solutions and their mixture before and after the heat treatment

7.3.4. CD spectroscopy

Conformational change of thermal aggregated OT in the presence and absence of napin was also studied using CD spectroscopy. Comparison of the spectrum of OT revealed that although random coil was the main secondary structure in both heated and unheated protein, the intensity of the negative ellipticity peak decreased and the positive part of the peak disappeared after heating (Figure 7.6). Similar results were reported by Tong et al. (2012) showing unordered and β-sheet structures increased in aggregated OT, while α-helix and β-turn decreased. However, the heat treatment had no significant influence on the napin spectrum; the spectra with an intense positive band at 190 nm, zero-crossing point near 200 nm and a negative peak at 208 nm (Bulheller et al., 2007; Ranjbar and Gill, 2009) indicated α-helix was the main secondary structure of napin.

In the OT/napin mixture, the presence of napin significantly changed the secondary structure of OT after heating compared to heated OT itself. The spectrum of the heated mixture was very similar to α-helix spectrum. This implied that napin prevented formation of β-sheet and random coils (the secondary structures of heated OT), and instead, the new structure in heated OT/napin mixture was re-ordered in favour of α-helix which is napin structure. Librizzi et al. (2014) also showed a very similar structure to α-helix for insulin aggregates in the presence of α-casein. Therefore the conformational change might be a reason for reducing fibril structures in the presence of napin.

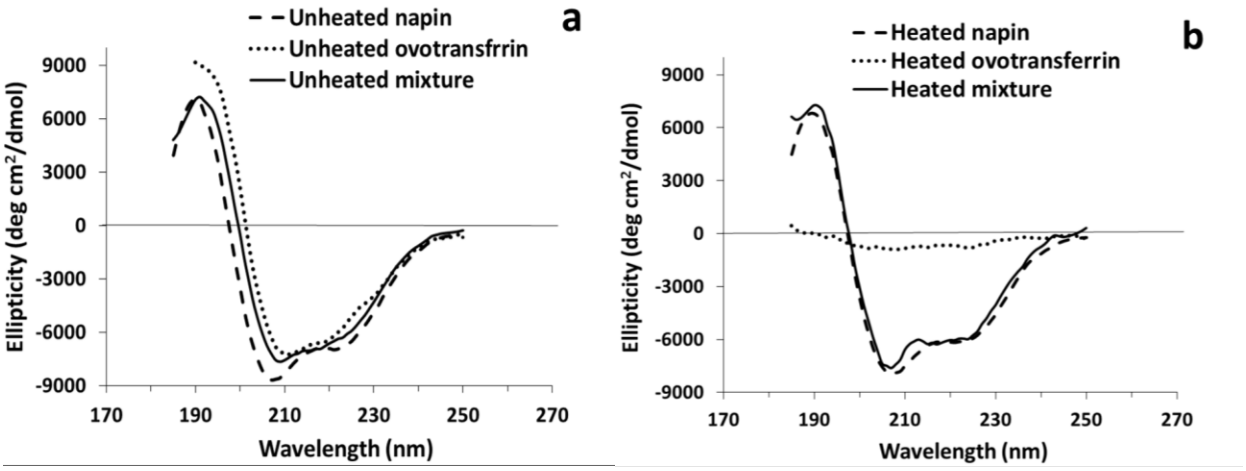

Figure 7.6. Far-UV CD spectra of ovotransferrin and napin solutions and their mixture before (a) and after the heat treatment (b).

7.3.5. FTIR study

Since the accuracy of CD for measuring turns and β-sheets is as low as 50 to 75% (compared to 97% for helices and 89% for other structures) (Ranjbar and Gill, 2009), the secondary structures of the samples were also studied using FTIR. Deconvoluted FTIR spectra of amide I band region of the samples were compared with the previously established wavenumber ranges (Kong and Yu, 2007; Pelton and McLean, 2000). The strong absorption of IR at 1654-1655 cm^{-1} indicated that α-helix was predominant in the secondary structure of unheated and heated napin (Figure 7.7). β-sheet structures, represented at 1634 and 1639 cm^{-1}, and random coil at 1650 cm^{-1}, were detected in unheated OT spectrum, while a mixture of β-sheet (1627 and 1695 cm^{-1}), α-helix (1652 cm^{-1}) and random structures (1645 cm^{-1}) were observed in the OT aggregates. However, the peaks assigned to β-sheet and random structures were disappeared/weakened in the spectrum of heated mixture. As a result, α-helix, represented at 1655 cm^{-1}, was the predominant secondary structure in the heated OT/napin mixture which confirmed our previous results in the CD study.

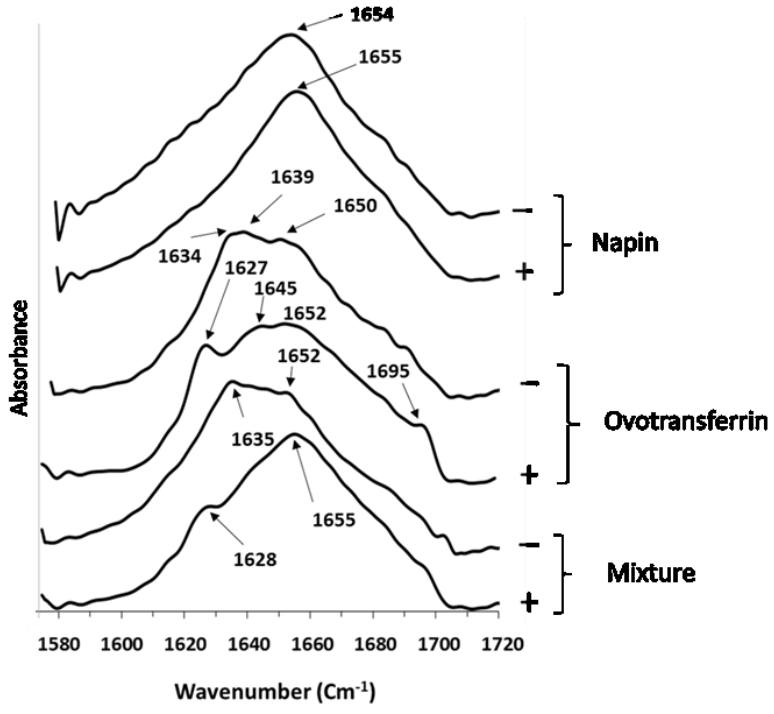

Figure 7.7. FTIR spectra of ovotransferrin and napin solutions and their mixture before (-) and after (+) heating

Although the conformational changes and surface hydrophobicity and zeta potential studies supported the Th T fluorescence study showing decrease of fibril formation, the chaperone-like activity of napin was lower than our expectation, and amorphous aggregates were not decreased effectively.

7.4.Conclusions

Napin shows a chaperone-like activity through limiting fibril formation. The presence of positive charges as well as hydrophobic groups could provide napin an amphiphilic nature which is an important factor for chaperone-like molecules (Koudelka et al., 2009). The mechanism of action might be through forming hydrophobic interactions between napin and OT fibril cores. Decrease of the surface hydrophobicity of heated OT/napin mixture compared to heated alone OT might confirm the suggested mechanism. With these interactions, the conformation of the aggregates re-ordered to some structures close to napin. The CD and FTIR results supported the conformational changes. Since the re-ordered structures might have low propensity to form fibrils, fibril formation was suppressed. The chaperone-like activity of napin might also be concentration-dependent. While at low concentrations, napin decreased fibril formation due probably to redirecting fibrillation into off-pathways intermediates leading amorphous aggregation; at high concentrations, napin decreased fibril formation more efficiently, but amorphous aggregation remained stable.

7.5. References:

Aider, M. & Barbana, C. (2011). Canola proteins: Composition, extraction, functional properties, bioactivity, applications as a food ingredient and allergenicity - A practical and critical review. *Trends in Food Science & Technology*, 22(1), 21-39.

Akbari, A. & Wu, J. (2015). An integrated method of isolating napin and cruciferin from defatted canola meal. *Lwt-Food Science and Technology,* 64(1), 308-315.

Alizadeh-Pasdar, N. & Li-Chan, E. C. Y. (2000). Comparison of protein surface hydrophobicity measured at various pH values using three different fluorescent probes. *Journal of Agricultural and Food Chemistry,* 48(2), 328-334.

Barciszewski, J., Szymanski, M., & Haertle, T. (2000). Minireview: Analysis of rape seed napin structure and potential roles of the storage protein. *Journal of Protein Chemistry,* 19(4), 249-254.

Bertenshaw, E. J., Lluch, A., & Yeomans, M. R. (2008). Satiating effects of protein but not carbohydrate consumed in a between-meal beverage context. *Physiology & Behavior, 93*(3), 427-436.

Borana, M. S., Mishra, P., Pissurlenkar, R. R. S., Hosur, R. V., & Ahmad, B. (2014). Curcumin and kaempferol prevent lysozyme fibril formation by modulating aggregation kinetic parameters. *Biochimica Et Biophysica Acta-Proteins and Proteomics,* 1844(3), 670-680.

Bulheller, B. M., Rodger, A., & Hirst, J. D. (2007). Circular and linear dichroism of proteins. *Physical Chemistry Chemical Physics,* 9(17), 2020-2035.

Chiti, F., & Dobson, C. M. (2006). Protein misfolding, functional amyloid, and human disease. *Annual Review of Biochemistry*, *75*, 333-366.

Duy, C. & Fitter, J. (2006). How aggregation and conformational scrambling of unfolded states govern fluorescence emission spectra. *Biophysical Journal,* 90(10), 3704-3711.

Ehrnhoefer, D. E., Bieschke, J., Boeddrich, A., Herbst, M., Masino, L., Lurz, R., Engemann, S., Pastore, A., & Wanker, E. E. (2008). EGCG redirects amyloidogenic polypeptides into unstructured, off-pathway oligomers. *Nature Structural & Molecular Biology,* 15(6), 558-566.

Ellis, R. J. (2006). Molecular chaperones: Assisting assembly in addition to folding. *Trends in Biochemical Sciences,* 31(7), 395-401.

Folawiyo, Y. L. & Apenten, R. K. O. (1997). The effect of heat- and acid-treatment on the structure of rapeseed albumin (napin). *Food Chemistry, 58*(3), 237-243.

Foley, J., Hill, S. E., Miti, T., Mulaj, M., Ciesla, M., Robeel, R., Persichilli, C., Raynes, R., Westerheide, S., & Muschol, M. (2013). Structural fingerprints and their evolution during oligomeric vs. oligomer-free amyloid fibril growth. *Journal of Chemical Physics,* 139(12), 121901.

Ghadami, S. A., Khodarahmi, R., Ghobadi, S., Ghasemi, M., & Pirmoradi, S. (2011). Amyloid fibril formation by native and modified bovine β-lactoglobulins proceeds through unfolded form of proteins: A comparative study. *Biophysical Chemistry,* 159(2-3), 311-320.

Gorinstein, S., Goshev, I., Moncheva, S., Zemser, M., Weisz, M., Caspi, A., Libman, I., Lerner, H. T., Trakhtenberg, S., & Martin-Belloso, O. (2000). Intrinsic tryptophan fluorescence of human serum proteins and related conformational changes. *Journal of Protein Chemistry,* 19(8), 637-642.

Gosal, W. S., Morten, I. J., Hewitt, E. W., Smith, D. A., Thomson, N. H., & Radford, S. E. (2005). Competing pathways determine fibril morphology in the self-assembly of beta(2)-microglobulin into amyloid. *Journal of Molecular Biology,* 351(4), 850-864.

Hudson, S. A., Ecroyd, H., Dehle, F. C., Musgrave, I. F., & Carver, J. A. (2009). (-)-Epigallocatechin-3-gallate (EGCG) maintains kappa-casein in its pre-fibrillar state without redirecting its aggregation pathway. *Journal of Molecular Biology,* 392(3), 689-700.

Jyothi, T. C., Singh, S. A., & Appu Rao, A. G. (2007). Conformation of napin (*Brassica juncea*) in salts and monohydric alcohols: Contribution of electrostatic and hydrophobic interactions. *Journal of Agricultural and Food Chemistry,* 55(10), 4229-4236.

Kehoe, J. J., & Foegeding, E. A. (2014). The characteristics of heat-induced aggregates formed by mixtures of β-lactoglobulin and β -casein. *Food Hydrocolloids, 39*, 264-271.

Khodarahmi, R., Soori, H., & Karimi, S. A. (2009). Chaperone-like activity of heme group against amyloid-like fibril formation by hen egg ovalbumin: Possible mechanism of action. *International Journal of Biological Macromolecules,* 44(1), 98-106.

Kong, J. & Yu, S. (2007). Fourier transform infrared spectroscopic analysis of protein secondary structures. *Acta Biochimica Et Biophysica Sinica,* 39(8), 549-559.

Koudelka, T., Hoffmann, P., & Carver, J. A. (2009). Dephosphorylation of alpha(s)- and beta-caseins and its effect on chaperone activity: A structural and functional investigation. *Journal of Agricultural and Food Chemistry*, 57(13), 5956-5964.

Liao, Y., Chang, Y., Yoshiike, Y., Chang, Y., & Chen, Y. (2012). Negatively charged gold nanoparticles inhibit Alzheimer's amyloid-beta fibrillization, induce fibril dissociation, and mitigate neurotoxicity. *Small,* 8(23), 3631-3639.

Liberek, K., Lewandowska, A., & Zietkiewicz, S. (2008). Chaperones in control of protein disaggregation RID F-5812-2011. *Embo Journal,* 27(2), 328-335.

Librizzi, F., Carrotta, R., Spigolon, D., Bulone, D., & San Biagio, P. L. (2014). alpha-Casein inhibits insulin amyloid formation by preventing the onset of secondary nucleation processes. *Journal of Physical Chemistry Letters,* 5(17), 3043-3048.

Machida, S., Ogawa, S., Shi, X. H., Takaha, T., Fujii, K., & Hayashi, K. (2000). Cycloamylose as an efficient artificial chaperone for protein refolding. *FEBS Letters,* 486(2), 131-135.

Matsudomi, N., Kanda, Y., Yoshika, Y., & Moriwaki, H. (2004). Ability of alpha s-casein to suppress the heat aggregation of ovotransferrin. *Journal of Agricultural and Food Chemistry,* 52(15), 4882-4886.

Miti, T., Mulaj, M., Schmit, J. D., & Muschol, M. (2015). Stable, metastable, and kinetically trapped amyloid aggregate phases. *Biomacromolecules,* 16(1), 326-335.

Nicolai, T. & Durand, D. (2013). Controlled food protein aggregation for new functionality. *Current Opinion in Colloid & Interface Science,* 18(4), 249-256.

Nielsen, L., Khurana, R., Coats, A., Frokjaer, S., Brange, J., Vyas, S., Uversky, V. N., & Fink, A. L. (2001). Effect of environmental factors on the kinetics of insulin fibril formation: Elucidation of the molecular mechanism. *Biochemistry,* 40(20), 6036-6046.

Oboroceanu, D., Wang, L., Brodkorb, A., Magner, E., & Auty, M. A. E. (2010). Characterization of beta-lactoglobulin fibrillar assembly using atomic force microscopy, polyacrylamide gel electrophoresis, and *in situ* Fourier transform infrared spectroscopy. *Journal of Agricultural and Food Chemistry,* 58(6), 3667-3673.

Pelton, J. T. & McLean, L. R. (2000). Spectroscopic methods for analysis of protein secondary structure. *Analytical Biochemistry,* 277(2), 167-176.

Perez, A. A., Andermatten, R. B., Rubiolo, A. C., & Santiago, L. G. (2014). Beta-Lactoglobulin heat-induced aggregates as carriers of polyunsaturated fatty acids. *Food Chemistry,* 158, 66-72.

Porat, Y., Abramowitz, A., & Gazit, E. (2006). Inhibition of amyloid fibril formation by polyphenols: Structural similarity and aromatic interactions as a common inhibition mechanism. *Chemical Biology & Drug Design,* 67(1), 27-37.

Potter, J. M., Roberts, M. A., McColl, J. H., & Reilly, J. J. (2001). Protein energy supplements in unwell elderly patients - A randomized controlled trial. *Journal of Parenteral and Enteral Nutrition, 25*(6), 323-329.

Ranjbar, B. & Gill, P. (2009). Circular dichroism techniques: Biomolecular and nanostructural analyses- A review. *Chemical Biology & Drug Design,* 74(2), 101-120.

Saglam, D., Venema, P., de Vries, R., & van der Linden, E. (2014). Exceptional heat stability of high protein content dispersions containing whey protein particles. *Food Hydrocolloids, 34*(1), 68-77.

Singh, P. K., Kotia, V., Ghosh, D., Mohite, G. M., Kumar, A., & Maji, S. K. (2013). Curcumin modulates alpha-synuclein aggregation and toxicity. *Acs Chemical Neuroscience,* 4(3), 393-407.

Tan, S. H., Mailer, R. J., Blanchard, C. L., & Agboola, S. O. (2011). Extraction and characterization of protein fractions from Australian canola meals. *Food Research International,* 44(4), 1075-1082.

Tong, P., Gao, J., Chen, H., Li, X., Zhang, Y., Jian, S., Wichers, H., Wu, Z., Yang, A., & Liu, F. (2012). Effect of heat treatment on the potential allergenicity and conformational structure of egg allergen ovotransferrin. *Food Chemistry,* 131(2), 603-610.

van der Linden, E. & Venema, P. (2007). Self-assembly and aggregation of proteins. *Current Opinion in Colloid & Interface Science,* 12(4-5), 158-165.

Vetri, V., Canale, C., Relini, A., Librizzi, F., Militello, V., Gliozzi, A., & Leone, M. (2007). Amyloid fibrils formation and amorphous aggregation in concanavalin A. *Biophysical Chemistry,* 125(1), 184-190.

Wanasundara, J. P. D. (2011). Proteins of *Brassicaceae* oilseeds and their potential as a plant protein source. *Critical Reviews in Food Science and Nutrition*, 51(7), 635-677.

Wang, J., Ho, L., Zhao, W., Ono, K., Rosensweig, C., Chen, L., Humala, N., Teplow, D. B., & Pasinetti, G. M. (2008). Grape-derived polyphenolics prevent A beta oligomerization and attenuate cognitive deterioration in a mouse model of Alzheimer's disease. *Journal of Neuroscience,* 28(25), 6388-6392.

Wu, J. & Muir, A. D. (2008). Comparative structural, emulsifying, and biological properties of 2 major canola proteins, cruciferin and napin. *Journal of Food Science,* 73(3), C210-C216.

Yong, Y. H., & Foegeding, E. A. (2010). Caseins: utilizing molecular chaperone properties to control protein aggregation in foods. *Journal of Agricultural and Food Chemistry, 58*(2), 685-693.

7.6. Appendix D: Supplementary Information

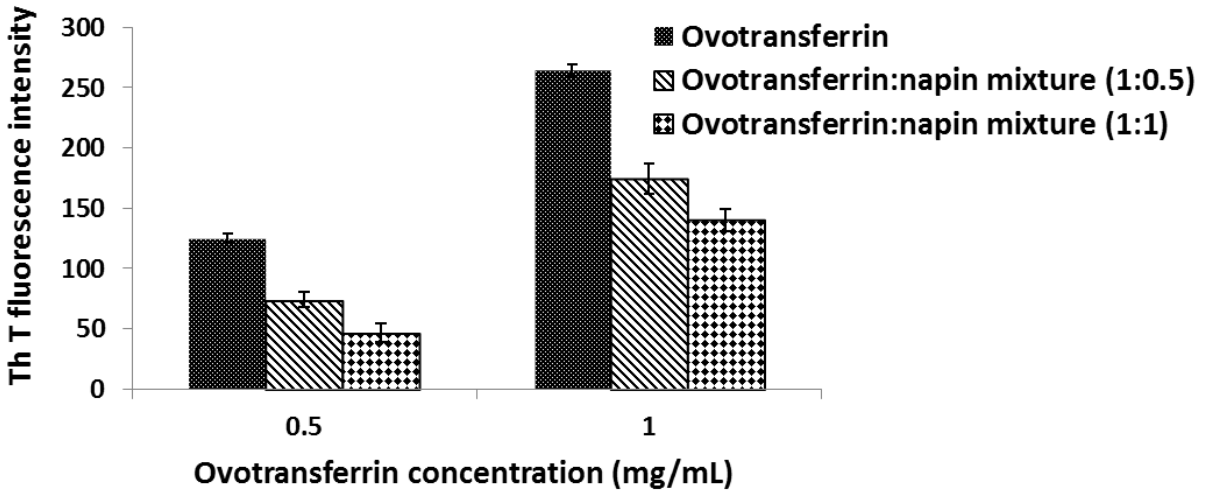

Supplementary Figure 7.1. Thioflavin T fluorescence intensity of ovotransferrin solution (in the absence and presence of different ratio of napin) after heating at 65 °C for 30min

CHAPTER 8-Conclusions and recommendations

8.1. Conclusion

The development of colloid-based delivery systems to encapsulate various bioactive compounds is a growing field in food industry. In addition to protection of bioactive compounds against harsh conditions in food processing and human digestive system, encapsulation can mask unpleasant off-flavor of some compounds, increase solubility and as a result, improve their bioavailability (Matalanis et al., 2011; Wan et al., 2015; McClements, 2015). The selection of a biopolymer to prepare a proper delivery system depends on several factors: 1) the ability of the polymer to form the delivery system; 2) the required properties of the system (e.g., charge, size and stability to environment conditions); 3) cost, application limits and consistency of the polymers and processing operations (Matalanis et al., 2011). Food proteins, GRAS, biocompatible and biodegradable biopolymers, possess various active groups which enable them to interact with both hydrophilic and hydrophobic compounds. The presence of three-dimensional network, which could be altered in different conditions such as temperature, pH and ionic strength, also provides an appropriate system to entrap or release bioactive compounds (Elzoghby et al., 2012). After successful encapsulation and protection of bioactive compounds, the release of the compounds in the target organ is very important which affects their health promoting influence. The absorption of the compounds in small intestine, the target organ for most orally-administrated compounds, is affected by important parameters such as short transit time, mucus barrier and transport across epithelial cells (Boegh and Nielsen, 2015; Martins et al., 2015). Mucoadhesive particles are able to prolong the transit time and sustainably release the encapsulated compounds (Smart, 2005), and the mucus barrier can be overcome using mucus-penetrating particles (Lai et al., 2009). Study the mechanisms of cellular uptake and also the physicochemical properties of particles (e.g. size, shape and charge) could help researchers to prepare appropriate carriers to transport the encapsulated compounds (Martins et al., 2015; Bernkop-Schnuerch, 2013; Sahay, et al., 2010). However, most of these studies have focused on synthetic polymers, while there is an increasing demand for edible biopolymer-based delivery systems.

In this research, for the first time, we prepared two delivery systems using cruciferin, a major canola protein. Canola proteins are extracted from an abundant and inexpensive source, canola meal, a by-product of oil extraction with global production of 38 million metric which is mainly used as animal feed and fertilizer. In addition to good gelling and emulsifying properties

(Schwenke et al., 1998; Wu and Muir, 2008b), cruciferin is resistant protein to gastric digestion (Bos et al., 2007) with high denaturation temperature of 91 °C (Wu and Muir, 2008b). Therefore, in this research, the potential of cruciferin to encapsulate model bioactive compounds against a heat treatment and gastric conditions and also to coat and protect chitosan particles at low pH of stomach was investigated. Release of encapsulated compounds in intestinal conditions was also studied. In the first study of this research, canola proteins were extracted using an integrated method. The protein content and yield were respectively 91 and 38.6% for cruciferin isolate, and 82 and 12.5% for napin product. Afterward, negatively-charged cruciferin/calcium (Cru/Ca) and positively-charged cruciferin/Cs (Cru/Cs) particles were prepared. The particles were spherical in shape with average size of 160-200 nm. Water-soluble and -insoluble model compounds were successfully encapsulated in the particles, and their thermal stability was significantly increased compared to un-encapsulated form. However, the resistance of the particles in GI tract was different; while Cru/Ca particles were resistant in simulated gastric fluid and released 70-90% of encapsulated in simulated intestinal fluids, Cru/Cs particles were resistant in both gastric and intestinal fluids and released less than 20% of the compounds. The difference in the stability of the particles could provide different applications for the particles. Cru/Ca particles could be an appropriate delivery system for encapsulation of sensitive compounds to low pH and/or enzymes in stomach. The bioactive compounds are released in small intestine to be absorbed or for treatment of intestinal diseases. However, Cru/Cs particles which can protect bioactive compounds against pH and enzymatic degradation in both stomach and intestine, are suitable for encapsulation of sensitive compounds to digestion in GI tract such as protein-based bioactive compounds. Cru/Cs particles might also help the absorption of fat-soluble compounds in the patients who have problem in digestion and absorption of the compound due to lack of bile salts. In addition, Cru/Cs particles could be a promising colon targeting delivery system for encapsulation and delivery of probiotics, protein-based anti-inflammatory and anti-cancer drugs to lower GI tract. Since the surface of Cru/Ca and Cru/Cs particles is composed of cruciferin, both particles are resistant in gastric conditions; however, their release behavior in intestinal fluid depends on the type of material in the interior parts of particles. For instance, the release rate of encapsulated compounds from chitosan cores with different molecular weights and degree of deacetylation might be different. Furthermore, the cruciferin coating of Cru/Ca and Cru/Cs particles is a single-layer coating, but multi-layer coating systems containing cruciferin as one of the layers can also be developed. In

comparison, a multi-layer coating has some advantages such as higher loading capacity, controlled release of encapsulated compounds, and improved mechanical stability compared to single-layer systems. In addition, desirable coating systems can be achieved by tailoring the composition and thickness of the multilayer coating (Keeney et al., 2015; Shchukina and Shchukin, 2012).

The effect of the presence of mucus on cellular uptake and transport of the particles across epithelial cells were investigated using Caco-2 and Caco-2/HT29 co-culture. To closely mimic GI tract condition, the particles were digested in simulated GI fluids and their cellular uptake and transport were compared with those of undigested forms. Our results showed that the cellular uptake and transport of the cruciferin-based particles in Caco-2/HT29 co-culture, in the presence of mucus, had no significant difference compared to those in Caco-2 cells. These results revealed that the presence of mucus had negligible influence on the particles uptake, implying that the particles might have mucus-penetrating property. The traverse of the particles across mucus layers could improve the absorption of bioactive compounds. The penetrated particles might be uptaken by epithelial cells and/or sustainably release the compounds in adherent mucus layer, the layer which is slowly cleared. Since the mucus-penetrating property is lost after digestion of the particles in GI tract, these particles might be appropriate carriers for drug delivery in non-digestive mucosal tissues.

Unlike undigested Cru/Cs particles which were not affected by mucus layers, the digested particles showed mucoadhesion property. The adhesion of digested Cru/Cs particles to mucus layers might be due to the exposure of chitosan core which is a well-known mucoadhesive polymer. Therefore, Cru/Cs particles after digestion in GI tract have ability to overcome short intestinal transit time and prolong residence time which results in release improvement. The mucoadhesion property is beneficial for release of compounds in both small and large intestine.

In the second part of this thesis, the chaperone-like activity of napin, the second major canola protein, was investigated. Chaperones, a diverse group of proteins, regulate folding of partially unfolded or intrinsically disordered proteins and as a result, inhibit protein misfolding, aggregation and fibrillation in the cells (Hartl et al., 2011; Ellis, 2006). The formation of amyloid fibrils is also recognized as a major contributing factor in amyloid-related diseases such as Alzheimer's and Huntington's (Hartl et al., 2011). Although protein aggregation/fibrillation result in new structures with different applications such as drug delivery and film formation, the aggregates/fibrils may lead to undesirable appearance and flow behaviour in high protein products (Nicolai and Durand,

2013). Ingested pre-formed aggregates might also act as fibrillization seeds to trigger extensive aggregation in the body (Chiti and Dobson, 2006).

Napin limited fibril formation of ovotransferrin (OT). Three key properties might be the reasons of napin chaperone-like activity: resistance to thermal denaturation, high positive charge, and presence of surface hydrophobic groups. The presence of positive charges and surface hydrophobic groups could provide napin an amphiphilic nature which is important for chaperone-like molecules (Koudelka et al., 2009). The chaperone-like activity of napin might be due to formation hydrophobic and electrostatic interactions between napin and OT fibril cores. Through these interactions, napin redirected OT fibrillation into off-pathways intermediates leading to amorphous aggregation and as result, fibril formation was decreased.

Based on the results, both thesis hypothese, encapsulating property of cruciferin and chaperone-like activity of napin, were accepte. Therefore, development of cruciferin-based delivery systems and also further investigation on chaperone-like activity of napin could be starting points to produce more value-added products from canola protein which is highly required for development of Canadian canola industry.

8.2. Recommendations for future studies:

To validate the results of *in vitro* cellular uptake and trans-cellular transport, further *in vivo* studies are needed. The labelled particles can be orally administrated to appropriate animal model, and then after sacrificing the animals, the intestinal uptake of the particles will be studied. The fate of the particles in the *in vivo* model can be investigated and quantified after collection of different tissues of the sacrificed animals.

An appropriate drug (insulin) can also be encapsulated in the particles and after oral administration to appropriate animal model, the concentration of insulin and glucose in the serum be determined and compared with intravenous and orally administration of un-encapsulated insulin. After *in vivo* validation of the delivery systems, the technology might be scaled up to industrial applications. Considering the abundant and inexpensive starting material, and also their simple preparation methods, the delivery systems could be commercialized.

Cru/Cs particles might be also a proper delivery system for targeting colon. Cru/Cs particles can protect probiotics and bioactive compounds in stomach and intestine and deliver them to colon. These bioactive compounds could be protein-based anti-inflammatory or anti-cancer drugs.

Napin redirected fibrillation into off-pathways intermediates leading less-toxic amorphous aggregates. To study the chaperone-like activity of napin on decrease of neurotoxicity, MTT assay can be performed. Chemical modifications such as alkylation and acylation of napin could improve chaperone-like activity of napin by adding more hydrophobic groups.

REFERENCES

Aachary, A. A. & Thiyam, U. (2012). A pursuit of the functional nutritional and bioactive properties of canola proteins and peptides. *Critical Reviews in Food Science and Nutrition*, 52(11), 965-979.

Aguilera, J. M. (1995). Gelation of whey proteins. *Food Technology*, 49(10), 83-89.

Aider, M. & Barbana, C. (2011). Canola proteins: Composition, extraction, functional properties, bioactivity, applications as a food ingredient and allergenicity - A practical and critical review. *Trends in Food Science & Technology*, 22(1), 21-39.

Akbari, A. & Wu, J. (2016). Cruciferin nanoparticles: Preparation, characterization and their potential application in delivery of bioactive compounds. *Food Hydrocolloids,* 54, 107-118.

Akbari, A. & Wu, J. (2015). An integrated method of isolating napin and cruciferin from defatted canola meal. *LWT-Food Science and Technology,* 64, 308-315.

Alizadeh-Pasdar, N. & Li-Chan, E. C. Y. (2000). Comparison of protein surface hydrophobicity measured at various pH values using three different fluorescent probes. *Journal of Agricultural and Food Chemistry,* 48(2), 328-334.

Almutawah, A., Barker, S. A., & Belton, P. S. (2007). Hydration of gluten: A dielectric, calorimetric, and fourier transform infrared study. *Biomacromolecules,* 8(5), 1601-1606.

Aluko, R. & McIntosh, T. (2005). Limited enzymatic proteolysis increases the level of incorporation of capola proteins into mayonnaise. *Innovative Food Science & Emerging Technologies*, 6(2), 195-202.

Aluko, R. & McIntosh, T. (2001). Polypeptide profile and functional properties of defatted meals and protein isolates of canola seeds. *Journal of the Science of Food and Agriculture*, 81(4), 391-396.

Antunes, F., Andrade, F., Araujo, F., Ferreira, D., & Sarmento, B. (2013). Establishment of a triple co-culture *in vitro* cell models to study intestinal absorption of peptide drugs. *European Journal of Pharmaceutics and Biopharmaceutics,* 83(3), 427-435.

AOAC. (2000). Official Methods of Analysis. (17th ed). Washington, DC: Association of Official Analytical Chemists.

Araujo, F., Shrestha, N., Shahbazi, M., Fonte, P., Makila, E. M., Salonen, J. J., Hirvonen, J. T., Granja, P. L., Santos, H. A., & Sarmento, B. (2014). The impact of nanoparticles on the mucosal translocation and transport of GLP-1 across the intestinal epithelium. *Biomaterials,* 35(33), 9199-9207.

Arntfield, S. D. & Cai, R. (1998). Protein polysaccharide interactions during network formation: Observations involving canola protein. *Paradigm for Successful Utilization of Renewable Resources*, 108-122.

Artemova, N. V., Bumagina, Z. M., Kasakov, A. S., Shubin, V. V., & Gurvits, B. Y. (2010). Opioid peptides derived from food proteins suppress aggregation and promote reactivation of partly unfolded stressed proteins. *Peptides, 31*(2), 332-338.

Awaad, A., Nakamura, M., & Ishimura, K. (2012). Imaging of size-dependent uptake and identification of novel pathways in mouse Peyer's patches using fluorescent organosilica particles. *Nanomedicine-Nanotechnology Biology and Medicine,* 8(5), 627-636.

Badley, R. A., Atkinson, D., Hauser, H., Oldani, D., Green, J. P., & Stubbs, J. M. (1975). Structure, physical and chemical properties of soy bean protein glycinin. *Biochimica Et Biophysica Acta*, 412(2), 214-228.

Balogh, L., Nigavekar, S. S., Nair, B. M., Lesniak, W., Zhang, C., Sung, L. Y., Kariapper, M. S. T., El-Jawahri, A., Llanes, M., Bolton, B., Mamou, F., Tan, W., Hutson, A., Minc, L., & Khan, M. K. (2007). Significant effect of size on the *in vivo* biodistribution of gold composite nanodevices in mouse tumor models. *Nanomedicine-Nanotechnology Biology and Medicine,* 3(4), 281-296.

Bandara, N., Chen, L., & Wu, J. (2011). Protein extraction from triticale distillers grains. *Cereal Chemistry*, 88(6), 553-559.

Barbut, S. & Foegeding, E. A. (1993). Ca^{2+}-Induced gelation of pre-heated whey-protein isolate. *Journal of Food Science*, 58(4), 867-871.

Barciszewski, J., Szymanski, M., & Haertle, T. (2000). Minireview: Analysis of rape seed napin structure and potential roles of the storage protein. *Journal of Protein Chemistry*, 19(4), 249-254.

Bartlett, A. I. & Radford, S. E. (2009). An expanding arsenal of experimental methods yields an explosion of insights into protein folding mechanisms. *Nature Structural & Molecular Biology*, 16(6), 582-588.

Bell, J. M. (1993). Factors affecting the nutritional-value of canola-meal - A review. *Canadian Journal of Animal Science*, 73(4), 679-697.

Bernkop-Schnuerch, A. (2013). Nanocarrier systems for oral drug delivery: Do we really need them? *European Journal of Pharmaceutical Sciences*, 49(2), 272-277.

Berot, S., Compoint, J., Larre, C., Malabat, C., & Gueguen, J. (2005). Large scale purification of rapeseed proteins (*Brassica Napus L.*). *Journal of Chromatography B-Analytical Technologies in the Biomedical and Life Sciences,* 818(1), 35-42.

Bertenshaw, E. J., Lluch, A., & Yeomans, M. R. (2008). Satiating effects of protein but not carbohydrate consumed in a between-meal beverage context. *Physiology & Behavior, 93*(3), 427-436.

Bier, J. M., Verbeek, C. J. R., & Lay, M. C. (2014). Thermal transitions and structural relaxations in protein-based thermoplastics. *Macromolecular Materials and Engineering,* 299(5), 524-539.

Blaicher, F., Elstner, F., Stein, W., & Mukherjee, K. (1983). Rapeseed protein isolates - effect of processing on yield and composition of protein. *Journal of Agricultural and Food Chemistry,* 31(2), 358-362.

Boegh, M. & Nielsen, H. M. (2015). Mucus as a barrier to drug delivery - understanding and mimicking the barrier properties. *Basic & Clinical Pharmacology & Toxicology*, 116(3), 179-186.

Boeris, V., Micheletto, Y., Lionzo, M., da Silveira, N. P., & Pico, G. (2011). Interaction behavior between chitosan and pepsin. *Carbohydrate Polymers,* 84(1), 459-464.

Boon, C. S., McClements, D. J., Weiss, J., & Decker, E. A. (2010). Factors influencing the chemical stability of carotenoids in foods. *Critical Reviews in Food Science and Nutrition*, 50(6), 515-532.

Borana, M. S., Mishra, P., Pissurlenkar, R. R. S., Hosur, R. V., & Ahmad, B. (2014). Curcumin and kaempferol prevent lysozyme fibril formation by modulating aggregation kinetic parameters. *Biochimica Et Biophysica Acta-Proteins and Proteomics,* 1844(3), 670-680.

Bos, C., Airinei, G., Mariotti, F., Benamouzig, R., Berot, S., Evrard, J., Fenart, E., Tome, D., & Gaudichon, C. (2007). The poor digestibility of rapeseed protein is balanced by its very high metabolic utilization in humans. *Journal of Nutrition,* 137(3), 594-600.

Bouwmeester, H., Dekkers, S., Noordam, M. Y., Hagens, W. I., Bulder, A. S., de Heer, C., ten Voorde, S. E. C. G., Wijnhoven, S. W. P., Marvin, H. J. P., & Sips, A. J. A. M. (2009). Review of health safety aspects of nanotechnologies in food production. *Regulatory Toxicology and Pharmacology,* 53(1), 52-62.

Bryant, C. M. & McClements, D. J. (2000). Influence of NaCl and $CaCl_2$ on cold-set gelation of heat-denatured whey protein. *Journal of Food Science*, 65(5), 801-804.

Bukau, B., Weissman, J., & Horwich, A. (2006). Molecular chaperones and protein quality control. *Cell*, 125(3), 443-451.

Bulheller, B. M., Rodger, A., & Hirst, J. D. (2007). Circular and linear dichroism of proteins. *Physical Chemistry Chemical Physics,* 9(17), 2020-2035.

Canola Council of Canada. (2007). Canola, growing great 2015. URL:

http://www.canolacouncil.org/media/502091/growing_great_pdf.pdf. Accessed December 12, 2013.

Capitani, C., Perez, O. E., Pacheco, B., Teresa, M., & Pilosof, A. M. R. (2007). Influence of complexing carboxymethylcellulose on the thermostability and gelation of alpha-lactalbumin and beta-lacto globulin. *Food Hydrocolloids,* 21(8), 1344-1354.

Carpenter, J., Katayama, D., Liu, L., Chonkaew, W., & Menard, K. (2009). Measurement of Tg in lyophilized protein and protein excipient mixtures by dynamic mechanical analysis. *Journal of Thermal Analysis and Calorimetry,* 95(3), 881-884.

Carver, J. A., Rekas, A., Thorn, D. C., & Wilson, M. R. (2003). Small heat-shock proteins and clusterin: Intra- and extracellular molecular chaperones with a common mechanism of action and function? *IUBMB Life*, 55(12), 661-668.

Cavallieri, A. L. F. & Da Cunha, R. L. (2008). The effects of acidification rate, pH and ageing time on the acidic cold set gelation of whey proteins. *Food Hydrocolloids*, 22(3), 439-448.

Chabanon, G., Chevalot, I., Framboisier, X. Chenu, S., & Marc, I. (2007). Hydrolysis of rapeseed protein isolates: Kinetics, characterization and functional properties of hydrolysates. *Process Biochemistry,* 42, 1419-1428.

Chang, M., Tsai, T., Lee, C., Wei, Y., Chen, Y., Chen, C., & Tzen, J. T. C. (2013). Elevating bioavailability of curcumin via encapsulation with a novel formulation of artificial oil bodies. *Journal of Agricultural and Food Chemistry,* 61(40), 9666-9671.

Chen, X., Elisia, I., & Kitts, D. D. (2010). Defining conditions for the co-culture of Caco-2 and HT29-MTX cells using Taguchi design. *Journal of Pharmacological and Toxicological Methods,* 61(3), 334-342.

Chen, L. Y., Remondetto, G. E., & Subirade, M. (2006). Food protein-based materials as nutraceutical delivery systems. *Trends in Food Science & Technology*, 17(5), 272-283.

Chen, L. & Subirade, M. (2005). Chitosan/beta-lactoglobulin core-shell nanoparticles as nutraceutical carriers. *Biomaterials*, 26(30), 6041-6053.

Chithrani, B. D., Ghazani, A. A., & Chan, W. C. W. (2006). Determining the size and shape dependence of gold nanoparticle uptake into mammalian cells. *Nano Letters,* 6(4), 662-668.

Chiti, F. & Dobson, C. M. (2006). Protein misfolding, functional amyloid, and human disease. *Annual Review of Biochemistry,* 75, 333-366.

Chourasia, M. K. & Jain, S. K. (2003). Pharmaceutical approaches to colon targeted drug delivery systems. *Journal of Pharmacy and Pharmaceutical Sciences,* 6(1), 33-66.

Chu, B., Ichikawa, S., Kanafusa, S., & Nakajima, M. (2007). Preparation and characterization of beta-carotene nanodispersions prepared by solvent displacement technique. *Journal of Agricultural and Food Chemistry,* 55(16), 6754-6760.

Chuah, A. M., Kuroiwa, T., Ichikawa, S., Kobayashi, I., & Nakajima, M. (2009). Formation of biocompatible nanoparticles via the self-assembly of chitosan and modified lecithin. *Journal of Food Science*, 74(1), N1-N8.

Cone, R. A. (2009). Barrier properties of mucus. *Advanced Drug Delivery Reviews*, 61(2), 75-85.

Cookman, D. J. & Glatz, C. E. (2009). Extraction of protein from distiller's grain. *Bioresource Technology*, 100, 2012-2017.

Coronel-Aguilera, C. P. & Martin-Gonzalez, M. F. S. (2015). Encapsulation of spray dried beta-carotene emulsion by fluidized bed coating technology. *Lwt-Food Science and Technology,* 62(1), 187-193.

Courraud, J., Berger, J., Cristol, J.P., & Avallone, S. (2013). Stability and bioaccessibility of different forms of carotenoids and vitamin A during *in vitro* digestion. *Food Chemistry,* 136, 871-877.

Cumby, N., Zhong, Y., Naczk, M., & Shahidi, F. (2008). Antioxidant activity and water-holding capacity of canola protein hydrolysates. *Food Chemistry*, 109(1), 144-148.

Deak, N. A., Murphy, P. A., & Johnson, L. A. (2006). Effects of NaCl concentration on salting-in and dilution during salting-out on soy protein fractionation. *Journal of Food Science,* 71(4), C247-C254.

Deat-Laine, E., Hoffart, V., Garrait, G., & Beyssac, E. (2013). Whey protein and alginate hydrogel microparticles for insulin intestinal absorption: Evaluation of permeability enhancement properties on Caco-2 cells. *International Journal of Pharmaceutics,* 453(2), 336-342.

de Kruif, C. G. & Tuinier, R. (2001). Polysaccharide protein interactions. *Food Hydrocolloids*, 15(4-6), 555-563.

de Paz, E., Martin, A., Estrella, A., Rodriguez-Rojo, S., Matias, A. A., Duarte, C. M. M., & Jose Cocero, M. (2012). Formulation of beta-carotene by precipitation from pressurized ethyl acetate-on-water emulsions for application as natural colorant. *Food Hydrocolloids,* 26(1), 17-27.

del Pozo-Rodriguez, A., Pujals, S., Delgado, D., Solinis, M. A., Gascon, A. R., Giralt, E., & Pedraz, J. L. (2009). A proline-rich peptide improves cell transfection of solid lipid nanoparticle-based non-viral vectors. *Journal of Controlled Release,* 133(1), 52-59.

Derbyshire, E., Wright, D. J., & Boulter, D. (1976). Legumin and vicilin, storage proteins of legume seeds. *Phytochemistry*, 15(1), 3-24.

des Rieux, A., Fievez, V., Garinot, M., Schneider, Y., & Preat, V. (2006). Nanoparticles as potential oral delivery systems of proteins and vaccines: A mechanistic approach. *Journal of Controlled Release*, 116(1), 1-27.

Doherty, S. B., Gee, V. L., Ross, R. P., Stanton, C., Fitzgerald, G. F., & Brodkorb, A. (2011). Development and characterisation of whey protein micro-beads as potential matrices for probiotic protection. *Food Hydrocolloids*, 25(6), 1604-1617.

Donhowe, E. G., Flores, F. P., Kerr, W. L., Wicker, L., & Kong, F. (2014). Characterization and *in vitro* bioavailability of beta-carotene: Effects of microencapsulation method and food matrix. *LWT-Food Science and Technology,* 57(1), 42-48.

Dudhani, A. R. & Kosaraju, S. L. (2010). Bioadhesive chitosan nanoparticles: Preparation and characterization. *Carbohydrate Polymers,* 81(2), 243-251.

Duval, S., Chung, C., & McClements, D. J. (2015). Protein-polysaccharide hydrogel particles formed by biopolymer phase separation. *Food Biophysics*, 10(3), 334-341.

Duy, C. & Fitter, J. (2006). How aggregation and conformational scrambling of unfolded states govern fluorescence emission spectra. *Biophysical Journal,* 90(10), 3704-3711.

Ecroyd, H. & Carver, J. A. (2009). Crystallin proteins and amyloid fibrils. *Cellular and Molecular Life Sciences*, 66(1), 62-81.

Ehrnhoefer, D. E., Bieschke, J., Boeddrich, A., Herbst, M., Masino, L., Lurz, R., Engemann, S., Pastore, A., & Wanker, E. E. (2008). EGCG redirects amyloidogenic polypeptides into unstructured, off-pathway oligomers. *Nature Structural & Molecular Biology,* 15(6), 558-566.

Ellis, R. J. (2006). Molecular chaperones: Assisting assembly in addition to folding. *Trends in Biochemical Sciences*, 31(7), 395-401.

Elzoghby, A. O., El-Fotoh, W. S. A., & Elgindy, N. A. (2011). Casein-based formulations as promising controlled release drug delivery systems. *Journal of Controlled Release*, 153(3), 206-216.

Elzoghby, A. O., Samy, W. M., & Elgindy, N. A. (2012a). Albumin-based nanoparticles as potential controlled release drug delivery systems. *Journal of Controlled Release*, 157(2), 168-182.

Elzoghby, A. O., Samy, W. M., & Elgindy, N. A. (2012b). Protein-based nanocarriers as promising drug and gene delivery systems. *Journal of Controlled Release*, 161(1), 38-49.

Ensign, L. M., Cone, R., & Hanes, J. (2012). Oral drug delivery with polymeric nanoparticles: The gastrointestinal mucus barriers. *Advanced Drug Delivery Reviews*, 64(6), 557-570.

Ezpeleta, I., Irache, J. M., Stainmesse, S., Chabenat, C., Gueguen, J., Popineau, Y., & Orecchioni, A. M. (1996). Gliadin nanoparticles for the controlled release of all-trans-retinoic acid. *International Journal of Pharmaceutics*, 131(2), 191-200.

Foged, C., Brodin, B., Frokjaer, S., & Sundblad, A. (2005). Particle size and surface charge affect particle uptake by human dendritic cells in an *in vitro* model. *International Journal of Pharmaceutics,* 298(2), 315-322.

Folawiyo, Y. L. & Apenten, R. K. O. (1997). The effect of heat- and acid-treatment on the structure of rapeseed albumin (napin). *Food Chemistry 58*(3), 237-243.

Foley, J., Hill, S. E., Miti, T., Mulaj, M., Ciesla, M., Robeel, R., Persichilli, C., Raynes, R., Westerheide, S., & Muschol, M. (2013). Structural fingerprints and their evolution during oligomeric vs. oligomer-free amyloid fibril growth. *Journal of Chemical Physics,* 139(12), 121901.

Galindo-Rodriguez, S., Allemann, E., Fessi, H., & Doelker, E. (2005). Polymeric nanoparticles for oral delivery of drugs and vaccines: A critical evaluation of *in vivo* studies. *Critical Reviews in Therapeutic Drug Carrier Systems*, 22(5), 419-463.

Gao, J. Y., Dubin, P. L., & Muhoberac, B. B. (1997). Measurement of the binding of proteins to polyelectrolytes by frontal analysis continuous capillary electrophoresis. *Analytical Chemistry*, 69(15), 2945-2951.

Garti, N. & Aserin, A. (2012). Micelles and microemulsions as food ingredient and nutraceutical delivery systems. *Encapsulation Technologies and Delivery Systems for Food Ingredients and Nutraceuticals*, (239), 211-251.

Gaumet, M., Gurny, R., & Delie, F. (2009). Localization and quantification of biodegradable particles in an intestinal cell model: The influence of particle size. *European Journal of Pharmaceutical Sciences,* 36(4-5), 465-473.

Ghadami, S. A., Khodarahmi, R., Ghobadi, S., Ghasemi, M., & Pirmoradi, S. (2011). Amyloid fibril formation by native and modified bovine β-lactoglobulins proceeds through unfolded form of proteins: A comparative study. *Biophysical Chemistry*, 159(2-3), 311-320.

Ghodsvali, A., Khodaparast, M. H. H., Vosoughi, M., & Diosady, L. L. (2005). Preparation of canola protein materials using membrane technology and evaluation of meals functional properties. *Food Research International*, 38(2), 223-231.

Gilbert, V., Rouabhia, M., Wang, H. X., Arnould, A. L., Remondetto, G., & Subirade, M. (2005). Characterization and evaluation of whey protein-based biofilms as substrates for *in vitro* cell cultures. *Biomaterials,* 26(35), 7471-7480.

Gillberg, L. & Tornell, B. (1976). Preparation of rapeseed protein isolates - dissolution and precipitation behavior of rapeseed proteins. *Journal of Food Science*, 41(5), 1063-1069.

Gorinstein, S., Goshev, I., Moncheva, S., Zemser, M., Weisz, M., Caspi, A., Libman, I., Lerner, H. T., Trakhtenberg, S., & Martin-Belloso, O. (2000). Intrinsic tryptophan fluorescence of human serum proteins and related conformational changes. *Journal of Protein Chemistry,* 19(8), 637-642.

Gosal, W. S., Morten, I. J., Hewitt, E. W., Smith, D. A., Thomson, N. H., & Radford, S. E. (2005). Competing pathways determine fibril morphology in the self-assembly of beta(2)-microglobulin into amyloid. *Journal of Molecular Biology,* 351(4), 850-864.

Gruener, L. & Ismond, M. (1997). Effects of acetylation and succinylation on the functional properties of the canola 12S globulin. *Food Chemistry*, 60(4), 513-520.

Han, Y., Alsayed, A. M., Nobili, M., Zhang, J., Lubensky, T. C., & Yodh, A. G. (2006). Brownian motion of an ellipsoid. *Science,* 314(5799), 626-630.

Han, S., Wan, H., Lin, D., Guo, S., Dong, H., Zhang, J., Deng, L., Liu, R., Tang, H., & Dong, A. (2014). Contribution of hydrophobic/hydrophilic modification on cationic chains of poly(epsilon-caprolactone)-graft-poly(dimethylamino ethylmethacrylate) amphiphilic co-polymer in gene delivery. *Acta Biomaterialia,* 10(2), 670-679.

Harde, H., Das, M., & Jain, S. (2011). Solid lipid nanoparticles: An oral bioavailability enhancer vehicle. *Expert Opinion on Drug Delivery*, 8(11), 1407-1424.

Hartl, F. U., Bracher, A., & Hayer-Hartl, M. (2011). Molecular chaperones in protein folding and proteostasis. *Nature*, 475(7356), 324-332.

Hattori, T., Hallberg, R., & Dubin, P. L. (2000). Roles of electrostatic interaction and polymer structure in the binding of beta-lactoglobulin to anionic polyelectrolytes: Measurement of binding constants by frontal analysis continuous capillary electrophoresis. *Langmuir*, 16(25), 9738-9743.

Haug, W. & Lantzsch, H. (1983). Sensitive method for the rapid-determination of phytate in cereals and cereal products. *Journal of the Science of Food and Agriculture,* 34(12), 1423-1426.

He, R., He, H., Chao, D., Ju, X., & Aluko, R. (2014). Effects of high pressure and heat treatments on physicochemical and gelation properties of rapeseed protein isolate. *Food and Bioprocess Technology,* 7(5), 1344-1353.

He, C., Hu, Y., Yin, L., Tang, C., & Yin, C. (2010). Effects of particle size and surface charge on cellular uptake and biodistribution of polymeric nanoparticles. *Biomaterials,* 31(13), 3657-3666.

He, B., Lin, P., Jia, Z., Du, W., Qu, W., Yuan, L., Dai, W., Zhang, H., Wang, X., Wang, J., Zhang, X., & Zhang, Q. (2013). The transport mechanisms of polymer nanoparticles in Caco-2 epithelial cells. *Biomaterials,* 34(25), 6082-6098.

He, C., Yin, L., Tang, C., & Yin, C. (2012). Size-dependent absorption mechanism of polymeric nanoparticles for oral delivery of protein drugs. *Biomaterials,* 33(33), 8569-8578.

He, J., Zhu, S., Mu, T., Yu, Y., Li, J., & Azuma, N. (2011). Alpha(s)-Casein Inhibits the Pressure-Induced Aggregation of beta-lactoglobulin through its molecular chaperone-like properties. *Food Hydrocolloids*, 25(6), 1581-1586.

Heger, M., van Golen, R. F., Broekgaarden, M., & Michel, M. C. (2014). The molecular basis for the harmacokinetics and pharmacodynamics of curcumin and its metabolites in relation to cancers. *Pharmacological Reviews*, 66(1), 222-307.

Hillaireau, H. & Couvreur, P. (2009). Nanocarriers' entry into the cell: Relevance to drug delivery. *Cellular and Molecular Life Sciences,* 66(17), 2873-2896.

Hu, B. & Huang, Q. (2013). Biopolymer based nano-delivery systems for enhancing bioavailability of nutraceuticals. *Chinese Journal of Polymer Science,* 31(9), 1190-1203.

Huang, A. H. C. (1992). Oil Bodies and Oleosins in Seeds. *Briggs, W.R.(Ed.).Annual Review of Plant Physiology and Plant Molecular Biology, Vol.43, 685p. Annual Reviews Inc.: Palo Alto, California, Usa.Illus,* 177-200.

Huang, G., Sun, Y., Xiao, J., & Yang, J. (2012). Complex coacervation of soybean protein isolate and chitosan. *Food Chemistry,* 135(2), 534-539.

Hudson, S. A., Ecroyd, H., Dehle, F. C., Musgrave, I. F., & Carver, J. A. (2009). (-)-Epigallocatechin-3-gallate (EGCG) maintains kappa-casein in its pre-fibrillar state without redirecting its aggregation pathway. *Journal of Molecular Biology,* 392(3), 689-700.

Ichikawa, S., Iwamoto, S., & Watanabe, J. (2005). Formation of biocompatible nanoparticles by self-assembly of enzymatic hydrolysates of chitosan and carboxymethyl cellulose. *Bioscience Biotechnology and Biochemistry*, 69(9), 1637-1642.

Ismond, M. A. H. & Welsh, W. D. (1992). Application of new methodology to canola protein-isolation. *Food Chemistry*, 45(2), 125-127.

Jiang, J., Chen, J., & Xiong, Y. L. (2009). Structural and emulsifying properties of soy protein isolate subjected to acid and alkaline pH-shifting Processes. *Journal of Agricultural and Food Chemistry,* 57(16), 7576-7583.

Jin, Y., Song, Y., Zhu, X., Zhou, D., Chen, C., Zhang, Z., & Huang, Y. (2012). Goblet cell-targeting nanoparticles for oral insulin delivery and the influence of mucus on insulin transport. *Biomaterials,* 33(5), 1573-1582.

Jones, O., Decker, E. A., & McClements, D. J. (2010). Thermal analysis of beta-lactoglobulin complexes with pectins or carrageenan for production of stable biopolymer particles. *Food Hydrocolloids*, 24(2-3), 239-248.

Jones, O. G., Decker, E. A., & McClements, D. J. (2009). Formation of biopolymer particles by thermal treatment of beta-lactoglobulin-pectin complexes. *Food Hydrocolloids*, 23(5), 1312-1321.

Jones, O. G. & McClements, D. J. (2011). Recent progress in biopolymer nanoparticle and microparticle formation by heat-treating electrostatic protein-polysaccharide complexes. *Advances in Colloid and Interface Science*, 167(1-2), 49-62.

Jones, O. G. & McClements, D. J. (2010). Functional biopolymer particles: Design, fabrication, and applications. *Comprehensive Reviews in Food Science and Food Safety*, 9(4), 374-397.

Joye, I. J., Davidov-Pardo, G., & McClements, D. J. (2014). Nanotechnology for increased micronutrient bioavailability. *Trends in Food Science & Technology*, 40(2), 168-182.

Jyothi, T. C., Singh, S. A., & Appu Rao, A. G. (2007). Conformation of napin (*Brassica juncea*) in salts and monohydric alcohols: Contribution of electrostatic and hydrophobic interactions. *Journal of Agricultural and Food Chemistry,* 55(10), 4229-4236.

Kamath, K. R. & Park, K. (1993). Biodegradable hydrogels in drug-delivery. *Advanced Drug Delivery Reviews*, 11(1-2), 59-84.

Karaca, A. C., Low, N., & Nickerson, M. (2011). Emulsifying properties of canola and flaxseed protein isolates produced by isoelectric precipitation and salt extraction. *Food Research International*, 44, 2991-2998.

Karlsson, J., Ungell, A. L., Grasjo, J., & Artursson, P. (1999). Paracellular drug transport across intestinal epithelia: Influence of charge and induced water flux. *European Journal of Pharmaceutical Sciences,* 9(1), 47-56.

Keeney, M., Jiang, X. Y., Yamane, M., Lee, M., Goodman, S., & Yang, F. (2015). Nanocoating for biomolecule delivery using layer-by-layer self-assembly. *Journal of Materials Chemistry B,* 3, 8757-8770.

Kehoe, J. J. & Foegeding, E. A. (2014). The characteristics of heat-induced aggregates formed by mixtures of β-lactoglobulin and β -casein. *Food Hydrocolloids,* 39, 264-271.

Khodarahmi, R., Soori, H., & Karimi, S. A. (2009). Chaperone-like activity of heme group against amyloid-like fibril formation by hen egg ovalbumin: Possible mechanism of action. *International Journal of Biological Macromolecules*, 44(1), 98-106.

Klockeman, D. M., Toledo, R., & Sims, K. A. (1997). Isolation and characterization of defatted canola meal protein. *Journal of Agricultural and Food Chemistry*, 45(10), 3867-3870.

Kong, F. & Singh, R. P. (2010). A human gastric simulator (HGS) to study food digestion in human stomach. *Journal of Food Science*, 75(9), E627-E635.

Kong, J. & Yu, S. (2007). Fourier transform infrared spectroscopic analysis of protein secondary structures. *Acta Biochimica Et Biophysica Sinica,* 39(8), 549-559.

Koudelka, T., Hoffmann, P., & Carver, J. A. (2009). Dephosphorylation of alpha(s)- and beta-caseins and its effect on chaperone activity: A structural and functional investigation. *Journal of Agricultural and Food Chemistry*, 57(13), 5956-5964.

Kulmyrzaev, A., Cancelliere, C., & McClements, D. J. (2000). Influence of sucrose on cold gelation of heat-denatured whey protein isolate. *Journal of the Science of Food and Agriculture*, 80(9), 1314-1318.

Kundu, S., Chinchalikar, A. J., Das, K., Aswal, V. K., & Kohlbrecher, J. (2013). Fe^{+3} ion induced protein gelation: Small-angle neutron scattering study. *Chemical Physics Letters,* 584, 172-176.

Kurita, K. (2006). Chitin and chitosan: Functional biopolymers from marine crustaceans. *Marine Biotechnology*, 8(3), 203-226.

Lacki, K. & Duvnjak, Z. (1998). Decrease of phenolic content in canola meal using a polyphenol oxidase preparation from *Trametes versicolor*: Effect of meal saccharification. *Biotechnology Techniques*, 12(1), 31-34.

Lai, S.K., O'Hanlon, D.E., Harrold, S., Man, S.T. Wang, Y.Y., Cone, R., & Hanes, J. (2007) Rapid transport of large polymeric nanoparticles in fresh undiluted human mucus, *Proceedings of the National Academy of Sciences U. S. A.* 104, 1482–1487.

Lai, S. K., Wang, Y., & Hanes, J. (2009a). Mucus-penetrating nanoparticles for drug and gene delivery to mucosal tissues. *Advanced Drug Delivery Reviews*, 61(2), 158-171.

Lai, S. K., Wang, Y., Wirtz, D., & Hanes, J. (2009b). Micro- and macrorheology of mucus. *Advanced Drug Delivery Reviews*, 61(2), 86-100.

Lee, P. S., Yim, S. G., Choi, Y., Thi Van Anh Ha, & Ko, S. (2012). Physiochemical properties and prolonged release behaviours of chitosan-denatured beta-lactoglobulin microcapsules for potential food applications. *Food Chemistry*, 134(2), 992-998.

Lefevre, T. & Subirade, M. (2000). Molecular differences in the formation and structure of fine-stranded and particulate beta-lactoglobulin gels. *Biopolymers*, 54(7), 578-586.

Leo, E., Vandelli, M. A., Cameroni, R., & Forni, F. (1997). Doxorubicin-loaded gelatin nanoparticles stabilized by glutaraldehyde: Involvement of the drug in the cross-linking process. *International Journal of Pharmaceutics*, 155(1), 75-82.

Leonard, F., Collnot, E., & Lehr, C. (2010). A Three-dimensional coculture of enterocytes, monocytes and dendritic cells to model inflamed intestinal mucosa *in vitro*. *Molecular Pharmaceutics,* 7(6), 2103-2119.

Li, X., Chen, D., Le, C., Zhu, C., Gan, Y., Hovgaard, L., & Yang, M. (2011). Novel mucus-penetrating liposomes as a potential oral drug delivery system: Preparation, *in vitro* characterization, and enhanced cellular uptake. *International Journal of Nanomedicine,* 6, 3151-3162.

Liao, Y., Chang, Y., Yoshiike, Y., Chang, Y., & Chen, Y. (2012). Negatively charged gold nanoparticles inhibit Alzheimer's amyloid-beta fibrillization, induce fibril dissociation, and mitigate neurotoxicity. *Small,* 8(23), 3631-3639.

Liberek, K., Lewandowska, A., & Zietkiewicz, S. (2008). Chaperones in control of protein disaggregation RID F-5812-2011. *Embo Journal*, 27(2), 328-335.

Librizzi, F., Carrotta, R., Spigolon, D., Bulone, D., & San Biagio, P. L. (2014). α-Casein inhibits insulin amyloid formation by preventing the onset of secondary nucleation processes. *Journal of Physical Chemistry Letters,* 5(17), 3043-3048.

Lim, J. P. & Gleeson, P. A. (2011). Macropinocytosis: An endocytic pathway for internalising large gulps. *Immunology and Cell Biology,* 89(8), 836-843.

Lindner, R. A., Carver, J. A., Ehrnsperger, M., Buchner, J., Esposito, G., Behlke, J., Lutsch, G., Kotlyarov, A., & Gaestel, M. (2000). Mouse Hsp25, a small heat shock protein - The role of its C-terminal extension in oligomerization and chaperone action. *European Journal of Biochemistry*, 267(7), 1923-1932.

Lodhia, J., Mandarano, G., Ferris, N., Eu, P., & Cowell, S. (2010). Development and use of iron oxide nanoparticles (Part 1): Synthesis of iron oxide nanoparticles for MRI. *Biomedical Imaging and Intervention Journal*, 6(2), e12-e12.

Luo, Y., Teng, Z., Wang, T. T. Y., & Wang, Q. (2013). Cellular uptake and transport of zein nanoparticles: Effects of sodium caseinate. *Journal of Agricultural and Food Chemistry,* 61(31), 7621-7629.

Luo, Y., Zhang, B., Whent, M., Yu, L., & Wang, Q. (2011). Preparation and characterization of zein/chitosan complex for encapsulation of alpha-tocopherol, and its *in vitro* controlled release study. *Colloids and Surfaces B-Biointerfaces,* 85(2), 145-152.

Machida, S., Ogawa, S., Shi, X. H., Takaha, T., Fujii, K., & Hayashi, K. (2000). Cycloamylose as an efficient artificial chaperone for protein refolding. *FEBS Letters,* 486(2), 131-135.

MaHam, A., Tang, Z., Wu, H., Wang, J. & Lin, Y. (2009). Protein-based nanomedicine platforms for drug delivery. *Small*, 5(15), 1706-1721.

Makhlof, A., Tozuka, Y., & Takeuchi, H. (2011). Design and evaluation of novel pH-sensitive chitosan nanoparticles for oral insulin delivery. *European Journal of Pharmaceutical Sciences,* 42(5), 445-451.

Maltais, A., Remondetto, G. E., Gonzalez, R., & Subirade, M. (2005). Formation of soy protein isolate cold-set gels: Protein and salt effects. *Journal of Food Science*, 70(1), C67-C73.

Maltais, A., Remondetto, G. E., & Subirade, M. (2008). Mechanisms involved in the formation and structure of soya protein cold-set gels: A molecular and supramolecular investigation. *Food Hydrocolloids*, 22(4), 550-559.

Mao, Z., Zhou, X., & Gao, C. (2013). Influence of structure and properties of colloidal biomaterials on cellular uptake and cell functions. *Biomaterials Science*, 1(9), 896-911.

Marangoni, A. G., Barbut, S., McGauley, S. E., Marcone, M., & Narine, S. S. (2000). On the structure of particulate gels - the case of salt-induced cold gelation of heat-denatured whey protein isolate. *Food Hydrocolloids,* 14(1), 61-74.

Marczak, E., Usui, H., Fujita, H., Yang, Y., Yokoo, M., Lipkowski, A., & Yoshikawa, M. (2003). New antihypertensive peptides isolated from rapeseed. *Peptides*, 24(6), 791-798.

Martins, J. T., Ramos, O. L., Pinheiro, A. C., Bourbon, A. I., Silva, H. D., Rivera, M. C., Cerqueira, M. A., Pastrana, L., Xavier Malcata, F., Gonzalez-Fernandez, A., & Vicente, A. A. (2015). Edible bio-based nanostructures: Delivery, absorption and potential toxicity. *Food Engineering Reviews*, 7(4), 491-513.

Matalanis, A., Jones, O. G., & McClements, D. J. (2011). Structured biopolymer-based delivery systems for encapsulation, protection, and release of lipophilic compounds. *Food Hydrocolloids,* 25(8), 1865-1880.

Matsudomi, N., Kanda, Y., Yoshika, Y., & Moriwaki, H. (2004). Ability of alpha s-casein to suppress the heat aggregation of ovotransferrin. *Journal of Agricultural and Food Chemistry,* 52(15), 4882-4886.

McClements, D. J. (2015). Nanoscale nutrient delivery systems for food applications: Improving bioactive dispersibility, stability, and bioavailability. *Journal of Food Science*, 80(7), N1602-N1611.

McClements, D. J. (2013). Edible lipid nanoparticles: Digestion, absorption, and potential toxicity. *Progress in Lipid Research*, 52(4), 409-423.

McClements, D. J. (2012a). Advances in fabrication of emulsions with enhanced functionality using structural design principles. *Current Opinion in Colloid & Interface Science*, 17(5), 235-245.

McClements, D. J. (2012b). Crystals and crystallization in oil-in-water emulsions: Implications for emulsion-based delivery systems. *Advances in Colloid and Interface Science*, 174, 1-30.

McClements, D. J. & Decker, E. A. (2000). Lipid oxidation in oil-in-water emulsions: Impact of molecular environment on chemical reactions in heterogeneous food systems. *Journal of Food Science*, 65(8), 1270-1282.

McClements, D. J., Decker, E. A., Park, Y., & Weiss, J. (2009). Structural design principles for delivery of bioactive components in nutraceuticals and functional foods. *Critical Reviews in Food Science and Nutrition*, 49(6), 577-606.

McClements, D. J. & Keogh, M. K. (1995). Physical-properties of cold-setting gels formed from heat-denatured whey-protein isolate. *Journal of the Science of Food and Agriculture*, 69(1), 7-14.

McClements, D. J. & Rao, J. (2011). Food-grade nanoemulsions: Formulation, fabrication, properties, performance, biological fate, and potential toxicity. *Critical Reviews in Food Science and Nutrition*, 51(4), 285-330.

McClements, D. J. & Xiao, H. (2014). Excipient foods: Designing food matrices that improve the oral bioavailability of pharmaceuticals and nutraceuticals. *Food & Function*, 5(7), 1320-1333.

McClements, D. J. & Xiao, H. (2012). Potential biological fate of ingested nanoemulsions: Influence of particle characteristics. *Food & Function*, 3(3), 202-220.

Mejia, L. A., Korgaonkar, C. K., Schweizer, M., Chengelis, C., Novilla, M., Ziemer, E., Williamson-Hughes, P. S., Grabiel, R., & Empie, M. (2009). A 13-week dietary toxicity study in rats of a napin-rich canola protein isolate. *Regulatory Toxicology and Pharmacology*, 55(3), 394-402.

Mensi, A., Choiset, Y., Haertle, T., Reboul, E., Borel, P., Guyon, C., de Lamballerie, M., & Chobert, J. (2013). Interlocking of beta-carotene in beta-lactoglobulin aggregates produced under high pressure. *Food Chemistry,* 139(1-4), 253-260.

Mikos, A. G., Mathiowitz, E., Langer, R., & Peppas, N. A. (1991). Interaction of polymer microspheres with mucin gels as a means of characterizing polymer retention on mucus. *Journal of Colloid and Interface Science*, 143(2), 366-373.

Miti, T., Mulaj, M., Schmit, J. D., & Muschol, M. (2015). Stable, metastable, and kinetically trapped amyloid aggregate phases. *Biomacromolecules,* 16(1), 326-335.

Morgan, P., Treweek, T., Lindner, R., Price, W., & Carver, J. (2005). Casein proteins as molecular chaperones. *Journal of Agricultural and Food Chemistry*, 53(7), 2670-2683.

Morshedi, D., Ebrahim-Habibi, A., Moosavi-Movahedi, A. A., & Nemat-Gorgani, M. (2010). Chemical modification of lysine residues in lysozyme may dramatically influence its amyloid fibrillation. *Biochimica Et Biophysica Acta-Proteins and Proteomics*, 1804(4), 714-722.

Murugan, K., Choonara, Y. E., Kumar, P., Bijukumar, D., du Toit, L. C., & Pillay, V. (2015). Parameters and characteristics governing cellular internalization and trans-barrier trafficking of nanostructures. *International Journal of Nanomedicine,* 10, 2191-2206.

Naczk, M., Diosady, L. L., & Rubin, L. J. (1985). Functional-properties of canola meals produced by a 2-phase solvent-extraction system. *Journal of Food Science*, 50(6), 1685-88.

Nagano, T., Akasaka, T., & Nishinari, K. (1995). Study on the heat-induced conformational-changes of beta-conglycinin by FTIR and CD analysis. *Food Hydrocolloids,* 9(2), 83-89.

Nesterenko, A., Alric, I., Silvestre, F., & Durrieu, V. (2013). Vegetable proteins in microencapsulation: A review of recent interventions and their effectiveness. *Industrial Crops and Products*, 42, 469-479.

Newkirk, R. & Classen, H. (1998). *In vitro* hydrolysis of phytate in canola meal with purified and crude sources of phytase. *Animal Feed Science and Technology*, 72(3-4), 315-327.

Niamprem, P., Rujivipat, S., & Tiyaboonchai, W. (2014). Development and characterization of lutein-loaded SNEDDS for enhanced absorption in Caco-2 cells. *Pharmaceutical Development and Technology,* 19(6), 735-742.

Nicolai, T. & Durand, D. (2013). Controlled food protein aggregation for new functionality. *Current Opinion in Colloid & Interface Science*, 18(4), 249-256.

Nielsen, L., Khurana, R., Coats, A., Frokjaer, S., Brange, J., Vyas, S., Uversky, V. N., & Fink, A. L. (2001). Effect of environmental factors on the kinetics of insulin fibril formation: Elucidation of the molecular mechanism. *Biochemistry,* 40(20), 6036-6046.

Oboroceanu, D., Wang, L., Brodkorb, A., Magner, E., & Auty, M. A. E. (2010). Characterization of beta-lactoglobulin fibrillar assembly using atomic force microscopy, polyacrylamide gel electrophoresis, and *in situ* Fourier transform infrared spectroscopy. *Journal of Agricultural and Food Chemistry,* 58(6), 3667-3673.

Owen, D. F., Chichest.Co, Granadin.J, & Monckebe.F. (1971). Process for producing nontoxic rapeseed protein isolate and an acceptable feed by-product. *Cereal Chemistry*, 48(2), 91-98.

Patel, A. R. & Velikov, K. P. (2011). Colloidal delivery systems in foods: A general comparison with oral drug delivery. *Lwt-Food Science and Technology*, 44(9), 1958-1964.

Patil, S., Sandberg, A., Heckert, E., Self, W., & Seal, S. (2007). Protein adsorption and cellular uptake of cerium oxide nanoparticles as a function of zeta potential. *Biomaterials,* 28(31), 4600-4607.

Paula, H. C. B., Sombra, F. M., Cavalcante, R. d. F., Abreu, F. O. M. S., & de Paula, R. C. M. (2011). Preparation and characterization of chitosan/cashew gum beads loaded with Lippia sidoides essential oil. *Materials Science & Engineering C-Materials for Biological Applications,* 31(2), 173-178.

Paulson, A. & Tung, M. Aulson, A. & Tung, M. (1988). Emulsification properties of succinylated canola protein isolate. *Journal of Food Science*, 53(3), 817-820.

Pelton, J. T. & McLean, L. R. (2000). Spectroscopic methods for analysis of protein secondary structure. *Analytical Biochemistry*, 277(2), 167-176.

Penalva, R., Esparza, I., Agueeros, M., Gonzalez-Navarro, C. J., Gonzalez-Ferrero, C., & Irache, J. M. (2015). Casein nanoparticles as carriers for the oral delivery of folic acid. *Food Hydrocolloids,* 44, 399-406.

Perez, A. A., Andermatten, R. B., Rubiolo, A. C., & Santiago, L. G. (2014). β-Lactoglobulin heat-induced aggregates as carriers of polyunsaturated fatty acids. *Food Chemistry,* 158, 66-72.

Piculell, L. (1995). Gelling carrageenans. Food Science and Technology (New York); *Food Polysaccharides and their Applications*, 67, 205-244.

Pinterits, A. & Arntfield, S. D. (2008). Improvement of canola protein gelation properties through enzymatic modification with transglutaminase. *Lwt-Food Science and Technology*, 41(1), 128-138.

Porat, Y., Abramowitz, A., & Gazit, E. (2006). Inhibition of amyloid fibril formation by polyphenols: Structural similarity and aromatic interactions as a common inhibition mechanism. *Chemical Biology & Drug Design,* 67(1), 27-37.

Potter, J. M., Roberts, M. A., McColl, J. H., & Reilly, J. J. (2001). Protein energy supplements in unwell elderly patients - A randomized controlled trial. *Journal of Parenteral and Enteral Nutrition, 25*(6), 323-329.

Powell, J. J., Faria, N., Thomas-McKay, E., & Pele, L. C. (2010). Origin and fate of dietary nanoparticles and microparticles in the gastrointestinal tract. *Journal of Autoimmunity,* 34(3), J226-J233.

Prakash, V. & Rao, M. S. N. (1986). Physicochemical properties of oilseed proteins. *CRC Critical Reviews in Biochemistry*, 20(3), 265-363.

Qian, C., Decker, E. A., Xiao, H., & McClements, D. J. (2012). Physical and chemical stability of beta-carotene-enriched nanoemulsions: Influence of pH, ionic strength, temperature, and emulsifier type. *Food Chemistry,* 132(3), 1221-1229.

Qin, Y., Chen, L., Wang, X., Zhao, X., & Wang, F. (2011). Enhanced mechanical performance of poly(propylene carbonate) via hydrogen bonding interaction with o-lauroyl chitosan. *Carbohydrate Polymers,* 84(1), 329-334.

Qiu, Y. & Park, K. (2001). Environment-sensitive hydrogels for drug delivery. *Advanced Drug Delivery Reviews*, 53(3), 321-339.

Ranjbar, B. & Gill, P. (2009). Circular dichroism techniques: Biomolecular and nanostructural analyses- A review. *Chemical Biology & Drug Design,* 74(2), 101-120.

Reddy, N. & Yang, Y. (2011). Potential of plant proteins for medical applications. *Trends in Biotechnology*, 29(10), 490-498.

Relkin, P. (1998). Reversibility of heat-induced conformational changes and surface exposed hydrophobic clusters of beta-lactoglobulin: Their role in heat-induced sol-gel state transition. *International Journal of Biological Macromolecules,* 22(1), 59-66.

Remondetto, G.E. & Subirade, M. (2003). Molecular mechanisms of Fe^{2+} -induced β-lactoglobulin cold gelation. *Biopolymers*, 69, 461–469.

Ren, C., Tang, L., Zhang, M., & Guo, S. (2009). Structural characterization of heat-Induced protein particles in soy milk. *Journal of Agricultural and Food Chemistry,* 57(5), 1921-1926.

Ridley, B. L., O'Neill, M. A., & Mohnen, D. A. (2001). Pectins: Structure, biosynthesis, and oligogalacturonide-related signaling. *Phytochemistry*, 57(6), 929-967.

Rinaudo, M. (2006). Chitin and chitosan: Properties and applications. *Progress in Polymer Science*, 31(7), 603-632.

Rodriguez-Amaya, B. (1999). *A guide to carotenoid analysis in foods.* (1st ed.). Washington, D.C.: ILSI Press.

Roger, E., Lagarce, F., Garcion, E., & Benoit, J. (2009). Lipid nanocarriers improve paclitaxel transport throughout human intestinal epithelial cells by using vesicle-mediated transcytosis. *Journal of Controlled Release,* 140(2), 174-181.

Rommi, K., Ercili-Cura, D., Hakala, T. K., Nordlund, E., Poutanen, K., & Lantto, R. (2015). Impact of total solid content and extraction pH on enzyme-aided recovery of protein from defatted rapeseed (*Brassica rapa L.*) press cake and physicochemical properties of the protein fractions. *Journal of Agricultural and Food Chemistry*, 63, 2997-3003.

Rouilly, A., Orliac, O., Silvestre, F., & Rigal, L. (2001). DSC study on the thermal properties of sunflower proteins according to their water content. *Polymer,* 42(26), 10111-10117.

Ryan, K. N., Vardhanabhuti, B., Jaramillo, D. P., van Zanten, J. H., Coupland, J. N., & Foegeding, E. A. (2012). Stability and mechanism of whey protein soluble aggregates thermally treated with salts. *Food Hydrocolloids,* 27(2), 411-420.

Sagalowicz, L. & Leser, M. E. (2010). Delivery systems for liquid food products. *Current Opinion in Colloid & Interface Science*, 15(1-2), 61-72.

Saglam, D., Venema, P., de Vries, R., & van der Linden, E. (2014). Exceptional heat stability of high protein content dispersions containing whey protein particles. *Food Hydrocolloids, 34*(1), 68-77.

Sahay, G., Alakhova, D. Y., & Kabanov, A. V. (2010). Endocytosis of nanomedicines. *Journal of Controlled Release*, 145(3), 182-195.

Saiz-Abajo, M., Gonzalez-Ferrero, C., Moreno-Ruiz, A., Romo-Hualde, A., & Gonzalez-Navarro, C. J. (2013). Thermal protection of beta-carotene in re-assembled casein micelles during different processing technologies applied in food industry. *Food Chemistry,* 138(2-3), 1581-1587.

Saskatchewan Canola Development Commission. Online. 2016. Available from URL: http://saskcanola.com/industry/index.php.

Schatz, C., Lucas, J. M., Viton, C., Domard, A., Pichot, C., & Delair, T. (2004). Formation and properties of positively charged colloids based on polyelectrolyte complexes of biopolymers. *Langmuir*, 20(18), 7766-7778.

Schlucker, S., Szeghalmi, A., Schmitt, M., Popp, J., & Kiefer, W. (2003). Density functional and vibrational spectroscopic analysis of beta-carotene. *Journal of Raman Spectroscopy,* 34(6), 413-419.

Schmitt, C., Moitzi, C., Bovay, C., Rouvet, M., Bovetto, L., Donato, L., Leser, M. E., Schurtenberger, P., & Stradner, A. (2010). Internal structure and colloidal behaviour of covalent whey protein microgels obtained by heat treatment. *Soft Matter,* 6(19), 4876-4884.

Schmitt, C., Sanchez, C., Desobry-Banon, S., & Hardy, J. (1998). Structure and technofunctional properties of protein-polysaccharide complexes: A review. *Critical Reviews in Food Science and Nutrition*, 38(8), 689-753.

Schwenke, K. D., Dahme, A., & Wolter, T. (1998). Heat-induced gelation of rapeseed proteins: Effect of protein interaction and acetylation. *Journal of the American Oil Chemists Society,* 75(1), 83-87.

Schwenke, K. D., Raab, B., Linow, K. J., Pahtz, W., & Uhlig, J. (1981). Isolation of the 12 S globulin from rapeseed (*Brassica napus* L) and characterization as a neutral protein on seed proteins .13. *Nahrung-Food*, 25(3), 271-280.

Sek, S. (2013). Review peptides and proteins wired into the electrical circuits: an SPM-based approach. *Biopolymers,* 100(1), 71-81.

Ser, W. Y., Arntfield, S. D., Hydamaka, A. W., & Slorninski, B. A. (2008). Use of diabetic test kits to assess the recovery of glucosinolates during isolation of canola protein. *Lwt-Food Science and Technology*, 41(5), 934-941.

Serranio, M. & Thompson, L. (1984). Removal of phytic acid and protein phytic acid interactions in rapeseed. *Journal of Agricultural and Food Chemistry*, 32(1), 38-40.

Seyrek, E., Dubin, P. L., Tribet, C., & Gamble, E. A. (2003). Ionic strength dependence of protein-polyelectrolyte interactions. *Biomacromolecules*, 4(2), 273-282.

Shahidi, F. & Abuzaytoun, R. (2005). Chitin, chitosan, and co-products: Chemistry, production, applications, and health effects. *Advances in Food and Nutrition Research*, Vol 49, 49, 93-135.

Shahidi, F., Gabon, J. E., Rubin, L. J., & Naczk, M. (1990). Effect of methanol ammonia water-treatment on the fate of glucosinolates. *Journal of Agricultural and Food Chemistry*, 38(1), 251-255.

Shchukina, E. M., & Shchukin, D. G. (2012). Layer-by-layer coated emulsion microparticles as storage and delivery tool. *Current Opinion in Colloid and Interface Science*, 17, 281-289.

Shen, L. (2009). Functional morphology of the gastrointestinal tract. *Molecular Mechanisms of Bacterial Infection Via the Gut*, 337, 1-35.

Shewry, P., Napier, J., & Tatham, A. (1995). Seed storage proteins - Structures and biosynthesis. *Plant Cell*, 7(7), 945-956.

Shimono, N., Takatori, T., Ueda, M., Mori, M., Higashi, Y., & Nakamura, Y. (2002). Chitosan dispersed system for colon-specific drug delivery. *International Journal of Pharmaceutics,* 245(1-2), 45-54.

Singh, P. K., Kotia, V., Ghosh, D., Mohite, G. M., Kumar, A., & Maji, S. K. (2013). Curcumin modulates alpha-synuclein aggregation and toxicity. *Acs Chemical Neuroscience,* 4(3), 393-407.

Slutter, B., Plapied, L., Fievez, V., Alonso Sande, M., des Rieux, A., Schneider, Y., Van Riet, E., Jiskoot, W., & Preat, V. (2009). Mechanistic study of the adjuvant effect of biodegradable nanoparticles in mucosal vaccination. *Journal of Controlled Release,* 138(2), 113-121.

Smart, J. D. (2005). The basics and underlying mechanisms of mucoadhesion. *Advanced Drug Delivery Reviews*, 57(11), 1556-1568.

Sonvico, F., Cagnani, A., Rossi, A., Motta, S., Di Bari, M. T., Cavatorta, F., Alonso, M. J., Deriu, A., & Colombo, P. (2006). Formation of self-organized nanoparticles by lecithin/chitosan ionic interaction. *International Journal of Pharmaceutics*, 324(1), 67-73.

Sorensen, H. (1990). Glucosinolates: Structure, properties, function. In F. Shahidi (Ed.), Canola and Rapeseed: Production, Chemistry, Nutrition, and Processing Technology (149-172). *New York: Von Nostrand Reinhold*.

Takeuchi, H., Thongborisute, J., Matsui, Y., Sugihara, H., Yamamoto, H., & Kawashima, Y. (2005). Novel mucoadhesion tests for polymers and polymer-coated particles to design optimal mucoadhesive drug delivery systems. *Advanced Drug Delivery Reviews,* 57(11), 1583-1594.

Tan, S. H., Mailer, R. J., Blanchard, C. L., & Agboola, S. O. (2011). Extraction and characterization of protein fractions from Australian canola meals. *Food Research International*, 44(4), 1075-1082.

Tanaka, N., Tanaka, R., Tokuhara, M., Kunugi, S., Lee, Y., & Hamada, D. (2008). Amyloid fibril formation and chaperone-like activity of peptides from alpha A-Crystallin. *Biochemistry*, 47(9), 2961-2967.

Tang, C. & Liu, F. (2013). Cold, gel-like soy protein emulsions by microfluidization: Emulsion characteristics, rheological and microstructural properties, and gelling mechanism. *Food Hydrocolloids*, 30(1), 61-72.

Teng, Z., Luo, Y., & Wang, Q. (2013). Carboxymethyl chitosan-soy protein complex nanoparticles for the encapsulation and controlled release of vitamin D-3. *Food Chemistry*, 141(1), 524-532.

Tergesen, J. F. (2010). Sustainability points to plant proteins. *Food Technology*, 64(11), 88-88.

Thanki, K., Gangwal, R. P., Sangamwar, A. T., & Jain, S. (2013). Oral delivery of anticancer drugs: Challenges and opportunities. *Journal of Controlled Release*, 170(1), 15-40.

Thorek, D. L. J. & Tsourkas, A. (2008). Size, charge and concentration dependent uptake of iron oxide particles by non-phagocytic cells. *Biomaterials,* 29(26), 3583-3590.

Tomczynska-Mleko, M. (2013). Structure and stability of ion induced whey protein aerated gels. *Czech Journal of Food Sciences*, 31(3), 211-216.

Tong, P., Gao, J., Chen, H., Li, X., Zhang, Y., Jian, S., Wichers, H., Wu, Z., Yang, A., & Liu, F. (2012). Effect of heat treatment on the potential allergenicity and conformational structure of egg allergen ovotransferrin. *Food Chemistry,* 131(2), 603-610.

Treweek, T. M., Thorn, D. C., Price, W. E., & Carver, J. A. (2011). The chaperone action of bovine milk alpha(S1)- and alpha(S2)-caseins and their associated form alpha(S)-casein. *Archives of Biochemistry and Biophysics*, 510(1), 42-52.

Turgeon, S. L., Beaulieu, M., Schmitt, C., & Sanchez, C. (2003). Protein-polysaccharide interactions: Phase-ordering kinetics, thermodynamic and structural aspects. *Current Opinion in Colloid & Interface Science*, 8(4-5), 401-414.

Turgeon, S. L., Schmitt, C., & Sanchez, C. (2007). Protein-polysaccharide complexes and coacervates. *Current Opinion in Colloid & Interface Science*, 12(4-5), 166-178.

Twomey, M., Keogh, M. K., Mehra, R., & OKennedy, B. T. (1997). Gel characteristics of beta-lactoglobulin, whey protein concentrate and whey protein isolate. *Journal of Texture Studies*, 28(4), 387-403.

Tzeng, Y. M., Diosady, L. L., & Rubin, L. J. (1990). Production of canola protein materials by alkaline extraction, precipitation, and membrane processing. *Journal of Food Science*, 55(4), 1147-1156.

Ullah, A., Vasanthan, T., Bressler, D., Elias, A. L., & Wu, J. (2011). Bioplastics from Feather Quill. *Biomacromolecules,* 12(10), 3826-3832.

Uruakpa, F. & Arntfield, S. (2006a). Structural thermostability of commercial canola protein-hydrocolloid mixtures. *Lwt-Food Science and Technology*, 39(2), 124-134.

Uruakpa, F. & Arntfield, S. (2006b). Impact of urea on the microstructure of commercial canola protein-carrageenan network: A research note. *International Journal of Biological Macromolecules,* 38(2), 115-119.

Uruakpa, F. & Arntfield, S. (2005). The physico-chemical properties of commercial canola protein isolate-guar gum gels. *International Journal of Food Science and Technology*, 40(6), 643-653.

USDA. (2013). Major oilseeds: World supply and distribution. United States Department of Agriculture. URL: http://apps.fas.usda.gov/psdonline/circulars/oilseeds.pdf. Accessed December 13, 2013.

Valette, P., Malouin, H., Corring, T., & Savoie, L. (1993). Impact of exocrine pancreatic adaptation on *in vitro* protein digestibility. *British Journal of Nutrition,* 69(2), 359-369.

van de Weert, M. & Stella, L. (2011). Fluorescence quenching and ligand binding: A critical discussion of a popular methodology. *Journal of Molecular Structure,* 998(1-3), 144-150.

van der Linden, E. & Venema, P. (2007). Self-assembly and aggregation of proteins. *Current Opinion in Colloid & Interface Science,* 12(4-5), 158-165.

Velikov, K. P. & Pelan, E. (2008). Colloidal delivery systems for micronutrients and nutraceuticals. *Soft Matter*, 4(10), 1964-1980.

Vetri, V., Canale, C., Relini, A., Librizzi, F., Militello, V., Gliozzi, A., & Leone, M. (2007). Amyloid fibrils formation and amorphous aggregation in concanavalin A. *Biophysical Chemistry,* 125(1), 184-190.

Visschers, R. W. & de Jongh, H. H. J. (2005). Disulphide bond formation in food protein aggregation and gelation. *Biotechnology Advances,* 23(1), 75-80.

Wan, Z., Guo, J., & Yang, X. (2015). Plant protein-based delivery systems for bioactive ingredients in foods. *Food & Function*, 6(9), 2876-2889.

Wanasundara, J. P. D. (2011). Proteins of *Brassicaceae* oilseeds and their potential as a plant protein source. *Critical Reviews in Food Science and Nutrition*, 51(7), 635-677.

Wang, J., Ho, L., Zhao, W., Ono, K., Rosensweig, C., Chen, L., Humala, N., Teplow, D. B., & Pasinetti, G. M. (2008). Grape-derived polyphenolics prevent A beta oligomerization and attenuate cognitive deterioration in a mouse model of Alzheimer's disease. *Journal of Neuroscience,* 28(25), 6388-6392.

Wang, X., Lee, J., Wang, Y., & Huang, Q. (2007). Composition and rheological properties of beta-lactoglobulin/pectin coacervates: Effects of salt concentration and initial protein/polysaccharide ratio. *Biomacromolecules*, 8(3), 992-997.

Wang, J., Ma, W., & Tu, P. (2015). The mechanism of self-assembled mixed micelles in improving curcumin oral absorption: *In vitro* and *in vivo*. *Colloids and Surfaces B-Biointerfaces*, 133, 108-119.

Waraho, T., McClements, D. J., & Decker, E. A. (2011). Mechanisms of lipid oxidation in food dispersions. *Trends in Food Science & Technology*, 22(1), 3-13.

Win, K. Y. & Feng, S. S. (2005). Effects of particle size and surface coating on cellular uptake of polymeric nanoparticles for oral delivery of anticancer drugs. *Biomaterials,* 26(15), 2713-2722.

Wu, J., Aluko, R. E., & Muir, A. D. (2009). Production of angiotensin I-converting enzyme inhibitory peptides from defatted canola meal. *Bioresource Technology,* 100(21), 5283-5287.

Wu, J., Aluko, R. E., & Muir, A. D. (2008a). Purification of angiotensin I-converting enzyme-inhibitory peptides from the enzymatic hydrolysate of defatted canola meal. *Food Chemistry,* 111(4), 942-950.

Wu, J. & Muir, A. D. (2008b). Comparative structural, emulsifying, and biological properties of 2 major canola proteins, cruciferin and napin. *Journal of Food Science*, 73(3), C210-C216.

Wu, Y., Loper, A., Landis, E., Hettrick, L., Novak, L., Lynn, K., Chen, C., Thompson, K., Higgins, R., Batra, U., Shelukar, S., Kwei, G., & Storey, D. (2004). The role of biopharmaceutics in the development of a clinical nanoparticle formulation of MK-0869: A Beagle dog model predicts improved bioavailability and diminished food effect on absorption in human. *International Journal of Pharmaceutics*, 285(1-2), 135-146.

Xu, L. & Diosady, L. (2000). Interactions between canola proteins and phenolic compounds in aqueous media. *Food Research International*, 33(9), 725-731.

Xu, L. & Diosady, L. (1997). Rapid method for total phenolic acid determination in rapeseed/canola meals. *Food Research International*, 30(8), 571-574.

Xu, Y. M. & Du, Y. M. (2003). Effect of molecular structure of chitosan on protein delivery properties of chitosan nanoparticles. *International Journal of Pharmaceutics,* 250(1), 215-226.

Yamada, Y., Iwasaki, M., Usui, H., Ohinata, K., Marczak, E. D., Lipkowski, A. W., & Yoshikawa, M. (2010). Rapakinin, an anti-hypertensive peptide derived from rapeseed protein, dilates mesenteric artery of spontaneously hypertensive rats via the prostaglandin IP receptor followed by CCK1 receptor. *Peptides,* 31(5), 909-914.

Yasuda, K., Nakamura, R., & Hayakawa, S. (1986). Factors affecting heat-induced gel formation of bovine serum-albumin. *Journal of Food Science*, 51(5), 1289-1292.

Yi, J., Lam, T. I., Yokoyama, W., Cheng, L. W., & Zhong, F. (2015). Beta-carotene encapsulated in food protein nanoparticles reduces peroxyl radical oxidation in Caco-2 cells. *Food Hydrocolloids,* 43, 31-40.

Yong, Y. H. & Forgeding, E. A. (2010). Caseins: Utilizing molecular chaperone properties to control protein aggregation in foods. *Journal of Agricultural and Food Chemistry*, 58(2), 685-693.

Yoshie-Stark, Y., Wada, Y., & Waesche, A. (2008). Chemical composition, functional properties, and bioactivities of rapeseed protein isolates. *Food Chemistry*, 107(1), 32-39.

Yu, S. Y., Hu, J. H., Pan, X. Y., Yao, P., & Jiang, M. (2006). Stable and pH-sensitive nanogels prepared by self-assembly of chitosan and ovalbumin. *Langmuir*, 22(6), 2754-2759.

Zhang, J., Field, C. J., Vine, D., & Chen, L. (2015a). Intestinal uptake and transport of vitamin B-12-loaded soy protein nanoparticles. *Pharmaceutical Research,* 32(4), 1288-1303.

Zhang, Z., Van Steendam, K., Maji, S., Balcaen, L., Anoshkina, Y., Zhang, Q., Vanluchene, G., De Rycke, R., Van Haecke, F., Deforce, D., Hoogenboom, R., & De Geest, B. G. (2015b). Tailoring cellular uptake of gold nanoparticles via the hydrophilic-to-hydrophobic ratio of their (co)polymer coating. *Advanced Functional Materials,* 25(22), 3433-3439.

Zhang, J., Liang, L., Tian, Z., Chen, L., & Subirade, M. (2012). Preparation and in vitro evaluation of calcium-induced soy protein isolate nanoparticles and their formation mechanism study. *Food Chemistry*, 133, 390–399.

Zhou, B., He, Z., Yu, H., & Mukherjee, K. (1990). Proteins from double-zero rapeseed. *Journal of Agricultural and Food Chemistry,* 38(3), 690-694.

Zimet, P. & Livney, Y. D. (2009). Beta-lactoglobulin and its nanocomplexes with pectin as vehicles for omega-3 polyunsaturated fatty acids. *Food Hydrocolloids,* 23(4), 1120-1126.